

**TOWARDS AN OPTIMAL CORE OPTICAL NETWORK USING
OVERFLOW CHANNELS**

by

Pratibha Menon

B.Tech, Calicut University, 1999

M.S, University of Pittsburgh, 2002

Submitted to the Graduate Faculty of
School of Information Sciences in partial fulfillment
of the requirements for the degree of Doctor of Philosophy

University of Pittsburgh

2009

UNIVERSITY OF PITTSBURGH

School of Information Sciences

This dissertation was presented

by

Pratibha Menon

It was defended on

April 17, 2009

and approved by

Dr. Abdullah Konak, Assistant Professor, Information Sciences and Technology, Penn State University.

Dr. David Tipper, Program Director of Telecommunications Program, School of Information Sciences,
University of Pittsburgh.

Dr. Jayant Rajgopal, Associate Professor and Graduate Program Director, Industrial Engineering
Department, University of Pittsburgh.

Dr. Taieb Znati, Professor, Department of Computer Science, University of Pittsburgh.

Dr. Abdelmounaam Rezgui, Visiting Professor, School of Information Sciences, University of Pittsburgh.

Dissertation Advisor: Dr. Richard. A. Thompson, Professor, Telecommunication Program,
School of Information Sciences, University of Pittsburgh.

Copyright © by Pratibha Menon

2009

TOWARDS AN OPTIMAL CORE OPTICAL NETWORKS USING OVERFLOW CHANNELS

Pratibha Menon, PhD

University of Pittsburgh, 2009

This dissertation is based on a traditional circuit switched core WDM network that is supplemented by a pool of wavelengths that carry optical burst switched overflow data. These overflow channels function to absorb channel overflows from traditional circuit switched networks and they also provide wavelengths for newer, high bandwidth applications. The channel overflows that appear at the overflow layer as optical bursts are either carried over a permanently configured, primary light path, or over a burst-switched, best-effort path while traversing the core network.

At every successive hop along the best effort path, the optical bursts will attempt to enter a primary light path to its destination. Thus, each node in the network is a Hybrid Node that will provide entry for optical bursts to hybrid path that is made of a point to point, pre-provisioned light path or a burst switched path. The dissertation's main outcome is to determine the cost optimality of a Hybrid Route, to analyze cost-effectiveness of a Hybrid Node and compare it to a route and a node performing non-hybrid operation, respectively. Finally, an example network that consists of several Hybrid Routes and Hybrid Nodes is analyzed for its cost-effectiveness.

Cost-effectiveness and optimality of a Hybrid Route is tested for its dependency on the mean and variance of channel demands offered to the route, the number of sources sharing the route, and the relative cost of a primary and overflow path called path cost ratio. An optimality condition that relates the effect of traffic statistics to the path cost ratio is analytically derived and tested. Cost-effectiveness of a Hybrid Node is compared among different switching fabric architecture that is used to construct the Hybrid Node. Broadcast-Select, Benes and Clos architectures are each considered with different degrees of chip integration. An example Hybrid Network that consists of several Hybrid Routes and Hybrid Nodes is found to be cost-effective and dependent of the ratio of switching to transport costs.

TABLE OF CONTENTS

1.0	INTRODUCTION.....	1
1.1	THE OPTIMALITY PROBLEM.....	1
1.1.1	CORE NETWORK INFRASTRUCTURE.....	1
1.1.2	OPTIMALITY PROBLEM.....	3
1.2	RESEARCH STATEMENT	5
1.2.1	PROBLEM STATEMENT	6
1.2.2	PURPOSE STATEMENT.....	7
1.3	RESEARCH QUESTIONS, HYPOTHESES AND GOALS.....	7
1.4	NATURE OF STUDY	11
1.4.1	MODELING	12
1.4.2	ANALYSIS	13
1.4.3	REPRESENTING RESULTS	15
1.5	SIGNIFICANCE OF STUDY.....	17
1.5.1	CONCEPTUAL AND THEORETICAL FRAMEWORK.....	17
1.5.2	CONTRIBUTIONS.....	18
1.5.3	SCOPE AND LIMITATIONS	20
1.6	CHAPTER CONCLUSION.....	23
2.0	LITERATURE REVIEW	24
2.1	FACILITY SWITCHING IN CORE NETWORKS.....	24
2.1.1	CHANNEL ACCESS SCHEMES	25
2.1.2	CAPACITY AND FACILITY SWITCHING.....	26
2.1.3	FACILITY SWITCHING ON TDM CHANNELS.....	27
2.2	HYBRID SWITCHING IN WDM NETWORKS.....	28
2.2.1	CIRCUIT SWITCHING IN WDM	29
2.2.2	OPTICAL PACKET/BURST SWITCHING	31
2.3	HYBRID NETWORKS.....	32
2.3.1	NON-HIERARCHICAL, PARALLEL SCHEMES.....	33

2.3.2	HIERARCHICAL SCHEMES.....	34
2.3.2.1	NON-STATIONARY, HIERARCHICAL AND INTERGRATED SCHEMES.....	34
2.3.2.2	STATIONARY, HIERARCHICAL SCHEMES.....	36
2.4	HYBRID SCHEME WITH OVERFLOW CHANNELS	37
2.5	OVERFLOW THEORY	38
2.5.1	STATE PROBAILITIES OF OVERFLOW CHANNELS	38
2.5.2	MOMENT MATCHING METHODS	40
2.5.2.1	EQUIVALENT RANDOM TRANSFORMATION.....	41
2.6	INTERRUPTED POISSON PROCESS.....	42
2.7	CONCLUSION	43
3.0	HYBRID PATH WITH OVERFLOW CHANNELS	44
3.1	INTRODUCTION	44
3.2	A HYBRID CORE NETWORK ARCHITECTURE	46
3.2.1	HYBRID NETWORK ARCHITECTURE	46
3.2.2	HYBRID NODES	50
3.2.3	TRUNCATION OF ARRIVAL PROCESS	53
3.2.4	PRIMARY AND OVERFLOW CHANNEL MECHANISM.....	58
3.3	HYBRID NODE.....	60
3.3.1	OVERFLOW PROCESS	60
3.3.2	GENERAL CORE NODE.....	62
3.4	MODELING THE GENERAL NODE	64
3.4.1	QUEUEING MODEL	64
3.4.2	COST RATIO OF A HYBRID ROUTE	65
3.4.2.1	COST RATIO, CR_{PATH} OF A PRIMARY AND AN OVERFLOW PATH	66
3.4.2.2	PATH COST RATIO OF MULTIPLE OVERFLOW PATHS	70
3.4.3	TOTAL COST OF A HYBRID ROUTE	73
3.5	RESULTS	76
3.5.1	OPTIMAL COMBINATION OF PRIMARY/OVERFLOW CHANNELS	76
3.5.1.1	THE OVERFLOW GAIN.	78
3.5.1.2	ANALYSIS OF OVERFLOW GAIN	79
3.5.2	RANGE OF HYBRID OPERATION	83
3.5.3	USEFULNESS AND LIMITATIONS OF USING PATH COST RATIO	86
3.6	EFFECT OF OPTICAL BURST FORMATION ON HYBID OPERATION.....	87
3.6.1	TRAFFIC ADAPTATION AT THE EDGE-CORE INTERFACE	87
3.6.1.1	ADAPTING TRAFFIC ARRIVAL DISTRIBUTION	87
3.6.1.2	ADAPTING CHANNEL HOLDING DURATION	89

3.6.2 AN EXAMPLE	90
3.7 CONCLUSION	91
4.0 DESIGN AND ANALYSIS OF A HYBRID CORE NODE.....	94
4.1 INTRODUCTION	94
4.2 ARCHITECTURE OF A HYBRID CORE NODE OB-SWITCH.....	97
4.2.1 PRIMARY AND OVERFLOW OB-SWITCHES	100
4.2.2 SPACE SWITCH ARCHITECTURE OF AN OB-SWITCH	102
4.2.2.1 SYMMETRIC SWITCHES.....	103
4.2.2.2 BROADCAST AND SELECT SWITCH	103
4.2.2.3 BENES ARCHITECTURE	105
4.2.2.4 CLOS INTERCONNECTION ARCHITECTURE	106
4.2.3 WAVELENGTH INTERCHANGERS.....	106
4.2.4 REALIZING OVERFLOW PROCESS IN A HYBRID SWITCH.....	107
4.3 SUMMARY OF HYBRID NODE SWITCH DESIGN CHOICES	109
4.4 ANALYSIS OF A HYBRID NODE SWITCH.....	112
4.4.1 TOTAL COST OF A NODE.....	113
4.4.1.1 COST COMPONENTS	113
4.4.2 COST ANALYSIS OF A HYBRID SWITCH.....	116
4.4.2.1 CROSS POINTS IN A HYBRID SWITCH	116
4.4.2.2 MULTI WAVELENGTH INTEGRATED SWITCH	119
4.4.2.3 WAVELENGTH CONVERTERS AND INTERCHANGERS	120
4.4.2.4 AMPLIFIERS	120
4.4.2.5 TOTAL COST	122
4.5 ANALYSIS OF TOTAL COST.....	122
4.5.1 ADVANTAGE OF HYBRID OPERATION	123
4.5.2 TEST CASES.....	127
4.6 RESULTS OF SWITCHING AND TRANSPORT ANALYSIS	128
4.6.1 SWITCH CONTACTS USING B-S ARCHITECTURE	128
4.6.2 B-S ARCHITECTURE WITH MULTI-WAVELENGTH CHIPS	135
4.6.3 BENES ARCHITECTURE USING 2X2 SWITCHES	139
4.6.4 BENES ARCHITECTURE USING MULTI WAVELENGTH INTEGRATED 2X2 SWITCHES	144
4.6.5 CLOS ARCHITECTURE USING 4X4 SWITCHES.....	145
4.6.6 TRANSPORT COSTS	147
4.6.6.1 TOTAL NUMBER OF CHANNELS	147
4.6.6.2 COST RATIO CR_{OUTPUT}	149
4.7 HYBRID COST ADVANTAGE.....	154
4.7.1 HYBRID COST ADVANTAGE FOR $CR_{AMP}=0$ AND $CR_{OUTPUT}=0$	154

4.7.2	EFFECT OF SWITCH FABRIC ARCHITECTURE.....	156
4.8	CHAPTER CONCLUSION.....	162
5.0	ANALYSIS OF A NETWORK OF HYBRID NODES	164
5.1	INTRODUCTION	164
5.2	HYBRID NETWORK MODELING.....	166
5.2.1	GRAPH DEFINITIONS AND EXAMPLES	167
5.2.2	ROUTE AND TRAFFIC LOAD MATRICES	172
5.2.2.1	ROUTE MATRIX	172
5.2.2.2	TRAFFIC LOAD MATRIX	174
5.3	LIGHTPATH ENTRY OF OVERFLOW TRAFFIC	179
5.3.1	ITERATING OVERFLOW TRAFFIC LOAD MATRIX	181
5.3.2	ADDING PRIMARY LIGHTPATHS IN EXAMPLE 1.....	182
5.3.3	RESULTS: PRIMARY AND OVERFLOW CHANNELS IN THE LINKS	193
5.3.4	SWITCHING COST OF NODES.....	196
5.4	COST OF A HYBRID NETWORK.....	201
5.4.1	SWITCHING COSTS	201
5.4.2	TRANSMISSION COSTS.....	205
5.5	COST OF ROUTES.....	207
5.5.1	COST OF ROUTES IN EXAMPLE 1	207
5.5.2	ANALYSIS OF NETWORK ROUTE COSTS FOR EXAMPLE 1	211
5.6	CHAPTER CONCLUSION.....	213
6.0	CONCLUSION	216
5.7	SUMMARY OF RESULTS	217
5.8	FUTURE WORK.....	219
	BIBLIOGRAPHY.....	221

LIST OF TABLES

Table 1.1 Structure of the dissertation, showing the 3 levels of modeling and analysis.	14
Table 3.1a Overflow gain	80
Table 3.2 Values of l_i and $\Delta(Ro(l_i))$ for different offered loads.....	81
Table 4.1 Design choices considered for the Hybrid Node analysis.	110
Table 4.2 Slopes of the primary and overflow layer OB-switch based on B-S architecture for an offered load of 0.75 Erlangs per source-destination.	157
Table 4.3 Slopes of the primary and overflow layer OB-switch based on B-S architecture for an offered load of 6 Erlangs per source-destination.	158
Table 4.4 Slopes of the primary and overflow layer OB-switch based on Benes architecture for an offered load of 0.75 Erlangs per source-destination.	159
Table 4.5 Slopes of the primary and overflow layer OB-switch based on Benes architecture for an offered load of 6 Erlangs per source-destination.	160
Table 5.1 Primary channels for each route at edge node.	180
Table 5.2 Value of T_o after Iteration 1	184
Table 5.3 Value of T_o after Iteration 2.....	186
Table 5.4 Iteration 3.....	188
Table 5.5 Iteration 4.....	189
Table 5.6 Final Iteration.....	190

Table 5.7 Number of input and out put fibers at each node.....	199
Table 5.8 Number of switching elements in each node.....	200
Table 5.9 Number of primary and overflow channels in each link.	210
Table 5.10 Total cost of the Hybrid Network.....	211

LIST OF FIGURES

Figure 1.1 Core Networks.....	1
Figure 1.2 Proposed OBS-based Overflow Layer	2
Figure 1.3 The optimality problem	4
Figure 1.4 Conceptual/theoretical framework.	19
Figure 2.1 A Literature review map of switching techniques.....	25
Figure 2.2 Light paths in an optical circuit switched network, with IP access layer [19]	30
Figure 2.3 State transition diagram for Kosten's system.....	39
Figure 2.4 Effect of peakedness on blocking probability [26].....	40
Figure 2.5 Equivalent Random Process.....	42
Figure 2.6 Interrupted Poisson Process.....	43
Figure 3.1 Alternate path routing along AD. Path AD carries overflow traffic to destinations B and C.	45
Figure 3.2 The Proposed Overflow Network.....	47
Figure 3.3 The Proposed Overflow Network and its access-core interface.....	49
Figure 3.4 A Hybrid Node.	51
Figure 3.5 The proposed overflow network (Hybrid Network) layers	53
Figure 3.6. Case 1. Truncation of offered arrival process in three steps.	54
Figure 3.7. Case 2. Truncation at two levels.....	56
Figure 3.8 Primary and Overflow channels	59

Figure 3.9 Operation in a Hybrid Node, showing header queues for primary and overflow channels.....	61
Figure 3.10 Possibilities of operation.	63
Figure 3.11 Queuing model of a Hybrid Node.	64
Figure 3.12 Path cost ratio, CR_{path}	67
Figure 3.13 Effect on light path entry on cost ratio.	70
Figure 3.14 Assumption in calculating cost of a hybrid route.....	75
Figure 3.15 Cost of primary, overflow and sum of primary and overflow channels, for a load of 3 Erlangs per traffic source; 100 sources and a peakedness of 2.....	77
Figure 3.16 Overflow Gain.....	82
Figure 3.17 Feasibility of a hybrid node with 100 traffic sources.....	85
Figure 3.18 Feasibility of a hybrid node with 10 traffic sources.....	85
Figure 3.19 Timer based assembly process.	88
Figure 4.1 A Hybrid-Node switch	94
Figure 4.2 Five stages of a Hybrid Node.	98
Figure 4.3 Primary and overflow layer of an OB-Switch.....	99
Figure 4.4 Source-specific switching modules in a primary OB-switch.	101
Figure 4.5 Constructing $K \times M$ space switches using $M \times M$ switch modules.....	103
Figure 4.6 N - ($M \times M$), Broadcast and Select space switch using a 1×1 WSC.....	104
Figure 4.7 N -($M \times M$) Benes space switch using a 2×2 Optical Add Drop Multiplexer (OADM).	105
Figure 4.8 Clos interconnection architecture	106
Figure 4.9 A Wavelength Interchanger.....	107

Figure 4.10(a). Passive overflow using 1:2 splitters. (b) Active overflow using gates.	108
Figure 4.11 Hybrid Node architecture, considered in the analysis.	110
Figure 4.12 Total number of 1x1 switches for an offered load is 0.75 Erlangs and $CR_{amp} = 0$..	128
Figure 4.13 Total number of 1x1 switches for an offered load is 3 Erlangs and $CR_{amp} = 0$	129
Figure 4.14 Total number of 1x1 switches for an offered load is 6 Erlangs and $CR_{amp} = 0$	129
Figure 4.15 Amplifiers to overcome switching loss. Offered load is 0.75 Erlangs.....	131
Figure 4.16 Amplifiers to overcome switching loss. Offered load is 3 Erlangs.	131
Figure 4.17 Amplifiers to overcome switching loss. Offered load is 6 Erlangs.	132
Figure 4.18 Total cost of switching for various values of CR amp. Offered load is 0.75 Erlangs	133
Figure 4.19 Total cost of switching for various values of CR amp. Offered load is 3 Erlangs	134
Figure 4.20 Total cost of switching for various values of CR amp. Offered load is 6 Erlangs.	134
Figure 4.21 Total number of multi-wavelength 1x1 switches. Offered load = 0.75 Erlangs ; CR amp=0.....	136
Figure 4.22 Total number of multi-wavelength 1x1 switches. Offered load = 3 Erlangs ; CR amp=0	136
Figure 4.23 Total number of multi-wavelength 1x1 switches. Offered load = 6 Erlangs ; CR amp=0.....	136
Figure 4.24 Total cost of switching for various values of CR amp. Offered load =0.75 Erlangs.	138
Figure 4.25 Total cost of switching for various values of CR amp. Offered load = 3 Erlangs.....	138
Figure 4.26 Total cost of switching for various values of CR amp. Offered load = 6 Erlangs.....	138
Figure 4.27 Total number of 2x2 switches. Offered load = .75 Erlangs.....	140
Figure 4.28 Total number of 2x2 switches. Offered load = 3 Erlangs.....	140

Figure 4.29 Total number of 2x2 switches. Offered load = 6 Erlangs.....	140
Figure 4.30 Amplifiers to overcome switching loss. Offered load is 0.75 Erlangs.....	141
Figure 4.31 Amplifiers to overcome switching loss. Offered load is 3 Erlangs.....	141
Figure 4.32 Amplifiers to overcome switching loss. Offered load is 6 Erlangs.....	142
Figure 4.33 Total cost of switching for various values of CR_{amp} . Offered load = 3 Erlangs.....	142
Figure 4.34 Total cost of switching for various values of CR_{amp} . Offered load = 3 Erlangs.....	143
Figure 4.35 Total cost of switching for various values of CR_{amp} . Offered load = 6 Erlangs.....	143
Figure 4.36 Total number of 2x2 chips. Offered load = 0.75 Erlangs.....	144
Figure 4.37 Total number of 2x2 chips. Offered load = 3 Erlangs.....	145
Figure 4.38 Total number of 2x2 elements. Offered load = 6 Erlangs.	145
Figure 4.39 Total cost of switching for various values of CR_{amp} for a load of 0.75 Erlangs	146
Figure 4.40 Total cost of switching for various values of CR_{amp} for a load of 3 Erlangs	146
Figure 4.41 Total cost of switching for various values of CR_{amp} for a load of 6 Erlangs	147
Figure 4.42 Total number of output channels.....	148
Figure 4.43 Total cost of a node.	150
Figure 4.44 Total cost of a node. Offered load = 3 Erlangs.....	151
Figure 4.45 Total cost of a node. Offered load is 6 Erlangs.	151
Figure 4.46 Total cost for a core node with an offered load of 0.75 Erlangs per source-destination.....	152
Figure 4.47 Total cost for a core node with an offered load of 3 Erlangs per source-destination.	153
Figure 4.48 Total cost for a core node with an offered load of 6 Erlangs per source-destination.	153

Figure 4.49 Percentage values of HCA for a core node made using B-S architecture.	154
Figure 4.50 Percentage values of HCA for a core node made using Benes architecture	155
Figure 4.51 Percentage values of HCA for a core node made using Integrated B-S architecture.	155
Figure 4.52 Percentage values of HCA for a core node made using Clos architecture.....	156
Figure 4.53 Number of 1x1 switches for a core node using B-S architecture and an offered load of .75 Erlangs, 10 sources and 1 destination.....	158
Figure 4.54 Number of 1x1 switches for a core node using B-S architecture and an offered load of .75 Erlangs, 10 sources and 1 destination.....	159
Figure 4.55 Number of 2x2 switches for a core node using Benes architecture and an offered load of .75 Erlangs, 10 sources and 1 destination.....	160
Figure 4.56 Number of 2x2 switches for a core node using Benes architecture and an offered load of 6 Erlangs, 10 sources and 1 destination.....	161
Figure 5.1 A example core-network topology	167
Figure 5.2 An example Network Graph and its Incidence matrix.	168
Figure 5.3 Example of a Virtual Primary layer graph.	169
Figure 5.4 An example physical primary layer graph.....	170
Figure 5.5 Example of an overflow layer graph	172
Figure 5.6 Physical Network in the example with link IDs	173
Figure 5.7 Calculating overflow traffic on each hop of the path.....	175
Figure 5.8 Number of overflow channels in the example network, with out any primary channels.	181
Figure 5.9 G_p for the given example network, after performing Step 10.	184

Figure 5.10 G_p for the example network, after Iteration 1	185
Figure 5.11 G_p after addition of 7 primary channels after Iteration 2.....	187
Figure 5.12 Addition of light-paths in Iteration 3.....	189
Figure 5.13 G_p after addition of primary channels on link 2.....	190
Figure 5.14 Initial and Final Overflow Graphs.....	191
Figure 5.15 Initial and final Primary Layer Graph.	192
Figure 5.16 Links showing overflows channels/overflow fibers of each link.....	198
Figure 5.17 Primary lightpaths/fiber emanating from nodes 2, 3 and 4.	198
Figure 5.18 Number of 1x1 elements for nodes 1, 6 and 5.....	202
Figure 5.19 Number of 1*1 elements for node 3	203
Figure 5.20 Number of 1x1 elements in nodes 2 and 4	204
Figure 5.21 Number of 1x1 elements in the entire network	204
Figure 5.22 Total number of channels in the network	205
Figure 5.23 Total cost of the network for different values of CR_{trans}	206

1.0 INTRODUCTION

Today, core optical networks are characterized by wavelength division multiplexed (WDM) channels, being able to provide cheap and bulk transport capability to edge traffic sources. Not only are the number of wavelengths per channel increasing, the bit rates of individual channels are also getting bigger. Today, a long haul fiber can support 40-100 wavelengths/fiber, with a speed of 10-40 Gbps each. In order to enable several end users to share a wavelength, the bandwidth of a single wavelength channel can be further divided into granular trunks using time division multiplexing (TDM).

Along with an increase in WDM transmission rates, there is also a proliferation of newer applications at the access layer that require both large and dynamic transmission capacity, from the core networks. Typical applications have been identified as GRID applications, Storage area networks (SANs), On-demand applications, etc [\[1\]](#). Current WDM circuit switched core networks can provide some degree of channel flexibility to the end users by using protocol based on MPLS, ATM, RSVP etc. All these protocols help regulate channel access, class based services, traffic smoothing and policing functions that enable judicious used of pre-provisioned channels. In order to enable a truly next generation optical core network, on demand automatic switching and connection of WDM channels will be required [\[1\]](#). However, development of such a dynamic optical WDM backbone network will depend on the development of fast optical switches, standardization of control planes and design of cost optimal network architectures. Among the different optical switching techniques, WDM circuit switching, burst switching and packet switching techniques have been proposed by the research community [\[2\]](#).

Edge sources that supply traffic to the core networks have benefited from the immense channel capacity of wavelengths. This benefit can be explained by the economy of scale, where a larger number of edge traffic sources can be aggregated onto a single wavelength than ever before. The economy of scale, however, becomes strained as the speed of the channel far outpaces the speed of aggregation at the edge. It is seen that at higher channel rates such as 40 Gbps, the aggregation may cost about 40% of the total node cost, compared to only 17% at 10 Gbps [35]. Optical aggregation schemes have been identified as a solution to bring scalability at the edge nodes. The optical packet (OPS) and burst switches (OBS) have been proposed at the edge nodes, to provide this high capacity aggregation [3]. However, the design of OPS and OBS switches are still in their research stages and their feasibility in core networks is still an open research problem.

OPS and OBS differ from the existing optical circuit switched scheme because they can enable core nodes to provide statistical multiplexing gains for the core links. Currently there exists a functional demarcation between edge and core nodes because edge nodes perform traffic aggregation and core nodes perform optical bypass. Optical bypass is the ability of optical channels to 'bypass' any switching/aggregation function at the core nodes. With the introduction of OPS/OBS switches in core nodes, the functional demarcation between edge and core nodes will disappear.

But the introduction of OPS and OBS switches in to the core nodes may result in expensive core nodes, compared to their optically-bypassed counterparts. Optical bypass enables simpler switching nodes, which can be constructed from optical cross-connects (OXCs) that can switch at slower speeds. However, optical bypass results in inefficient use of core link wavelengths, which cannot be reconfigured fast enough to support dynamic channel demand. Capacity inefficiency of optically bypassed channels may become more acute as the offered traffic shows high statistical variance. In an OPS/OBS scheme, statistical access of channel capacity can help provide efficient use of channels in response to a statistically varying channel demand. However, compared to an optically bypassed scheme, OPS/OBS has more complex switching requirements, such as: high switching speeds (order of ns), the need for optical buffers due to the statistical nature of the traffic and high fabric cost due to immature devices and integration technology [11][15][39]. Part of the problem may be alleviated by framing packets

into optical bursts. However, even an OBS switch has similar requirements, except that switching speed may be relaxed to milliseconds by putting up with more framing delay. Thus, it can be seen that statistical channel gains provided by OPS/OBS switches comes with a higher switching costs and penalties.

The stringent requirements that OPS/OBS switches may place on the core node makes one re-think about the possibility of optical bypass. It may be possible to provide some degree of optical bypass, along with statistical channel gains, in core nodes. A core node's switching capability may be divided between the two complementary switching schemes, OPS/OBS and OCS. Doing so will also divide the channels of the core links. Thus, we may envision a core network, whose channels are divided between OPS/OBS and OCS schemes.

If we consider the current optical circuit switching and optical packet/burst switching schemes, as opposite ends of the switching spectrum, the question becomes how much each type of switching scheme is optimal in a core network? Alternatively, one might ask, if it is possible to divide the core network capacity into OCS and OPS/OBS schemes in the most optimal manner? This obviously raises questions about the design of a hybrid OCS/OPS/OBS core node that will help divide incoming traffic load into OCS and OPS/OBS channels. A Hybrid Network will also be able to provide some degree of channel over provisioning along with better channel performance, in a cost efficient manner. A research study aimed at this issue would be of practical interest to systems designers and researchers aiming to create optimal core network architecture

In order to realize optimal hybrid operation in a core network, a theoretical framework to partition the network channel capacity into OCS and OPS/OBS channels is required. The channels can be partitioned if the channel demand offered to the node is divided between the two schemes. The concept of overflow provides a simple threshold based rule, to partition demand for channels into circuit switched and packet/burst switched layers of the core network. The overflow mechanism can be extended to establish end to end paths using an alternate switching scheme (alternate to circuit switching). In effect, partitioning the traffic via overflow provides a mechanism to study, the existence of complementary switching schemes within the same core node/network.

1.1 THE OPTIMALITY PROBLEM

1.1.1 CORE NETWORK INFRASTRUCTURE

Consider a core WDM network, as shown in [Figure 1.1](#). The nodes in the network perform the function of aggregating regional access network traffic onto core WDM channels and for this reason, the nodes function as an edge node. [Figure 1.1](#) shows that the edge node numbered Region 11 aggregating regional traffic from the four central states, of the USA that constitute Region 11. The same node also functions as a core node, containing optical cross connects, in order to complete a light path between other network nodes. In [Figure 1.1](#) Region 11 concatenates wavelengths of light paths to/from Regions 6, 7 and 12. Thus, any node in the given core network can function as an edge node or as a core node.

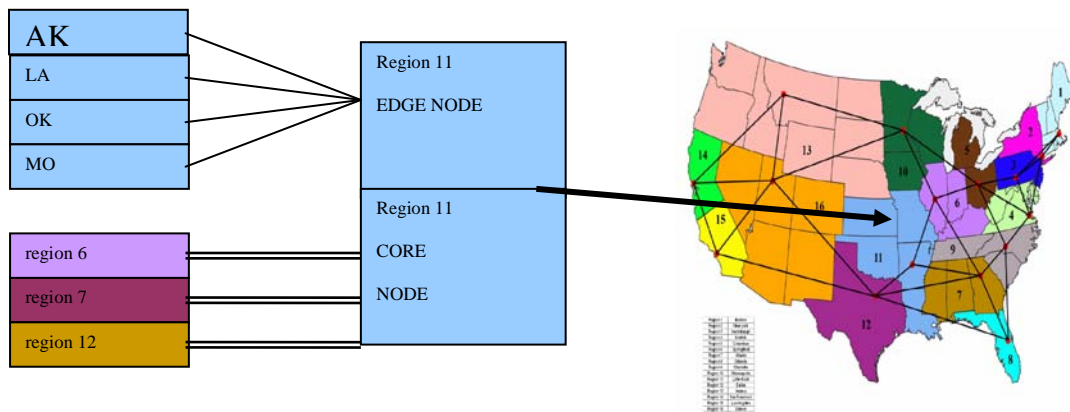


Figure 1.1 Core Networks

If the core network shown in [Figure 1.1](#) contained burst switched channels, there will be no pre-provisioned point-to-point connection between any two regions. Instead, sections of a path between any two regions will be shared by several other paths between other regions. In such a case, a core node will aggregate optical bursts belonging to several paths that share the same link. For instance, the path from Region 6 to Region 12 and the path from Region 7 to Region 12, will intersect at Region 11. In this case, the core node in Region 11 will aggregate

bursts from regions 6 and 7. In an OBS based core network, both core nodes aggregate bursts belonging to different regions and edge nodes aggregate bursts belonging to different states of a region.

Optical burst switching can be introduced into the core WDM network in the form of an overflow layer. The overflow layer may carry channel overflows from traditional Facility-Switched WDM light paths or offered traffic from newer applications that require dynamic channel access. [Figure 1.2](#) shows the OBS-based overflow layer, which accepts overflows from the Facility-Switched light-paths and also from another access-source.

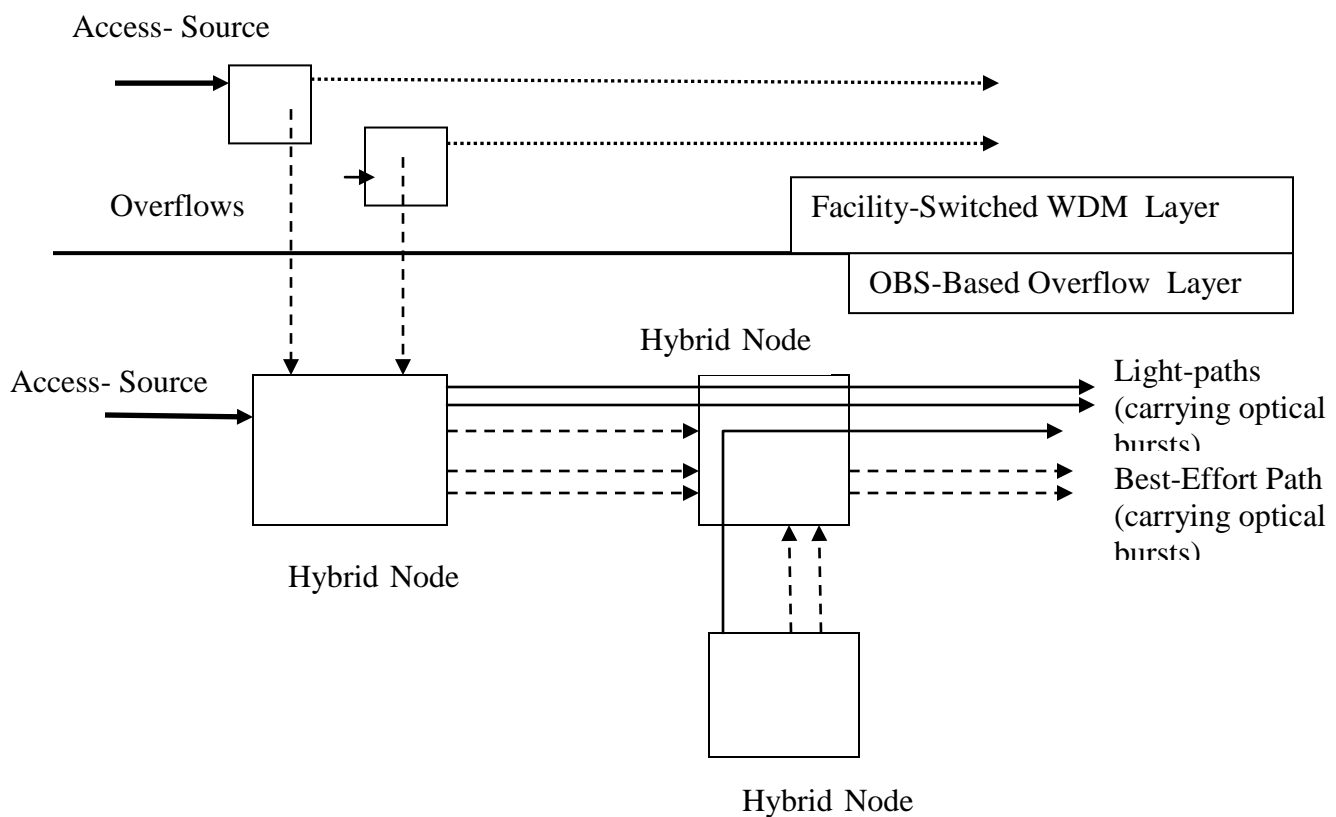


Figure 1.2 Proposed OBS-based Overflow Layer

Although the proposed overflow layer uses a burst transport mechanism, it is possible for the channels to enter a pre-provisioned light-path or remain on the best-effort, OBS path. Entry of the bursts into a light-path provides a guaranteed direct path to carry optical bursts between a pair of nodes. A light-path is provisioned between a pair of nodes if there is enough optical burst traffic to keep the light-paths loaded at a fixed value. In case the light-paths are loaded above the

fixed value, an overflow occurs, which is handled by the OBS channels. The optical bursts carried along OBS channels will appear at the next core node along its path, where they try to enter a light path.

Each edge/core node in the network performs the operation of filling its outgoing light-paths with incoming optical bursts and diverting the overflows along OBS channels. We may call each node a Hybrid Core Node, since it functions as a point of entry to either a light-path or a best-effort path. The light-path behaves like a pre-provisioned circuit switched path that will carry optical bursts and the best effort-path is an OBS path. In [Figure 1.2](#), Hybrid Node 1 provides light path and best-effort path entry to access sources, while Hybrid Node 3 provides light path and best effort path entry to optical bursts from Hybrid Node 1 and Hybrid Node 2. If Hybrid Node 3 is attached to its access source, it will also function as an edge node like Hybrid Node 1. The proposed overflow network, which is made of Hybrid Nodes, will be called a 'Hybrid Network'.

Managing the channel load offered to the core network using the hybrid mechanism is viable only if it is cost optimal to do so. Combining OCS and OBS features is advantageous only if it results in a synergy that occurs due to the combined operation. In the dissertation, an attempt is made to study cost optimality of hybrid operation with regards to total cost of a network.

1.1.2 OPTIMALITY PROBLEM

Consider an edge traffic source, whose channel demand is relatively smooth with respect to time. Since traffic demand remains invariant with respect to time, the number of channels to be provided by the core network also remains static. Now consider an edge traffic source with a highly variable channel demand. In order to provide a statically configured light-path to the traffic source, the traffic demand must be estimated to be a constant over a time period. By assuming a constant demand equal to the peak demand, sufficient carrying capacity may be provided at the cost of severe channel underutilization. In order to achieve better channel efficiency, several traffic sources may be allowed to access the net fixed capacity in a statistical

manner. We may assume that the traffic sources may access the core channels in the form of optical bursts.

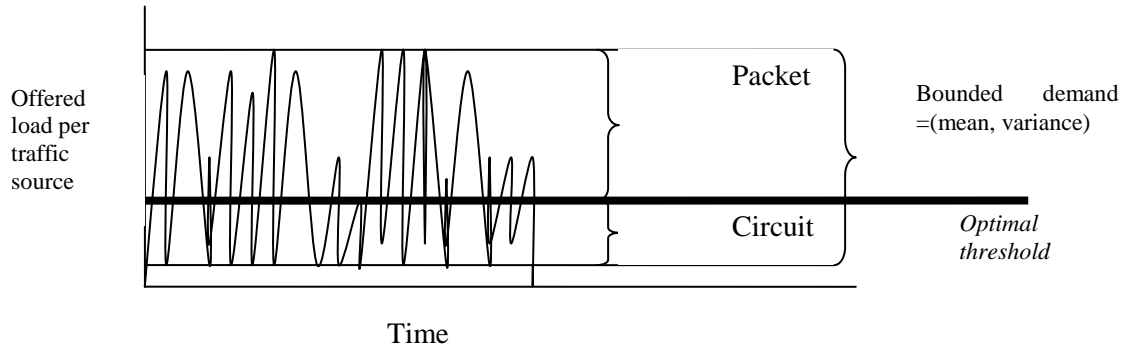


Figure 1.3 The optimality problem

The number of core network channels required by an edge node is dictated by the highly aggregated access level traffic coming from regional networks. The traffic aggregation and optical burst assembly may take place at a point of presence, POP, which is the edge node. Aggregation and burst assembly partially smoothes out some of the variance in traffic demand, although it may not provide a completely smooth traffic. Thus, it becomes possible to envision an edge source channel demand, consisting of a smooth average and a residual variable / ‘peaked’ component. Statistically, the smoothness and the Peakedness components can be gauged by the steady state mean and variance of the offered load. Depending on the mean and variance of the channel demand, the core network channels accessed by the traffic source can be divided into statically accessed OCS and dynamically accessed OBS channels. In this manner, it may be possible to achieve an optimal division of access channel demands between OCS and OBS schemes.

The optimality achieved by partitioning the core node capacity into OCS/OBS parts, is a trade off between costs of statistical multiplexing gains and switching simplicity. In a Hybrid Node, balancing these features may result in a cost optimal switching node. This may be especially true in optical networks, where there exists a wide discrepancy between the realization complexity of OCS and OBS switches. If the cost of an OBS switch is much higher than its OCS counterpart, part of statistical multiplexing gains attained by OBS may be offset by higher

switching costs. Thus, partitioning the node capacity between OCS and OBS schemes not only depends on traffic mean and variance, but also on relative costs of both the channel types.

The optimal split of the core network into OCS and OBS channels also depends on the performance conditions to be achieved at the node. Performance criteria, such as blocking of channel requests will decide how many channels may be required in each category. The general assumption that we make here, is that there exists a hierarchical relationship between OCS and OBS channels and the blocking constraint is met by the joint effort of OCS and OBS schemes. The hierarchical relationship between OCS and OBS channels is via the overflow process and the percentage of channel demand offered to the OBS channels depends on available OCS channels.

The hierarchical relation between OCS and OBS channels, via the concept of overflow, brings forth the notion of a channel threshold. A channel threshold is the number of OCS channels available to a traffic source and it will be henceforth called, “primary channels”. If the threshold is high, there are more OCS primary channels that can be exclusively accessed by a traffic source and subsequently, there will be a smaller overflow load. A high threshold will thus mean a smaller requirement of OBS channels, which will be henceforth called the “overflow channels”. The primary channel threshold available to each access source and the overflow channels required to support all primary channel overflows, will depend on channel demand statistics (mean and variance), cost/complexity of the OCS and OBS channels and the blocking performance required for the access source. In this dissertation, we analyze a hybrid scheme consisting of primary/overflow channels for an optimal operation.

1.2 RESEARCH STATEMENT

The research statement includes the problem statement and the research purpose statement. The problem statement explains the research problem in light of the optimality problem. The purpose statement draws from the problem statement to formally state the research purpose.

1.2.1 PROBLEM STATEMENT

Optical circuit switching (OCS) and optical burst switching (OBS) can be viewed as complementary schemes, with regards to their switching complexity and channel efficiency. In order to improve efficiency of OCS channels and help OBS become more practical/ feasible, a hybrid operation can be considered in core networks. The Hybrid Networks may neither provide channel efficiency of pure OBS, nor switching simplicity of OCS. In stead, feasibility of Hybrid Networks depends on their ability to balance the features of OBS and OCS, to provide cost optimal networks for a given level of performance. In order to study the optimality, as well as feasibility of such Hybrid Nodes/networks, suitable design and analysis of Hybrid Node operation is required.

Previous researches on hybrid optical networks were concerned with partitioning the network capacity to aid the migration of core networks to a pure OPS/OBS system [22]. A set of conditions, under which pure OBS, pure OCS or a hybrid of OCS/OBS may be feasible, is a problem to which only minimal attention has been paid. Hybrid Networks consisting of hybrid edge nodes have also been proposed in some researches [17][18]. In this research, the traffic is split into circuit and burst switched channels, only once, at the edge nodes. It still needs to be found out if core nodes too, can function in a hybrid mode and be able to optically split the traffic into circuit and burst switched channels. Currently lacking in the literature is a general method to analyze feasibility and optimality of hybrid operation in either edge or core nodes.

In order to answer the questions concerning optimality and feasibility of hybrid operation in edge and core nodes, a mechanism of partitioning/splitting the offered packet traffic into OCS and OBS channel is required. The optimality problem discussed in Section 1.1 is approached via the concept of overflow.

Feasibility of optimal hybrid operation in core networks can be quantitatively analyzed, by studying the total cost of a Hybrid Network. In order to do so, the cost of a Hybrid Network is analyzed by using two approaches. One approach is to consider the role played by hybrid operation in reducing the cost of routes between two Hybrid Nodes of the network. The other approach is to study the role played by hybrid operation in reducing switching cost in the network. In both cases, hybrid operation is compared with non-hybrid operation, which is either pure OCS or pure OBS operation. The effects of various parameters such as traffic mean and

variance, channel utilization, number of traffic sources and cost structure of hybrid switching nodes on optimal hybrid operation is also studied.

1.2.2PURPOSE STATEMENT

The purpose of this study is to (1) quantitatively test the feasibility of optimal hybrid OCS/OBS operation in core WDM networks that support channel overflow, (2) by relating the effect of variables such as traffic statistics, cost structure of OCS and OBS paths, switching architecture and network topology, and to (3) determine the optimal number of OCS and OPS channels for a given blocking probability at the Hybrid Node.

1.3 RESEARCH QUESTIONS, HYPOTHESES AND GOALS

A Hybrid Network that combines OCS and OBS operations is feasible only if some sort of cost optimality can be achieved by the hybrid operation. Cost optimality of hybrid operation occurs when total cost of network is minimum for a hybrid operation, compared to purely OCS or OBS operations in the same network. In order to assess the total cost of a network, the network may be viewed either as a collection of hybrid routes, or as a collection of switching nodes and transmission links. If the network is seen as a network of hybrid routes, the total network cost is the total costs of primary light paths and best effort paths for every route in the network. If cost of a network is viewed as cost of a collection of switching and channel entities, total costs of switching nodes and channels are required. In the dissertation, optimal hybrid operation is tested by considering both the approaches. In order to test optimality of hybrid operation, following questions are put forth.

- Cost optimality of a hybrid route.

1) How to determine cost of a route that consists of primary and overflow channels?

A hybrid route consists of a path between two nodes in a network. A hybrid route is made of primary and overflow paths. While number of primary light paths is the same as number of primary channels originating at the source node, the number of overflow channels in the best effort path is not the same as number of overflow channels available in the first hop. In the same route, there are as many overflow paths, as there are overflow channels between the source and destination nodes of a route. In order to determine number of overflow channels required for a route, one needs to consider the possibility of light path entry and loss within the route. Total cost of the route depends on total number of primary light paths and overflow paths in the route.

2) How do factors such as channel load statistics, relative costs of primary and overflow paths and the number of sources sharing the overflow path determine feasibility of a hybrid route?

Channel load statistics such as mean and variance of the offered load will determine number of primary and overflow channels in the links. If the load is such that benefit of statistical sharing of overflow channels is high, higher cost of overflow path is compensated by smaller channel requirement. Benefit of statistical sharing is expected to increase for loads that have high variance relative to its mean load value. Also if there are more sources sharing the overflow channels, optimal hybrid operation can be realized even if relative cost of an overflow path is higher than the cost of a primary path.

- Cost optimality of a Hybrid Node

1) How does cost optimality of a Hybrid Node depend on the switching fabric architecture used to construct the switch?

Cost of a Hybrid Node depends on the cost of switching hardware. Partitioning the channels of all output links of a Hybrid Node may also result in partitioning the switch within the node. A partitioned switch fabric, with lesser interconnection among switching elements may

help reduce the total cost of a switch. The number of switching elements within a hybrid switch depends on the switching fabric architecture used to construct the switch. Switching fabric architectures can be classified based on wide-sense and rearrangably non-blocking properties provided by the Broadcast-Select and Benes architecture, respectively. The cost of a hybrid switch made from the Benes architectures requires a minimum number of switching elements and it grows ‘slowly’ with an increase in number of output channels. On the other hand, the Broadcast-Select architecture requires a larger number of switching elements, and the switch size grows faster with an increase in number of output channels. It is expected that the proposed hybrid switch architecture may greatly help minimize number of elementary switches in a Broadcast–Select architecture switch, when compared to a Benes switch that is already optimal to begin with.

- 2) How does the cost optimality of a Hybrid Node depend on the relative cost of switching elements compared to other non-switching elements, such as amplifiers and transmission costs?

The total cost of a node not only depends on its switching elements, but also on non switching elements that depend on the number of channels in outgoing links of a Hybrid Node. Channel-dependent costs increase with output channels, which increases when there are more primary channels. Even if hybrid operation may minimize switching costs, other non-switching costs may grow with an increase in the number of output channels. This may undo the hybrid advantage.

- Network analysis of Hybrid Network

- 1) How does total cost of a network depend on average channel utilization at the primary layer?

Average channel utilization of the primary layer will determine the amount of load offered to the overflow layer. A high value of average primary channel utilization can be obtained if there are fewer primary channels. Fewer primary channel results in a larger overflow at the edge node, which will try to enter a light path at the next node along the path. At the next node, light path entry is provided for the incoming overflow, such that the light paths are

utilized by the same fixed amount. Light path entry reduces the amount of overflow load that remains in the overflow layer, by providing a high probability of light path entry for the overflow path. Thus, to provide high channel utilization, there are fewer primary light paths originating at the edge node, but more light paths in the core node. Analysis of an example network will provide the overall effect of average channel utilization of total cost of network.

2) How does the optimal hybrid operation depend on the ratio of switching to transmission costs in a network?

Due to the aggregation of optical burst at hop of its path, an overflow path requires more switching resources than the corresponding primary path. At the same time, due to dedicated light-paths, primary path requires more channels than the corresponding overflow path. Thus, the ratio of channel transmission to switching costs will determine number primary and overflow paths in a route. This ratio, along with the average probability of light-path entry, will provide the cost ratio of the route. A network consists of several such routes and the links are shared by several routes. Analysis of an example network will show the effect of ratio of switching to transmission costs in a network.

The above questions are answered sequentially in the following chapters:

1) Chapter 3: Analysis of a hybrid route

A hybrid route, which contains primary and overflow paths, will be analyzed for its cost optimality by varying the offered load and cost-ratio of primary and overflow paths. The goal is to discover how the offered traffic, along with the ratio of primary and overflow path costs will affect optimal number of primary/overflow channels in the route.

2) Chapter 4: Analysis of a Hybrid Node

A Hybrid Node, consisting of a hybrid switch, is analyzed for optimal hybrid operation by varying the switching fabric architecture and the load offered to the Hybrid Node. The goal is to understand if the optimality of the underlying switching fabric architecture will determine the possibility of hybrid cost advantage. The sensitivity of this hybrid cost advantage towards offered load and the relative cost of non-switching components will also be studied.

3) Chapter 5: Analysis of a Hybrid Network

Since Chapters 3 and 4 consider an isolated hybrid route and an isolated Hybrid Node, they only provide the conditions for a local optimum when subjected to varying external load and cost conditions. However, when we consider a Hybrid Network, some of the load values and cost conditions are modulated by the network. For instance, in a core node, the load offered by other nodes will depend on the primary and overflow channels in the incoming link. In the same way, the number of primary channels in the outgoing links of the core node will determine how much load will be offered to its neighboring nodes. The cost ratio of primary and overflow paths, are also modulated by the network, since possibility of light path entry within the path depends on number of primary channels in the links that constitute the path. Thus, the primary/overflow channels in a network link will affect the number of primary/overflow channels in other links. Optimality of an example Hybrid Network is analyzed by considering the total cost of all routes and the total cost of switching and transmission.

1.4 NATURE OF STUDY

The purpose of the research is to study the optimality of hybrid operation. The effect of hybrid operation on the total cost of a hybrid route, a Hybrid Node, and a Hybrid Network, is studied analytically. Out of all combinations of number of primary and overflow channels in the link, optimal hybrid operation is expected to be achieved only for a particular combination of primary and overflow channels. The optimum number of primary and overflow channels in a hybrid route is tested for its dependence, on independent variables such as traffic mean and variance, the number of sources, relative cost of primary and overflow paths. Optimality of a Hybrid Node is studied for the underlying switch fabric architecture used to construct the node switch and load offered to the core node. An example network that consists of hybrid routes and Hybrid Nodes is tested for optimal hybrid operation by varying the utilization of primary channels.

The study consists of quantitative analyses, where the Hybrid Node is analyzed in three different ways. As shown in Table1, the Hybrid Node is positioned independently (Level 2), within a network (Level 1) and at the switch level (Level 3). Appropriate independent/dependent variables, which may affect the hybrid operation is identified, along with the system constants and assumptions appropriate for each level. Results of the study provide information on the effect of each of the independent variables, on optimal hybrid operation.

1.4.1 MODELING

The study follows four different models, in which each model considers the Hybrid Node from a particular level of detail. In Chapter 3, the source node attached to a hybrid route is modeled as a loss node consisting of GI/M/C primary and overflow queues. Costs of primary and overflow paths are made comparable using the notion of path cost ratio, which gives the total cost of an overflow path to the total cost of a primary path. The total cost of an overflow path takes into account the probabilities of light-path entry in the intermediate hops of the overflow path and the ratio of costs of a path within a node and a link.

In Chapter 4, the Hybrid Node is modeled as a switching node consisting of primary and overflow layers. The primary layer consists of smaller dedicated switches and the overflow layer consists of a single big switch shared by all sources. The primary and overflow switches can be fabricated using any of the common architectures, out of which Benes and Broadcast-select are selected as examples of re-arrangably and wide-sense non-blocking fabrics. In the two layered hybrid switch model, switching elements can also be integrated on a chip. The cost of a hybrid switch is expressed as a function of the basic switching element and the cost of all non-switching operations can be described relative to the cost of the basic switching element.

Chapter 5 considers a network topology, which can be modeled as a graph. The Hybrid Network consists of different graphs, representing the physical topology, primary layer, and the overflow layer. Vertices of each graph represent the Hybrid Nodes and the edges represent the network links. The weight of each link is equal to number of wavelengths in the link. Chapter 5 devises a technique to determine the weight of links in each of the three network graphs. The technique calculates the traffic load of all routes in the links, by taking into account the

possibility of light path entry and loss experienced at the overflow path. Once the link loads are known, the number of overflow channels is calculated and the graphs are updated. The procedure is repeated and the graphs are updated for each value of primary channel utilization, which is assumed to be a constant on all primary channels of the network. Chapter 5 extends the analyses in chapters 3 and 4 to calculate total costs of all routes and all nodes in the network.

1.4.2 ANALYSIS

The Hybrid Node, depending on its level of detail, is analyzed for its optimality. In Chapter 3, the total cost of a hybrid route is obtained for different values of offered access load, Peakedness of access load, the number of access sources and cost ratio of hybrid path.

The total cost of a hybrid route is obtained for values of primary channels per access source, varying from zero to P , where, P is the total number of primary channels if there were absolutely no overflow channels. Once the number of overflow channels is obtained for all values of primary channels, the primary/overflow channel combination that gives the minimum total cost is selected as the one that provides optimal hybrid operation. A parameter called 'overflow gain', which is the slope of the overflow channel curve with respect to the primary channel curve, is analyzed for different values of offered load. The overflow gain relates the traffic load to the path cost ratio of primary/ overflow paths and provides the condition for optimal hybrid operation.

In Chapter 4, the total cost of a Hybrid Node is represented in terms of the cost of a basic switching element used to construct the hybrid switch. The number of basic elements for a hybrid switch made out of Benes, Broadcast-select and Clos architectures, is determined. In addition, for each of the three switching architectures, the degree of switch integration is varied. The sensitivity of total node cost to switching and non-switching costs is analyzed by varying the cost ratios of non-switching elements with respect to the cost of a switching element.

Optimality of a Hybrid Node is studied by measuring a parameter called the 'hybrid advantage' which is the cost saving achieved by a Hybrid Node as opposed to the corresponding non-Hybrid Node. The strength of this hybrid advantage is studied by measuring if some degree of hybrid advantage occurs for all cases of hybrid operation. The hybrid cost advantage is

analyzed for Hybrid Nodes made of different switching fabrics, when offered with different load values.

Table 1.1 Structure of the dissertation, showing the 3 levels of modeling and analysis.

I. Network Level		
Independent variables <ul style="list-style-type: none"> • Primary channel utilization Relative cost of switching to transmission of a channel. 	Constants <ul style="list-style-type: none"> • Overflow Loss rate • Switching arch. • Offered load 	Dependent variables <ul style="list-style-type: none"> • Primary/overflow link loads. • Number of primary /overflow channels /link. • Cost Ratio of hybrid routes • Optimality of Hybrid Network.
	Assumptions <ul style="list-style-type: none"> • Independent access load • Buffer less operation. • Homogenous access load • One access source per Hybrid Node. 	
II. Route Level		
Independent Variables <ul style="list-style-type: none"> • Offered load (mean, variance). • Relative cost of primary and overflow path • Primary channels per source 	Constants <ul style="list-style-type: none"> • Fixed overflow loss probability. 	Dependent Variables <ul style="list-style-type: none"> • Number of overflow channels. • Optimum number of primary and overflow channels. • Total cost of the route.
	Assumptions <ul style="list-style-type: none"> • Homogenous inputs. • General independent arrival, exponential holding. • Probability of lightpath entry and path loss given by path cost ratio. • Cost ratio is independent of primary/overflow channels 	
III. Node Level		
Independent Variables <ul style="list-style-type: none"> • Offered load (mean, variance). • Switching architecture • Ratio of costs of active/passive elements. • Number of input traffic sources. • Number of wavelengths/fiber • Primary channels per source. 	Constants <ul style="list-style-type: none"> • Loss probability. 	Dependent Variables <ul style="list-style-type: none"> • Number of overflow channels. • Optimum number of primary/overflow channels. • Channels dependent cost ratio at point of optimality. • Cost of the optimal node.
	Assumptions <ul style="list-style-type: none"> • Non blocking switching architecture. • Buffer less operation. • Full wavelength conversion. • Cost of transport scales linearly with number of channels. • Cost of switching is a function of number of switching elements. • Homogenous inputs 	

The network level analysis in Chapter 5 consists of determining the primary/overflow channels in each link of the network. An iterative procedure is used to determine the number of primary/overflow channels in all links of the network for a given value of primary channel utilization. The number of primary and overflow links in the network is determined for all links of the network. Once the input and output channels of all nodes in the network are known, the total cost of a node is determined using the procedure developed in Chapter 4. The total cost of each node is obtained for different values of primary channel utilization. The effect of node degree, on total node cost is analyzed for different values of primary channel utilization.

The total cost of a network can also be obtained as the sum of the cost of all routes in the network. The effect of varying primary channel utilization on total cost of the network is analyzed. By varying primary channels utilization, the probability of light-path entry within the routes will vary for each route. The effect of varying primary channel utilization will show up in the path cost ratios of each path and on the average path cost ratio of the entire network. In addition to the primary channel utilization, the ratio of the cost of switching a channel through the node to the cost of a transmitting the channel on a link also affects the cost ratio of the routes. The effect of switching to transmission cost ratio on optimality of hybrid operation is also studied in Chapter 5.

The optimization carried on to determine the number of optimal primary/overflow channels in a link, will be performed numerically using Matlab package. Simulation studies used to validate the queuing models is performed using CSIM simulation package.

1.4.3 REPRESENTING RESULTS

The results of Chapter 3 will consist of a graphical representation of results showing the feasibility of hybrid operation. The results show the total cost of hybrid operation obtained for different values of cost ratios and when subjected to different load condition. The feasibility graphs are provided to routes containing ten and one hundred access sources respectively. Chapter 3 will also provide a table of results comparing the overflow gain for each addition of primary channels, for different values of average load, Peakedness and number of sources.

Results from the table and the graphs will be used to validate an equation that relates overflow gains to path cost ratio and number of sources.

Chapter 4 will provide cost curves for total switching costs and total node costs for different number of primary channels provided to each access source. The cost curves are obtained for different cases of switching architecture, load and relative cost of amplifiers and channel transmission elements. Cost optimality of hybrid operation can be visually inspected from the total cost curves, which also gives sensitivity of hybrid operation to non-switching parameters. In addition to the total cost curves, there are bar charts that represent hybrid cost advantage for each test case.

Chapter 4 will also contain tables that show the slopes of the overflow and primary switch costs for Broadcast and select and Benes architectures. The table will represent the condition for hybrid optimal operation, which depends on incremental values of primary and overflow switch costs. Results from chapter 4, will be used to validate the condition for optimality that relates the incremental cost of overflow and primary layers to the overflow gain

Chapter 5 illustrates an iterative technique to determine the number of primary and overflow channels in all the links, of a given example network topology and offered access load and primary channels utilization. For each value of primary channel utilization, an adjacency matrix of primary and overflow layer graphs are provided. For each set of primary and overflow adjacency matrices, total cost of Hybrid Nodes is calculate. The primary channels utilization that corresponds to minimum total cost is represented as a graph. In the graphs, the x-axis consists of values of primary channels provided to each access source. For a fixed value of primary channel utilization and fixed value of offered load, number of primary channels for each access source is fixed. Chapter 5 also contains a total cost curve represented as the sum of total route cost.

1.5 SIGNIFICANCE OF STUDY

1.5.1 CONCEPTUAL AND THEORETICAL FRAMEWORK

The research study can be broadly classified under the research field of hybrid optical networks. Hybrid optical networks have been classified based the interaction between OCS and OBS/OPS paradigms. The three classifications are *parallel*, *integrated* and *client server* architectures [17]. The benefits of the OCS layer have been previously identified as the ability to optically bypass switching operation by providing a virtual connection between the end nodes. This dissertation quantitatively analyzes the feasibility and optimality of a hybrid OCS/OBS mechanism, by subjecting it to varying traffic parameters, node architectures and network topology.

Much of the motivation for the study comes from the need to match channel demand profiles to channel allocation policies. Historically, attempts have been made to allocate a pool of shared capacity in addition to fixed capacity, for a global TDM based network architecture [5]. Such networks have been called *Capacity Switched Networks* [2]. In the existing literature, all nodes under this architecture access network capacity in the form of time slots and performed electronic switching. This study extends the same idea to a WDM network, where an entire wavelength channel is accessed for duration of an asynchronous, variable length burst and switching is performed all optically. It has to be noted, however, that the TDM based networks with fixed and shared capacity didn't address the impact of alternate switching schemes in the network,; instead the fixed and variably accessed channels were all circuit switched.

The approach used to study a hybrid operation in this dissertation, is based on an overflow mechanism. Overflow channels, in the form of circuit switched channels have been used to carry traffic overload in toll telephone networks [28]. The general concepts of overflow paths and overflow switching come from the literature on alternate path routing. However, alternate path routing generally considers only path diversity, without any form of switching diversity. In this study, we consider a special case of alternate paths, with two different switching schemes. The paths of OBS wavelengths, considered in this dissertation, is a shadow of the paths followed by the OCS network. The figure shown below maps the dissertation among the related

historical, seminal and current research. A more detailed mapping of the dissertation among the existing literature will be provided in Chapter 2.

1.5.2 CONTRIBUTIONS

The basic question in the dissertation study is: how many of OBS and OCS channels result in cost-optimal core networks? The motivation for answering the question lies in the fact that there exists a wide discrepancy in the switching and transportation capabilities of OBS and OCS paradigms, as discussed in the previous sections.

The main contribution of this dissertation is that it proposes a hybrid operation characterized by primary channel overflows and it aims to find the optimum number of primary and overflow channels, in order to minimize the total cost of a network. Optimality of hybrid operation may depend on the method by which we may assess total cost. In the dissertation, total cost of network is calculated by considering the total cost of all routes and the constructional cost of all nodes and links in the network. The two fold approach used in the dissertation to analyze optimality of Hybrid Network operation is not present in the current literature.

Some of the literature on hybrid networks proposes a combination of circuit switching with other switching schemes such as OBS/OPS in order to facilitate the migration of core networks to more complex switching paradigms [22]. In this work, no such migration strategy is formulated; instead it provides a cost optimization mechanism that may serve as one of the decision criteria to aid a migration strategy.

In this research, we consider a particular kind of hybrid network, which is characterized by overflow capability. The optimality problem is solved for a particular kind of stationary hybrid network involving overflow channels. Compared to the literature on hybrid networks, the contribution of this work is to present a mechanism for splitting traffic/capacity into OCS and OBS domains, via the process of overflow. Although the publication by Gauger et.al, has used OBS to carry the overflow traffic, the capability to split channel demand is limited to the edge nodes. This research study provides this traffic splitting capability to all nodes within the network, which includes optical traffic splitting, in core nodes. The feasibility of such an operation in edge and core optical nodes is analyzed in the research.

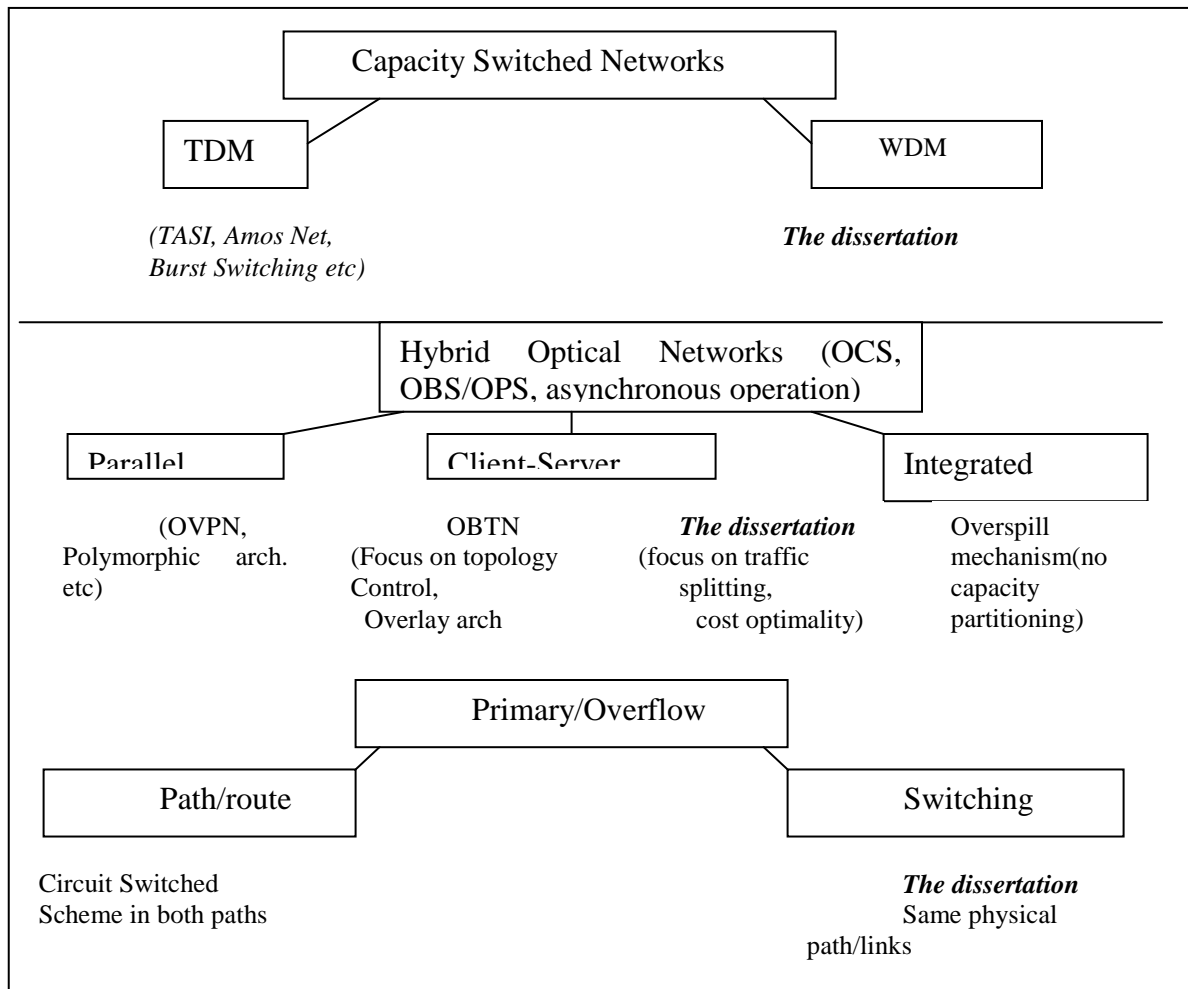


Figure 1.4 Conceptual/theoretical framework.

The dependence of optimal hybrid operation on channel load, switching parameters and network topology is analyzed. The relationship between the optimal number of primary/overflow channels and parameters such as load statistics, nodal cost structure, and network topology is examined in various levels of detail. Hybrid operation is analyzed for general traffic types with known load statistics, instead of the Poisson arrival used in most previous studies.

The dissertation makes use of the overflow theory to perform modeling and analysis of the Hybrid Node [28]. The literature on overflow theory, involving circuit switched primary and overflow channels, is extended to WDM systems with burst switching in overflow channels. Traditionally, overflow channels have been used to provide cost optimal alternate routing for

telephone traffic. The possibility of using an alternate burst switching scheme, in addition to the existing circuit switching scheme, is considered in the dissertation. The overflow path provides channel efficiency for bursty overflow via statistical multiplexing gains. Thus, function of the overflow process is extended to provide an alternate switching scheme in an optimal Hybrid Node.

The general approach to design and analyze an optimal hybrid network is based on partitioning the channels in a link and diversifying the switching techniques in a node/network. In general, the dissertation attempts to answer the larger question of the feasibility of partitioning traffic demand and capacity in to circuit/packet switched channels of core optical networks

In a Hybrid Node, this partitioning of channel capacity also leads to partitioning the switching fabric. This means that in a Hybrid Node, a single large packet switch is partitioned into two smaller modules, primary and overflows switching. Within a primary/overflow switching module, the switching fabric may be constructed using smaller switching modules. In the dissertation, the criteria of partitioning the switching capacity into primary/overflow modules is examined based on their output channels, the number of elementary modules required and cost relationship between switching and transport elements in the node. So far, this is the first known attempt to relate the cost of switching and transport resources, to the optimality of a Hybrid Node.

1.5.3 SCOPE AND LIMITATIONS

The dissertation analyses hybrid OCS/OBS operation by optimizing the hybrid routes and Hybrid Nodes that belong to a hybrid network. Chapter 3 of the dissertation presents design, modeling, and analysis of a hybrid route for cost-optimal operation. Chapter 4 proposes a hybrid switch architecture, which is tested for cost optimality. Chapter 5 provides an adhoc optimization of a hybrid network, by working out an example. The scope and limitations of each chapter are provided below.

- Chapter 3

The operation of a hybrid edge and core node is shown in [Figure 1.2](#). The dotted lines in the figures demarcate the scope of hybrid operation considered in the dissertation. Although Chapter 3 includes a brief description of burst assembly, it just shows that burst formation can affect the load offered to the hybrid layer. An efficient assembly mechanism, which may result in cost optimal hybrid operation is beyond the scope of this dissertation. It is assumed that channel request for optical bursts, arrive to the Hybrid Node as an ON-OFF process that can be represented as a second order hyper exponential process. It is also assumed that channel holding times are exponentially distributed, which may not be the case in real networks. However, the analysis of a Hybrid Node queue, which has both general arrival rates and general holding distributions, can only be approximate and is not considered in the dissertation.

The function of a Hybrid Node is to allocate primary light-paths to channel requests arriving from the access source or from other core nodes. A Hybrid Node will also aggregate the primary channel request overflows, and allocate them to available overflow channels. The process of overflow takes place at the electronic control plane whenever optical burst headers arrive at the Hybrid Node. The control plane will possess all the route information required to transport the burst to the destination node. The control plane doesn't choose among multiple alternative routes, because hybrid routes in the dissertation don't have alternate physical paths. The control plane also doesn't perform any kind of scheduling other than random scheduling of primary/overflow channels. Both alternate route paths and intelligent channel scheduling may help improve performance of the Hybrid Network. However, in the dissertation, the function of the control plane is to read the final destination of the burst header and randomly allot a free primary light path or overflow channels along a fixed route path.

In analyzing the cost of a hybrid route, it is assumed that total cost of route path is equal to the cost of traversing several nodes and links along the route path. The cost of traversing a node is assumed to be the same for all nodes and the cost of traversing a link is assumed to be the same for all links. However, the cost of traversing a node and the cost of passing along a link are not equal. It is assumed that there already exists a method to calculate the cost of passing through a node and a link and that the costs are already given. The dissertation does not provide a method to calculate these costs. The two costs are related by a transmission to switching cost ratio that appears in the path cost ratio.

The optical bursts travelling along overflow channels of a hybrid path will have a certain probability that it will enter a light path on the successive hops toward the destination. The bursts will keep along the overflow channels until it enters a light path and keeps itself in the light path all the way to the destination. A dual to this process of light path entry is the case where bursts belonging to several routes are aggregated onto primary channels and later split into overflow channels at successive hops towards the destination node. The dissertation does not consider the light path entry process as described in the dual problem.

- Hybrid Node

A Hybrid Node contains the necessary hardware required to switch and transmit/receive optical bursts. The switch present in a Hybrid Node contains interconnected switching elements. Cost of the switch greatly depends on number of switching elements present in the node. Number of elements depends on the switch architecture used to fabricate the switch. Other than the switching elements, the node also contains amplifiers to combat switching losses, wavelength converters to resolve channel contention and provide wavelength adaptation and transmitters/receivers for all the channels. Cost of wavelength converters and transmitter/receiver is assumed to grow linearly with number of channels.

In analyzing the cost of Hybrid Node, it is assumed that relative cost of transmission with respect to the cost of switching elements is a quantity that is pre-determined. Total cost of the Hybrid Node is expressed in terms of cost of a switching element, since it is difficult to obtain absolute costs of switching and transmission elements from the vendors.

The Hybrid Node analysis is limited to three non-blocking fabric architectures, namely Benes, Broadcast-Select and Clos. The analysis considers switching elements ranging from 1x1 for Broadcast-Select, 2x2 for Benes and 4x4 for Clos. The load values range from 0.75 Erlangs to 6 Erlangs.

- Hybrid Network

The dissertation provides an adhoc solution for optimality of Hybrid Network. Cost of the network is assumed to depend on the constructional costs, such as cost of switching and transmission elements and on route costs, which depends on cost of channel paths. The

dissertation keeps the two approaches to be unrelated, although in reality both the approaches may be related.

The example network represents a network with varying node degrees and multiple hops between sources and destinations. All access sources provide a fixed load to the core nodes. While calculating total cost of route, it is assumed that cost of traversing all nodes is equal and cost of traversing the links are the same too. While calculating the constructional cost of the network, the nodes are assumed to contain Broadcast-Select switches.

The Hybrid Network performance is limited to a fixed average channel load of primary layer and a fixed channel blocking probability at each hop of the overflow layer. Since the nodes do not contain optical buffers, delay is not a valid performance measure.

1.6 CHAPTER CONCLUSION

In this chapter, the motivation for the research and the approaches used for the research has been outlined. The underlying research problem is identified as an optimality problem for Hybrid Nodes supporting overflow channels. The research problem is approached in a quantitative manner, by considering the variables and situations that may affect the optimal operation of a Hybrid Node. In effect, feasibility of hybrid operation in core nodes is analyzed. The optimality and feasibility of optimal hybrid operation is analyzed at the node, switch and network levels and the dissertation chapters are designed to focus on the three levels. Questions, hypothesis and goals, addressed by each chapter is provided, along with modeling, analysis and expected deliverables. The dissertation is identified for its contribution to the existing literature on optical Hybrid Networks and overflow theory. Scope and limitations of the research has also been provided, that may clearly mark the bounds, within which the study is based.

2.0 LITERATURE REVIEW

In this chapter, literature closely associated with the dissertation problem and approach is reviewed and summarized. The past and current state of knowledge about this topic is discussed and the need for the proposed study is identified with respect to the existing literature on the topic. Past studies on the concept of TDM-based capacity switching and emerging studies on WDM hybrid switching will be covered in this chapter. The bulk of the review will focus on capacity switching schemes, termed *Hybrid Networks* in the current literature, on WDM networks. An explanation of key methods used in overflow traffic analysis is also provided since overflow theory will be extensively used throughout the dissertation.

2.1 FACILITY SWITCHING IN CORE NETWORKS

Historically, attempts were made to combine static and dynamic channel allocation/access schemes in Time Division Multiplexed (TDM) systems. Prior to the advent of WDM networks, core networks were typically TDM-based fiber channels. Hence, most of the research efforts were based on enhancing the capabilities of traditional circuit-switched TDM channels by enabling dynamic/shared access to an additional/spare pool of channels.

2.1.1 CHANNEL ACCESS SCHEMES

Access to a core network channel by an edge traffic source can be classified into *static* or *statistical* access schemes. The channels can be accessed in the form of fixed/variable number of timeslots, or single/multiple wavelengths. The traffic entity provided by the traffic source, for a single event of channel access, can be fixed/variable length packets, framed packets (bursts), flows or calls/connections. A channel is accessed by the traffic entity for a holding time that depends on the duration of the traffic entity and the channel rate.

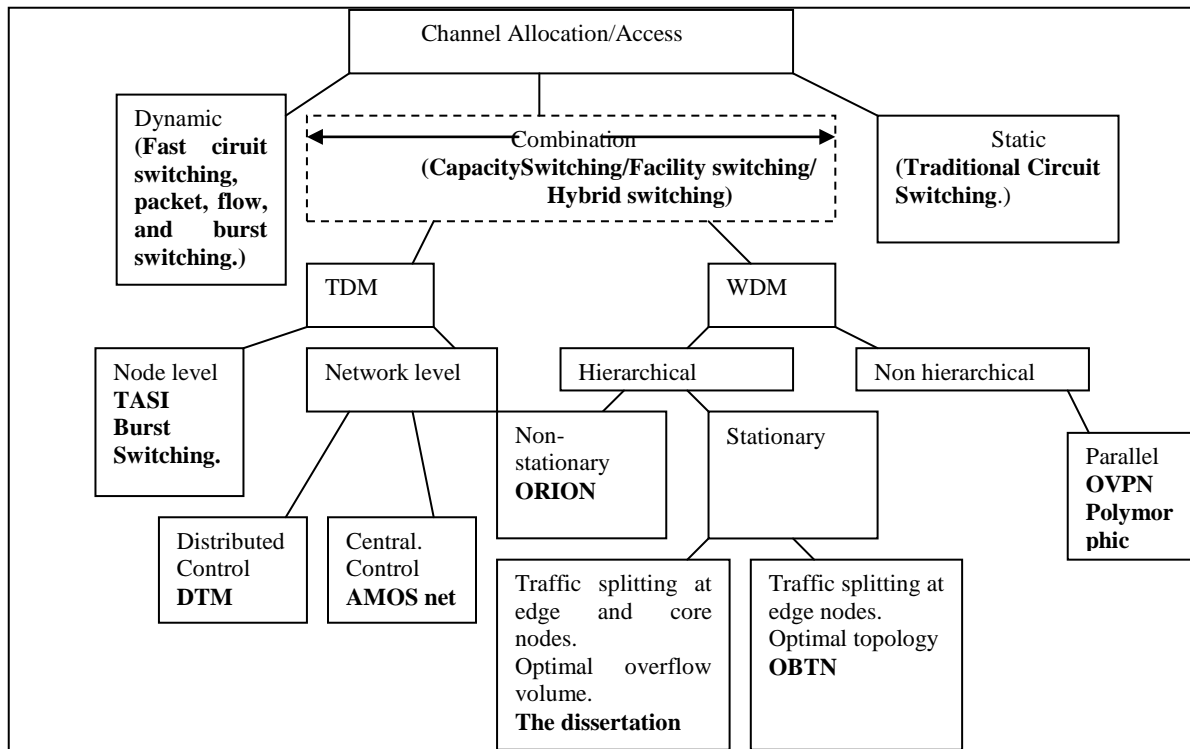


Figure 2.1 A Literature review map of switching techniques.

An edge traffic source's access to the core network channels can be classified as either *static* or *dynamic* in nature. Dynamic access can also be called *statistical access* to better reflect the statistical nature of edge-traffic demand. In a statistical channel access scheme, a given set of channel is accessed by the traffic source with a probability dependent on the arrival of the traffic entity. Once again, the traffic entity can be a packet (IP, ATM etc), a framed packet (burst), a long flow or a call (voice). In contrast to dynamic access, static access restricts channel

availability to a traffic source. One, or a group of, outgoing channel(s) are exclusively ‘reserved’ for access by a traffic source and channels allocated to a particular traffic source cannot be accessed by any other traffic sources. This is unlike dynamic/statistical access where there is usually statistical sharing of available channels.

Examples of dynamic access schemes are packet, burst, and flow switching schemes where there is statistical sharing of a given set of channels by several traffic sources. In addition to these switching schemes, there can be fast circuit switching schemes, where end to end circuits are created or destroyed as per demand. Such schemes are typically used for protection switching or during events such as congestion or demand overloads.

2.1.2 CAPACITY AND FACILITY SWITCHING

Additional core channels may be required by an edge node in events such as link failure, temporary overloads etc. Protection switching may be invoked by the edge and core node by re-configuring the existing channels to transport the edge traffic. It is not just during contingency situations, but also during routine traffic peaks hours, capacity that can be added to existing statically allocated channels. Since, peak hour’s demand can be predetermined; the core nodes can be pre-configured to provision additional channels between a pair of nodes. Such a scheme is circuit switched at the core and fast provisioned at the physical layer on a regular schedule.

A capacity switched scheme is an extension of fast provisioning, where capacity is reallocated at the physical layer in a statistical manner. A combination of circuit and packet switching scheme has been identified by Thompson, as a possibility to implement capacity switching in core networks [\[1\]](#). Capacity switching does not try to bring circuit and packet switching schemes under an “integrated paradigm”; rather it tries to carry circuit and packet switched signals over an “integrated set of facilities”. Thompson also identifies a spectrum of switching paradigms that considers capacity switching, protection switching and fast provisioning under the general scheme of “facility switching”. Facility switching is the scheme that supports static and dynamic or quasi-dynamic channel access over an integrated set of facilities. Capacity switching is the term used to describe the kind of facility switching where channel access is relatively more dynamic /statistical in nature.

2.1.3 FACILITY SWITCHING ON TDM CHANNELS

Historically, facility switching schemes began as enhanced circuit-switched schemes. Facility switching can be performed on TDM networks by reallocating channel time slots available to a traffic source. A traffic source is assigned a fixed set of time-slots, to which they have exclusive access. Additionally, there are latent time-slots that can be shared by traffic sources, either periodically or statistically.

Fast circuit switching was proposed for use in telephone systems way back in the 1980s [2]. A fast circuit switched telephone network allocates a circuit-switched channel to users only when they are actively transmitting any information and makes use of channel idle time to accommodate more calls. Fast circuit switching relies on more intelligent and faster signaling than traditional circuit switching. Fast circuit switching can be enabled for interactive data applications while traditional circuit switching applies to bulk data and voice applications. This means that the decision between fast and traditional circuit switching depends on the gap between the interactive messages. The switchover between methods would be a function of the size of the interactive message, the transmission rate, and implementation costs.

Time Assigned Speech Interpolation is an example of fast/enhanced circuit switching used for voice and data applications [3]. The dynamic synchronous architecture, DTM, is yet another fast circuit-switching architecture with dynamic resource allocation capability [4]. Channels of DTM are made of time-slots and each source can possess any number of slots based on its requirements. DTM also supports multicasting by defining a channel as a set of time slots between a sender and an arbitrary number of receivers. During system start up, the nodes are allocated time-slots in some pre-determined fashion and it can be said that nodes 'own' these time-slots. In order to reallocate time-slots, a distributed control system is used to distribute a pool of available time slots among the nodes. Upon receiving a request for bandwidth, a node first looks into its local pool of time slots and sends a connection request to the next hop. If a node cannot find any time slots in its local pool, it requests free time slots from other nodes. Each node contains updated information on time slots available to other nodes. A distributed scheme of using local pool of time slots to set up a channel provides a relatively faster and more adaptable response to varying demands, compared to using a central pool of time slots. However,

the disadvantage of a distributed scheme lies in the high signaling overhead to maintain neighboring node information, compared to a centralized scheme.

A nation-wide TDM based photonic network was proposed by Amos Joel [5] [2]. A centralized scheme allows for certain time-slots to be permanently reserved for communication between certain pre determined pairs of nodes. Other than these reserved time-slots, there exists a pool of latent time slots that can be used by the nodes when required. The latent time slots may be assigned by making arrangements with the neighboring nodes. The simplicity of this scheme lays in the fixed time pre assigned time- slots between pairs of nodes, which means the TDM switch doesn't need to be reconfigured frequently. The scheme is also flexible by allowing the latent time-slots to be shared by the nodes.

It can be seen from the above examples that facility switching schemes for TDM channels does not involve multiple switching schemes, as in Hybrid Networks. Rather, in all the examples discussed above, static circuit switching is enhanced by dynamic set up or teardown of channels. This is an important difference compared to hybrid switching schemes proposed for WDM channels. In a hybrid switching scheme, there may exist two or more alternative switching schemes, which may complement each other's capabilities. For instance, the traffic intensity based alternate routing for WDM networks, proposed by Lin. et.al, propose alternate paths of circuit-switched channels [65]. This scheme is not a Hybrid Switched scheme because it uses circuit-switching (fast circuit switching) in alternate paths. In fact, most hybrid switching schemes proposed for WDM networks are a combination of circuit and packet switching schemes, which is very much the idea of capacity switching. Hybrid switching, as mentioned in the existing literature, can be termed as special kind of capacity switching scheme applicable to WDM networks.

2.2 HYBRID SWITCHING SCHEMES IN WDM NETWORKS

The proliferation of data traffic in the access layer led to the need for high capacity transport in the core networks. Wavelength division multiplexing is a scalable solution currently deployed in the core network, to provide cheap bulk carrying capacity for the ever growing access traffic.

Currently, the core network traffic is circuit-switched, where a circuit consists of concatenated wavelengths that are pre-configured between a pair of edge nodes. Research initiatives may be taken to provide on all optical core switching capability that is dynamic in nature. Dynamic light paths, optical burst switching, and optical packet switching are some examples of schemes that support the dynamic/statistical access of core network wavelengths.

Unlike a statically-provisioned light-path, dynamic schemes do not nail-down wavelengths between a pair of nodes. Dynamic schemes treat wavelengths as fluid entities that can be switched among traffic sources as per demand. Although dynamic schemes provide flexibility to core networks, they nevertheless introduce additional complexities compared to static schemes. Partly due to the immaturity of high speed photonic devices and partly due to uncertainty regarding the applications and bandwidth demands, a hybrid approach is considered for core networks. Most of the existing literature on this topic combines OCS and OPS/OBS schemes in different ways. In this section, different optical switching schemes, including hybrid schemes will be reviewed in sufficient detail.

2.2.1 CIRCUIT SWITCHING IN WDM

The basic component of a WDM core network is the circuit-switched light-path. A light-path is an end-to-end path set up by concatenating wavelengths at each intermediate node of the path. The light paths are circuit switched channels that are dedicated to a pair of source-destination nodes. The intermediate nodes in a light-path serve to switch wavelengths/fibers either statically or dynamically. Optical patch panels are used to perform static switching and either reconfigurable optical add-drop multiplexers (ROADMs) or optical cross connects (OXC) are used for dynamic switching [7]. Using OXC or ROADMs, light-paths can be dynamically set up, or torn down, depending on traffic demands. Such optical circuit switched WDM network, is also called wavelength switched network. In a wavelength switched network, wavelength converters may also be needed if the light path has to maintain continuity of multiple wavelengths [7][8].

Once a light path is set up, the traffic on the light-path does not undergo further processing, which maintains switching simplicity and the scalability attributed to the circuited-

switched paradigm. [Figure 2.2](#) shows two light paths of wavelengths λ_1 and λ_2 set up within the core optical network. The light paths are created between the client access networks, which in [Figure 2.2](#) are the IP networks. The light-paths and the optical cross connects are transparent to the traffic unit they carry. In [Figure 2.2](#), filling the transport wavelengths the light-path carries IP packets and packet switching is performed only at the edge nodes of the IP network.

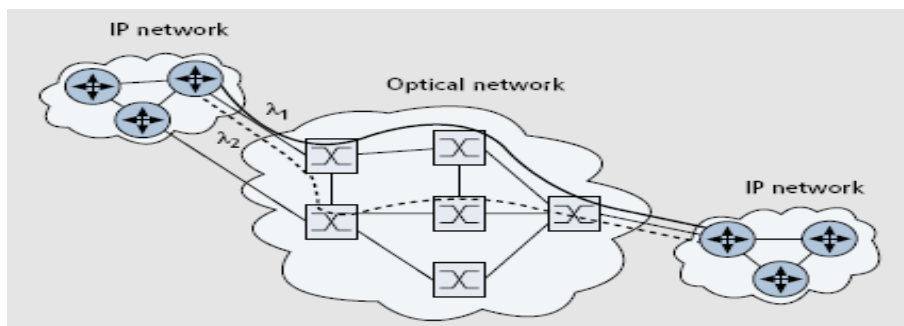


Figure 2.2 Light paths in an optical circuit switched network, with IP access layer [19]

Light-paths can be set up statically or dynamically within the core network. Routing and Wavelength Assignment (RAW) are important tasks to be performed while setting up a light-path, [\[65\]](#). Dynamic wavelength switched networks enable automated provisioning of light paths and capacity adaptation in the optical core network. They also provide shared protection paths in case of failure situations.

Wavelength switched networks can support client traffic of multiple granularities by transporting different services along different light paths. In carrying client traffic of a smaller granularity than an entire wavelength, the wavelength needs to be packed for transport efficiency. Such a process of packing wavelengths is termed grooming [\[63\]](#). Grooming is performed electronically at the edge nodes, using SONET/SDH or MPLS standards. Although grooming allows efficient use of wavelength capacity, it introduces additional layers between the client traffic (for instance IP) and the WDM transport layers.

404"OPTICAL PACKET/BURST SWITCHING

Due to the coarse granularity of circuit switched wavelengths, the access layer traffic needs to be aggregated and statistically multiplexed onto WDM channels. This makes the architecture of a core network layered as IP/SONET/WDM or MPLS/ WDM etc. Typically the aggregation and multiplexing is performed electronically and such schemes have scalability problems as the channel rate increases [1] [8]. In order to overcome the scalability problem, optical aggregation/statistical multiplexing schemes have been proposed [12]. Optical packet switching was initially proposed for IP/WDM, by removing all intermediate layers [64]. OPS, however, requires fast packet switches that can reconfigure in nanoseconds. Due to slow switching rates (ns) of optical switches or due to the inability to integrate switching elements in a cost effective manner, OPS switching has not been commercially implemented.

OPS is also constrained by lack of efficient optical processors and optical buffers [10][12]. Dynamic channel allocation, which comes naturally to packet switches, is highly dependent on fast processors and efficient buffers. All optical buffers can only be implemented using fiber delay lines. Fiber delay lines (FDL) of various graduated lengths may be used to produce delay if there is a contention for wavelengths. Yet another option to provide contention resolution in OPS is to use wavelength converters [6]. Even though wavelength conversion provides an efficient mechanism for contention resolution, they are more expensive than FDLs.

In order to overcome the constraints posed by switching, processing and buffering devices in OPS, Optical burst switching (OBS) has been proposed [15][16]. While OPS switches every packet, OBS does so for a train of packets called bursts. Burst switching times may range from milliseconds to seconds and MEMS based switching devices can easily support these switching rates. Also, MEMS devices can be integrated into large port count switches. OBS also simplifies header processing by doing it electronically and transmitting the header in a different channel than the bursts. The header is sent shortly before the bursts are sent, in order to reserve the switching resources, prior to the burst arrival. Both the offset duration and the burst length may be optimized for maximum through put.

OBS has some features common to circuit and packet switching. While OBS provides statistical multiplexing gains and dynamic channel allocation, it also uses reservation and out of band signaling mechanisms that are similar to circuit-switching. It is also assumed that

contention resolution is obtained by reserving resources prior to the burst's arrival at the switch. Contention of bursts may still be a problem at heavy loads, in which case huge buffers may be required.

OBS may be asynchronous or time synchronized. A time synchronous OBS will synchronize the arrival of each burst at the switch and it is seen that synchronization enables use of re-arrangably non-fabric that requires lesser cross points [\[54\]\[55\]](#).

2.3 HYBRID NETWORKS

The literature of Hybrid Networks classifies optical Hybrid Networks into client-server, parallel, and integrated schemes based on the method of interaction between the two alternative switching schemes [\[17\]](#). This literature review uses a different approach to classify the Hybrid Networks, one based on the hierarchy among the circuit and packet/burst switched paradigms, as shown in [Figure 2.1](#). In a non-hierarchical paradigm, the switching schemes do not directly interact with each other. A non-hierarchical scheme is referred to as parallel scheme in the literature. In such a scheme the edge traffic is usually partitioned based on its performance requirements. This kind of traffic partitioning, is different from a hierarchical scheme, where the traffic is partitioned based on its capacity requirements in a strictly hierarchical manner. The hierarchical scheme is characterized by a traffic overload situation, in which the packet/burst switched (or an alternative scheme) is allowed to carry the overload. Yet another approach of conceiving the hierarchical approach is to, consider the circuit switched layer as providing a virtual point to point topology for the burst/packet switched layer. Such an approach is also called a client-server approach, where the "client" OBS layer, requests a virtual topology from the "server" OCS layer [\[18\]](#). In this section, some of the current and emerging literature on optical Hybrid Networks is discussed.

2068 NON-HIERARCHICAL, PARALLEL SCHEMES

In a parallel hybrid switching scheme, packet and circuit switched channels exist in parallel, serving different kinds of traffic, in order to meet their respective performance goals [17][18]. For instance, services requiring deterministic service guarantees can use the circuit switched channels and those requiring best effort service can use separate packet switched channels. Such services create separate circuit/packet switched logical networks based on the service requirements. The edge nodes segregate traffic into circuit/packet switched networks based on the traffic bandwidth requirement, grade of service etc. Parallel circuit/packet switched networks may involve greater degree of interaction if they are set dynamically based on changing traffic pattern. In such a case, the hybrid switches may need to support circuit/packet switching capabilities for all available channels and the switches need to be flexible enough to be able to function in circuit/packet mode.

In most of the parallel schemes, the edge node selects the appropriate transport method. For instance, an IP packet can be transported as an optical byte stream along a permanent or dynamic light-path or as packets (or bursts), along the same or different paths. There are also parallel schemes where it is not the edge node, but the user, who selects the appropriate switching scheme [21]. In CHEETAH, an end user can select among a primary SONET/SDH path or a secondary TCP/IP path.

In addition to meeting various performance goals of different traffic types, the multi service architecture also aids migration of core networks into more sophisticated schemes [22]. For instance, in the Polymorphic architecture, different kinds of switching schemes may exist at different times, depending on the evolution of complex switching schemes such as OBS and OPS etc.

While this sharing of network channels by different switching schemes provides resource efficiency, it may also call for a unified control plane to facilitate network operation. In order to do so, the details of all the technologies need to be considered and the process itself may take much time and effort. The time and effort may become a more crucial issue if the constantly changing switching technology may introduce newer schemes into the core network. As is the case with most Hybrid Networks there is a clear tradeoff between resource sharing and realization complexity.

4.5.1 HIERARCHICAL SCHEMES

A hierarchical scheme is characterized by a distinct hierarchy between the operations of the circuit and packet/burst switching schemes. The hierarchy causes the traffic to be split into primary and alternative switching schemes. The primary switching scheme is usually a circuit switched scheme and the alternative packet/burst switched scheme is accessed during an overload at the primary level. The hierarchy also causes the wavelengths in a link to be partitioned between circuit and packet/burst mode operation, at any instance of time. Although a link's wavelengths are partitioned, they are not independent of each other. The switching operations on the partitioned wavelengths are bound to each other by the overflow process. This kind of hierarchical relationship between the primary and alternative switching schemes makes hierarchical schemes different from the parallel schemes. Although the concept of hierarchical operation, characterized by the event of overflow, has not been explicitly categorized in the literature, several papers have alluded to this concept in different ways. In this section, such papers will be identified and compared among each other.

Hierarchical schemes can be further classified into stationary and non-stationary methods. In a stationary approach, the number of partitioned wavelengths available for circuit and packet/burst switched operations are relatively static in nature. In a non-stationary approach, a wavelength can operate in circuit or packet switched mode, depending on the traffic conditions. In such schemes, the proportion of wavelengths that carry circuit and packet switched traffic vary with time.

2.3.2.1 NON-STATIONARY, HIERARCHICAL AND INTEGRATED SCHEMES

In a non-stationary approach, the wavelengths operate in circuit or packet switched mode depending on overload conditions. Such a hybrid operation is also classified under the name of Integrated Hybrid Operation in the existing literature because the wavelengths that support hybrid operation are enabled to function in circuit and packet switched modes depending on the traffic loads. Thus, a wavelength may be accessed by, both, the packet and circuit switched components of an integrated switch. In the ORION and 'OpiMigua' project, an integrated network is made of nodes that can set up dynamic circuit switched light-paths and perform packet switching at the same time [23][24]. If a certain light path is overloaded with traffic,

additional packet switched paths are accessed to carry the overload. Packet switched paths are created from idle light paths, by inserting marked ‘overspill’ packets onto these light paths. The light path is said to function in ‘overspill’ mode for the duration it carries the over-spilled packets. The ‘over-spill’ packets are switched at every hop of the path, unlike the primary light-path accessed by the non-overspill packets.

The ORION project provides the router architecture and routing policies that may influence the network performance. Cases of constrained and unconstrained routing policies are considered, along with cases where the ‘overspill’ packets enter or do not enter a light path along its path. Performance evaluation of utilization, delay, and packet loss has been performed for examples of non-stationary IP traffic. It can be seen that the ORION can absorb temporary overloads, provided sufficient buffering is provided at the nodes.

In case of ORION, the number of packet switched ports is conserved by concentrating the number of incoming packets at the receiving side of the packet switch. It can be seen that the concentration ratio plays an important role in the loss performance of the node. Decreasing the size of the packet switch may impact the dimension of the buffers and the complexity of the routing technique to achieve the same performance. It still is not known how much ORION’s complexity trades off against the size of the packet switch. In other words, whether there exists an optimal size of an ORION packet switch, to achieve a required performance level.

Besides the ORION project, there is also the HOTNET architecture, which can be classified as an integrated architecture [20]. In the case of HOTNET, the time multiplexed OCS and slotted OBS operate on a given set of wavelengths in an integrated manner. The traffic offered to an edge node is classified, based on its flow duration and bandwidth needs and forwarded to an appropriate forwarding queue. The mode of transport for the given traffic stream is selected from the circuit or burst switching schemes. Long flows are wavelength routed, whereas short flows are ‘message’/burst switched. The architecture of HOTNET provides a control structure consisting of resource managers and bandwidth brokers that help assign bandwidth to the traffic sources in real time.

Although HOTNET and ORION are similar with respect each other in their integrated use of wavelengths, HOTNET does not contain any hierarchy between the OCS and OBS schemes. Both the schemes work parallel to each other and the traffic is partitioned based on Qos

requirements, rather than any overload situation. Thus, we can include HOTNET under an integrated scheme but not under a hierarchical scheme.

Both ORION and HOTNET are optical networks, where the OCS paradigms have dynamic light path capabilities. The difference between invoking a new light path and the packet/burst mode operation, depends on the time scale of traffic overload or flow duration, for ORION and HOTNET respectively. Light paths may be set up for larger timescales and packet/burst mode for smaller ones. For a given time scale / time frame, the traffic overload situation can be measured by its statistical variance and mean parameters. It would be a worthwhile study to examine the effect of traffic mean and variance on the number of wavelengths using circuit and packet/burst switched modes. This would provide the relationship between the number of circuit and packet switched channels and the traffic mean and variance at various time scales.

2.3.2.2 STATIONARY, HIERARCHICAL SCHEMES In a stationary hierarchical scheme, the OBS/OPS layer is used to absorb overloads from the OCS scheme. The OCS layer is assumed to consist of static or quasi-static wavelength switched network (WSN) channels. This means, the reconfiguration of OCS channels occur at a very large time scale compared to time scales of end to end delay.

Example of a stationary hierarchical scheme is the Optical burst Switched Transport Network (OBTN) architecture [18]. In an OBTN, burst switched traffic offered by the edge node, is transported over a primary OCS channel or an alternative path of shared OBS channels. The hierarchy proposed in the paper has more levels consisting of OCS channels (no contention resolution), OCS channels with wavelength conversion and then with buffering, alternative channels without and with contention resolution, respectively. OCS channels, without contention resolution gets the highest priority and OBS channels with buffering gets the lowest priority. In case of OBTN, the alternative path is a shadow of the primary physical path.

The OBTN scheme is classified under the client-server approach of Hybrid Networks. The burst switched ‘client’ layer requests a virtual topology service from the ‘server’ OCS layer. The virtual one hop path is created by the OCS layer by optically bypassing the intermediate physical hops. The virtual topology in OBTN can be created using a demand based or path based approach. In the demand based approach, virtual paths are created only if the demand exceeds a

certain threshold. In the path based approach, virtual paths are created only if the number hops exceeds a certain number. The effect of both approaches on the number of OBS switch ports has been studied.

The OBTN, which has both OBS and OCS layers, can be extended to pure OBS and ‘Burst over Circuits’ (BoCs) schemes [18]. In BoCs, the burst traffic is carried to its destination by a circuit switched virtual hop. It has been found that number of OBS switches ports and fiber hops of OBTN lies in between that of OBS and BoCs schemes. Relative to OBS and BoCs, OBTN provides an optimal performance regarding resource usage (switch ports and hops) for intermediate loads. As the load increases, the margin shifts towards BoCs and for smaller loads OBS is favored.

2.4 HYBRID SCHEME WITH OVERFLOW CHANNELS

The hybrid scheme presented in this dissertation can be classified as a stationary hierarchical approach. There exists a clearly defined hierarchy between the primary circuit switched and alternative packet/burst switched layer. The two layers are connected through the overflow process. In this respect the proposed approach is more or less similar to the OBTN. However, the proposed Hybrid Node, because of the optimality condition it has to satisfy, is different from an OBTN core node. The number of primary and overflow channels for a given traffic load, performance, and cost should satisfy the optimality condition. Although OBTN does relate traffic load to the number of switch ports and fiber hops, it does not explicitly state that the demand or path threshold used to dimension the links should be optimal. Thus, it needs to be shown quantitatively that a hybrid link is more beneficial than purely OCS or OBS links.

The dimensioning procedure used in this dissertation is different from the one used in OBTN. In OBTN the offered traffic is split in a certain arbitrary ratio between the OCS and OBS layers. The split in demand causes the traffic in OBS to be more bursty than the traffic carried by the OCS layer. The effect of traffic burstiness in the overflow layer is to require more resources (switch ports) for a given loss/delay performance. Thus, overflow theory is used, in order to

determine the dimension of OCS and OBS channels by considering the effect of burstiness in traffic overflow.

The proposed hybrid scheme uses overflow theory to determine the number of overflow channels required for a given size of primary channels. The number of primary channels provides the threshold in this case, which would trigger an overflow into the alternate layer. The optimum threshold is then determined by balancing the switching and transport costs of both layers in the nodes. The optimality is specified as minimum node cost, achieved by balancing the number of primary and overflow channels in the node. In the next section, an overview of overflow theory will be provided.

2.5 OVERFLOW THEORY

A brief introduction of overflow theory is a pre-requisite to understanding the traffic models used in this chapter. In the classical Erlang-B formula, traffic arrival is assumed to be pure chance traffic described by the Poisson distribution. However, in networks that use overflow channels, the overflow traffic is no longer a pure chance traffic. Since classical Erlang B formula cannot accurately calculate the blocking probability for the overflow traffic, a new model for the overflow traffic had to be developed. In principle the study of overflow models can be split into vertical and horizontal methods [\[25\]](#). By vertical studies we can calculate the state probabilities of the overflow system and by horizontal studies, we analyze the distance between the overflow call arrival processes.

2.5.1 STATE PROBABILITIES OF OVERFLOW CHANNELS

The overflow process can be described by the distribution of busy circuits when overflow traffic is offered to a group of servers. Kosten derived the state probabilities when the overflow channels constituted an infinite server group [\[27\]\[28\]](#). The distribution of calls in the overflow channel group is linked to the states in the primary channel group. Thus, in order to consider the

states of an overflow system, we need a two-dimensional approach that considers the primary and overflow channel groups. The state transition diagram of the Kosten system is shown in [Figure 2.3](#). It is assumed in this case, that the traffic offered to the primary group is a Poisson arrival process with mean λ . Brockmeyer extended the state transition diagram to limited channel systems [\[29\]](#). The mean and variance of the busy circuit distribution used to characterize the overflow process, is given by

The mean of the overflow traffic offered to overflow channels, $M = A * E(A, N)$,

where $A = \lambda / \mu$ and $E(A, N)$ is the Erlang blocking probability of the primary channel system with N channels.

The variance of the overflow traffic $V = M \left(1 - M + \frac{A}{(N + 1 - A + M)} \right)$ and the

Peakedness $Z = V / M$, $Z > 1$

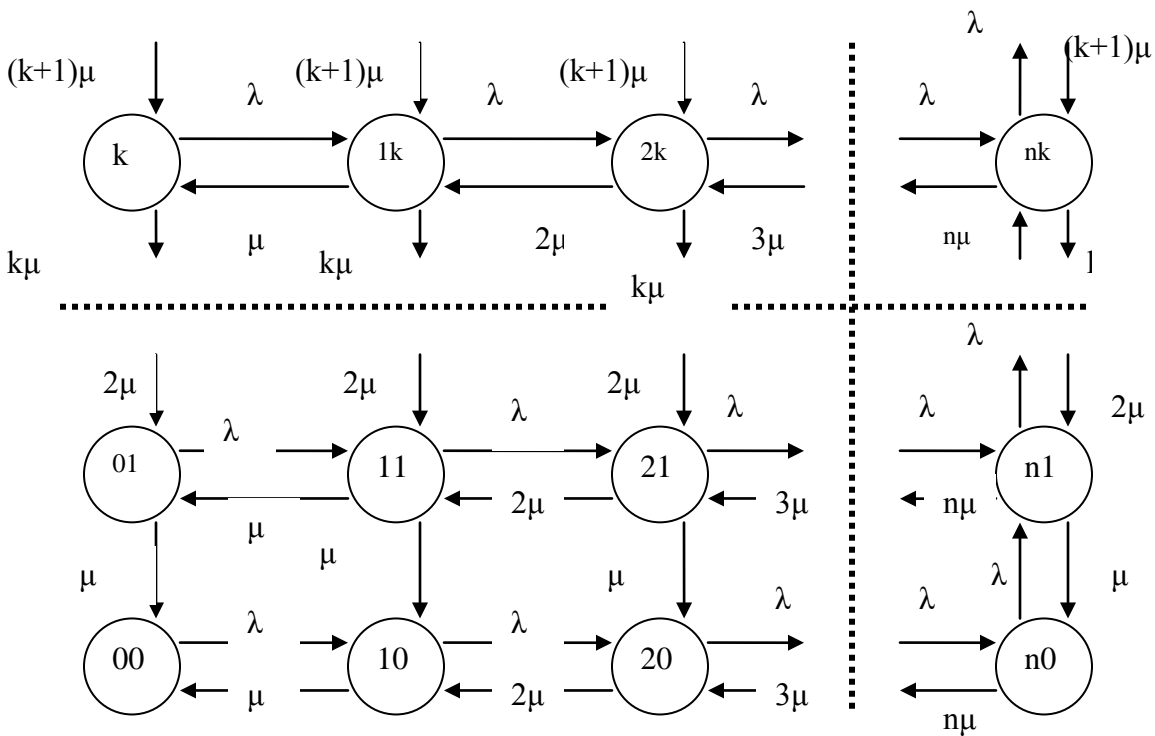


Figure 2.3 State transition diagram for Kosten's system.

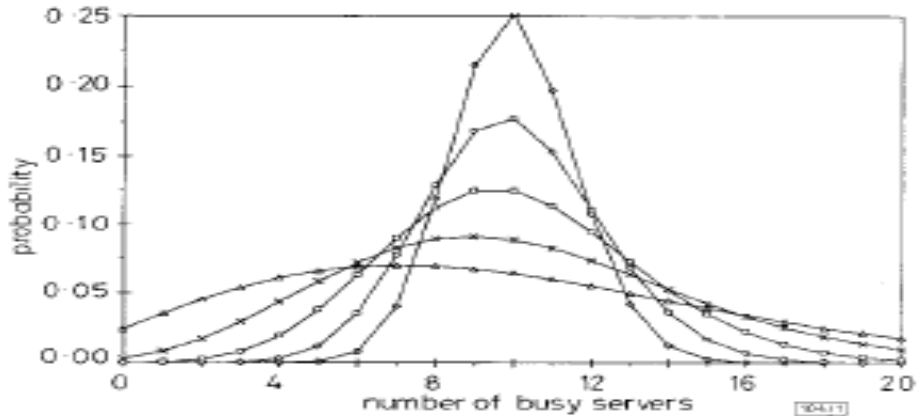


Fig. 1 Generalised erlang distribution where intended traffic is $A_s = 10\text{erl}$, number of servers $n = 20$, number of sources $s = 100$ and peakedness z from 0.25 to 4
 —◇— $z = 0.25$, —○— $z = 0.5$, —□— $z = 1$, —×— $z = 2$, —△— $z = 4$

Figure 2.4 Effect of peakedness on blocking probability [26].

For a peaked traffic, unlike Poisson traffic, the mean number of arrivals during an instance is not equal to its variance. An offered traffic is considered to be peaked or smooth, if its variance is greater or lesser than its mean, respectively. We call the traffic ‘bursty’ or ‘smooth’ if the Peakedness is greater or less than one, respectively. For Poisson traffic, the Peakedness is equal to one. The effect of a peaked traffic compared to a Poisson arrival, is to produce more blocking, when offered to the same number of ‘markovian’ servers. Thus, the basic Erlang formula, that we apply for Poisson traffic needs to be modified /generalized for peaked traffic [26]. One of the effects of peaked traffic is to actually spread the probability of busy server over a wider range compared to Poisson distribution. [Figure 2.4](#) shows the effect of Peakedness on generalized Erlang distribution.

2.5.2 MOMENT MATCHING METHODS

The moment matching method forms the basis of all techniques used in network analysis and synthesis of overflow traffic [37]. The moment matching technique works as follows. The arrival process is represented by a small set of parameters, which are its first two (or at most three) moments. Another process, called the equivalent process, is selected to represent the arrival process. The equivalent process is represented by a set of parameters such that the traffic it

generates has moments similar to the moments of the real arrival process. The equivalent process is then used to compute performance measures of interest such as call congestion, delay etc. The Equivalent Random Transformation and the Interrupted Poisson Process are the two equivalent processes that we use for blocking analysis and simulation of bursty traffic. Both methods use the mean and Peakedness of the offered /overflow traffic to analyze the performance of the primary and overflow channel system.

2.5.2.1 EQUIVALENT RANDOM TRANSFORMATION The Equivalent Random Transformation is the earliest application of the moment matching method [28] [31] [32]. We have already seen in the previous discussion on state transition diagram of overflow process that the overflow is always more peaked than the offered traffic. This overflow model can be used to generate a bursty arrival process by the moment matching method. This is done by assuming the bursty process, with mean M and variance V , is an overflow from a fictitious group of primary channels. The fictitious primary channels are given by parameters A^* and N^* , where A^* represents the equivalent Poisson load and N^* the number of primary channels that produced an overflow with mean M and variance V , as shown in [Figure 2.3](#). From Kosten's model, M and V must satisfy the relation

$$M = A^* E(A^*, N^*) \text{ and } V = M \left(1 - M + \frac{A^*}{(N^* + 1 - A^* + M)} \right) \quad (1)$$

Approximate values of A^* and N^* are given by Rapp [31][32] as

$$\begin{aligned} A^* &\approx V + 3Z(Z - 1) \\ N^* &\approx \frac{A^*(M + Z)}{M + Z - 1} - M - 1 \end{aligned} \quad (2)$$

If the traffic described by M and V are offered to a group of N servers, the resulting overflow M' and V' , can be calculated from the Brockmeyer model given by [Girard]:

$$\begin{aligned} M' &= A^* E(A^*, N + N^*) \\ V' &= M' \left(1 - M' + \frac{A^*}{N + N^* + 1 - A^* + M'} \right) \end{aligned} \quad (3)$$

The Brockemeyer model is similar to Kosten's model shown in [Figure 2.4](#), except that the state space is truncated at N overflow servers (instead of infinite servers).

2.6 INTERRUPTED POISSON PROCESS

In order to model the bursty traffic pattern for our performance analysis, we use the Interrupted Poisson Process. The Interrupted Poisson Process (IPP) is an ON/OFF model that can be described by three parameters; the on-to-off rate γ , the off-to-on rate ω and the arrival rate during on period, λ . The inter arrival time of an IPP stream can be characterized by a second order hyper exponential distribution, H_2 , $A(t)$ given by [32][33];

$$A(t) = k(1 - e^{(-r_1 t)}) + (1 - k)(1 - e^{(-r_2 t)});$$

where,

$$\{r_1, r_2\} = \frac{(\lambda + \gamma + \omega) \pm \sqrt{(\lambda + \omega + \gamma)^2 - 4\lambda\omega}}{2}, \quad (4)$$

and

$$k = \frac{\lambda - r_2}{r_1 - r_2}$$

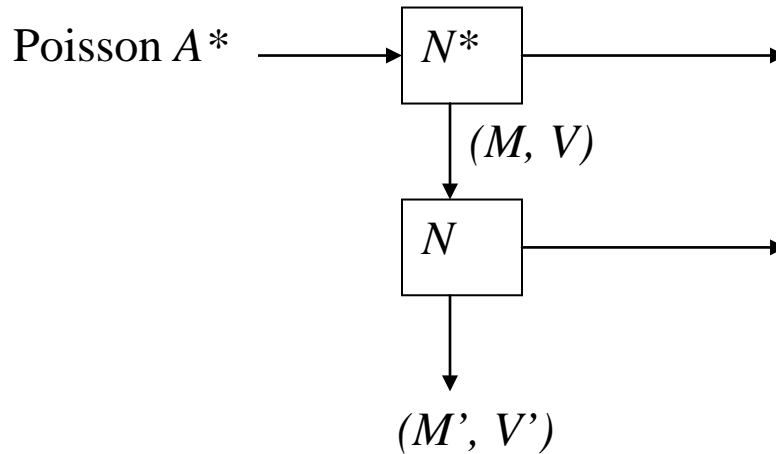


Figure 2.5 Equivalent Random Process.

Mean, M , and Peakedness, Z , of any non-random (bursty) load can be mapped into its corresponding IPP parameters λ , γ and ω , by the 2-moment match method [28].

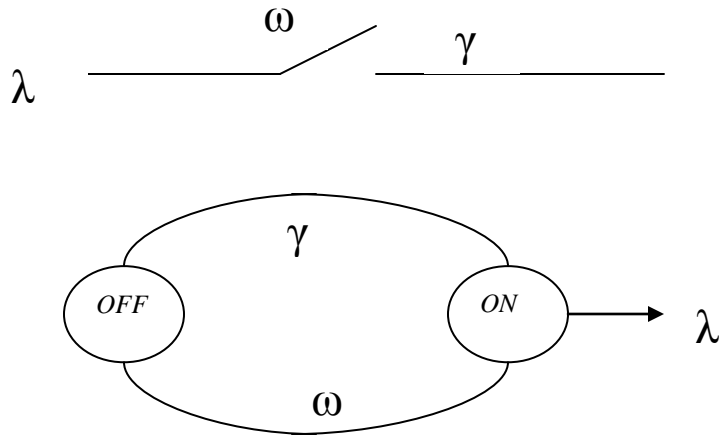


Figure 2.6 Interrupted Poisson Process.

$$\lambda \approx A = MZ + 3Z(Z - 1);$$

$$\gamma = \omega \left(\frac{\lambda}{M} - 1 \right), \omega = \frac{M}{\lambda} \left(\frac{\lambda - M}{Z - 1} - 1 \right). \quad (5)$$

2.7 CONCLUSION

As a part of the literature review, past and current research on capacity switching scheme has been discussed. The literature review provides a classification of capacity switched scheme, which includes the upcoming topic of hybrid optical networks. Some of the current researches on hybrid optical networks that come close to the proposed dissertation topic have been explained in detail. Since the dissertation topic makes extensive use of the overflow concept, a sufficiently detailed explanation of the overflow theory is also provided.

3.0 HYBRID PATH WITH OVERFLOW CHANNELS

3.1 INTRODUCTION

Alternate path routing is typically used in networks to alleviate traffic congestion during busy hours. Fixed hierarchical alternate routing is traditionally used in toll telephone networks to absorb call overflows during peak busy hours [31]. Typically, an alternate path is dynamically shared by several overflowing calls during busy hours. Calls overflow whenever call volume exceeds the carrying capacity of a call's primary path. In hierarchical alternate routing schemes, a primary path does not carry any overflows from other primary paths. Instead it only provides overflows to be carried by the overflow channels. However, in non-hierarchical schemes, the primary path for one traffic source may be the overflow path for another. In both cases, the function of alternate paths is to provide 'path redundancy' to absorb primary channel overflows, as shown in [Figure 3.1](#).

Overflow channels behave like a 'bandwidth-buffer' that is statistically shared by several sources during traffic overloads. Overflow channels are the extra channel capacity, statistically accessed by the sources, whenever their dedicated primary channels cannot keep up with their channel demand. Apparently, the combination of primary and overflow channel usage by a traffic source mirrors the statistical nature of channel demand offered by the traffic source to the core network. Channel demand of a source can be statistically classified into a static average demand, which is stable over a given time, and a variable demand that fluctuates in the same time frame. Intuitively, primary channels can carry the 'relatively static' part of offered traffic, while the overflow channels can be used to meet the capacity demand variation above the primary channel capacity.

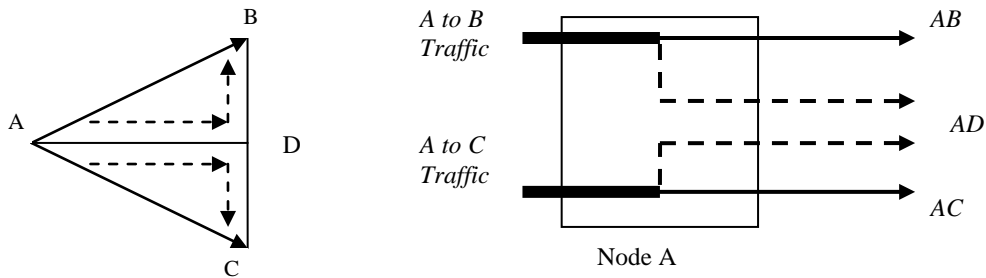


Figure 3.1 Alternate path routing along AD. Path AD carries overflow traffic to destinations B and C.

It is intuitively apparent that static and variable components of the offered traffic load may be related to the number of primary and overflow channels.

Overflow theory, developed over the past decades provides the method to determine the number of overflow channels, once we know how many primary channels are present to carry the source traffic load. However, the question of how many primary channels to provide may depend on factors other than just the traffic demand placed by the source.

Factors that will decide the number of primary/overflow channels available to carry a given traffic demand may depend on several assumptions such as: the core network architecture, performance requirements, the transport mechanism, and the cost structure of the network. The proposed hybrid network architecture consists of a primary layer with OCS light paths and an overflow layer with OBS channels. The performance requirement of interest for the primary layer is the average primary channel utilization and that for the overflow layer is a fixed blocking probability. The transport unit for both primary and overflow channels is the optical burst. The cost structure assumes that an overflow path, due to its rapidly switched paths will require more resource than a similar primary path that bypasses any fast switching at the intermediate hops. The assumptions are explained in detail in sections 3.1 and 3.2

The assumed hybrid network contains several routes that connect the hybrid nodes among themselves. A ‘hybrid route’ is characterized by its source and destination hybrid nodes. Each route consists of a possible ‘hybrid path’ that contains a primary path and an overflow path. The primary and overflow paths are made of several primary and overflow channels, respectively. Thus, a route between any two hybrid nodes may be composed of a different

number of primary and overflow channels. The number of primary and overflow channels in a route may depend on several factors such as: the load offered to the route, the relative cost of the primary and the overflow paths and number of access sources sharing the route. Sections 3.2 and 3.3 will examine the dependency of an optimal hybrid route on all these factors. In addition, section 3.4 will show how the optical burst formation at the edge node can impact the hybrid operation of a route.

3.2 A HYBRID CORE NETWORK ARCHITECTURE

Functionally, the nodes in a core network can be classified as edge and core nodes. The edge nodes aggregate traffic load from low-speed access-layer channels and place it on high speed core channels. For a core WDM network, the high speed channels are made of multiple wavelengths operating at 10 or 40 Gbps. The edge node aggregates low speed access traffic and it packs the high speed links appropriately. Typically, lower speed SONET/SDH streams in the access layer are aggregated into higher speed SONET/SDH streams in the core layer. There is, however, a growing trend in the industry to replace SONET standards with carrier-grade Ethernet at the access layer. Also, optical packet/burst switching concepts have been discussed as a possible method to aggregate and transport edge-traffic in an asynchronous manner. In this dissertation, a core-network architecture based on OBS is proposed.

3.2.1 HYBRID NETWORK ARCHITECTURE

The proposed overflow network is an OBS-based network that will provide end to end paths for the access networks that are connected to it. The existing core network consists of the facility-switched paths that carry both telephone traffic and Internet traffic. The PSTN and the Internet form ‘virtual networks’ that use the same underlying core network infrastructure, as shown in [Figure 3.2](#). Any overflows from the ‘virtual networks’ are absorbed by the proposed overflow network that also uses the same underlying core-network infrastructure.

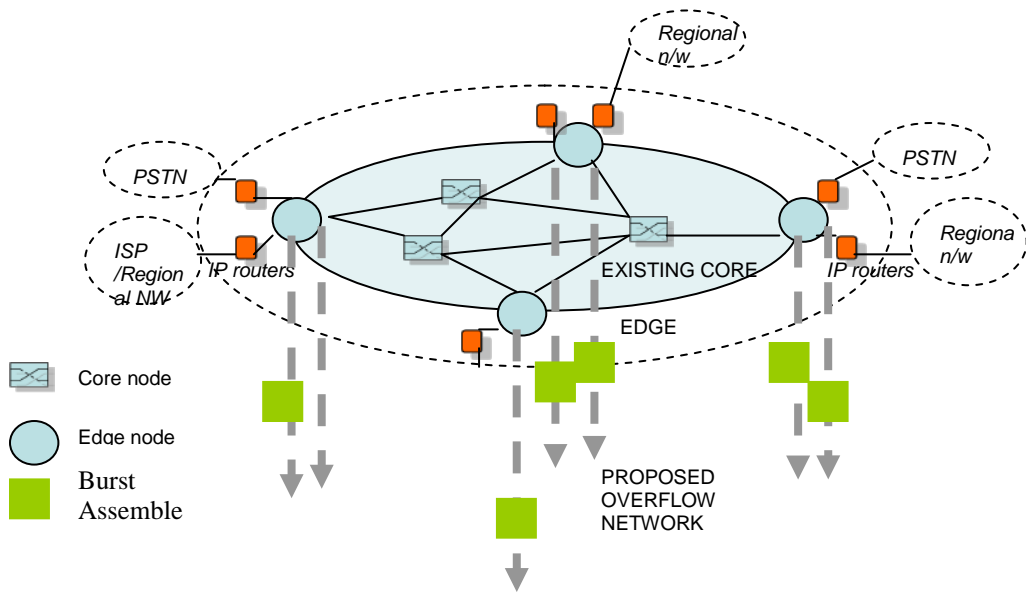


Figure 3.2 The Proposed Overflow Network.

For instance, during overload situations, a gateway router may divert a portion of its incoming packets to the proposed overflow layer. The overflows are assembled into optical bursts and then offered to the proposed network. The proposed network will provide a guaranteed primary light-path for a portion of the offered bursts and a best-effort secondary overflow path, for the remaining offered bursts. The bursts are lost if the proposed network cannot provide either of these paths within the core network. Both, the primary and the secondary overflow paths are fabricated from the same traditional facility-switched infrastructure that is used by the PSTN and the Internet. However, the channels that constitute the primary and the secondary overflow paths are solely used to carry the optical bursts offered to the proposed overflow layer.

The access-core interface to the proposed network handles overflows that occur at edge nodes of each ‘virtual network’. For instance, if the ‘virtual network’ that uses the core network infrastructure is the Internet, then overflow occurs at the gateway routers. Overflows occur when the router cannot send its packets through its facility switched paths without significant performance penalty. During such situations, the router will deflect some or all of its packets to the proposed network. The proposed network will provide an alternate path to the packets.

However, these packets access the alternate overflow paths as optical bursts and burst assembly has to be performed at the access-core interface to the proposed network.

The optical bursts, which carry overflows from several access sources (virtual networks), are aggregated at the nodes of the proposed network. Some of these bursts are provided with a primary path and some of them take the secondary overflow path. The primary path, for which the channel configurations are permanently set up, is facility- switched. It appears that the channels in the primary path 'by-pass' any fast switching operation at the intermediate nodes.

The bursts that enter the secondary overflow channels (shown as vertical dotted lines) are further aggregated with other overflows. If the burst remains on the secondary overflow path throughout its transit to the destination, it will be aggregated with more overflows at each hop.

A burst that enters the overflow path, may attempt to enter a primary path at each hop of its path. If the burst enters a primary path, it will remain in the primary path, all the way, to the destination. For instance, in [Figure 3.3](#) incoming bursts along the overflow channels from Nodes 1 and 2 will enter a primary light-path at Node 4. The figure shows the access-core interface of the proposed overflow network. As an example, in the figure, Nodes 1, 2 and 3 sends bursts to node 6, via Nodes 4 and 5. In Figure 3.3, Nodes 1, 2 and 3 aggregate the incoming overflows and put those on primary and secondary overflow paths that go to edge-node 6.

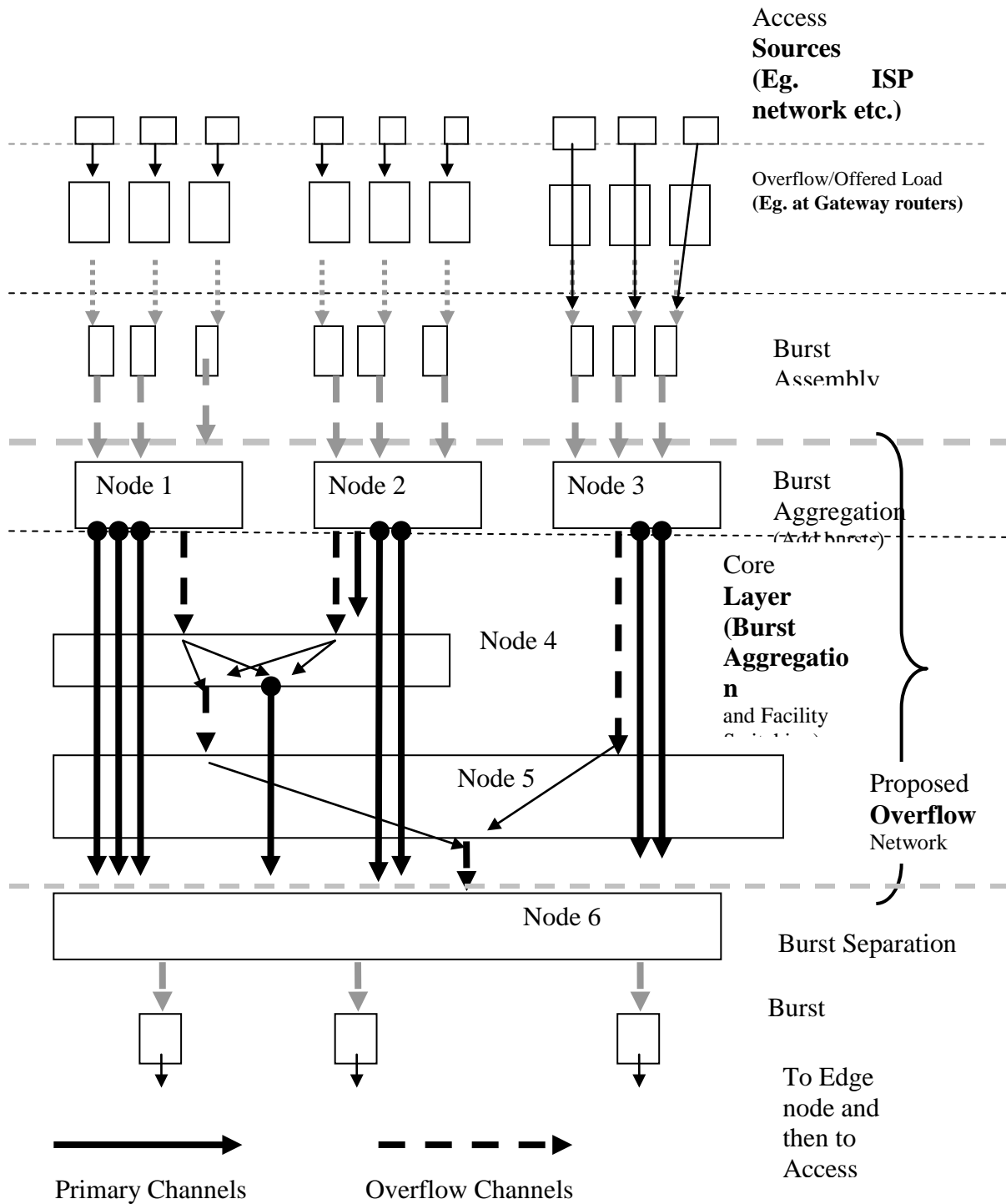


Figure 3.3 The Proposed Overflow Network and its access-core interface

At Nodes 4 and 5, the bursts that appear on the incoming primary channels ‘by-pass’ any aggregation. Bursts along the incoming overflow channels are aggregated and switched using optical burst switches. These bursts are aggregated on outgoing primary and overflow channels. When all bursts reach Node 6 (along different paths), they are segregated and segmented and then sent to appropriate access networks.

All nodes within the proposed overflow network perform both Facility-Switching and optical burst switching. Nodes perform Facility-Switching on incoming primary channels and they forward the bursts arriving via a primary channel, to a fixed output primary channel. Bursts that arrive at a node, via overflow channels can be destined to any of the output channels and thus, Optical-Burst switching is performed for bursts arriving the nodes via overflow channels. In [Figure 3.3](#), the overflow channels are depicted by dotted lines and primary channels by dark lines. Facility switched primary channels are shown as ‘bypassing’ the Optical Burst switching operation and they have a hardwired ‘internal’ path within the Nodes. On the other hand, there is no hardwired ‘internal’ path between an incoming overflow channel and outgoing primary/overflow channels.

3.2.2 HYBRID NODES

All the nodes depicted in the proposed overflow network in [Figure 3.3](#), do not perform the same functions. While Nodes 1, 2 and 3 perform aggregation of bursts formed at the access-core interface, Nodes 4 and 5 aggregate bursts that overflow from nodes 1, 2 and 3. In general, a node in the proposed network may perform some, or all of the functions, as shown in [Figure 3.4](#). The node depicted in [Figure 3.4](#) is called a Hybrid Node because it performs both Facility Switching and Burst Switching, in the same ‘physical’ node.

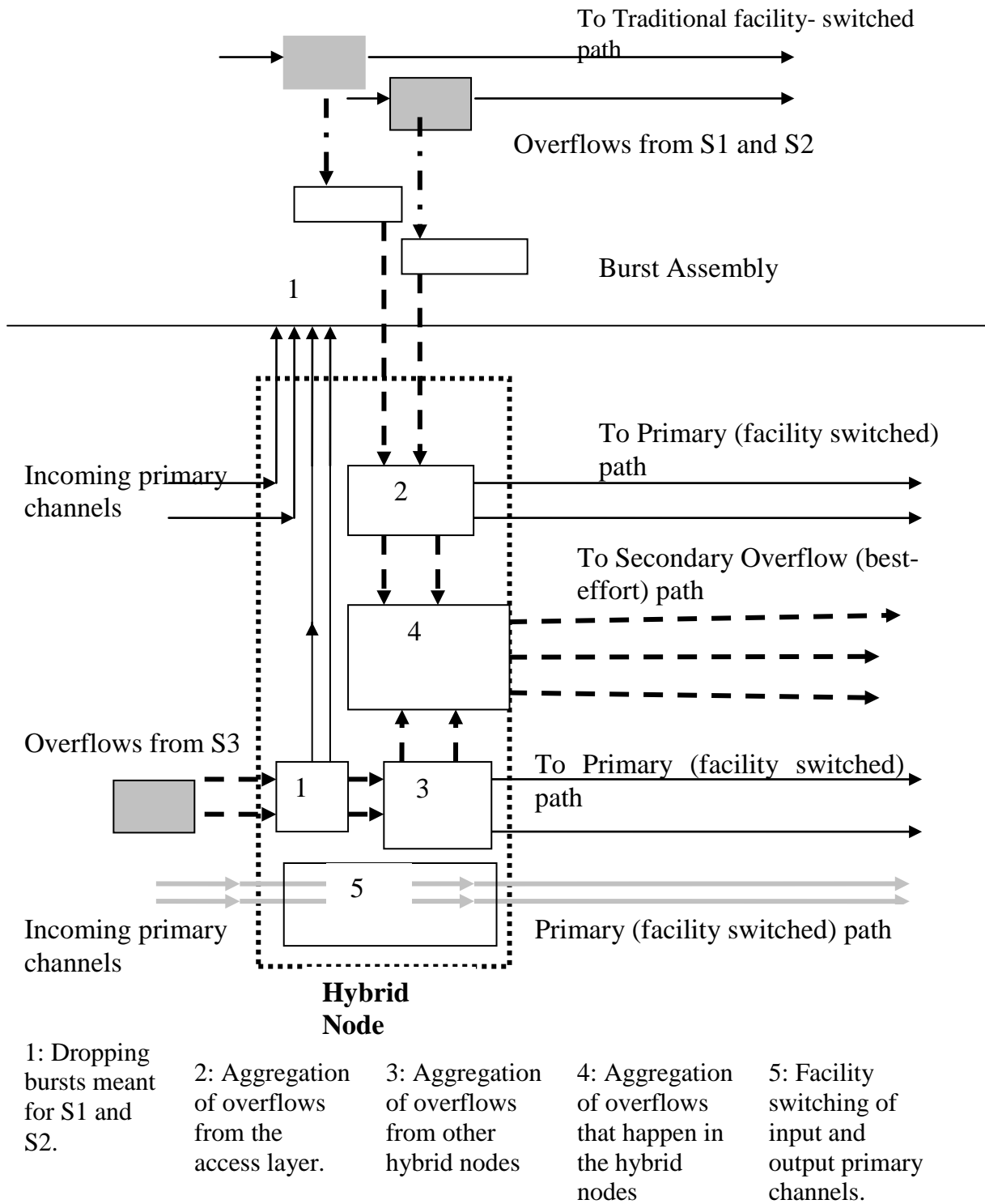


Figure 3.4 A Hybrid Node.

A Hybrid Node may obtain overflows from the access-core interface, or from other Hybrid Nodes in the proposed network. For instance, in [Figure 3.4](#), S1 and S2 may be two gateway routers and S3 may be another Hybrid Node in the proposed network. The Hybrid nodes may have incoming primary channels, which may be the last leg of a primary path and all bursts arriving through this path may have to be dropped at the Hybrid Node. There may also be incoming primary channels that belong to a facility switched, primary path.

The Hybrid Node contains primary and secondary overflow channels as its outputs. The Hybrid Node will place some of the input overflows on the respective outgoing primary channels. For instance, part of the overflows from S1 and S2 are placed to two different sets of primary channels. A portion of the overflow from S3 is placed on a different set of primary channels. Whatever portion of input overflows could not be placed on primary channels, are called 'internal overflows' in the Hybrid Node. The internal overflows are aggregated onto outgoing overflow channels. These outgoing overflow channels will appear as inputs to a subsequent Hybrid Node along the path.

The proposed network, which is made of Hybrid Nodes, will be called the Hybrid Network. The Hybrid Network will contain a primary layer consisting of primary channels and the overflow layer consisting of the secondary overflow channels. The primary layer, which consists of facility-switched light-paths, may operate with certain fixed average channel utilization. The higher the primary-channel utilization, the lower the degree of over-provisioning in the network. In the same vein, under-utilized primary channels implies, too much over-provisioning in the core network. The secondary overflow channels, unlike the primary channels, enable statistical sharing of channels, which results in efficient use of the channels. Since better channel efficiency also results in contention for channels, some degree of burst blocking probability occurs at the secondary overflow layer.

The network architecture shown in [Figure 3.5](#) contains a secondary overflow layer that provides a fixed maximum blocking rate. Over this fixed blocking rate, the core network provides a better burst loss-performance by providing primary channel paths with guaranteed delivery of bursts for part of the offered edge traffic. The primary channels provide service guarantees by increasing the degree of over-provisioning, which occurs by decreasing the degree of channel utilization. The main question that we seek to answer is how many primary channels

can be put in the network, in addition to the secondary overflow channels that provide a fixed maximum blocking rate, in order to achieve an optimal proposed overflow network.

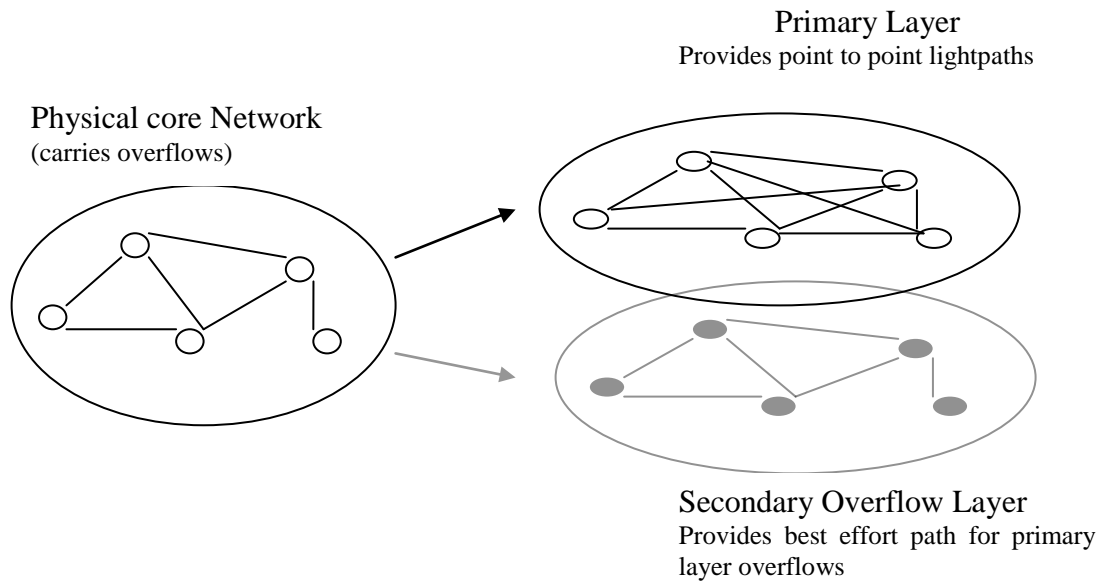


Figure 3.5 The proposed overflow network (Hybrid Network) layers

3.2.3 TRUNCATION OF ARRIVAL PROCESS

We have seen in [Figure 3.3](#) that overflows may occur both, inside and outside the realms of the proposed overflow network. An overflow may occur first, outside the proposed network, which we call “primary overflows”. In [Figure 3.6](#), this overflow occurs, when buffers and channels of system S1, which is outside the realms of the proposed network system S2, allows only part of the offered arrivals to be carried. System S1 may consist of the gateway router, whose output ports and buffer-size limitations may result in primary overflows. The primary overflows are assembled into optical bursts and offered to the primary channels. In [Figure 3.6](#), the primary overflows are carried by the primary channels of system S2. All those optical bursts not carried by the primary channels are offered to the secondary overflow channels of system S2. Throughout the dissertation, the focus is on the design and optimization of system S2. However, it is important to see how systems S2 and S1 may be related and how they may affect the statistics of the arrival processes.

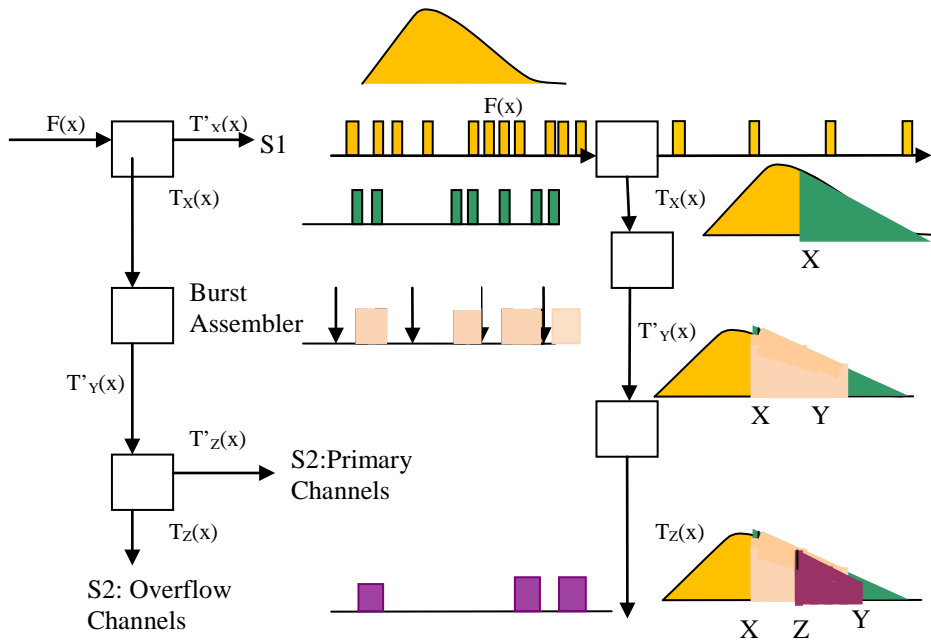


Figure 3.6. Case 1. Truncation of offered arrival process in three steps.

The statistics of the primary and the secondary overflow traffic can be obtained by truncating the arrivals offered to system S1. [Figure 3.6](#) shows an offered traffic arrival process whose probability distribution function, *pdf*, is given as $F(x)$. The arrival process is truncated when a part of the arriving packets are allowed to enter channels corresponding to system S1. The *pdf* of the truncated process that depicts the primary overflow is given as, $T_X(x)$, where system S1 will absorb all arrivals up to X . $T_X(x)$ expressed as a conditional probability, whose numerator is function $F(x)$ and denominator is the cumulative distribution function, *cdf*, for $x > X$. The denominator term scales $F(x)$, so that the value of *cdf* for the truncated function $T_X(x)$ over region $x > X$ is one. $T_X(x)$ contains the tail of the distribution of $F(x)$ and, hence, burstiness of $T_X(x)$ is expected to be greater than that of $F(x)$. The process $T'_X(x)$ that appears at system S1, is relatively smooth, since it contains $F(x)$, but with its tail truncated.

$$T_X(x) = \frac{F(x)}{1 - \sum_{i=0}^x F(i)}; \text{ where } \sum_{j=X}^{\infty} T(j) = 1 \dots \dots \dots (3.1a)$$

$$T'_Y(x) = \frac{T_X(x)}{\sum_{k=X}^Y T_X(k)} = \frac{\frac{F(x)}{1 - \sum_{i=0}^x F(i)}}{\sum_{k=X}^Y \frac{F(k)}{1 - \sum_{i=0}^x F(i)}} = \frac{F(x)}{\sum_{k=X}^Y F(k)}; \text{ where } \sum_{l=X}^Y T'_Y(l) = 1 \dots \dots \dots (3.1b)$$

$$T_Z(x) = \frac{T'_Y(x)}{1 - \sum_{m=X}^Z T'_Y(m)} = \frac{\frac{F(x)}{\sum_{k=X}^Y F(k)}}{1 - \frac{\sum_{m=X}^Z F(m)}{\sum_{k=X}^Y F(k)}} = \frac{F(x)}{\sum_{k=X}^Y F(k) - \sum_{m=X}^Z F(m)}; \text{ where } \sum_{p=X}^Z T_Z(p) = 1 \dots \dots (3.1c)$$

The distribution of $T_X(x)$ is further altered by the burst assembly process. It is known that burst assemblers smooth the incoming traffic arrival process[] . Section 3.6 contains an example that shows the smoothing process. During burst assembly, say by using a timer, all packets that arrive in the time interval T are considered to be part of an optical burst. The next burst is formed when the first overflow packet arrives in the next time interval T. The inter-arrival time of bursts is equal to the inter-arrival time of the packets, plus some deterministic time T. In this way, the burst assembly process ‘smoothes’ the arrival distribution, as it appears to overflow system S2 in [Figure 3.6](#). It can be seen that burst formation, cuts of the ‘head’ portion of the *pdf* of the packet arrival distribution $T_X(x)$. Probability of a burst-arrival is equal to the probability that the first packet arrives in time interval T. All other packets that arrive within time interval T will not be considered as a burst arrival; instead they will be part of the burst formed in the respective time interval. Even if the burst assembly process is not timer-based, but based on a fixed number of packets per burst, similar smoothing of the arrival process is expected to take place.

The distribution $T'_Y(x)$ gives the *pdf* of the arrival process of the optical bursts to the primary channels in system S2. $T'_Y(x)$ is obtained by truncating $T_X(x)$ and considering only the portion between X and Y (including Y). The denominator of $T'_Y(x)$ contains the *cdf* of $T_X(x)$ up to $x = Y$.

The optical burst-arrivals, whose distribution is given by $T'_{Y(x)}$ are further truncated by the primary channels of system S2. This time the tail of $T'_{Y(x)}$ is truncated and offered to the secondary overflow channels. Let's assume that, depending on the number of primary channels, the tail of $T'_{Y(x)}$ gets truncated at $x=Z$. We thus have $T_Z(x)$, which is obtained by scaling $T'_{Y(x)}$ by the *cdf* of $T'_{Y(x)}$ at $x=Y$. Let the offered arrival-process $F(x)$ be truncated successively to obtain $T_X(x)$, $T'_{Y(x)}$ and $T_Z(x)$, respectively. [Figure 3.6](#) depicts *pdf* of $T_X(x)$, $T'_{Y(x)}$ and $T_Z(x)$. We may call such a truncation as “case 1”.

[Figure 3.6](#) depicts Case 1, in which, $T_Z(x)$, which is offered to the secondary overflow channels, is obtained by truncating the tail of the *pdf* of $F(x)$ twice; once by system S1 and then once again by the primary channels of system S2. As an alternative, we may consider Case 2, where primary channels may be removed from system S2, so that it contains only overflow channels. In such a case, system S1 contains only primary channels that may not carry optical bursts. Let system S1, truncate the *pdf* of the arrival $F(x)$ by an amount X' and let $T_{X'}(x)$ be the truncated arrival *pdf*. The truncated arrival is then offered to a burst assembler, which will then, result in a *pdf* $T'_{Y'(x)}$. The truncated arrival $T'_{Y'(x)}$ is offered to the overflow channels of system S2. [Figure 3.7](#) shows the distribution of the arrival process at different stages.

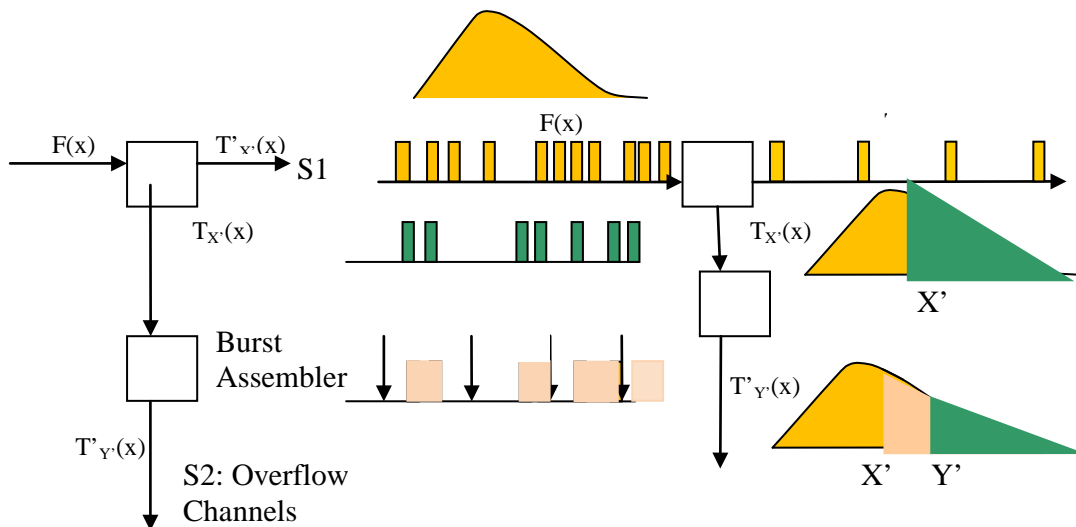


Figure 3.7. Case 2. Truncation at two levels.

$$T_{X'}(x) = \frac{F(x)}{1 - \sum_{i=0}^{X'} F(i)}; \text{ where } \sum_{j=X}^{\infty} T_{X'}(j) = 1 \dots \dots \dots (3.2a)$$

$$T'_{Y'}(x) = \frac{T_{X'}(x)}{\sum_{k=X'}^{Y'} T_X(k)} = \frac{\frac{F(x)}{1 - \sum_{i=0}^{X'} F(i)}}{\frac{\sum_{k=X'}^{Y'} F(k)}{1 - \sum_{i=0}^{X'} F(i)}} = \frac{F(x)}{\sum_{k=X'}^{Y'} F(k)}; \text{ where } \sum_{l=X'}^{Y'} T'_{Y'}(l) = 1 \dots \dots (3.2b)$$

$T'_{Y'}(x) = T_Z(x)$; if

$$\frac{F(x)}{\sum_{k=X'}^{Y'} F(k)} = \frac{F(x)}{\sum_{k=X}^Y F(k) - \sum_{m=X}^Z F(m)}; \text{ or } \dots \dots \dots (3.3a)$$

$$\sum_{k=X'}^{Y'} F(k) = \sum_{k=X}^Y F(k) - \sum_{m=X}^Z F(m) \dots \dots \dots (3.3b)$$

The overflow arrivals offered to the secondary overflow channels in Case 1 and to the overflow channels in Case 2, are equal if the section of $F(x)$, between Z and Y for Case 1 is equal to the section of $F(x)$, between X' and Y' for Case 2. This means, if truncation by the burst assemblers in the two cases is equal, then the double truncation of the tail of $F(x)$ in Case 1 is equal to the single ‘deeper’ truncation of the tail of $F(x)$ in Case2.

Since there is no end to end primary overflow path between any two pairs of nodes for Case 2, the primary path of Case 2 lies exclusively in system S1, and system S2 is used to carry only the overflows using OBS. In Case 1, however, the OBS based system S2, provides primary and secondary paths for overflows from system S1. In addition, system S2 also provides the possibility of primary path entry after the optical bursts take subsequent hops along the secondary overflow channels. In the dissertation, Case 1 is focused upon and Case 2 is represented as a limiting condition of Case 1 when there are no primary paths in the overflow system S2.

In the rest of the document we may focus only on system S2 and we assume that the distribution of optical burst arrival to system S2 is known. Hence, we consider only one truncation, which will result in secondary overflow arrival process. We may call the secondary

overflow channels as overflow channels and the primary overflow channels as the primary channels

3.2.4 PRIMARY AND OVERFLOW CHANNEL MECHANISM

In the proposed architecture, WDM links connected to each Hybrid Node is partitioned into primary and overflow channels. On a given outgoing link, sets of primary light paths are exclusively pre-provisioned between pairs of source and destination Hybrid Nodes to carry bursts belonging to each traffic source, attached to the Hybrid Node. At the same time, a number of wavelengths are dedicated to collect bursts that overflow from the primary channels, which must also be routed along that link. While primary channels are light paths reserved for each traffic sources connecting to specific destinations, overflow channels are shared by all the sources.

[Figure 3.8](#) shows an example of primary and overflow paths for two kinds of traffic sources using the core node. Primary path P1 is reserved for source S1 to send traffic to destination D1, and P2 is similarly reserved between S1 and D2. Source 2 (S2) has a bundle of primary light-paths P3 and P4 going to D1 and D2 respectively. Overflow channels O1 are shared by S1 and S2 and are used to send traffic to D1 and D2. Any burst that is sent along O1 will appear at core node N1, where it will contend with bursts from other overflow channels from other nodes. Assume that a burst from S1, going to D1, appears at N1. The burst will first try to enter a set of primary light-paths P5 that goes to D1 and is reserved for overflow traffic that appears on O1 and goes to D1. It is to be noted that traffic that appears along O1 will contain bursts that belong to source S1 and S2. If the burst finds P5 to be all occupied, it will look for a free overflow channels in O2 that go to node N2, which is on the way to D1. Meanwhile, primary light-paths P5 will cut through N2, without performing any fast switching. The bursts that enter N2 along O2 will once again try to enter a set of primary light-paths P6 reserved for traffic that arrives along O2 and goes to D1.

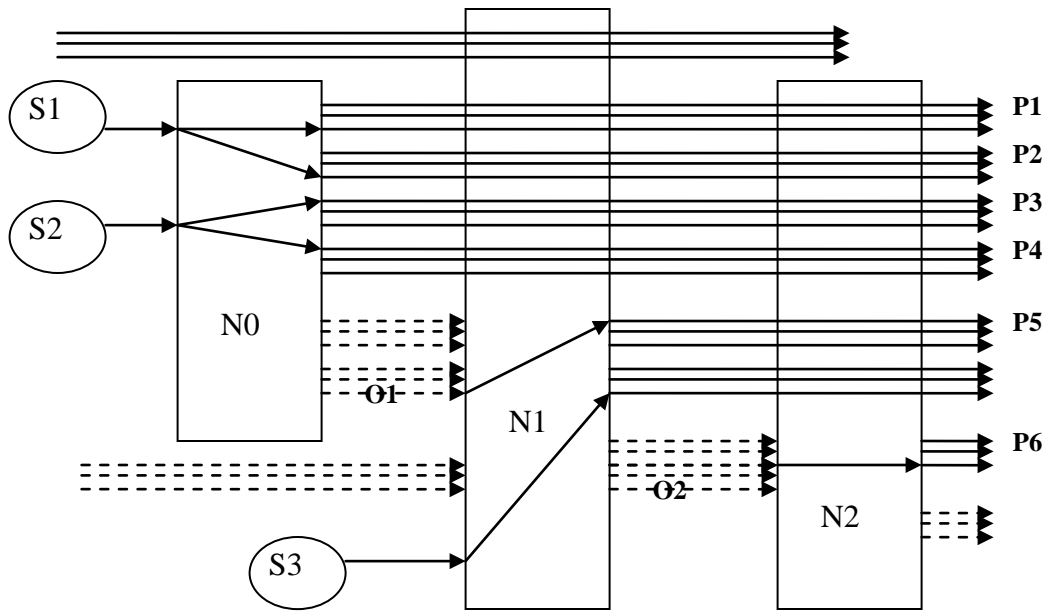


Figure 3.8 Primary and Overflow channels

At each core node, bursts that arrive along the overflow channels will try to enter an appropriately reserved light path. Once the burst enters a light path, it has a guaranteed path to the destination node. If the burst cannot enter a light path, it will contend for the overflow channels. Contention at the overflow channels will result in the loss of some of the bursts that may find all overflow channels to be busy. If a burst is not lost at the overflow channels, it will enter the overflow channels and look to enter a primary light path at the next hybrid core node.

The main entity of the proposed network architecture, which will manage channel allocation for the optical bursts, is the Hybrid Node. The Hybrid Node is an edge node if it accepts incoming optical bursts directly from the access layer. Although an edge node may also perform burst assembly, the scope of the dissertation is limited to the switching and queuing of bursts performed by the nodes. However, a brief explanation of the compatibility of the burst assembly process with the proposed architecture appears in section 3.4. A core node performs no assembly and it merely groups incoming bursts onto primary/overflow channels via switching operation.

3.3 HYBRID NODE

A core node/edge node depicted in [Figure 3.3](#) and [Figure 3.4](#), are Hybrid Nodes because they serve as entry points to a facility (circuit) switched and burst switched path. The Hybrid Node control layer makes a routing decision for an incoming optical burst. Once the control layer decides on the route path for the burst, it will make the decision of placing an optical burst on either a primary or an overflow channel. The probability that an incoming burst takes either a primary, or an overflow channel, depends on the relative amount of primary/overflow channels available in the links. By appropriate dimensioning, the probability of primary/overflow channel availability can be tuned. Once the control layer decides the route path, the switching hardware in the core /edge node will switch the incoming optical bursts into the primary and overflow channel groups.

3.3.1 OVERFLOW PROCESS

The process of overflow takes place prior to the actual arrival of an optical burst at a core node. [Figure 3.9](#) shows the queuing of burst headers for node N0 in [Figure 3.8](#). A burst header, sent prior to the actual burst, will request an appropriate primary light path through the core node. The control layer of the core node will queue the header based on its incoming link and destination node. If there is a primary light path available to satisfy the request made by the header, the light path is reserved on a first-come first-served basis. The link on which the burst arrives is connected to the reserved primary light path by reconfiguring the core node switch.

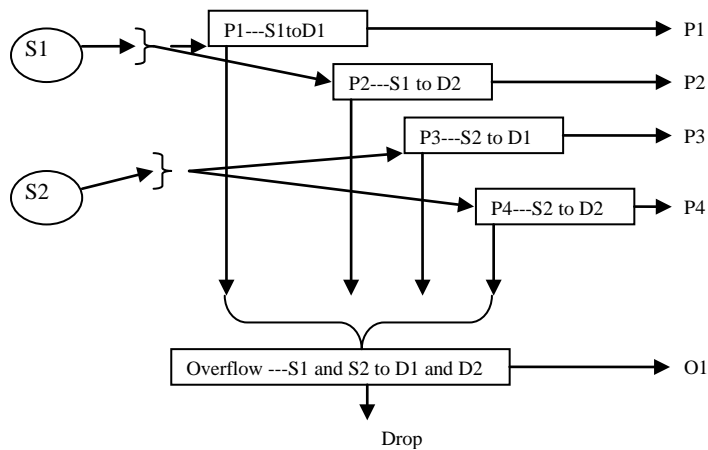


Figure 3.9 Operation in a Hybrid Node, showing header queues for primary and overflow channels.

If the channel request made by the header cannot be provided by any of the primary light paths associated to the header queue, the request overflows to an overflow queue. An overflow queue aggregates headers from all overflowing primary queues. There are as many overflow queues, as there are output links attached to the hybrid node. It is assumed that there is mapping between final destination of the headers and the output links. Once an overflow channel on an appropriate link is identified for the header, the core switch is reconfigured to connect the input link on which the burst corresponding to the header arrives, to the overflow channel that is reserved by the header. If the overflow channel request made by a header cannot be satisfied, the header is dropped from the core node. Along with the header, the incoming burst is also dropped.

Scheduling primary and overflow channels in response to a burst request may depend on several criteria. One such criterion could be to minimize the need for wavelength conversion within a switch. In our case, we assume that full range wavelength conversion is possible and there are enough wavelength converter devices to make all interchanges possible. Thus, we may assume random scheduling of channels. It has to be kept in mind that bursts from a particular traffic source can only occupy a fixed set of reserved primary channels and each source has its own set of such channels that it can randomly access.

In the overflow layer, there is the possibility of finding multiple paths between a pair of source-destination nodes. These alternate paths could span different intermediate core node hops. However, in the analysis of the proposed network architecture, we restrict the routing path to just one fixed physical path. In addition, an overflow path is assumed to be a shadow of the primary

path. The only difference between the two paths is that the overflow channels perform switching at all hops, while primary channels bypass any switching at the intermediate hops.

The hybrid node function can be classified into two parts. First, the hybrid node schedules an incoming burst to either primary/overflow channels along a route path. Second, the node provides the required hardware to perform the switching function upon burst arrival. The remaining sections of this chapter focus on the first function and chapter 4 focuses on the second function. Both functions can be viewed as two aspects of hybrid network that can be cost-optimized.

3.3.2 GENERAL CORE NODE

This description of a general core node is an attempt to generalize and model the function of the edge and core nodes in a network. An edge node has, as its traffic source, the access networks. A core node on the other hand, connects to several edge and other core nodes. The incoming traffic to a core node consists of primary and overflow traffic from other core/edge nodes as shown in [Figure 3.8](#). While the primary channels bypass any fast switching operation within the core node, the overflow traffic will be fast-switched. If we ignore the primary channels bypassing through a core node, its functions are similar to that of an edge node. The function of any general node, be it edge or core node, is to split the incoming traffic into primary and overflow channels. A core node performs this general node operation as well as optical bypass of incoming primary channels; an edge node performs only the general node operation.

A general node can do any of the following three functions. First, it can decide to have only primary channels carry the incoming traffic; that is, there are only primary channel groups for each traffic source. [Figure 3.10](#) shows the case, where core Node 3 has only dedicated primary channels in its outgoing ports. Second, a node can also decide to switch all incoming traffic onto shared outgoing channels. In this case, the traffic sources are not provided with any primary channels; rather they are all aggregated and switched onto the next node. In [Figure 3.10](#), Node 2 performs such a function. As a third option for the nodes, a node can decide to split its incoming traffic from each source into primary and overflow channels. Overflows from each primary channel group (attached to a traffic source) are statistically multiplexed along with other

overflows onto the overflow channels. Node 4 in [Figure 3.10](#) performs this function. It may be assumed that the first two cases are limiting conditions of the third case.

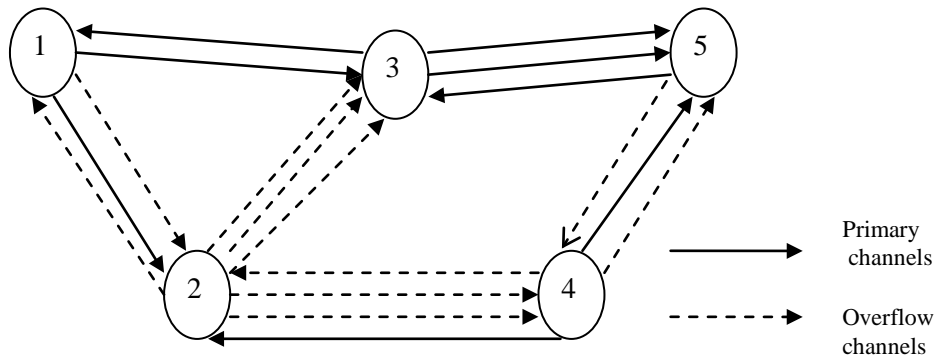


Figure 3.10 Possibilities of operation.

As far as a general node is concerned, we have the following questions to answer:

- 1) How many primary and overflow channels are feasible in a core node for a given required blocking performance in the overflow layer? What is the optimal combination?
- 2) Under what conditions will the core node have only primary, only overflow, and a combination of primary and overflow channels?
- 3) How do questions 1) and 2) respond to various traffic characteristics and the relative cost of operating primary/overflow channels?

Thus, the question is to determine the optimal number of primary and overflow channels in a path, subject to measurable traffic load statistics, and channel cost conditions, in order to satisfy a given blocking performance at the overflow layer. In order to perform the performance modeling of a system, we first need to create a traffic model, a cost model, and a queuing model for the system. The traffic model is derived from the overflow theory discussed in chapter 2. In the coming sections, the cost and queuing model is explained.

3.4 MODELING THE GENERAL NODE

The optimal design of a general node, mentioned in [Section 3.3.2](#), entails optimizing the number of primary and overflow channels. The optimality condition needs to be satisfied for any given load and loss probability. In addition to performance and traffic demand, the cost structure of the node may affect the optimum number of primary and overflow channels. In this section, a general node is modeled as a loss node, operating for a given loss probability and offered traffic. In addition, the cost structure of the node is represented by the notion of cost ratio.

3.4.1 QUEUEING MODEL

Traffic modeling for the offered and overflow arrival process was mentioned in section 2.3 of chapter 2. In this section, we develop a queuing model for the general node that will use the traffic model developed in the overflow theory.

The queuing model of a node consists of nodes called LossNode1 and LossNode2, which are connected together, as shown in [Figure 3.11](#). Both the nodes are modeled as a GI/M/C queue.

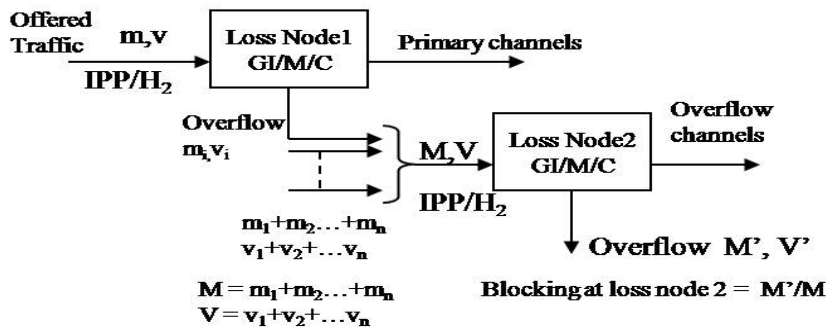


Figure 3.11 Queuing model of a Hybrid Node.

There is a LossNode1 for every incoming channel group and outgoing primary channel group. Input traffic to a LossNode1 queue, is assumed to be a 2- moment matched Interrupted Poisson Process (IPP). The IPP parameters can be mapped into the corresponding second-order

hyper-exponential (H₂) parameters, r_1 , r_2 and k . Using a recursive formula, the k th Factorial moments (F_k), of the overflow, can be calculated [41]. The first and second factorial moments, F_1 and F_2 respectively, are then used to calculate the mean, m_i and the variance v_i of the overflow process.

Mean overflow, $m_i = F_1$;

Variance overflow, $v_i = F_2 - F_1^2 + 1$ (3.4a)

$$\frac{1}{F_k} = \sum_{m=0}^C \binom{C}{m} \frac{(k+m-1)!}{(k-1)! M_{(m+k)}} ; \dots\dots\dots(3.4b)$$

Where C = number of channels.

$$M_k = \prod_{j=0}^{k-1} \frac{r_1 r_2 + (k r_1 + (1-k) r_2) j}{k r_2 + (1-k) r_1 + j} \dots\dots\dots(3.4c)$$

Overflows from LossNode1 are aggregated and offered to a single LossNode2. Since we assume independent overflows, the moments of all the overflow processes algebraically add up during aggregation. Thus, the moments of the aggregated traffic offered to LossNode2 can be characterized by a single set of moments, M and V, as shown in [Figure 3.11](#). This set of moments, is used to model the aggregated overflow as an IPP. The aggregated overflow arrival process can be approximated by a second-order hyper-exponential [32][41]. Thus, LossNode2 is modeled as a general independent arrival process. The first moment of overflow from LossNode2 can be calculated using the same recursive algorithm used for LossNode1, as shown in [equations \(3.4a\), \(3.4b\) and \(3.4c\)](#).

3.4.2 COST RATIO OF A HYBRID ROUTE

In order to dimension the channels in the primary and overflow layers, it is important to balance cost of the two layers. For a given traffic load offered to the core network by a number of traffic

sources, the primary layer may provide better service guarantees, because it isolates bursts from each source. However, isolating the channels will result in under utilization or over provisioning of channels, particularly if the load offered to the channels is peaked. In order to carry the same offered traffic load offered by the same number of sources, the overflow layer helps provide better channel utilization. Overflow channels improve channel efficiency in the core network, by allowing traffic sources to share available link capacities.

For the sources to be able to statistically share overflow channels, the core nodes should be able to reconfigure input and output channel connections for each arriving burst. While there are some commercial products, fast switches working in the order of microseconds will be expensive until a large market develops. Although the overflow layer may save channels due to statistical sharing, these channels incur higher switching cost. On the other hand, a static/semi static primary layer need not reconfigure wavelengths along its route very often, thereby reduces the need for expensive fast switches.

Due to the current lack of scalability and prohibitive cost of terabit electronic routers, the research community is investigating optical switching schemes. However, as of now, there are few commercially manufactured optical packet and burst switches and the cost of an OBS switch is not known. Thus, at this point we can only speculate the cost of switching and transporting over an overflow channel path, in relation to doing the same operations over a primary channel path. We define the relative cost of using an overflow channel and a primary channel by the path cost ratio, CR_{path} . The cost ratio depends on the switching and transportation costs of both the channels.

3.4.2.1 COST RATIO, CR_{PATH} OF A PRIMARY AND AN OVERFLOW PATH

The Path Cost Ratio is the relative cost of a primary path to the cost of an overflow path. A primary path consists of a light path between the source and destination nodes of a route. An overflow path originates at the source of a route and consists of a concatenation of wavelengths at each hop of the path, until the destination node. The cost of a primary path includes both the transmission cost of channels that make a light- path and the switching costs to interconnect the wavelengths of the links, as shown in [Figure 3.12](#). Just like the primary path, cost of an overflow path includes transmission and switching costs. If the routing path between two ends is the same for primary and overflow paths, the physical hops traversed by the two paths, and any channel

amplification/regeneration performed on the paths, are the same. Further, if the transmission costs do not depend on the wavelength of the channel, we may assume that transmission costs of a primary and overflow path are the same between any two given end points.

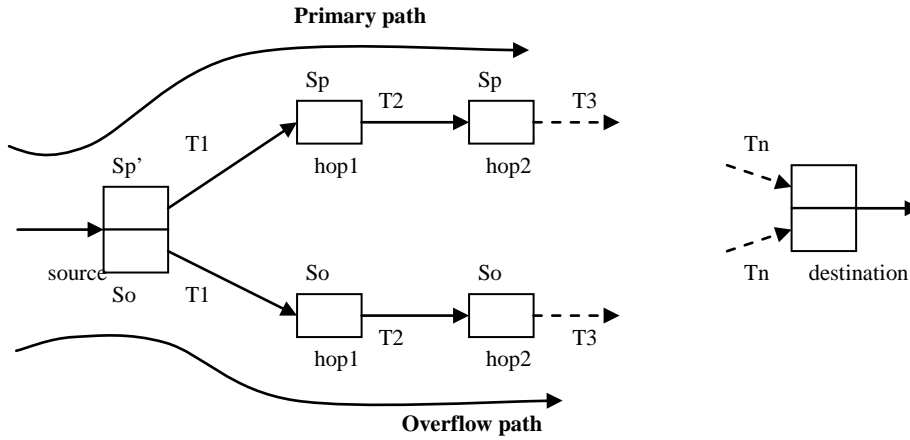


Figure 3.12 Path cost ratio, CR_{path}

Unlike the transmission costs for primary and overflow paths, switching costs may not be the same for both the layers. The configuration of the primary layer is assumed more or less static, in which case, there is no need to reconfigure the wavelengths that may constitute a light path. Thus, the nodes that constitute intermediate hops of a primary path do not need a fast switching capability. We may assume the cost of concatenating the wavelength channels of a light-path to be some constant average value, Sp , as shown in [Figure 3.12](#). There is, however, a need for a fast switching operation to groom the incoming channels to a primary light path. The cost of switching these incoming channels to a primary light-path may be much more than the cost of just concatenating the wavelengths at each hop. The cost of finding an internal path through a grooming switch at the source of each route is assumed to be some constant average value, Sp' , where Sp' is much higher than Sp .

In an overflow path there is fast reconfiguration of the wavelengths that may constitute the path. The hops of an overflow path are made up of fast switches and cost of finding an internal path through the hop is assumed to be some average constant value, So , as shown in [Figure 3.12](#). It may be assumed that So is equal to Sp .

Equation (3.5a) expresses cost of a primary path and its corresponding overflow path, in terms of per-hop switching and transmission costs, by assuming negligible loss at the

intermediate hops and no chance of light-path entry for the overflow channels. The cost of the overflow path is expressed in terms of the ratio of the costs of per-hop switching to transmission, CR_{path} . If we assume that So equals Sp' and if Sp is very small compared to Sp' , then CR_{path} depends on number of hops in the path and to the ratio of So to channel costs T_i , CR_{path} . Further, if we assume that CR_{path} is the same for all hops, we can express the path cost ratio, as shown in equation (3.5c).

$$C_{primary_path} = \left(\sum_{i=1}^{hops} (Sp_i + T_i) \right)$$

$$C_{overflow_path} = \sum_{i=1}^{hops} (So_i + T_i)$$

if, $CR_{path} = \frac{So_i}{T_i}$

$$C_{overflow_path} = \sum_{i=1}^{hops} (CR_{path} + 1) * T_i \dots \dots \dots (3.5a)$$

if

- 1) $So_i \approx So_{i+1}$
- 2) $Sp_1 = Sp' = So$
- 3) $Sp_i = Sp_{i+1}; i = 2, 3, \dots, hops$
- 4) $Sp_i \ll So; i = 2, 3, \dots, hops$

then

$$CR_{path} = \frac{hops * (So) + \sum_{i=1}^{hops} T_i}{So + \sum_{i=1}^{hops} T_i} \dots \dots \dots (3.5b)$$

also,

if

$T_i \approx T_{i+1}; i = 1, 2, 3, \dots, hops,$

$$CR_{path} = \frac{hops * (So + T_i)}{So + (hops * T_i)}$$

putting, $CR_{path} = CR_{path}$

$$CR_{path} = \frac{hops * (CR_{path} + 1)}{CR_{path} + hops} \dots \dots \dots (3.5c)$$

Equations (3.5a), (3.5b) and (3.5c) assume that there is no light-path entry at intermediate hops along the overflow path. Without light-path entry, the bursts travelling along the overflow path have to be fast-switched among input and output links at every hop. However, if there is light-path entry for the optical bursts at intermediate hops, there is no need to perform fast-switching on the bursts for the portion of the route path travelled along the light-path. If there is light-path entry for optical bursts at intermediate hops, the route's overflow path may be realized in multiple ways, as shown by [Figure 3.13](#). The multiple overflow paths associated with a route will each provide different switching costs. Thus, if there is possibility of light-path entry within an overflow path of a route, the total switching costs of the overflow path will be less than $C_{\text{overflow_path}}$ in equation (3.5a).

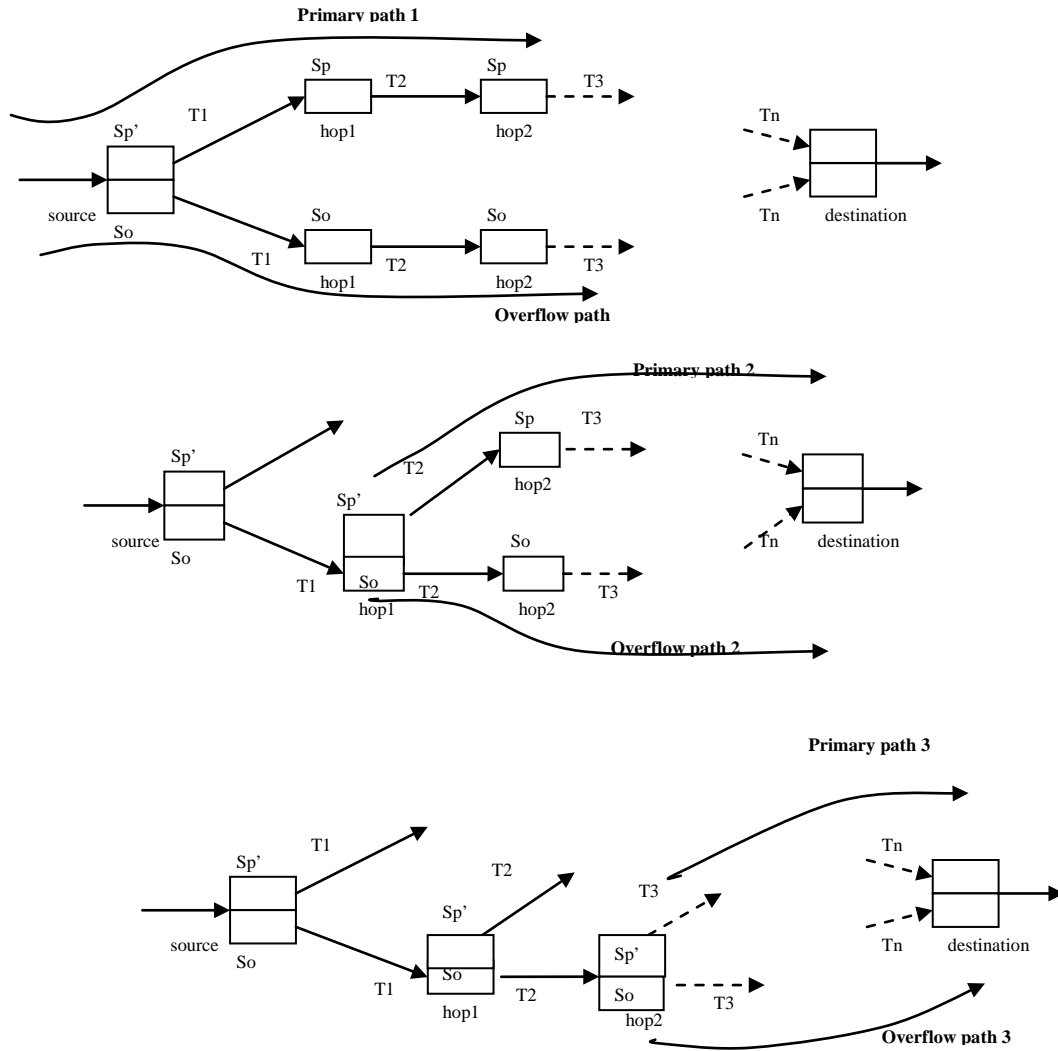


Figure 3.13 Effect on light path entry on cost ratio.

3.4.2.2 PATH COST RATIO OF MULTIPLE OVERFLOW PATHS Optical bursts entering an overflow path at a node may enter a primary light-path at any of the successive hops. Therefore, a burst may not always keep along the overflow path until it reaches the destination node. [Figure 3.13](#) shows several possibilities of transporting an overflow burst. If a burst enters a light path, it will not incur a switching cost, Sp' on any of the successive hops. Let the possibility that an overflow burst enters a primary light path at hop i , be p_i . Then, the cost of the overflow path, given by equation (3.5a) must be modified to include the possibility of light path

entry for the overflow bursts. In addition, chance of using the overflow path depends on the probability of blocking at each node.

If we assume a fixed blocking probability, B , at each node, we may derive the total cost of an overflow path as shown below. In this derivation, the cost of each overflow path is given as $C_{overflow_path_N}$, where N identifies the overflow path by its N th hops on the overflow path, prior to light-path entry.

$$C_{overflow_path_hops} = \left[(1-p_1)(1-p_2)\dots(1-p_{hops}) * (1-B)^{hops} \right] * \sum_{i=1}^{hops} S_{O_i} + \sum_{j=1}^{hops} T_j$$

$$C_{overflow_path_hops-1} = \left[(1-p_1)(1-p_2)\dots(1-p_{hops-1})(p_{hop}) * (1-B)^{hops-1} \right] * \sum_{i=1}^{hops-1} S_{O_i} + Sp'_{hops} + \sum_{j=1}^{hops} T_j$$

$$C_{overflow_path_hops-2} = \left[(1-p_1)(1-p_2)\dots(1-p_{hops-2})(p_{hops-1}) * (1-B)^{hops-2} \right] * \sum_{i=1}^{hops-2} S_{O_i} + Sp'_{hops-1} + \sum_{j=1}^{hops} T_j$$

In general if the overflow path makes a light-path entry at the $N+1$ th hop after the source node, where $N = 1, 2, \dots, hops$, then,

$$C_{overflow_path_N} = \left[(1-p_1)(1-p_2)\dots(1-p_N)(p_{N+1}) * (1-B)^N \right] * \sum_{i=1}^N S_{O_i} + Sp'_{N+1} + \sum_{j=1}^{hops} T_j$$

where,

$$p_{hops+1} = 0;$$

and

$$Sp'_{hops+1} = 0$$

The average switching cost, $C_{overflow_path_switch}$ of multiple overflow paths in a route is given as,

$$C_{overflow_path_switch} = \sum_{N=1}^{hops} \left[\left[\prod_{k=1}^N (1-p_k) \right] * p_{N+1} * (1-B)^N \right] * \sum_{i=1}^N S_{O_i} + Sp'_{N+1} \right] \dots\dots\dots(3.6a)$$

Total cost of an overflow path, $C_{overflow_path}$ may be expressed as,

$$C_{overflow_path} = C_{overflow_path_switch} + \sum_{j=1}^{hops} T_j \dots\dots\dots(3.6b)$$

Where, $C_{overflow_path_switch}$ gives the average switching cost for all multiple overflow paths between a source and destination route.

Cost of primary path for the route is given as,

$$C_{primary_path} = Sp'_1 + \sum_{j=1}^{hops} T_j \dots\dots\dots(3.6c)$$

If we make the same assumptions as in equation (3.5b) and (3.5c), then

$$C_{overflow_path} = \left[\sum_{N=1}^{hops} \left[\prod_{k=1}^N (1 - p_k) \right] * p_{N+1} * (1 - B)^N * (N + 1) * So \right] + hops * T$$

$$C_{primary_path} = So + hops * T \dots\dots\dots(3.6d)$$

So the Cost ratio, CR_{path} is the ratio of the cost of an overflow path to the cost of a primary path:

$$CR_{path} = \frac{C_{overflow_path}}{C_{primary_path}} \dots\dots\dots(3.6e)$$

As the values probability of light-path entry (p_i), increases, the cost of an overflow path decreases. A high value of p_i signifies a greater chance that the overflow burst will enter a light-path at the i th hop. If an overflow burst has a high chance of entering a light-path at intermediate hops of a route path, then there is a high probability that it will cost less to switch the burst along the route path. The value of p_i depends on the number of primary light-paths available at the i th hop to transport incoming bursts to the destination node. A method to

determine number of light paths on all links of the route and, as a result, the values of p_i for a Hybrid Node is provided in Chapter 5.

3.4.3 TOTAL COST OF A HYBRID ROUTE

A hybrid route path that originates at the hybrid node and ends at a destination node is composed of primary and overflow components. The costs of a primary and an overflow path are related via the notion of cost path ratio, CR_{path} . In order to determine total cost of a path, we must determine number of primary light-paths and overflow channels that are required at the source node.

While a primary light-path is made of wavelengths dedicated to a traffic source, in order to carry bursts belonging to a fixed route, overflow channels may carry bursts belonging to several sources that offer traffic to the same destination. It is to be noted that a route is described as the connection between the source Hybrid Node, to which the traffic sources are attached, to another destination Hybrid Node. A route is not a connection between a traffic source and a destination Hybrid Node.

The total cost of a hybrid route is calculated by sum of total number of primary light-paths belonging to all sources and the total number of overflow channels on the output link of the source Hybrid Node, each weighed by the cost of a primary path and the cost of an overflow path, respectively. The total cost of a hybrid route may be expressed as,

$$\begin{aligned}
 &Total_cost_route = \\
 &number_of_primary_ligtpaths * C_{primary_path} + number_of_overflow_channels.* C_{overflow_path} \\
 &.....(3.7a)
 \end{aligned}$$

Dividing both sides of equation 3.7a, by $C_{primary_path}$ gives:

$$\begin{aligned}
 &Total_cost_path_{primary_path} = \\
 &number_of_primary_ligtpaths + number_of_overflow_channels.* CR_{path} \\
 &.....(3.7b)
 \end{aligned}$$

The total number of overflow channels required for a route in the intermediate links of the route path is actually less than what is required at the first hops of the path. Due to losses and light-path entry at the intermediate hops, traffic belonging to the route that may remain in the overflow layer decreases. It can be inferred from [equation \(3.6d\)](#) that CR_{path} takes into account, the probability that a burst will remain on an overflow channel from source to destination nodes.

It appears from [equation \(3.7b\)](#) that both primary and overflow channels behave, as if they are part of an end-to-end light-path. Figure 3.14 shows the overflow channels of Route1 as an ‘equivalent light-path’. Such an assumption is required to compare cost of a primary path to the cost of an overflow path despite the fact that the overflow path, unlike the primary path, is not a true light-path.

The ‘equivalent light path’ representation of overflow channels for Route 1 gives each overflow channel a probability that it will be concatenated to yet another overflow channel at the intermediate hops of a route. This probability depends, on the probability of light-path entry for a burst belonging to Route 1 in all intermediate hops and on the probability of blocking experienced at each hop. Since the cost ratio, CR_{paths} , is related to this probability, it is possible to map an overflow path into its equivalent light- path. If we assume probability of light path entry is p_i on the i th hop and the loss probability as B on each hop, [equation \(3.6e\)](#) gives the cost ratio CR_{path} .

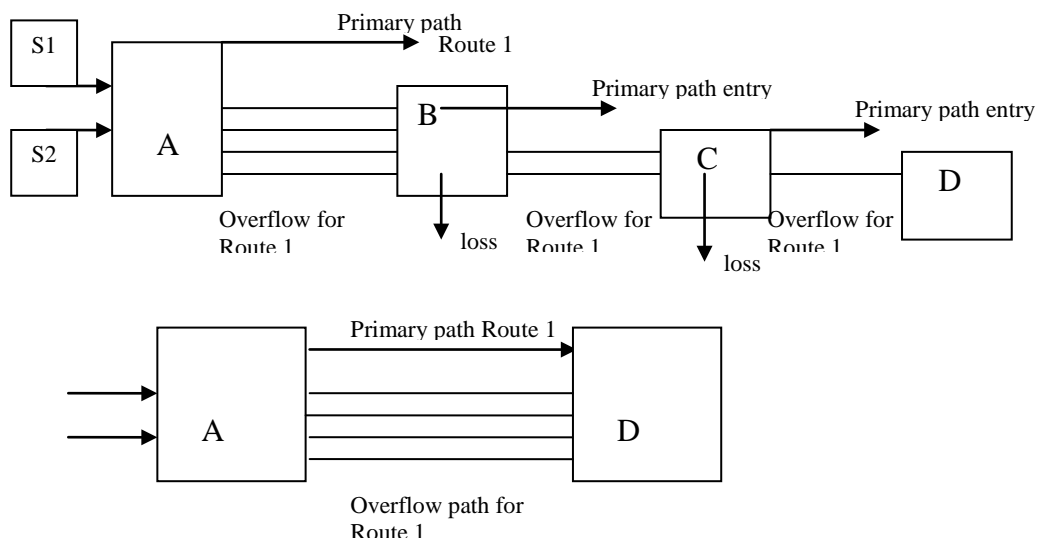


Figure 3.14 Assumption in calculating cost of a hybrid route

In Figure 3.14, Route 1 consists of a path between nodes A and B. Node A, aggregates overflows from all primary paths belonging to S1 and S2 that go to node D. At node B part of the aggregated route traffic enters light-paths going to node D. There is also some loss occurring at node B. Similarly, route 1 traffic may incur loss at node C. In order to compare primary and overflow channel costs of a single path it is assumed that an overflow channels for Route 1 behaves like a light-path. Since the path cost ratio accounts for the reduction in number of overflow channels at each successive hop, it enables us to calculate total cost of the entire overflow path, by just knowing the number of channels in the first link.

In real networks, a multi-channel overflow link between two nodes may carry several routes simultaneously. The same link may also originate some of the routes it actually carries. So the total overflow cost of these routes is calculated by knowing the average cost ratio of the entire network. Chapter 5 shows the method to calculate cost of the overflow layer of a network by determining average path cost ratio for the entire network.

A hybrid path is said to be *cost optimal* if minimum total cost can be obtained by hybrid operation. A path between a source and a destination is said to operate in a *hybrid mode* if the path can be realized using both primary light-paths and overflow channels. A path is said to operate in a *non-hybrid mode*, if the path is made of either primary light-paths, or overflow channels, but not both. For a given hybrid path R , the number of primary and overflow channels R_p and R_o can be given as a function of primary light-paths per source, l_i , as shown in equation (3.8a). If there are S sources attached to the Hybrid Node, then the total cost of the hybrid path, given by [equation \(3.7b\)](#) can be modified as shown in equation (3.8b). In equations (3.8a) and (3.8b), the path is said to operate in hybrid mode only if l_i is not equal to either 0, or P . When $l_i = 0$, there is absolutely no primary layer and if $l_i = P$ there is absolutely no overflow layer.

$$Total_{cost_{path_i}} = cost(R_p(l_i)) + cost(R_o(l_i)) \dots\dots\dots(3.8a)$$

or,

$$Total_{cost_{path_i}} = S * l_i + R_o(l_i) \dots\dots\dots(3.8b)$$

where, $i = 1,2,3,\dots,N$ and $l_1 = 0$ and $l_N = P$

Throughout the remaining analysis, it is assumed that the cost of a primary channel group increases linearly with the number of wavelengths in the group. This will be the case if the wavelengths in the fiber do not produce significant non-linear effects [35]. If the wavelengths within the fiber are very dense and closely spaced, non-linear compensation may be required. Non-linear compensation may require complex devices within the transmission path, which may drive the transportation costs. We ignore such a scenario and assume that the cost of a channel remains fixed at all times. Thus, we assume that the cost of primary channels scale linearly with the number of wavelengths in the group.

3.5 RESULTS

The queuing model in [Figure 3.11](#), is used to analyze the number of primary and overflow channels, needed to provide a blocking probability of 0 .001. The moments of overflow from LossNode1 and blocking probability at LossNode2, are determined using the recursive algorithm mentioned in the previous section. Alternatively, computer simulation of a GI/M/C queue was also used to check the accuracy of the results obtained from the recursive algorithm. The accuracy of the recursive algorithm was found to be comparable to that of the simulation. The number of overflow wavelengths obtained from the simulation and recursive algorithm varied by only 0.002% in the worst case. However, due to constraints on the simulation tool (CSIM) used, we could not simulate the LossNode2 queue, for more than 100 sources attached to the node.

3.5.1 OPTIMAL COMBINATION OF PRIMARY/OVERFLOW CHANNELS

[Figure 3.15](#) shows the cost optimization obtained by using the hybrid approach. In the figure, the dotted line called the ‘primary channels’ gives the cost of the primary path. Number of primary paths is also equal to the number of primary channels in each link and hence, the X-axis

is termed ‘Primary Channels’. In the analysis, cost of a primary path is assumed to be of unit value and cost of an overflow path is assumed to be equal to the path cost ratio (CR_{path}). In the figure, the path cost ratio is denoted as ‘CR’ and the curve named ‘Overflow Channels CR =1’ is the cost of the overflow paths in the route for a path cost ratio of one and this curve also gives the number of overflow paths, for a given number of primary paths and a given blocking probability. Similarly, the curve named ‘Overflow Channels CR=2’ gives the cost of the overflow paths in the route when the path cost ratio is two. By adding the values on the ‘Overflow Channel’ curve, with that of the ‘Primary Channel’ curve, we obtain the ‘Total Cost’ curve for the respective value of CR.

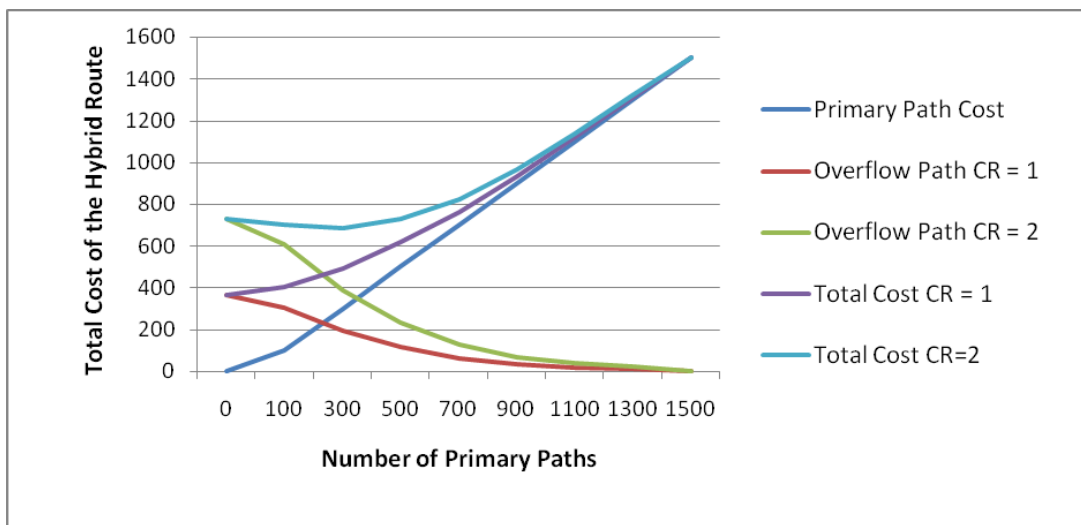


Figure 3.15 Cost of primary, overflow and sum of primary and overflow channels, for a load of 3 Erlangs per traffic source; 100 sources and a peakedness of 2.

The cost of a Hybrid Node in [Figure 3.15](#) spans two extremes. One extreme point on each hybrid cost curve occurs at the right edge, where there are only primary channels in the hybrid path. The other extreme point occurs at the left edge, where all traffic offered to a Hybrid Node is multiplexed onto overflow channels. In between these two extremes there may exist a point at which the total cost of primary and overflow paths is at a minimum. This minimum point occurs for a certain optimal number of primary and overflow channels, such that there is a balance between operational costs and statistical multiplexing gains.

The minimum cost of a hybrid path can be determined by taking the derivative of equation (3.8b)

$$\frac{\Delta(\text{Total_cost_path}_i)}{\Delta l_i} = \frac{\Delta(S * l_i)}{\Delta l_i} + \frac{\Delta(\text{Ro}(l_i) * CR_{\text{path}})}{\Delta l_i}$$

or,(3.9)

$$\frac{\Delta(\text{Ro}(l_i))}{S(\Delta l_i)} = -\frac{1}{CR_{\text{path}}}$$

3.5.1.1 THE OVERFLOW GAIN Overflow gain measures the savings in the average number of overflow channels accessed per source, when each source is provided an additional primary channel. The overflow advantage plays an important role in determining the optimal number of primary/overflow channels in a hybrid route. The left hand side of [equation \(3.9\)](#), represents the overflow gain, whose value depends on system parameters such as the number of sources and the path cost ratio. In order to obtain the cost of the optimal hybrid route, the cost savings due to overflow gain has to balance the cost incurred due to the addition of an extra primary channel for each source.

The overflow gain of a hybrid path depends on the load experienced in the overflow layer. Overflow load not only depends on load offered to the primary layer, but also on the number of primary channels from which the overflow occurred. This means, every increment in primary channels may yield a different amount of overflow gain. Overflow gain may also depend on the number of sources sharing the overflow channels. Overflow gain, as observed from [equation \(3.9\)](#), decreases with an increase with number of sources sharing overflow channels.

Overflow gain also depends on the smoothness of the load offered to the hybrid node. In general, for a peaked load of a given mean value, channel requirements are higher than what is required for a smooth load of the same mean value. Compared to channel requirements for a smooth load, an increment in primary channels will not substantially reduce the load on overflow channels for a peaked load condition. In effect, channel requirements of the overflow layer do not reduce due to an additional primary channel. Hence, overflow gain for a peaked load may be smaller than the overflow gain of a smooth load.

Overflow gain is related to the notion of statistical multiplexing gain in the overflow channels. Overflow gain is inversely proportional to number of sources, but statistical multiplexing gain is directly proportional to the number of sources that share the overflow channels. Statistical multiplexing gains obtained by aggregating a large number of sources at the overflow layer tend to equalize channels requirements, due to which channels requirement at the overflow layer decreases. In this manner, statistical multiplexing gains provides a better channel gain, which is otherwise small due to higher Peakedness of offered load. In effect, statistical multiplexing gains at the overflow layer tend to reduce the possibility of improving the overflow gain. Thus, lowering of overflow channel requirement upon addition of a primary channel, is small because of an already high channel gain due to aggregation.

Statistical multiplexing gain for a peaked-load is possibly higher than what can be obtained for a smooth load. Since the effect of statistical multiplexing gains is to reduce overflow gains, from [equation \(3.9\)](#), we may infer that statistical multiplexing gains is directly proportional to path cost ratio. Hence, higher statistical multiplexing gains may possibly balance high path cost ratio of the hybrid path.

Overflow gain provides the condition for optimal hybrid operation by relating the loading on the primary and overflow channels to the cost ratio of the primary and overflow paths. Loading on the primary channels is determined by the mean and Peakedness of the load offered by each source. Loading on the overflow channels is determined by mean and Peakedness of the load offered by each source and also on the number of sources sharing the overflow channels.

3.5.1.2 ANALYSIS OF OVERFLOW GAIN For example, let there be 100 sources, each with an offered load of 3 Erlangs and a Peakedness of 2. Table 3.1a shows the values of overflow channels $Ro(l_i)$ for some given values of primary channels, l_i . A curve fitting tool in Matlab is used to determine the polynomial that best represents the function $Ro(l_i)$. The curve fitting process maps the data points in Table 3.1a into a polynomial of a certain degree. The polynomial is selected to closely represent the data points and goodness of fit parameters is obtained. An R-square that is very close to one means a good fit.

Table 3.1a Overflow gain

l_i	0	1	3	5	7	9	11	13	15
$Ro(l_i)$	364	302	193	115	63	33	18	12	0

Curve fitting parameters for the data:

$$R_o(l_i) = p_1 * l_i^4 + p_2 * l_i^3 + p_3 * l_i^2 + p_4 * l_i + p_5$$

Where, $p_1 = -6.407e-11$; $p_2 = 7.12e-8$; $p_3 = 0.000327$; $p_4 = -0.677$; $p_5 = 364.5$

Goodness of fit: SSE=3.41, R-square =1

Table 3.1b Results from curve fitting

l_i	0	1	2	3	4	5	6	7	8	9	10	11	12	13	14	15
Overflow gain	>.6	.6	.53	.46	.39	.32	.26	.20	.14	.10	.07	.05	.03	.03	.02	.01

[Table 3.1 b](#) shows the decrease in the number of overflow channel for each increase in primary channels. If we are given a $CR_{path} = 1$ and $S = 100$, then from [equation \(3.9\)](#), the minimum total cost is obtained for an overflow gain is equal to 1. But since, such a value of overflow gain does not appear in [Table 3.1 b](#), it is not possible to obtain optimal hybrid operation for a $CR_{path} = 1$. However, if $CR_{path} = 2$, optimal hybrid operation is obtained for overflow gain equals to 0.5, which occurs for $l_i \approx 3$, in [Table 3.1 b](#). [Figure 3.15](#) depicts this example graphically. It can be seen from the total cost curves of [Figure 3.15](#), that optimal hybrid operation occurs only for $CR = 2$, where CR is also the path cost ratio, CR_{path} . This optimum occurs at approximately 300 primary channels. Since the total cost value is equal to cost of 700 primary channels, the number of overflow channels is about $((700 - 300)/2) 200$.

The relative position of the minimum cost point, between the two extreme points depends on the cost ratio. For a very high cost ratio, the minimum point leans towards more primary channels. On the contrary, for a lower cost ratio, the optimum hybrid path can afford more overflow channels.

A hybrid route can afford more overflow channels if the cost of overflow gain equals the cost of adding an extra primary channel. The overflow gain is not the same for every addition of

primary light-path; instead, it decreases with every successive addition of primary light-paths. Thus, we obtain a range of values for the overflow advantage, as we increase primary channels one by one.

The values of overflow gain may depend on the offered load characteristics and on the number of sources using the hybrid path. [Table 3.2](#) provides various data sets classified according to the load offered by each traffic source. [Figure 3.16](#) plots overflow gain for different values of offered load and number of sources. The offered load may be characterized by mean load and Peakedness of the load.

It can be observed from [Table 3.2](#) and [Figure 3.16](#) that with an increase in the average value of offered load, overflow gain increases if Peakedness is maintained constant. For a fixed number of primary channels, overflow gain is greater when offered load is higher. For instance, if primary channels are held at 4, overflow gain for data set 1, is smaller than overflow gain for data set 2. At the same time, for a fixed mean offered load, overflow gain decreases, as Peakedness increases. Thus, overflow gain increases whenever the smoothness of load offered to the primary channels increases. Smoothness of load may increase either due to an increase in average load or due to a decrease in Peakedness of offered load.

Table 3.2 Values of l_i and $\Delta(Ro(l_i))$ for different offered loads.

Data Set 1: 3 Erlangs, Peakedness=2 and 100 sources																
l_i	0	1	2	3	4	5	6	7	8	9	10	11	12	13	14	15
$Ro(l_i)$	365	300	244	194	150	115	85	62	45	32	24	19	15	11	8	0
Overflow Gain	>.65	.60	.53	.46	.39	.32	.26	.20	.14	.10	.07	.05	.04	.04	.03	
Data Set 2: 6 Erlangs, Peakedness=2 and 100 sources																
l_i	0	2	4	6	8	10	12	14	16	18	20					
$Ro(l_i)$	687	536	402	287	193	123	73	42	26	17	7					
Overflow Gain	.79	.72	.63	.52	.41	.29	.20	.11	.06	.04						
Data Set 3: 3 Erlangs, Peakedness=1 and 100 sources																
l_i	0	1	2	3	4	5	6	7	8	9	10					

$Ro(l_i)$	343	269	199	140	92	56	33	19	12	8	0					
Overflow Gain	.77	.73	.65	.53	.41	.29	.18	.09	.05	.05						
Data Set 4: 3 Erlangs, Peakedness=2 and 10 sources																
l_i	0	1	2	3	4	5	6	7	8	9	10	11	12	13	14	15
$Ro(l_i)$	57	50	44	38	32	26	22	18	15	13	12	11	10	9	6	0
Overflow Gain	.65	.7	.6	.58	.55	.49	.42	.34	.25	.16	.08	.08	.08	.02	.03	

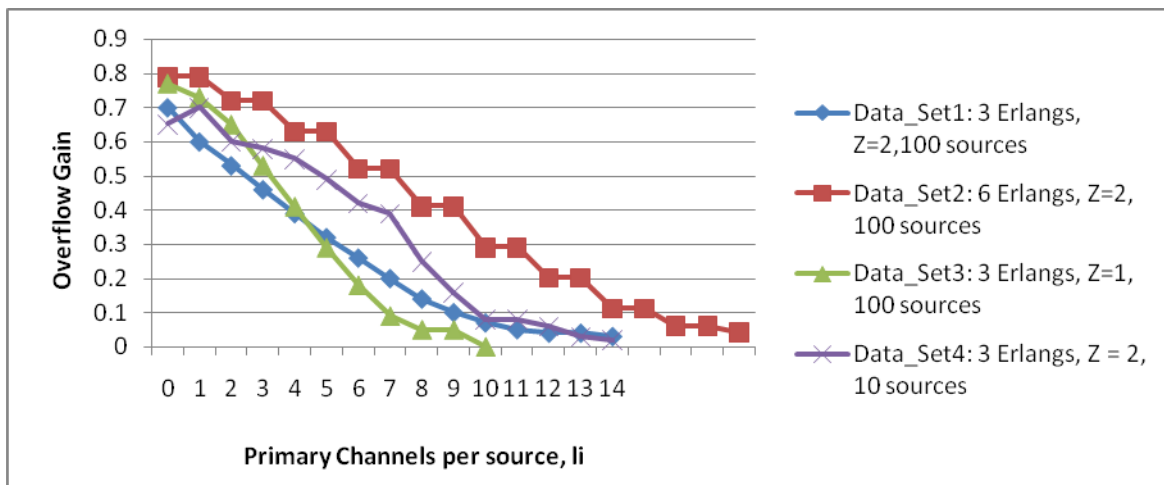


Figure 3.16 Overflow Gain

The overflow gain also depends on the total load offered to the overflow layer by all traffic sources. As number of traffic sources increases, the aggregate load that is carried by the overflow layer becomes smoother. It is observed that, as long as the load offered by a traffic source to the primary layer is a constant and if there is an increase in number of sources, overflow gain decreases. This is because aggregation of more number of traffic sources lowers the net channel requirement at the overflow layer. Hence, the relative effect of adding a primary channel will not be substantial, when compared to the effect of statistical multiplexing gains at the overflow layer. Figure 3.16 shows an increase in overflow gain for Data_Set4, which contains 10 sources, when compared to the overflow gain of Data_Set1, which contains 100 sources.

Overflow gain is depends on the average value of load offered at the primary layer. The effect of adding a primary channel results in a relatively fewer overflow channels, when the load offered to the primary layer is high. For instance, in Figure 3.16, overflow gain of Data_Set2, which has 6 Erlangs, is consistently higher than the overflow gain of Data_Set1, which has 3 Erlangs.

Overflow gain is seen to increase, as smoothness of load offered by a traffic source (at the primary layer) increases. However, the increase in overflow gain is not consistent for all values of l_i , as observed in Figure 3.16 for Data_Set1, with a Peakedness (Z) of 2 and for Data_Set3, with a Z of 1. This is possibly due to the modulation of Peakedness by the primary channels, especially at lower values of overflow load. The results can be observed from [Figure 3.16](#) and inferred from [Table 3.2](#).

Each value of overflow gain, can provide an optimal hybrid path for a certain fixed value of cost ratio. From [equation \(3.9\)](#), CR_{path} needed to provide a cost-optimal hybrid path can be determined for a given value of overflow gain.

3.5.2 RANGE OF HYBRID OPERATION

The window of the CR_{path} values for which hybrid operation yields minimum cost gives the range of hybrid operation. The range of hybrid operation represents the feasibility of hybrid operation and its sensitivity to values of CR_{path} . The path cost ratio, CR_{path} , itself depends on several parameters, such as switching and channel costs and the probability of light-path entry at intermediate nodes. None of these parameters may be constant at all times and any change will result in a new value of CR_{path} for the hybrid route. In response to such a change in the values of the path cost ratio, the number of primary/overflow channels in the route can be changed. Although the proposed overflow-layer architecture is not analyzed for dynamic operation, possibility of such an operation can be assessed by the range of hybrid operation.

Via the notion of overflow gain, the range of hybrid operation depends on the number of sources and the mean load and traffic Peakedness,. As overflow gain increases, either through an increase in smoothness (decrease in Peakedness) of the offered primary load or due to an increase in the number of sources sharing the overflow channels, the feasibility of hybrid

operation increases. As represented by [equation 3.9](#), overflow gain is the benefit seen by a traffic source, in reducing its share of overflow channels, by increasing its access to primary channels. As overflow gain increases, the benefit of adding primary channels increases. At the same time, an increase in overflow gain tends to reduce the CR_{path} at which optimal hybrid operation can be obtained. The result is that window of optimal hybrid operation will approach its non-hybrid (primary channel only) value, for smaller values of cost ratio. [Figures 3.17](#) and [3.18](#) show the range of hybrid operation for 100 and 10 sources respectively [57][59].

In [Figures 3.17](#) and [3.18](#), total cost of a hybrid route is determined in terms of cost of a primary channel. The total cost is determined for different values of average offered load and Peakedness. The range of hybrid operation for a given load and Peakedness is obtained for a range of path cost ratios. The dark curves in the figures show the range of hybrid operation in terms of its cost ratio and the dotted curves shows the cost ratios for which hybrid operation becomes infeasible. A hybrid operation is feasible only if it provides minimum total cost, when compared to a non-hybrid operation.

The range of hybrid operation decreases for higher values of primary offered loads values. We have seen in [Figure 3.16](#) that overflow gains are smaller on 3-Erlang traffic than on the 6-Erlang traffic for the same value of Peakedness. A smaller overflow gain causes the hybrid operation to achieve a high CR_{path} in the 3- Erlang curve compared to a 12-Erlang curve in [Figures 3.17](#) and [3.18](#).

If we assume the average load and the number of sources to be constants, an increase in the Peakedness corresponds to an increase in value of CR_{path} . With an increase in CR_{path} (at the point of optimality) optimal hybrid operation can be achieved despite high cost of overflow path. When peakedness of offered load reduces, overflow gain increases and CR_{path} for optimal hybrid operation reduces.

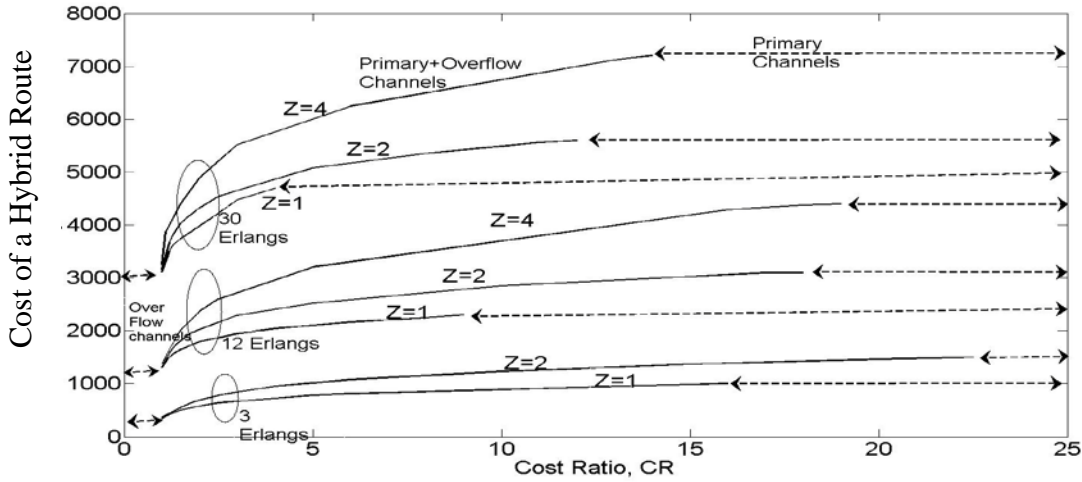


Figure 3.17 Feasibility of a hybrid node with 100 traffic sources.

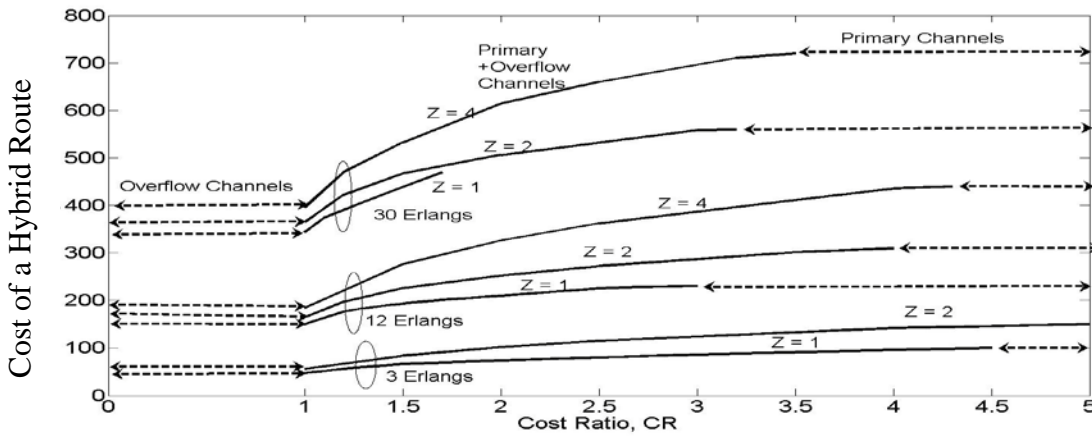


Figure 3.18 Feasibility of a hybrid node with 10 traffic sources

An increase in number of traffic sources results in a decrease in overflow gain, as is apparent from [equation 3.9](#). This means that the addition of primary channels results in only a small cost benefit. Due to the possibility of greater statistical multiplexing gains, it may be more cost-effective to save dedicated primary channels despite the high cost of the overflow path. The range of hybrid operation across the x-axis in [Figure 3.17](#), where there are 100 sources, is greater than the range in [Figure 3.18](#), which has only 10 sources.

The feasibility of hybrid operation depends on the range of values of CR_{path} for which hybrid operation is cost-optimal. An increase in overflow gain means there is greater cost benefit

by adding primary channels and the range of hybrid operation approaches non-hybrid (primary channels only) operation faster.

An increase in overflow gain also means a smaller value of CR_{path} at which optimal hybrid operation occurs. A large offered primary load and small number of sources sharing the overflow channels results in high overflow gain and subsequently causes the value of CR_{path} to be low. At the same time, a large value of offered Peakedness reduces overflow gain and thus, increases the CR_{path} at which not adding primary channels becomes optimal. It is observed that, as the value of CR_{path} for optimal hybrid operation becomes small, the range of values of CR_{path} for which optimal hybrid operation occurs too shrinks.

3.5.3 USEFULNESS AND LIMITATIONS OF USING PATH COST RATIO

The path cost ratio, CR_{path} compared the cost of a primary and an overflow path in a system. There are advantages and disadvantages to use the cost ratio as a measure to describe the cost of a switching node.

The path cost ratio, considers the cost disparity between the primary and overflow sections of a hybrid node. The cost disparity may stem from differences in switching and transport complexities in their respective sections. The switching complexity of the system may be due to an increase in required switching speed or the greater size of the control of switching elements. Increasing the number of channels may increase the cost of transportation devices and switch size. However, the cost ratio is oblivious to the details of the switching techniques within a node. Thus, cost ratio considers the hybrid node to be a black box.

The black box nature of the hybrid node omits several details that may help understand the practical feasibility of the hybrid node. For instance, in [Figure 3.17](#), at a cost ratio of 3, for a traffic of 12 Erlangs and $Z=2$, hybrid operation is theoretically feasible. But looking at [Figure 3.17](#), it cannot be said, if it is practically possible to design a switch with a cost ratio of 3. It may also be the case that different switching-fabric architecture may yield different cost ratios within a node, for the same load. Thus, the measure of cost ratio may be dependent on several factors internal and external to the switch.

3.6 EFFECT OF OPTICAL BURST FORMATION ON HYBRID OPERATION

One of the main assumptions of the network architecture is the adaptation of access layer traffic into bursts at the access-core interface, as shown in [Figure 3.3](#). Bursts are created by collecting multiple streams of input traffic coming from a source and assembling them into bursts. A timer-based assembly of input traffic streams may limit the size of the burst.

The process of framing/assembling the input traffic may change the statistical properties of traffic arrival rates and holding times when a burst arrives at the hybrid network. If the access traffic stream consists of bursty arrivals, assembling these smaller frames into larger bursts may result in a smoother burst arrival at the hybrid nodes. The smoothness of the burst arrival rates and burst holding-times can be varied by adjusting the timer value associated with the burst assembler. The value of the assembler timer may be limited by the delay requirements at the edge node.

Optical bursts may also be created by fragmenting large input frames into smaller bursts and ‘dispersing’ them along primary/channels. Fragmentation causes the opposite effect of burst assembly, namely it offers a peaked traffic to the hybrid network. Both the assembly and segmentation processes at the access-hybrid core interface will tend to equalize input traffic characteristics, in order to conform to the operational requirements of the hybrid network.

3.6.1 TRAFFIC ADAPTATION AT THE EDGE-CORE INTERFACE

OBS enables traffic adaptation to make it possible to realize all-optical switching, along with statistical multiplexing at the core network. Typically, OBS performs packet assembly at the edge node. In the proposed hybrid network architecture, traffic adaptation is performed only at the edge node. Traffic adaptation can be the assembly of small packet/frames or the segmentation of large frames/streams. It is also assumed that each traffic source may differ with the kind of traffic adaptation it uses.

3.6.1.1 ADAPTING TRAFFIC ARRIVAL DISTRIBUTION By adjusting the Peakedness of the traffic-arrival process, it may be possible to realize the required overflow advantage for a

hybrid path. It is possible to come up with situations where the cost ratio of a path remains fixed and it may not be possible to realize hybrid operation. But traffic adaptation can help shape the traffic arrival process, in order to make it possible to realize optimal hybrid operation for the given cost ratio.

Figure 3.19 shows the time sequence of the assembly process. It is assumed that each source offers packets/frames via multiple input channels to the hybrid core node. At $t = 0$, the assembly begins with the arrival of the first packet/frame. At $t = t_1$, the second packet/frame arrives with an inter-arrival time of t_2 . The inter-arrival time distribution of packet/frame arrival may be described by a second-order-hyper exponential process [44]. By time T , the timer expires and a total of $N+1$ packets/frame arrive. After collecting $N+1$ frames, a burst is scheduled to be transported on the channel. At t_{n+1} , the next channel overflow arrives and a different assembly begins.

If the inter arrival distribution of the access traffic is given by a 2-order, hyper-exponential process, the burst inter-arrival time is a time shifted process of the packet inter-arrival time. The inter-arrival time distribution is given by :

$$\text{interarrival_time} = q_1 * \lambda_1 * e^{-\lambda_1 x} + q_2 * \lambda_2 * e^{-\lambda_2 x} ; \dots\dots\dots (3.10a)$$

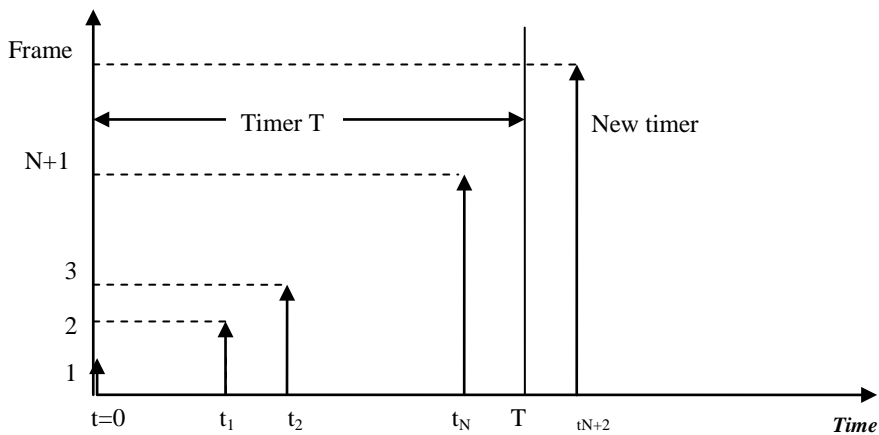


Figure 3.19 Timer based assembly process.

Where q_1 and q_2 are the probabilities with whether phase 1 or 2 of the arrival rates occurs. Phase1 can be assumed to be the on-state of the overflow process and phase2 the off-state. λ_1 and λ_2 give the mean on-rate and off-rate of the arrival process. It is assume that the on and off periods are exponentially distributed.

The mean and variance of the inter arrival time is given by:

$$\text{Mean_time} = \frac{q_1}{\lambda_1} + \frac{q_2}{\lambda_2} = \frac{1}{\lambda} \dots\dots\dots(3.10b)$$

$$\text{Variance_time} = 2 * \left(\frac{q_1}{\lambda_1^2} + \frac{q_2}{\lambda_2^2} \right) - \frac{1}{\lambda^2} \dots\dots\dots(3.10c)$$

The Burstiness of the arrival rates can be measured using the square coefficient- of-variation given by,

$$\text{Sq_coeff_of_variation} = \text{SCOV_arrival} = \frac{\text{Variance_time}}{\text{Mean_time}}$$

The burst inter arrival time is derived by time shifting equation (3.10a) by T.

$$\text{Mean_burst_time} = T + \text{Mean_time}$$

$$\text{Variance_burst_time} = \text{Variance_time} \dots\dots(3.11)$$

$$\text{Sq_coeff_of_variation} = \text{SCOV_arrival_time} = \frac{\text{Variance_time}}{\left(T + \frac{1}{\lambda} \right)^2}$$

3.6.1.2 ADAPTING CHANNEL HOLDING DURATION Traffic adaptation not only results in altering the arrival process, but it also alters the channel-holding distribution. Traffic assembly via a timer may result in a more deterministic channel holding duration. The process of segmentation does just the opposite; it creates a more stochastic component.

The frames/packet sizes are assumed to be exponentially distributed, with mean holding time of one unit if it is offered to the channels. In such a case, the burst holding time is given by the number of packets/frames assembled in period T. The average number of packets/frames assembled in time T equals the product of the average arrival rate and the timer value T plus one, to account for the first request that arrived when the timer began. The timer always begins with

the arrival of the first channel request. The variance of the burst holding-time is dependent on the convolution of frame service times [45].

$$\begin{aligned}
 \text{Mean_holding_time} &= n = \lambda * T + 1 \\
 \text{Variance_holding} &= 2n + 1 \\
 \text{SCOV_holding} &= \frac{1}{(\lambda * T + 1)^2} + \frac{2}{(\lambda * T + 1)} \dots\dots\dots(3.12)
 \end{aligned}$$

3.6.2 AN EXAMPLE

As an example, let's assume that each packet/frame is converted into an optical burst without any form of assembly. Let total burst traffic offered by each access source be 3 Erlangs with a Peakedness of 2. Let's assume that the offered traffic stream follows a hyper-exponential distribution, whose parameters can be mapped from its load values in Erlangs. Chapter 2 gives the mapping between the load in Erlangs, the Peakedness, and its corresponding hyper-exponential parameters.

The square coefficient-of-variations of the arrival process can be calculated using [equations \(3.11\)](#) and [\(3.12\)](#). Since we assume that the burst holding distribution is exponential, it *SCOV_holding* is one.

$$\begin{aligned}
 (\text{Avg.Load}, Z) &\Leftrightarrow 2\text{-order_hyperexponential}(q_1, q_2, \lambda_1, \lambda_2) \\
 (3, 2) &\Leftrightarrow 2\text{-order_hyperexponential}(0.6147, 0.3853, 18.718, 1.282) \\
 S_q\text{-coeff_var} &= \text{SCOV_arrival} = 3.25 \\
 \text{SCOV_holding} &= 1(\text{exponential}).
 \end{aligned}$$

Now, let's assume that the burst size is made big by assembling more packets/frames into a burst using a timer value of T=0.3 time units. In this case, using [equations \(3.11\)](#) and [\(3.12\)](#), the *SOCV_arrival* and *SOCV_holding* are 0.9 and 0.95 respectively. An *SOCV_arrival* of 0.9 suggests a nearly Poisson arrival-rate of the assembled burst. The holding-time distribution is slightly smoother than the exponential distribution. If we approximate holding time distribution

to be exponential, then assembly process leads to an offered load of 3 Erlangs and Peakedness of approximately one, to be offered to the hybrid path.

Smoothing the arrival process leads to greater overflow gain, which is greater than the gain obtained by retaining the Peakedness of offered access traffic. Compared to the optimal overflow gain of the original offered traffic, the smoothed traffic can provide the same optimal overflow gain with a greater number of primary channels. For instance, it can be observed in [Table 3.2](#) that for an overflow gain of .65 to be optimal, it requires 0 primary channels if offered load is 3 Erlangs, with a Peakedness of 2. If Peakedness is reduced to 1, it takes 2 primary channels to support an optimal overflow gain of .65. A given value of optimal overflow gain corresponds to a fixed cost ratio, as in [equation \(3.9\)](#). Thus, smoothing allows a hybrid path to achieve optimality for a given cost ratio by adding more primary channels.

The addition of primary light-paths, implies better end to end blocking performance for the traffic source. Smoothing the arrival process also implies an additional assembly delay at the edge node. This is the performance penalty paid in order to achieve optimal operation along with better blocking performance.

Segmenting the offered traffic frames provides an effect opposite to that of smoothing. Segmentation may cause an increase in traffic burstiness of the traffic offered to the hybrid network. If we assume the cost ratio of the path is a constant, segmentation serves to decrease the primary channels in order to provide optimal hybrid path. From [Figures 3.17](#) and [3.18](#) it is seen that the feasibility of hybrid operation extends over a wider range of cost ratios if the traffic offered to the Hybrid Node is more peaked. Segmentation, however, affects the blocking probability attainable with an optimal hybrid path.

3.7 CONCLUSION

A hybrid path consisting of primary and overflow channels may result in greater cost-effectiveness than purely OBS or OCS paths. Cost optimality of a hybrid path is found to depend on several factors such as traffic-load characteristics, the number of traffic sources and the relative costs of a primary and an overflow path. It is seen that optimal hybrid operation of a

hybrid route occurs when the incremental cost of adding a primary path to each source is equal to the corresponding decremented cost of channels in the overflow path.

The optimality condition for hybrid routes is related to the offered load statistics via a ratio called overflow gain. Overflow gain is the reduction in the number of overflow channels accessed by a traffic source for each addition of a primary light-path per traffic source. Overflow gain increases with an increase in the average load offered to the primary channels. Overflow gain also increases when the Peakedness of the offered load decreases. In both these cases, addition of a primary channel will result in a substantial reduction of number of overflow channels. Hence, for an optimal hybrid operation, the path cost ratio, decreases, with an increase in the smoothness of load and with an increase in the average offered load. In addition to the offered load, the optimality condition also depends on the number of sources sharing the overflow channels. If there are more number of sources sharing the overflow channels, the aggregate load that appears on the overflow channels will appear smooth. However, overflow gain decreases when there are more sources sharing the overflow channels.

The optimality condition shows that overflow gain has an inverse relationship with the path cost-ratio, which relates the relative costs of an overflow and a primary path. The feasibility of hybrid operation depends on the range of cost ratios for which hybrid operation remains cost-effective (optimal). The feasibility of hybrid operation increases whenever overflow gain decreases, either due to an increase in the Peakedness of the load offered to the primary channels or due to an increase in number of sources sharing the overflow channels.

The optical burst formation process may manipulate the smoothness of traffic offered to the hybrid network. The assembly or segmentation of packets/frames arriving via multichannel access channels form bursts. This burst assembly process may smooth the access traffic offered to the hybrid path; and such smoothing can cause an increase in overflow gain. With an increase in overflow gain, optimal hybrid operation is achieved with a greater number of primary channels for a hybrid path with a fixed cost ratio. Burst formation by segmentation of access frame results in an optimal hybrid path with fewer primary channels. With an increase in Peakedness, hybrid operation becomes cost- optimal over a larger range of cost ratios.

In this chapter, the cost ratio of a hybrid route is assumed a constant, even if number of primary channels is varied ([Figure 3.15](#)). However, it possible that cost ratio is a function of number of primary channels provided per source, or on the load per primary channel

(utilization). In such a case, the cost ratio of a route, whose value depends on the possibility of light-path entry within the path, may vary for different values of primary channel utilization. In Chapter 5, the cost of a hybrid network is analyzed by considering the possibility of light-path entry within a hybrid path.

The cost ratio of a hybrid route depends on the cost of a path within a switching node. The cost of a switching node may be sensitive to the number of incoming and outgoing channels from the switch ports. The number of incoming and outgoing channels from a switch depends on the number of primary and overflow channels in the links. In Chapter 4, it is shown that the cost of switching, expressed as number of switching elements used to construct the switch, depends on the number of input and output channels and also on the fabric architecture of the switch.

4.0 DESIGN AND ANALYSIS OF A HYBRID CORE NODE

4.1 INTRODUCTION

A basic Hybrid-Node, allocates incoming optical bursts, onto outgoing primary and overflow channels. In order to perform such an operation, the core node should at least be able to switch an incoming traffic entity to an appropriate output channel. In addition to its switching capability, the core node is attached to a network control plane. The control plane routes the traffic entity across the network and schedule incoming traffic onto appropriate switch outputs. In this chapter, the switching operation of a Hybrid Node will be considered and the resulting hardware complexity of constructing such a node will be analyzed.

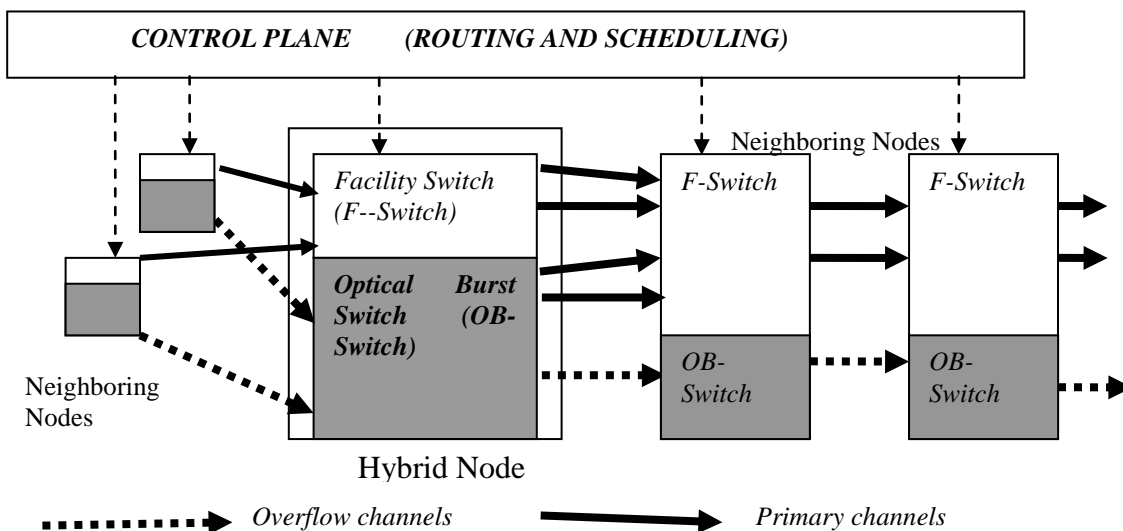


Figure 4.1 A Hybrid-Node switch

[Figure 4.1](#), depicts a Hybrid-Node switch, that contains a facility switched cross-connect, and called the F-Switch and the optical burst switch called the OB-Switch. Although not shown in the figure, in addition to the F-Switch and the OB-Switch, the core node contains devices such as wavelength interchangers/converters, multiplexers /de-multiplexers etc, which are associated with channel transmission. The input ports of the OB-switch connect to incoming overflow channels from the neighboring nodes. The output ports of the OB-switch are attached to outgoing primary and overflow channels, shown by the dotted and dark lines, respectively. The main function of an OB-Switch is to groom/pack primary light-paths and overflow channels, beginning at the Hybrid Node.

The F-switches help cross-connect incoming and outgoing primary channels that form a primary light-path. The primary light-paths that traverse an F-Switch, are groomed at a previous Hybrid Node, which initiates the primary path began. In this chapter, the cost of an F-switch is assumed to be negligible compared to the cost of an OB-Switch. Therefore, in order to optimize the cost of a Hybrid-Switch, it is important to focus on the design and analysis of the OB-Switch. Thus, the main focus of this Chapter will be on the design and analysis of the OB-Switch that constitutes a Hybrid-Node.

The core nodes are controlled by a control plane that may be either distributed or centralized. The control plane makes routing and scheduling decisions prior to connecting each input channel to the appropriate output channel. Once the appropriate output channel is selected by the control plane, the OB-switch fabric is configured to provide an ‘internal path’ between the input and output ports. The ‘internal path’ is configured within an OB-switch fabric by setting appropriate switching elements. The OB-switch elements are each controlled electrically by the switching logic circuit. In addition to the OB-switching elements, there are amplifiers and wavelength converters associated with the OB-switch hardware.

The size of the switching hardware (in terms of number of switching elements in the OB-switch fabric, amplifiers and wavelength converters) constitute the most expensive part of a core node. Thus, assuming that the OB-switching operation is the most expensive part of a Hybrid Node operation, it can be assumed that the cost of primary and overflow layers can be weighed by the associated OB-switching costs, in addition to the channel transport costs.

The total hardware cost of a Hybrid Node may be represented by [equation 4.1](#). The hardware cost includes all switching and transport costs for primary and overflow channels.

$$Total_Cost = T_p + S_p + T_{ov} + S_{ov} + K_{fac} \dots\dots\dots (4.1)$$

T_p and T_{ov} are the transport (channel) costs of outgoing primary and overflow channels that begin at the Hybrid-Node, respectively. S_p and S_{ov} are the OB-switching costs (along with the cost of wavelength converters and amplifiers) for primary and overflow channels respectively. In [equation \(4.1\)](#), it is assumed that the cost of the F-switch and the outgoing facility switched channels is a constant, K_{fac} , which does not depend on the Hybrid operation of the core node in which it is located.

Total cost is obtained minimized with respect to the number of primary channels, for a given value of outgoing primary channel, p , and a corresponding value of overflow channel, ov , by differentiating [equation \(4.1\)](#) as follows:

$$\frac{\Delta Total_cost}{\Delta p} = \frac{\Delta T_p}{\Delta p} + \frac{\Delta S_p}{\Delta p} + \left(\frac{\Delta T_{ov}}{\Delta ov} * \frac{\Delta ov}{p} \right) + \left(\frac{\Delta S_{ov}}{\Delta ov} * \frac{\Delta ov}{\Delta p} \right) + \frac{\Delta K_{fac}}{\Delta p} = 0$$

or,

$$\frac{\Delta T_p + \Delta S_p}{\Delta p} + \frac{\Delta T_{ov} + \Delta S_{ov}}{\Delta ov} * \frac{\Delta ov}{\Delta p} = 0 \dots\dots\dots(4.2)$$

or,

$$\left(\frac{\Delta T_p + \Delta S_p}{\Delta p} / \frac{\Delta T_{ov} + \Delta S_{ov}}{\Delta ov} \right) = - \frac{\Delta ov}{\Delta p}$$

The above equation gives the condition for obtaining minimum total cost of the core node. If either p , or ov is non-zero, the core node can be considered to be a Hybrid Node. If a particular value of $\{p, ov\}$ provides minimum cost, then the point of optimality is found when the ratio of incremental hardware (transport and switching) cost of primary channels to the

incremental hardware cost of overflow channels is equal to the negative of the slope of the overflow channels curve given by $ov = f(p)$.

The rest of this chapter focuses on determining the total cost of a core node for a given set of values of $\{p, ov\}$ and a given overflow blocking probability B:

$$ov = f(p,B).....(4.3)$$

The design of the OB-switch will be discussed in part A of this chapter. The OB-switching fabrics that may be constructed using some well-known architectures such as Broadcast-Select, Benes etc. Part B of this chapter will analytically determine the total cost of a Hybrid Node, whose OB-switch design is proposed in part A.

The main goal of this chapter is to determine if hybrid operation can help minimize the total cost of a core node, compared to a core node that performs a non-hybrid operation. [Equation \(4.2\)](#), which states a condition for optimal hybrid operation, is tested for different OB-switch fabric architectures. A metric called *Hybrid Cost Advantage* is used to quantify the benefit of hybrid operation in minimizing OB-switching cost. The sensitivity of the hybrid cost advantage is analyzed for different switch fabric architectures, different offered loads, and core-node cost parameters.

PART A

4.2 ARCHITECTURE OF A HYBRID CORE NODE OB-SWITCH

A Hybrid Node OB-switch is an all-optical fabric that switches a large number of input channels (overflow only) to outgoing primary and overflow channels. In its most basic form, an optical OB-switch that connects F input fibers to F output fibers, each with w wavelengths, consists of

five stages [45]. These stages are de-multiplexing, wavelength interchange/adaptation, space switching, wavelength interchange/adaptation and a multiplexing stage, as shown in Figure 4.2.

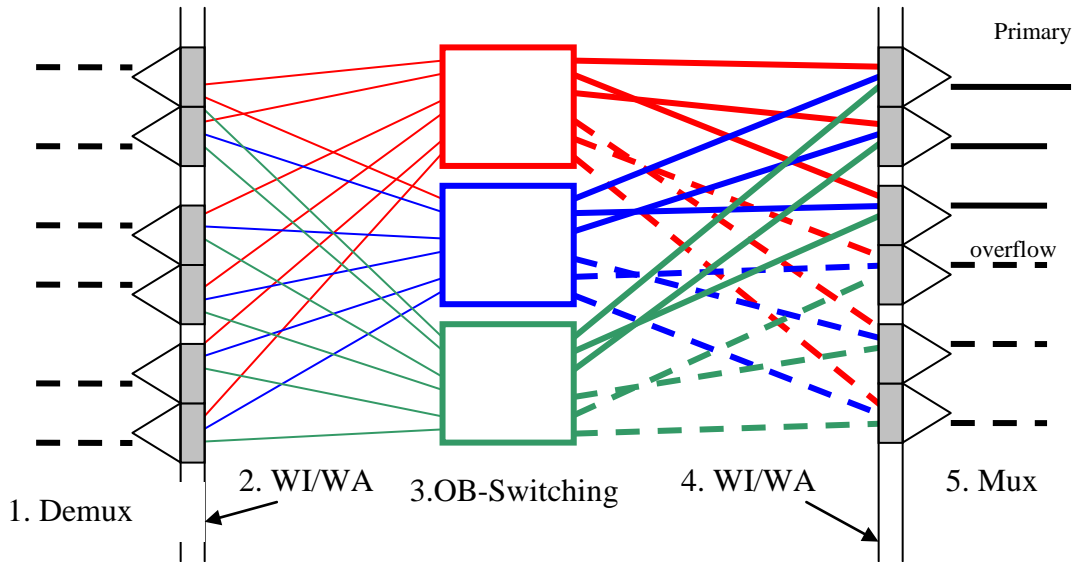


Figure 4.2 Five stages of a Hybrid Node.

[Figure 4.2](#) shows that incoming ‘overflow’ fibers are each de-multiplexed into their constituent (3) wavelengths using a de-mux (de-multiplexer). The wavelength channels may then undergo a wavelength interchange (WI) if there is channel contention at the output. Wavelength adaptation (WA) may be needed for multi-vendor equipments, or if the set of output wavelengths are different from the input ones. In stage three, space switching is performed.

The OB-switching stage in [Figure 4.2](#) is made of OB-switches, each tuned to operate on single wavelength. In the figure, there are three OB-switches operating on red, blue and green wavelengths. The OB-switches are used to switch incoming channels (overflow only) to outgoing primary and overflow channels. Thus, an OB-switch of [Figure 4.2](#), consists of two stages, which are the primary and overflow switching stages, as shown in [Figure 4.3](#).

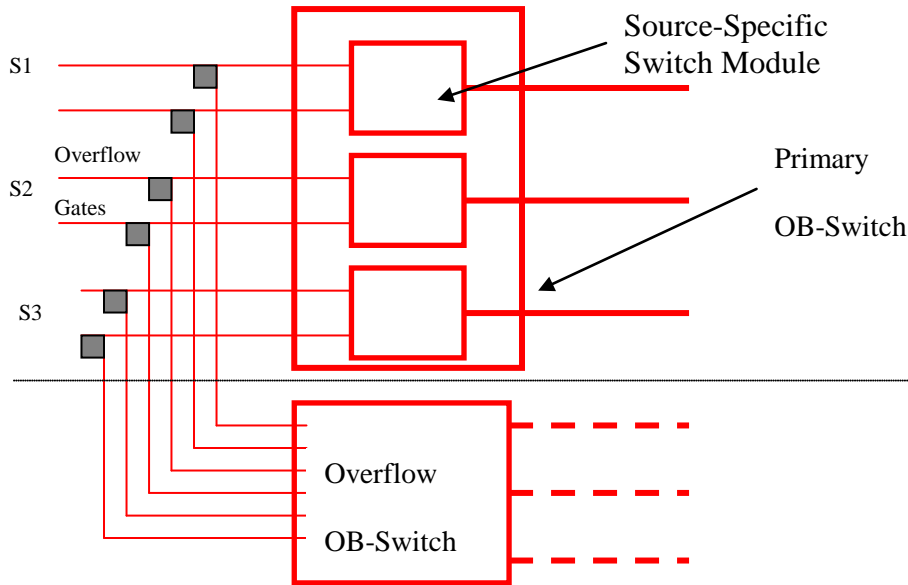


Figure 4.3 Primary and overflow layer of an OB-Switch

The OB-switches operate on a particular wavelength and in [Figure 4.3](#), the primary space switch (operating on the red wavelength) connects two input fibers of each source, to one primary output fiber (shown by the dark lines on the output of the primary OB-switch). In the same figure, the overflow switch connects the three inputs, S1, S2 and S3, to three outputs (shown by the dotted lines at the output of the overflow OB-switch). The primary OB-switch in [Figure 4.3](#) is shown to contain three mutually exclusive, *source-specific switch modules*. Each of these *source-specific switch module* is a space switch fabric between each input channel group (S1, S2 and S3) and their respective output primary channels. Section 4.2.1 explains the need for source specific modules in a primary OB-switch and the reason for their absence in an overflow OB-switch.

In some designs, it is also possible to contain wavelength interchange/ adaptation succeeding the space switch, as shown in [Figure 4.2](#). In such a case, receivers of the next hop node should be tuned to the appropriate wavelengths as the transmitter, in the preceding hop. In the fifth stage, the wavelengths are de-multiplexed.

The primary and the overflow layers of the OB-switch are connected by optical splitters/1x2 switches. While the splitter is a passive device, the 1x2 switch is an active device,

which is set up by the switch control layer. The space switch fabric of the primary and overflow OB-switches are disconnected except for the splitter/1x2 switches.

4.2.1 PRIMARY AND OVERFLOW OB-SWITCHES

A primary OB-switch consists of source-specific switch modules, while an overflow OB-switch does not contain any. The primary channel assignment is such that, output channels are exclusively assigned to a group of input channels (shown as S1, S2 and S3 in Figure 4.3). Therefore, a source-specific switch module in a primary OB-switch provides a space switching fabric, to switch input channels of a group, to its respective output primary channels. Unlike the primary channels, the overflow channels are shared by all sources (input groups) and hence, they do not require source-specific switching modules.

[Figure 4.4](#) shows an example containing output channel and output fiber assignment, to explain why source-specific switch modules are required in a primary OB-switch. In [Figure 4.4](#), there are two wavelengths per input and output fibers and there are two sources (input groups), S1 and S2 and two destinations, D1 and D2. The primary path from S1 to D1 are made of channels R1 and B1, which is part of output fiber 1 and channel R2 of fiber 2. Primary channels from S1 to D2 are made of channels R3 and B3 of fiber 3 and channel R4 of fiber 4. Similarly, for source S2, channels R5, B5 and B2 are the primary channels to D1 and channels B4, R6 and B6 are the primary channels to D2. The primary channel assignment between each source and destination is shown in the table within [Figure 4.4](#).

[Figure 4.4](#) shows the required interconnections in primary OB-switches that operate in R and B wavelengths. For instance, Source S1 uses the R wavelengths, which are R1, R2, R3 and R4 to switch to destinations D1 and D2. The same source uses the B wavelengths B1 and B3 to switch to D1 and D2. Thus, the primary OB-switch requires a 3x4 switch fabric to interconnect S1 with D1 and D2 in R wavelength and it requires a 2x2 switch fabric in B wavelength. These switch fabrics are independent of the switch fabric used to interconnect S2 to its primary channels. Thus, the primary OB-switches are source specific, as shown in [Figure 4.4](#).

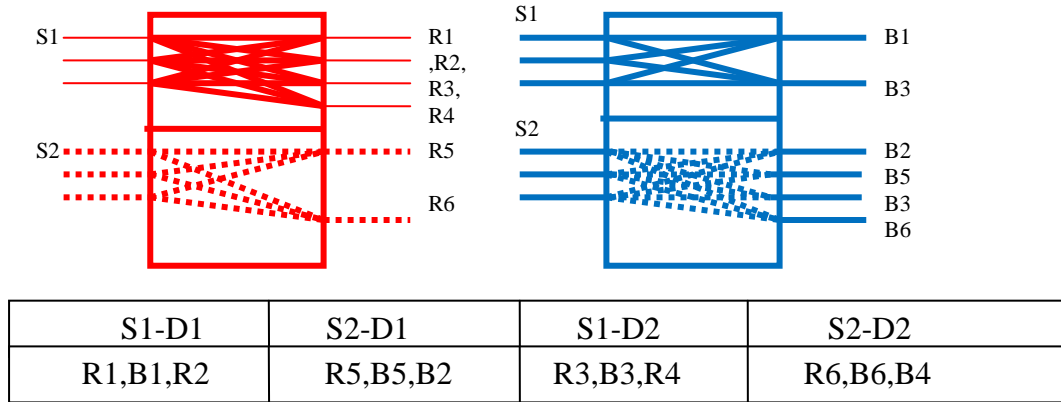


Figure 4.4 Source-specific switching modules in a primary OB-switch.

If all the traffic sources have identical primary channel requirements, as assumed in this chapter, the primary space switches are replicated as many times, as there are traffic sources. In addition, due to the space switches being wavelength specific, there is further replication of primary space switches for different wavelengths. For instance, there are two traffic sources and two wavelengths in the primary OB-switch of Figure 4.4 and therefore, there are four source-specific switches. Altogether, the primary layer consists of several independent source-specific switch modules. It is an important property of the primary layer that a ‘source-specific primary switch’ module is not interconnected to any other ‘source-specific primary switch’.

While the primary layer separates primary channel groups and switches among the traffic sources, the overflow layer does just the opposite. The overflow channels are shared by all traffic sources and the overflow switch aggregates all input channels to a common set of output channels. The space switch enables sharing of overflow channel among all the traffic sources. Thus, there is a requirement to create switch modules, in which all input fibers (of all sources) are connected to all output fibers, without the formation of any exclusive groups. However, like the primary OB-switch, the overflow-layer OB-switch is wavelength specific and the space-switches have to be replicated as many times, as there are wavelengths.

A hybrid core node differs from a non-Hybrid Node, due to the presence of the primary and overflow-layer space switches with the OB-Switch, which is depicted in [Figure 4.1](#). For all other operations other than the space switching function, such as wavelength conversion and multiplexing /demultiplexing, Hybrid and non-Hybrid Nodes are alike. Thus, it is the space-

switch stage of the core node OB-Switch that characterizes hybrid operation. Such a partitioning of space switch fabric may lead to different cost characteristics of the primary switch, S_p and the overflow switch, S_{ov} . In part B, values of S_p and S_{ov} are analyzed for various switch fabric architectures of the primary and overflow layer modules. Meanwhile, the rest of part A will explain the design of the space switch modules in the primary and overflow layers of the OB-Switch. Practical implementation issues for a Hybrid Node cross connect are also discussed in part A.

4.2.2 SPACE SWITCH ARCHITECTURE OF AN OB-SWITCH

In general, a ‘stand-alone space switch’ module is an entity that is not inter-connected to any other space switch module in the OB-Switch. For instance, the primary layer consists of source-specific switch modules that can be considered as stand-alone space switch modules. The overflow switch is also a stand-alone space switch module, whose inputs or outputs are not interconnected to any of the primary standalone modules. Internal architecture of a stand-alone space switch module may itself be modular, as in [Figure 4.5](#) . For instance, a standalone asymmetrical $K \times M$ space switch may be constructed using N number of symmetrical $M \times M$ modules, where N may be less than or equal to M .

Each $K \times M$ switch may be a standalone primary switch, dedicated to one source, or it may be a standalone overflow switch. If a $K \times M$ switch belongs to the primary layer, then M equals to the number of primary ‘fibers’ used to carry the primary channels. If the $K \times M$ switch is a stand-alone overflow switch, it has M equal to the number of overflow channels. For both, primary and overflow layers, the $K \times M$ switches are replicated as many times, as there are distinct wavelengths in the primary or overflow channel group. In [Figure 4.5](#), the shadow boxes show replication of a $K \times M$ space-switch into another two wavelengths.

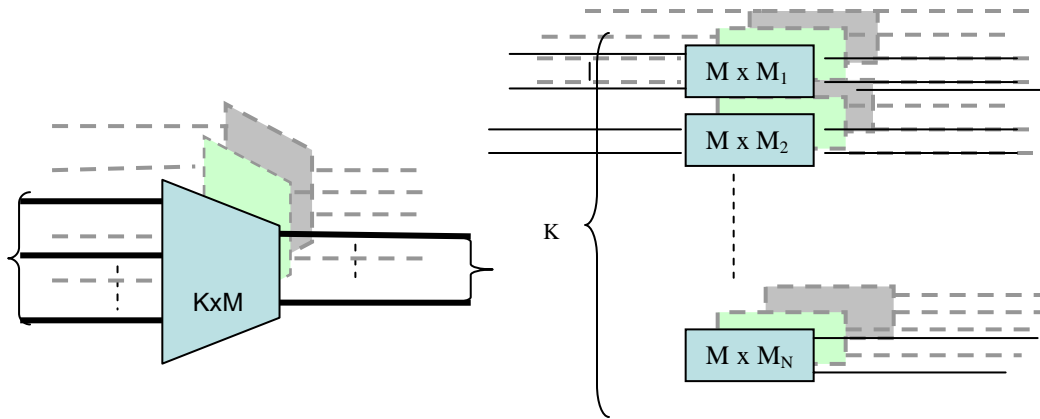


Figure 4.5 Constructing $K \times M$ space switches using $M \times M$ switch modules.

4.2.2.1 SYMMETRIC SWITCHES A symmetric $M \times M$, shown in [Figure 4.5](#), may be constructed using different kinds of ‘non-blocking’ switch fabric architectures. The $M \times M$ switch fabrics are non-blocking because there is an internal path for every input to output connection within the fabric. An internal path is formed by setting a certain set of elementary switches within the $M \times M$ switch fabric. An “ N -($M \times M$)” switch may be realized using a Broadcast-Select or Benes architecture, where N represents the number of wavelengths in the system and M the fiber input-outputs. In the two cases, the elementary switch is either a 1×1 switch or a 2×2 switch, respectively.

4.2.2.2 BROADCAST AND SELECT SWITCH An $M \times M$ switch may be constructed as per the Broadcast and Select architecture using fiber splitters, combiners and 1×1 gates. In B-S architecture, signal arriving on an input fiber are split M times and selected for an appropriate fiber output using a 1×1 gate. The 1×1 may be implemented as a wavelength selective cross-connect (WSC), as shown in [Figure 4.6](#).

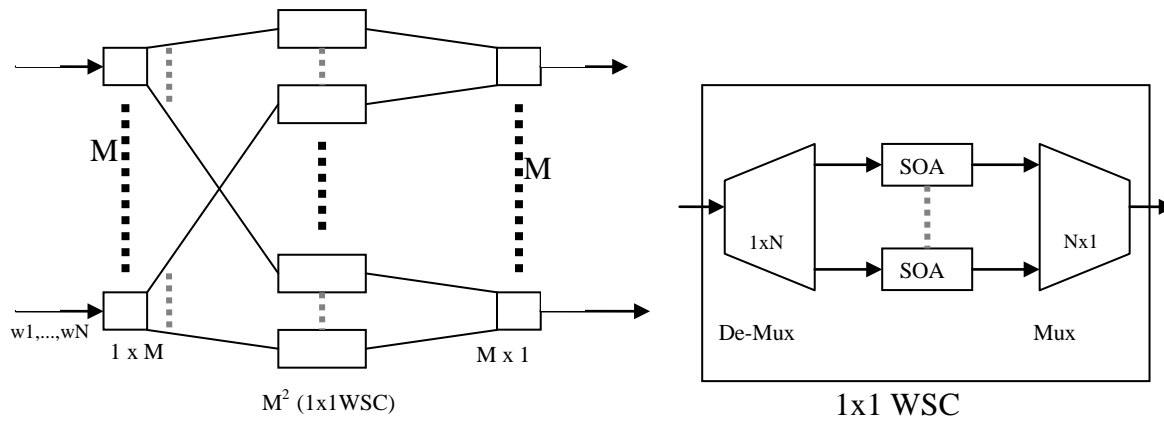


Figure 4.6 N- ($M \times M$), Broadcast and Select space switch using a 1×1 WSC.

The WSC may consist of an array of Semiconductor Optical Amplifiers (SOA), tuned to switch a particular wavelength [46]. The center-stage of a B-S switch contains M^2 WSC elements to provide a non-blocking performance. Since a 1×1 WSC has N SOAs in it, there are $N \times M^2$ SOAs in a strictly non-blocking multi-wavelength space switch. The B-S architecture also provides a multicasting capability. Signal on a particular channel of an input fiber can be sent to multiple output fibers by setting appropriate SOA, on appropriate WSCs. A B-S space switch along with wavelength interchangers can provide multicasting of an input signal on several output channels.

An SOA device provides gain-based switching by controlling the current provided to the device. Since the switching speed of an SOA, is less than a micro-second, they can be used to provide fast reconfiguration in the cross-connect. An array of SOAs, along with the mux-demux used to construct a WSC, can be monolithically integrated using InP [47]. Monolithic integration of SOAs in InP is attractive due to compactness and cost of production. In order to ease coupling the active SOA arrays with the passive Mux-Demux, hybrid integration can also be performed. Hybridization of SOA arrays on silicon motherboard provides a more scalable approach than monolithic integration [49]. Also, the hybrid silicon platform may contain passive devices along with the SOAs, in order to provide greater functionality. For instance, the De-mux/mux, which are passive devices can co-exist with active SOAs in a hybrid scheme.

A B-S switch also contains passive elements such as splitters and combiners. Passive splitters can cause power loss of signals arriving on WSCs. In the analysis, we may assume the

splitters to be independent elements connected to the WSCs using fiber. There is power loss of about 10 dB at the fiber interface between the splitters-combiners and a WSC.

4.2.2.3 BENES ARCHITECTURE Benes architecture can be constructed using basic 2×2 switching elements, as shown in figure 4.6. A Benes fabric can provide re-arrangeable non-blocking performance with lowest number of cross-points, possible to attain non-blocking performance. Multi wavelength Benes switch can be fabricated using Optical Add-drop multiplexers (OADMs), as shown in [Figure 4.7](#).

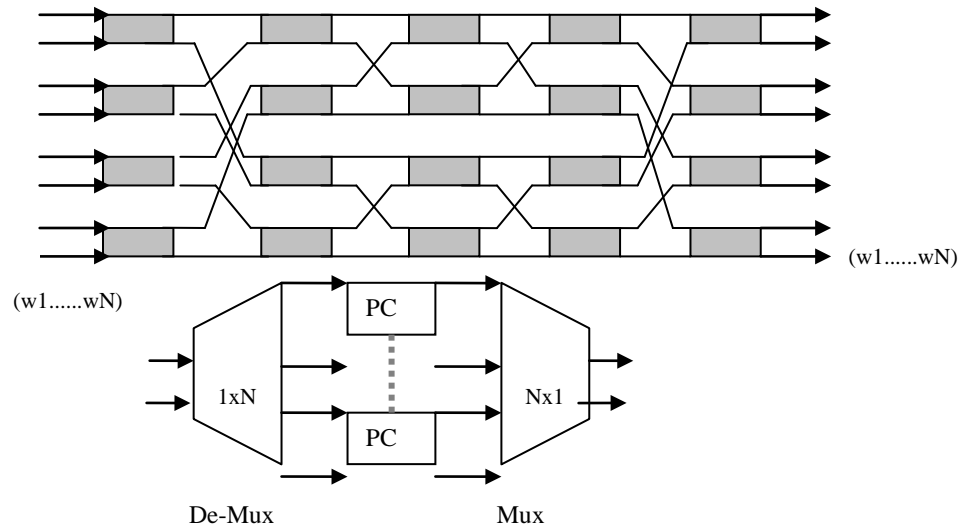


Figure 4.7 N-(MxM) Benes space switch using a 2x2 Optical Add Drop Multiplexer (OADM).

An OADM is a 2×2 switching device that can be put in either a cross or a bar state [45]. The 2×2 device may be realized using directional couplers such as those based on SOAs, integrated on a single chip. Once again, the 2×2 active switch can be integrated with other passive elements such as mux/demux.

Compared to B-S switch, a Benes switch of comparable size will need more stages, as well as, more interconnections among stages. For an $M \times M$ switch, total number of Benes stages is $2\log_2 M - 1$. While a B-S switch needs M^2 WSCs, a Benes needs $M(2\log_2 M - 1)/2$. However, complexity of a 2×2 WSC is roughly twice that of a 1×1 WSC. An $M \times M$ B-S switch needs M^2 fibers to interconnect the splitter to the switching stage. On the other hand, a Benes switch of

comparable size needs $4 \times (\text{number of } 2 \times 2 \text{ WSC})$ fibers to interconnect the 2×2 WSCs. The fiber interconnections introduce loss, at the junction of fibers and WSCs, within the switch fabric. Thus, integration of as many active elements on a single chip can minimize fiber interconnections and yield lower loss within the switch.

4.2.2.4 CLOS INTERCONNECTION ARCHITECTURE Integrated 4×4 or 8×8 space switches have been realized on Lithium Niobate/ Indium Phosphide substrates [49]. These space switches can be realized using the Benes / dilated Benes internal architecture, which in turn can be interconnected under Clos architecture to realize larger $M \times M$ switches. The Clos architecture consists of three stages, as shown in Figure 4.8, where the switch fabric provides a re-arrangably non-blocking performance.

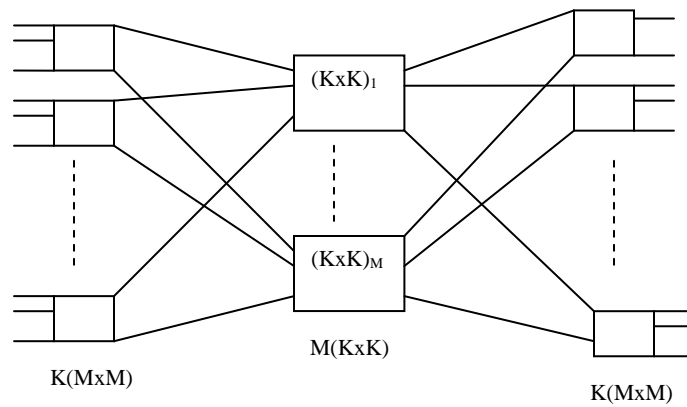


Figure 4.8 Clos interconnection architecture

4.2.3 WAVELENGTH INTERCHANGERS

In a hybrid OB-switch, channel contention is solved by using full-range wavelength interchanger. An N wavelength interchanger is constructed by de-multiplexing the N channels and individually converting the channels to the required wavelength using wavelength translators. Power combiners may be required at the output. The translators can be all optical non-linear devices or opto-electronic devices requiring tunable lasers [50]. Thus, wavelength combiners are expensive components requiring N active elements.

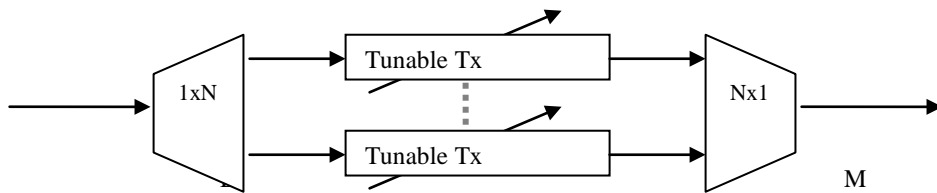


Figure 4.9 A Wavelength Interchanger

Wavelength interchangers are placed either near the input or near the output of the hybrid switch. In either case, the fiber wavelengths should be compatible with the ones in the succeeding or preceding Hybrid Nodes, respectively. A wavelength adapter is yet another class of tunable device that may be needed either at the input or at the output of a node to realize wavelength conformity among the nodes. It is assumed in the dissertation that wavelength compatibility among nodes already exists and that wavelength adapters are not part of the design. However, wavelength interchangers will be included in the design in order to realize non-blocking performance in the node.

4.2.4 REALIZING OVERFLOW PROCESS IN A HYBRID SWITCH

A Hybrid-Node OB-Switch is characterized by the overflow process that links the primary layer to the overflow layer. Overflow is realized either by active 1x2 switches, or by passive 1 x 2 splitters and the two schemes will be henceforth called, active and passive overflows, respectively. While the active 1x2 switches use an SOA switch array for every input channel, a passive splitter is required for every input fiber.

In both cases, wavelength interchange can be performed in the input or output side of the space switch. Active overflow switches (1x2 switches) may also be placed within the integrated chip that performs wavelength interchange, at the input side.

Active 1 x 2 switches may be realized by setting gain-based switches, as shown in [Figure 4.10 b](#). The switches are placed at the input side of the switch , after the input fibers are de-

multiplexed and the channels are passed through the tunable transmitters for wavelength translation. In the passive overflow scheme, 1:2 splitters are present at the input fibers. [Figure 4.10](#) shows such an arrangement, where splitters are placed after the wavelength interchangers. Such a scheme may lead to splitting loss, which may need to be compensated within the core node switch. If the space switch is B-S, there is an additional splitter within the B-S fabric, which can be combined back to back, with the 1:2 overflow splitter.

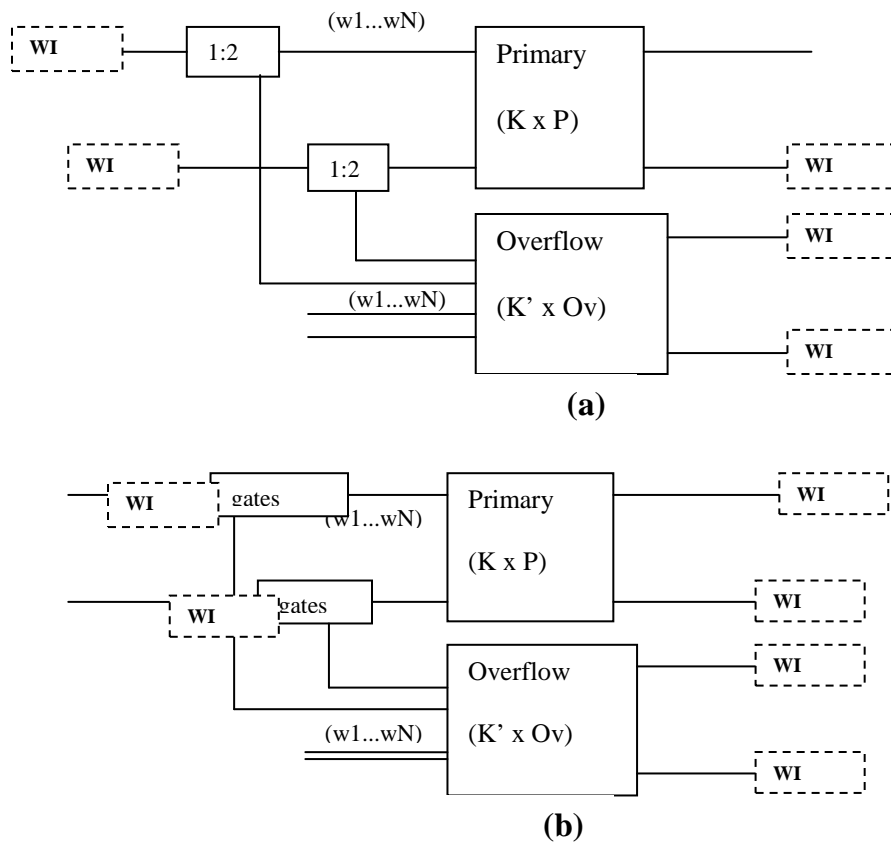


Figure 4.10(a). Passive overflow using 1:2 splitters. **(b)** Active overflow using gates.

Thus, the choice between active and passive overflows would primarily depend on loss occurring within the core node and the impact of the number of overflow gates in realizing cost effectiveness in the node. Loss offered by the overflow process depends on several features such

as integratability of 1x2 switches, choice of space switch architecture and placement of wavelength interchangers within the core node.

4.3 SUMMARY OF HYBRID NODE SWITCH DESIGN CHOICES

There are several design choices in order to implement the OB-Switch of a Hybrid Node. The design choices may be based on the architecture of the MxM switch and the granularity of the basic space switch element used to construct an M x M switch. In addition to the space switch, the overflows can be implemented using active gates or by using passive splitters. The active switch arrays can be monolithically integrated or it can exist as a standalone element.

In order to analyze the cost of an OB-Switch, three main architectures for the standalone M x M switch were considered. They are, B-S, Benes using OADMs and Clos architecture using integrated switches. While the B-S architecture will provide strictly non-blocking performance, Benes and Clos will be considered for re-arrangably non- blocking [43]. Also, the three architectures differ in the granularity of basic switching elements used. The B-S architecture may use 1 x 1 SOAs, either as standalone elements or as an array of multi-wavelength gates, integrated on a chip. The Benes architecture uses, 2 x 2 OADM modules, which like the 1 x 1 gates can be implemented as an array of multi-wavelength switches. The Clos architecture is used to interconnect elements of larger size, like a multi-wavelength 4 x 4 switching element.

Wavelength switching will be performed using wavelength translators, as shown in [Figure 4.9](#). Wavelength Interchangers may be placed either at the input or at the out put side of the space switch. In the analysis, wavelength interchangers are placed at the output side, in order to study the cost effect of varying primary and overflow channels.

In addition to the space switch, overflow 1x2 switch/splitter and wavelength converters, there might also be amplifiers to combat losses within the core node. Erbium- doped fiber/ SOA amplifiers will be placed whenever there is a 30 dB net loss in the core node. In addition, an EDFA/SOA could be placed at the core node inputs to overcome power loss during transmission.

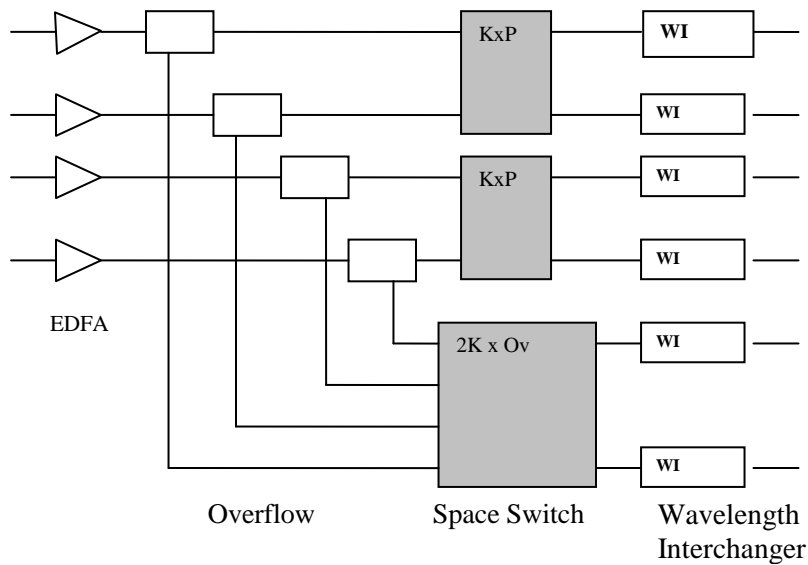


Figure 4.11 Hybrid Node architecture, considered in the analysis.

[Figure 4.11](#) shows the Hybrid Node architecture considered from a high level. There are two sources, each with K fibers on the input side of the node. [Table 4.1](#) shows some of the methods used to realize the architecture in [Figure 4.11](#). Part B of this chapter will analyze the cost of a Hybrid Node, in terms of elementary switch modules, for the design choices outlined in [Table 4.1](#).

Table 4.1 Design choices considered for the Hybrid Node analysis.

Overflow	M x M Space Switch	Wavelength Interchanger
Active	Broadcast and Select (strictly non blocking)	Integrated multi wave-length Tunable transmitters
<i>Integrated Gates</i>	<i>Non integrated 1 x 1 SOA</i>	
<i>Standalone Gates</i>	<i>Integrated multi-wavelength 1 x 1 SOA arrays.</i>	

<p>Passive</p> <p><i>1:2 Splitters</i></p>	<p>Benes (Re-arrangably non-blocking)</p> <p><i>Integrated multi-wavelength 2 x 2 OADMs</i></p> <p><i>Clos (Re-arrangably non-blocking)</i></p> <p><i>Integrated multi-wavelength 4 x 4 switches</i></p>	
---	---	--

PART B

4.4 ANALYSIS OF A HYBRID NODE SWITCH

Hybrid operation in a network calls for a Hybrid Switch architecture in the nodes, as represented in [Figure 4.1](#). Just like the Hybrid Routes, the OB-Switches within a Hybrid Switch are divided into primary and overflow OB-switches. The primary OB-switch is made of mutually exclusive source-specific switch modules and the overflow OB-switch interconnects all sources, as explained in part A of this chapter. In this part of the chapter, the effect of such a hybrid operation on the cost of a node is studied.

The cost of a Hybrid Node depends on both the switching and transport costs associated with the node. The transport cost associated with a node is primarily the cost of the receiver and transmitter ports associated with the Hybrid Node. The transport cost in a Hybrid Node is expected to scale linearly with number of output channels. Thus, transport costs depend on the sum of all primary channels and overflow channels. As the number of primary channels increases, the number of overflow channels (that provide a fixed blocking probability) decreases. However, with the increase in the number of primary channels, the total number of channels per Hybrid Node increases, which causes higher channel costs. Thus, transport cost is expected to increase with increase in number of primary channels.

Unlike transport costs (channel costs), the total switching cost may not increase/decrease linearly with an increase/decrease in the number of channels. For instance, the number of cross-points in a cross-bar switch has a square relation with the number of channels, while the number of cross-points in a Benes switch follows a log relation. A non-linear relationship between switch-size and channel-count suggests that the incremental increase in the cost of a switch is not the same for all channel counts. It means that while this increase in the number of primary channels leads to an increase in the primary switch cost, this increase may not always have a corresponding decrease, by the same amount, in the cost of an overflow switch.

Such differences in the incremental costs of switching at the primary and overflow layers suggest the possibility of an optimal point, where the total cost of switching is at a minimum. If switching cost dominates over other non-switching costs, the total cost of the node also attains a minimum value. Minimization of total cost, and the sensitivity of optimal operation to changes in the cost of non-switching components may strongly depend on the underlying switch fabric architecture and the load offered to the node. Thus, the goal of this chapter is to investigate the effect of the underlying fabric architecture and offered load values on realizing this minimum total cost in the core node by operating in hybrid mode. The sensitivity of the optimal hybrid operation on transport/channel cost components is also studied.

4.4.1 TOTAL COST OF A NODE

By performing cost analysis of a Hybrid Node, the benefits and/or penalties of hybrid operation are studied at the level of a core node. In this analysis, the cost of a facility switch and facility switched primary channels are assumed to be a constant and that they do not contribute to the optimality of the Hybrid-Node. In addition, the number of input channels is assumed to be a constant, while the number of output channels, which depends on the number of outgoing primary and overflow channels, is a variable quantity. Thus, the total cost of a Hybrid Node, which is equal to the sum of transport and switching costs, varies with the number of output channels. The transport costs of interest are the cost of the output ports/line cards, amplification, synchronization etc. for all the output channels. The switching cost is calculated in terms of the number of elementary ‘off the shelf’ switches used to construct the large core switch. It is assumed in this chapter that the number of elementary switching modules depends on the switching architecture, in addition to the number of primary/overflow channels.

4.4.1.1 COST COMPONENTS The total cost of a node is divided into two main parts, the channel-dependent cost and the switching cost. The channel-dependent cost results from any operation performed at the input and/or output channels. Such operations may include fiber amplification, synchronization, full-range wavelength conversation, signal regeneration etc. We can further classify the channel costs into input and output channel costs. In the analysis

performed in this chapter, it is assumed that the number of output channels varies with the number of primary and overflow channels, while the number input channels remains a constant.

Switching (space switching) costs result from any operation performed on both input and output fibers simultaneously. Such operations are the space switching operations and any amplification that may result from switching losses. The cost of a space-switching operation is quantified in terms of the cost of the elementary switching module used to construct the space switch. We define the following elementary switch modules:

- Array of w, multi-wavelength 1 x 1 switches per elementary module: ES_{1x1_w}
- Array of w, multi-wavelength 2 x 2 switches per elementary module: ES_{2x2_w}
- In general Array of w multi-wavelength N x N switches per elementary module: ES_{NxN_w}

The total cost of a core node can be expressed as the sum of three different costs, the cost of the input side, the cost of the output side, and the switching costs.

$$Total\ cost = Input\ costs + Switching\ costs + Output\ costs \dots\dots\dots(4.4)$$

Where *Input costs* = Cost of Input fiber ports, transmission, amplification, channel adaptation and synchronization.

And, *Output costs* = cost of output fiber ports, transmission, amplification/regeneration, channel adaptation, wavelength conversion

Both Input and Output costs are expressed as a function of the total number of input and output fibers respectively. Switching costs can be represented as a function of both input and output fibers.

$$Total\ cost = f(input\ fibers) + f(input\ fibers, output\ fibers) + f(output\ fibers) \dots\dots(4.5)$$

Since Input fibers are assumed to be a constant in this chapter, the only variable to determine total cost is the set of output fibers. Thus,

$$Total\ cost = K_{input} + K_{switch} * f_{switch}(output\ fibers) + K_{output} * f_{transport}(output\ fibers) \dots\dots\dots(4.6)$$

where, K_{input} , K_{switch} , and K_{output} are the constants associated with the input, switching, and output costs, respectively. $f_{switch}(output\ fibers)$ and $f_{transport}(output\ fibers)$ are the switching and transport functions that relate node costs to the number of output fibers, respectively. The number of output fibers is a variable quantity that depends on the number of primary and overflow channels assigned to the output links. Since the number of overflow channels is a function of the number of primary channels, as discussed in Chapter 3, we can re-write total cost as,

$$Total\ cost = K_{input} + K'_{switch} * f'_{switch}(p) + K'_{output} * f'_{transport}(p) \dots\dots\dots(4.7)$$

where, K'_{switch} and K'_{output} are the constants associated with the switching and output costs, respectively and $f'_{switch}(p)$ and $f'_{transport}(p)$ are the switching and transport functions that relate node costs to the number of primary channels. It is assumed that $f'_{transport}(p)$ is equal to the total number of output channels, given as,

$$f'_{transport}(p) = p * D * I + f_{Ov}(p) \dots\dots\dots(4.8)$$

where $f_{Ov}(p)$ is the total number of overflow channels that provide a fixed blocking probability for overflows from a given value of p channels per source-destination nodes; and D and I are the total number of destination nodes and source (input) nodes attached to the core Hybrid Node.

This cost analysis of a hybrid switch is classified into three main parts, based on the switching architecture used to construct the stand-alone MxM switch described in section 4.2.3. The three architectural choices are B-S, Benes and Clos. For each of these architectural choices, the two cases of implementing overflow, namely, active and passive overflow scheme are considered. For each case, the number of elementary SOA switches, ‘off-the-shelf’ integrated elementary switches, amplifiers and wavelength converters will be calculated.

4.4.2 COST ANALYSIS OF A HYBRID SWITCH

As described in part A of this chapter, there are several design choices for a hybrid core node switch. We consider multi-wavelength 1x1 or 2x2 switches as basic elements used to construct a switch. The cost of a Hybrid Node will be quantified in terms of the number of elementary switch modules.

4.4.2.1 CROSS POINTS IN A HYBRID SWITCH The cross points in the hybrid switch may be 1x1 switches for a B-S architecture or 2x2 switches for the Benes architecture. The number of cross-points in a hybrid switch may depend, not only on the space switch architecture, but also on external parameters, such as the number of traffic sources, fiber-links per source (neighbor node), wavelengths per fiber and destination nodes. We may denote these parameters as follows:

- Number of Input groups = I
- Number of fibers/input group = K
- Number of Destinations = D
- Number of next-hop nodes = G
- Number of wavelengths/Fiber = W

The internal variables that may affect size of a hybrid switch may be given by:

- Number of primary channels/source-destination beginning at the Hybrid Node = p
- Number of outgoing overflow channels = $v = f_{ov}(p)$

As discussed in part A of the chapter, the primary and overflow switches are assumed to consist of symmetric $M \times M$ switches. From our design choices, the switch architecture function for a standalone $M \times M$ switch, given as $S_{switch}(M)$, where

$$\begin{aligned}
 S(M)_{B-S} &= M * M \\
 S(M)_{Benes} &= M(2 * \log M - 1) / 2 \dots\dots\dots(4.9)
 \end{aligned}$$

Each input group, which corresponds to each traffic source, has all $W * K$ wavelengths connected to p primary channels. The asymmetrical primary space-switch(OB-switch), which has K input fibers and M_{prim} primary output fibers, is made of N_{prim} switches per input group which have M_{prim} ports, similar to what is shown in [Figure 4.5](#). The primary switch is used to interconnect input fibers to all the outgoing fibers used by the group. In order to determine the number of output primary fibers, the value of M_{prim} , is deduced from the given value of p . In fact, the value of p may not be an integral multiple of the number of wavelength per fiber W . There are m wavelengths out of W that have space switches with P_{large} output fibers and $(W-m)$ wavelengths that have space switches with P_{small} output fiber. The value of m is determined using the ‘floor’ function of the ratio of p and W as:

$$m = p - \left(\left\lfloor \frac{p}{W} \right\rfloor * W \right) \dots\dots\dots(4.10)$$

It is assumed that there are dedicated fibers to each destination. So, M_{prim} , can be expressed as:

$$M_{prim} = \{P_{small} * P_{large}\} ;$$

$$\text{where } P_{small} = \left\lfloor \frac{p}{W} \right\rfloor * D \text{ and } P_{large} = \left\lceil \frac{p}{W} \right\rceil * D \dots\dots\dots(4.11)$$

In the above equation, P_{small} and P_{large} is determined using the ‘floor’ and ‘ceiling’ functions respectively, on the ratio of p and W .

Due to P_{small} and P_{large} components of the set M_{prim} , the number of switches required to construct the asymmetrical primary space switches of size $K * P_{small}$ and $K * P_{large}$ are given by N_{prim_small} and N_{prim_large} , respectively as:

$$N_{prim} = \{N_{prim_small}, N_{prim_large}\}$$

$$\text{where } N_{prim_small} = \left\lceil \frac{K}{P_{small}} \right\rceil * (W - m) \text{ and } N_{prim_large} = \left\lceil \frac{K}{P_{large}} \right\rceil * m$$

$$\dots\dots\dots(4.12)$$

Assuming all input groups have same number of primary channels to all destinations, the total number of ‘primary’ elementary switches, C_p is given by,

$$C_p = I * (N_{prim_small} * S(P_{small}) + N_{prim_large} * S(P_{large})) \dots\dots\dots(4.13)$$

For the overflow switch, n out of W wavelengths possess V_{large} output fibers in total, going to all neighboring nodes and $(W-n)$ wavelengths possess V_{small} output fibers.

$$\begin{aligned} V_{small} &= \left\lfloor \frac{V}{W} \right\rfloor * G \\ V_{large} &= \left\lceil \frac{V}{W} \right\rceil * G \\ n &= V - \left\lfloor \frac{V}{W} \right\rfloor * G \end{aligned} \dots\dots\dots(4.14)$$

Once again, number of overflow switches may be either $N_{overflow_large}$ or $N_{overflow_small}$, where

$$\begin{aligned} N_{overflow} &= \{N_{overflow_large}, N_{overflow_small}\}; \\ N_{overflow_large} &= \left\lceil \frac{K * I}{V_{lar}} \right\rceil * n \dots\dots\dots(4.15) \\ N_{overflow_small} &= \left\lceil \frac{K * I}{V_{small}} \right\rceil * (W - n) \end{aligned}$$

The number of elementary switches in an overflow switch is given by

$$C_o = N_{lar} * S_{switch}(V_{large}) + N_{small} * S_{switch}(V_{small}) \dots\dots\dots(4.16)$$

In addition to the primary and overflow switches, there may be gates at the input to primary/overflow switches,

$$Gates = I * F * W \dots\dots\dots(4.17)$$

The Total number of cross-points/elementary switches in the core node is given by

$$Total_crosspts = Cp + Co + Gates \dots\dots\dots(4.18)$$

4.4.2.2 MULTIWAVELENGTH INTEGRATED SWITCH Integrating the arrays of elementary switches of multiple wavelengths, to a single substrate can minimize the number of interconnections and the loss within a switch fabric. Let W be number of switching elements of different wavelengths that can be integrated on a single chip. In this case, the total cross-points/elementary switch, as given by [equations \(4.11\),\(4.12\)](#) and [\(4.13\)](#) changes in the following ways,

$$\begin{aligned}
 M_{prim} &= P_{large} \\
 N_{prim} &= \left\lceil \frac{K}{M_{prim}} \right\rceil \dots\dots\dots(4.19) \\
 Cp_w &= N_{prim} * S(P_{large})
 \end{aligned}$$

Similarly for the overflow layer

$$\begin{aligned}
 N_{overflow} &= \left\lceil \frac{K * I}{V_{large}} \right\rceil \dots\dots\dots(4.20) \\
 Co_w &= N_{overflow} * S(V_{large})
 \end{aligned}$$

It is also possible to integrate the gates which gives total number of overflow gates as,

$$Gates_w = I * F \dots\dots\dots(4.21)$$

The Cost of a multi-wavelength 1x2 switch $cost(1x2_switch)$, is compared to the cost of an elementary switch $cost(ES_{NxN_W})$ by a cost ratio CR_{1x2_switch} ,

$$CR_{1x2_switch} = \frac{cost(1x2_switch)}{cost(ES_{NxN_W})} \dots\dots\dots(4.22)$$

4.4.2.3 WAVELENGTH CONVERTERS AND INTERCHANGERS A wavelength interchanger is a device that converts the wavelength of a channel. They are needed if there is contention among the bursts to access a particular wavelength. To construct a wavelength interchanger (WI) for W channels in a fiber, we need to de-multiplex the W channels and convert them individually. Each channel in the WI module passes through a tunable translator/transmitter, which are active elements. For a $K \times K$ switch, where each fiber has W wavelengths, a WI with W active elements makes the WI rearrangably non-blocking. The WIs may be provided at the input to each space switch, in which case number of active elements is equal to total number of input channels.

$$WI_{input} = I * W * K \dots\dots\dots(4.23)$$

Multi-wavelength integration of w wavelength translators on a single chip will yield:

$$WI_{input} = I * K \dots\dots\dots(4.24)$$

4.4.2.4 AMPLIFIERS Signal amplification may have to be performed within the switch fabric to overcome loss introduced by the switching elements. Let's assume that each integrated element introduces 10dB of splicing loss and that an amplifier can overcome 30dB of noise. Ideally, then, an amplifier is needed whenever the signal passes through three switching elements. The number of amplifiers Amp_{switch} required for an $M \times M$ switch depends on fabric architecture. The total number of amplifiers in core node composed of a general switch fabric 'switch' is given by,

$$Amp_{switch} = N_{lar} * Amp_{switch}(P_{lar}) + N_{overflow_lar} * Amp_{switch}(V_{lar})$$

Where,

$$Amp_{switch} = \{ Amp_{B-S}, Amp_{Benes} \} \dots\dots\dots(4.25)$$

In a Broadcast and Select switch, there is just one stage of space-switch elements, which will introduce about 10 dB noise. In addition, the passive splitter may split the power M times. Also, the degree of integration, as mentioned in Part A of this chapter, will affect the loss. The total loss between an input and output for an $M \times M$ B-S switch is given by:

$$Loss_{B-S}(K) = 10 + 20 * \log_{10}(K) \dots\dots\dots(4.26)$$

The number of amplifiers per $K \times K$ fabric is given by

$$Amp_{B-S}(K) = \frac{(K * Loss_{B-S}(K))}{30} \dots\dots\dots(4.27)$$

For a $K \times K$ Benes switch, there are $2 * \log_2 K - 1$ stages and each stage produces a loss of 10 dB. The loss through a Benes fabric, and number of amplifiers per input-output path is given by

$$Loss_{Benes} = 10 * (2 \log_2(K) - 1)$$

$$Amp_{Benes} = \frac{Loss_{Benes}}{3} \dots\dots\dots(4.28)$$

The total switching cost is obtained by adding the cost of amplifiers to the switching costs. It is assumed that the cost of a fiber amplifier, $cost(Amp)$, is compared to the cost of a multi-wavelength integrated $N \times N$ switch element, via the amplifier cost ratio, CR_{amp_N} ,

$$CR_{amp_N} = \frac{cost(Amp)}{cost(ES_{N \times N_W})} \dots\dots\dots(4.29)$$

4.4.2.5 TOTAL COST The total cost of a Hybrid Node can be written in terms of the cost of an elementary switch as,

$$\begin{aligned}
 \text{Total cost} = & (CR_{input_{trans}} + CR_{WT} + CR_{1x2_{switch}}) \\
 & + (Cp + Co + CR_{amp} * Amp_{switch}) \\
 & + [(CR)_{output_{trans}} * f'(p)] \\
 & \dots\dots\dots(4.30)
 \end{aligned}$$

$$\text{Here, } (CR_{input_{trans}} + CR_{WT} + CR_{gates}) * I * F = \frac{K_{input}}{\text{cost}(ES_{NxN_W})} \dots\dots\dots(4.31)$$

Equation (4.31) gives the relative cost of the input components, with respect to the cost of an elementary switch. The constant K_{input} is the cost of the input channels, as defined in [equation \(4.6\)](#) and $\text{cost}(ES_{NxN_W})$ is the cost of an NxN multi-wavelength elementary switch, as defined in [Section 4.4.1.1](#). Similarly, the cost of output channel transport can also be expressed relative to the cost of an elementary switch as:

$$\text{And } (CR_{output_{trans}}) = \frac{K'_{output_{trans}}}{\text{cost}(ES_{NxN_W})} \dots\dots\dots(4.32)$$

The quantity $K'_{output_{trans}}$ is defined in [equation \(4.7\)](#), and it represents the cost of an output channel.

4.5 ANALYSIS OF TOTAL COST

Total cost, as derived in [equation 4.30](#), has three main parts. The first part, which contains the input costs, is assumed to be a constant, because the number of input channels is assumed to remain the same. The second part, which consists of OB-switching costs, varies non-linearly with respect to the number of output channels and the relationship depends on the switching

architecture used to construct the standalone OB-switches. The third part, which consists of output costs, varies linearly with the number of channels.

Total cost varies with the total number of output channels and the total number of output channels depends on the number of primary and overflow channels. For a given load, the number of overflow channels depends on the number of primary channels. Hence, [equation 4.30](#) can be parsimoniously, modeled as a function of the number of primary channels. The input, output and switching parts of the equation can then be studied as a function of the number of primary channels.

Total cost may depend only on the switching costs if CR_{input_trans} , CR_{output_trans} and CR_{WT} are very small compared to cost of an elementary switch. In this case, it is of interest to learn if hybrid operation will produce a cost optimal core node switch. Cost optimality of a hybrid switch will be tested for various internal fabric architectures. In addition, the effect of chip integration is also studied.

As discussed in [equation \(4.2\)](#), earlier in this chapter, at this point of optimality, the incremental growth in overflow channels (with respect to the primary channels) should equal the ratio of the incremental growth of primary and overflow layer costs. The incremental cost of a switch may strongly depend on the switch fabric architecture used to construct the standalone MxM switches, as described in part A of this chapter. This incremental cost will also depend on the value of M, which may depend on the number of output channels of the switch.

Analysis of the total cost can also be extended to the case in which the cost of an elementary switch is negligible compared to the cost of transportation. In this case, only transport costs are considered and the optimal number of primary/overflow channels is obtained.

In this chapter, total cost analysis is performed by considering the switching and transport costs individually. Such an analysis will test cost-optimality under very special conditions and it can help explain the effect of switching and transport costs on hybrid operation.

4.5.1 ADVANTAGE OF HYBRID OPERATION

A hybrid operation is said to be cost advantageous compared to its non-hybrid counterpart, if there is a reduction in total node cost due to hybrid operation. In order to quantify the hybrid

advantage due to switching, the cost of hybrid operation is compared to the cost of non-hybrid operation. In a non-hybrid operation, offered traffic is exclusively transported either along overflow channels or via primary channels, but not both. Non-hybrid operation offers a fixed blocking probability to each traffic source, where the blocking probability of the overflow layer in hybrid operation is assumed to equal the blocking probability in non-hybrid operation. The remaining sections show if hybrid operation can help reduce the cost of a node. In section 4.5 the advantage of the hybrid operation is tested for its sensitivity to the OB-switch architecture, offered load, degree of integration and cost of non-switch components (such as channels and amplifiers).

In order to quantify this cost advantage due to hybrid operation we introduce a metric called ‘hybrid cost advantage’, HCA , which is represented as a function of number of primary channels per source-destination, p . The $HCA(p)$ function relates a hybrid operation to non-hybrid operation by the difference in total costs of the two operation modes. A non-hybrid operation could be either an exclusively primary operation or an exclusively overflow operation at a fixed blocking rate. Thus $HCA(p)$ is actually a 2-tuple function defined by [equation \(4.33\)](#). In this equation $HCA_{prim}(p)$ and $HCA_{overflow}(p)$ are hybrid cost advantages of operating a hybrid node with p primary channels, with respect to operating a hybrid node exclusively with primary and overflow channels, respectively.

$$\begin{aligned}
 HCA(p) &= \{HCA_{prim}(p), HCA_{overflow}(p)\} \\
 &\text{where, } HCA_{prim}(p) = Total\ cost(P) - Total\ cost(p) \\
 &\text{and } HCA_{overflow}(p) = Total\ cost(0) - Total\ cost(p) \\
 &\text{and } p = 0, 1, 2, 3, \dots, P \\
 &\dots\dots\dots(4.33)
 \end{aligned}$$

In the above set of equations, a non-Hybrid Node that operates with P primary channels, contains no overflow channels and the total cost of such a node, which is given by $Total\ cost(P)$, is used to obtain $HCA_{prim}(p)$. In the same set of equations, total cost of a non-Hybrid Node that operates with zero primary channels is given by $Total\ cost(0)$ and it is used to obtain $HCA_{overflow}(p)$. Total cost of a Hybrid Node, which is given by $Total\ cost(p)$ in [equation \(4.33\)](#), is calculated using [equation \(4.30\)](#).

Hybrid cost advantage of a node can also be represented using its percentage values such as:

$$\begin{aligned}
 \text{percentHCA}_{\text{prim}}(p) &= \frac{HCA_{\text{prim}}(p)}{\text{Total cost}(p)} \\
 \text{percentHCA}_{\text{overflow}}(p) &= \frac{HCA_{\text{overflow}}(p)}{\text{Total cost}(p)}
 \end{aligned}
 \dots\dots\dots(4.34)$$

A Hybrid Node with p primary channels is said to possess hybrid cost advantage if both $HCA_{\text{prim}}(p)$ and $HCA_{\text{overflow}}(p)$, are positive values. If hybrid cost advantage is obtained for all values of p between 0 and P , then it is called ‘complete hybrid cost advantage’, as defined in [Definition 4.1](#). In the definitions below a set Π contains all integer values between 1 and $(P-1)$. On the other hand, if hybrid cost advantage is obtained only for a subset of Π , then it is called ‘partial hybrid cost advantage’, as in [Definition 4.2](#).

Definition 4.1

‘Complete Hybrid Cost Advantage’ is said to occur in a Hybrid Node if, for all values of y in the set Π ,

$$\begin{aligned}
 &HCA_{\text{prim}}(y) > 0 \text{ and } HCA_{\text{overflow}}(y) > 0; \\
 &\text{where } y \in \Pi \text{ and } \Pi = \{1, 2, 3, \dots, (P - 1)\}
 \end{aligned}$$

Definition 4.2

‘Partial Hybrid Cost Advantage’ is said to occur in a Hybrid Node if, for all values of y' ,

$$\begin{aligned}
 &HCA_{\text{prim}}(y') > 0 \text{ and } HCA_{\text{overflow}}(y') > 0 \\
 &\text{where } y' \subset \Pi' \text{ and } \Pi' \subset \Pi
 \end{aligned}$$

Although a complete hybrid cost advantage provides hybrid cost advantage for all elements of Π , there may or may not be a global minimum for the Total Cost. At the same time,

a partial hybrid cost advantage in a Hybrid Node may still yield a unique, global minimum value of total cost. A ‘global maximum hybrid cost advantage’ is obtained, if the hybrid cost advantage occurs for a total cost, which is a global minimum over the set Π .

Definition 4.4

A Hybrid Node attains a ‘Global Maximum Value of Hybrid Cost Advantage’, $HCA(x)$, at x^* if

$$\text{Total cost}(x^*) < \text{Total cost}(y);$$

where $y \in \Pi, x^* \in \Pi$ and $y \neq x^*$

A complete or partial hybrid cost advantage may occur, for which there may not be a global maximum value. This happens when the total cost of a Hybrid Node doesnot incur a global minimum for the set Π ; instead attains a strong local minimum over a subset of Π .

Definition 4.5

A Hybrid Node attains a ‘Strong Local Maximum value of Hybrid Cost Advantage’, $HCA(x)$ at y^* if

$$\text{Total cost}(y^*) < \text{Total cost}(y);$$

where $y^* \in N(y^*, \delta), y \in N(y^*, \delta)$ and $N(y^*, \delta) \subset \Pi$

$N(y^*, \delta)$ is a set of feasible points that belongs to Π and lies in the neighborhood of y^* . Value of δ is such that $y^* + \delta < P$ and $y^* - \delta > 0$. There could be multiple local maximum for $HCA(x)$ in the set of Π .

4.5.2 TEST CASES

As discussed in the part A of this chapter, the total cost of a Hybrid Node depends on several design parameters and variables. Each choice of design parameter or variable will be considered as a test case.

For the test cases, the following choice of design parameters is considered.

- Architecture: B-S, Benes or Clos (Re-arrangably non-blocking).
- Size of basic space switch element, $N \times N$:
1x1 (for B-S) , 2x2 (for Benes) and 4x4 (for Clos).
- Number of wavelengths per $N \times N$ switch, W :
1 (single wavelength gates) or W (multi-wavelength gate array).
- Overflow: Active or Passive
- Number of sources sharing the overflow channels: 10 sources
- Number of different destinations: 8 destinations
- Load: Total offered load in Erlangs per Hybrid Node between every input source and final destination. Since the load is assumed to be peaked, we define the load by its average Erlang units and long term average Peakedness.
- Cost ratios are as defined in section 4.4.

While performing switching cost analysis, we may assume the transport costs to be zero, by setting CR_{input_trans} and CR_{output_trans} to be zero. Main components of the switching cost are total cost of basic switching elements, cost of fiber amplifiers needed due to switching loss and cost of overflow gates.

4.6 RESULTS OF SWITCHING AND TRANSPORT ANALYSIS

4.6.1 SWITCH CONTACTS USING B-S ARCHITECTURE

Broadcast and select switches have 1x1 gates as the main switching element, so the cost of switching is expressed in terms of the cost of one 1x1 element. For the B-S architecture, we consider the value of W , the number of wavelengths per switching element, to be either one or 10, which is also the number of wavelengths per fiber. For each of these cases, either active or passive overflows are possible. In the latter case, the cost ratio of overflow gates may be set to zero. The cost of amplification and switching are considered separately in order to study the individual effect of each of the components. In this analysis, total cost of a hybrid node containing B-S architecture is considered for 0.75 Erlangs, 3 Erlangs and 6 Erlangs of offered load per source. In all the three cases, the value of CR_{amp} , which gives the cost ratio of fiber amplifiers with respect to the cost of an elementary switch, can range from 0 to infinity.

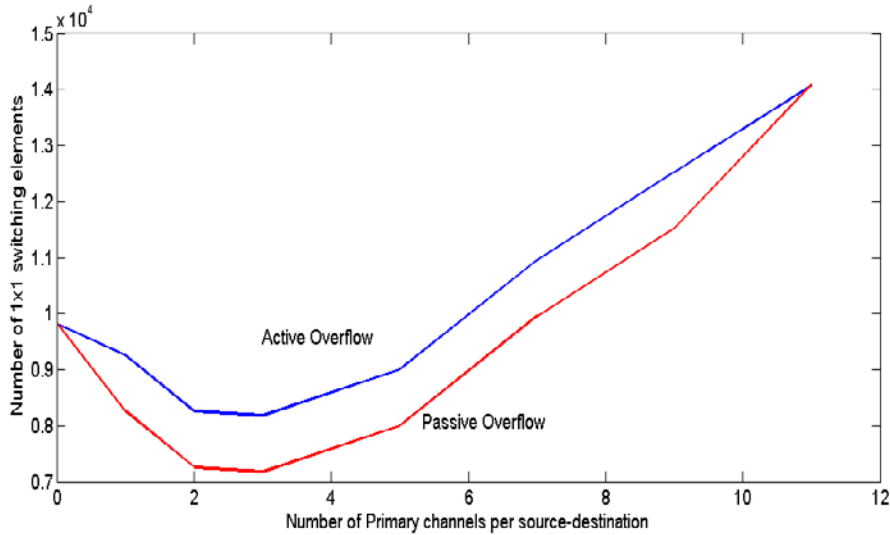


Figure 4.12 Total number of 1x1 switches for an offered load is 0.75 Erlangs and $CR_{amp} = 0$

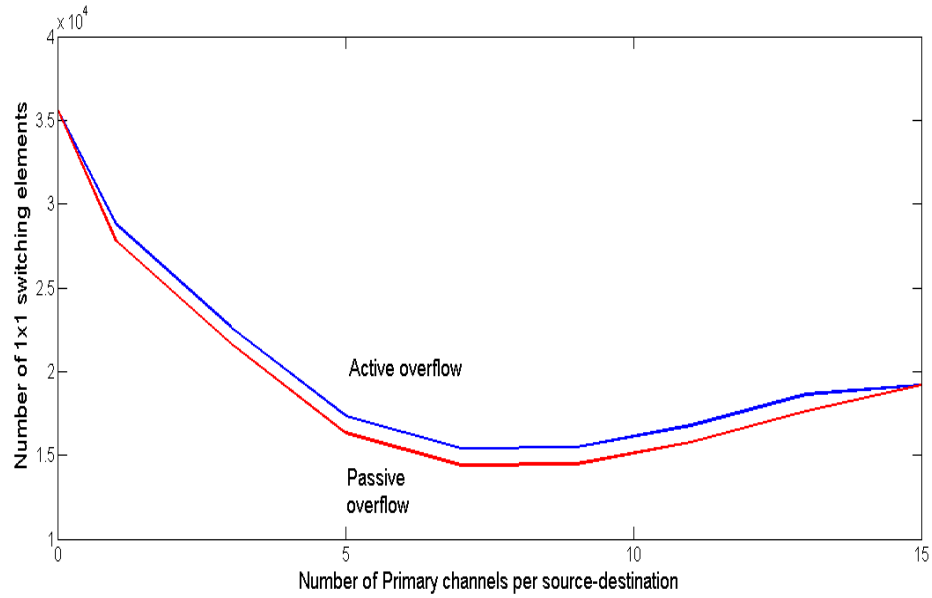


Figure 4.13 Total number of 1x1 switches for an offered load is 3 Erlangs and $CR_{amp} = 0$

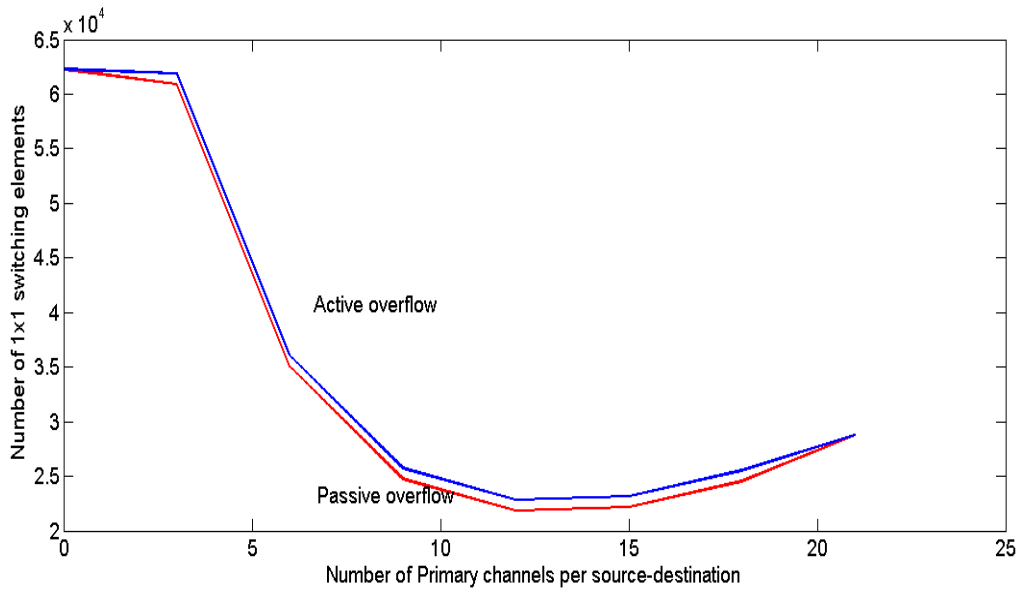


Figure 4.14 Total number of 1x1 switches for an offered load is 6 Erlangs and $CR_{amp} = 0$

It is observed from the above plots that the number of 1x1 elements reaches a minimum value for all three considered load values. Thus, hybrid operation may help lower the number of gates required, when compared to a non-hybrid operation of having only primary channels or

only overflow channels, in the Hybrid Node. This lowering of total switching element cost occurs despite the fact that hybrid operation requires ‘extra’ overflow switches, when compared to a non-hybrid operation. From Figures [4.12](#), [4.13](#) and [4.14](#), we observe that ‘partial hybrid advantage’ occurs for an offered load of 0.75 3 and 6 Erlangs, respectively. For a load of 0.75 Erlangs, hybrid cost advantage occurs for a value of p from 1 to 6 and outside this range, it is cost effective to have only overflow channels (and no primary channels). When the offered load is 3 Erlangs, the values of p for hybrid cost advantage is from 5 to 15 and for the values of p outside this range, it is cost effective to have only primary channels. Finally, for a load of 6 Erlangs hybrid cost advantage is seen for p varying from 7 to 21, and outside this range it is cost efficient to have only primary channels.

Figures [4.12](#), [4.13](#) and [4.14](#) exhibit a ‘global hybrid cost advantage’ occurring at the point of minimum total cost. At all three loads, it is possible to obtain a unique global minimum cost, which occurs due to the hybrid operation. For the offered loads of 0.753 and 6 Erlangs, the global minimum occurs at p equal to 3, 7 and 12, respectively. As the load increases, the value of p at which the global minimum occurs also increases. This means that at higher loads, it is cost effective to introduce source-specific stand-alone switches, rather than build a single large overflow OB-switch. Introducing more source-specific stand-alone switches in lieu of more interconnections in a single large switch, minimizes the number of switching elements and helps bring down total cost of the OB-switch.

It can be observed that for an offered load of 0.75 Erlangs the cost curve is skewed to the left and for a load of 6 Erlangs, it is skewed to the right. This is because, at low loads, one can build a single large switch which is cheaper than building a large number of smaller switches. Therefore, a non-hybrid operation containing only primary channels will be expensive than the non-hybrid operation with only overflow channels. On the other hand, for a large offered load, building a single large switch is far more expensive than building several small switches. Hence, when we consider the two non-hybrid operation, it is cheaper to have only primary channels, compared to overflow channels. This skewness in the cost curve is reflected in the position of the global minimum point, in the three figures above.

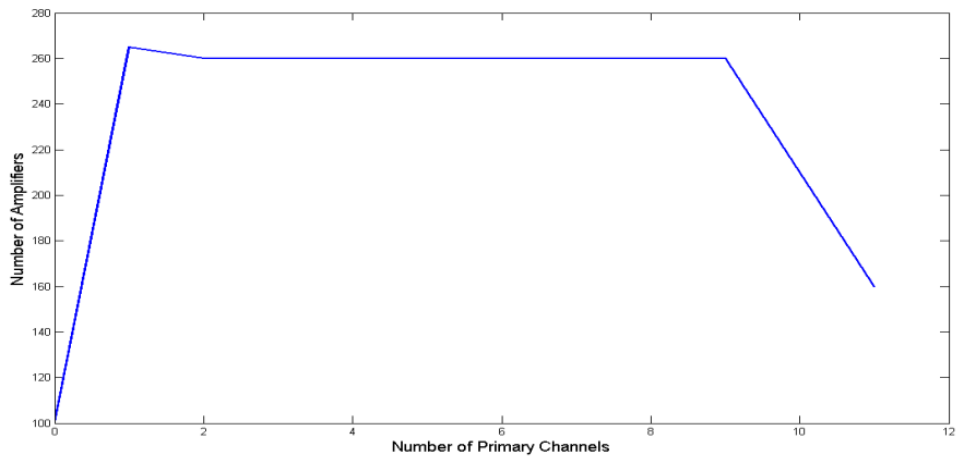


Figure 4.15 Amplifiers to overcome switching loss. Offered load is 0.75 Erlangs.

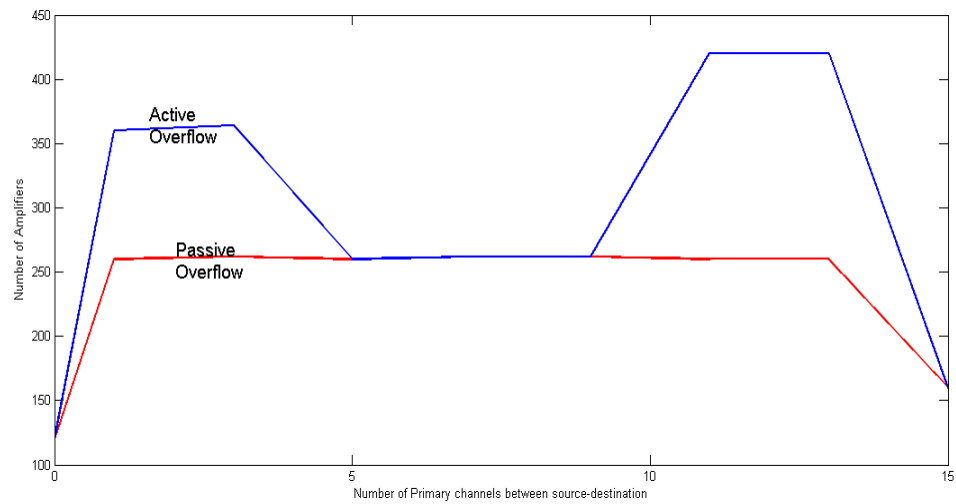


Figure 4.16 Amplifiers to overcome switching loss. Offered load is 3 Erlangs.

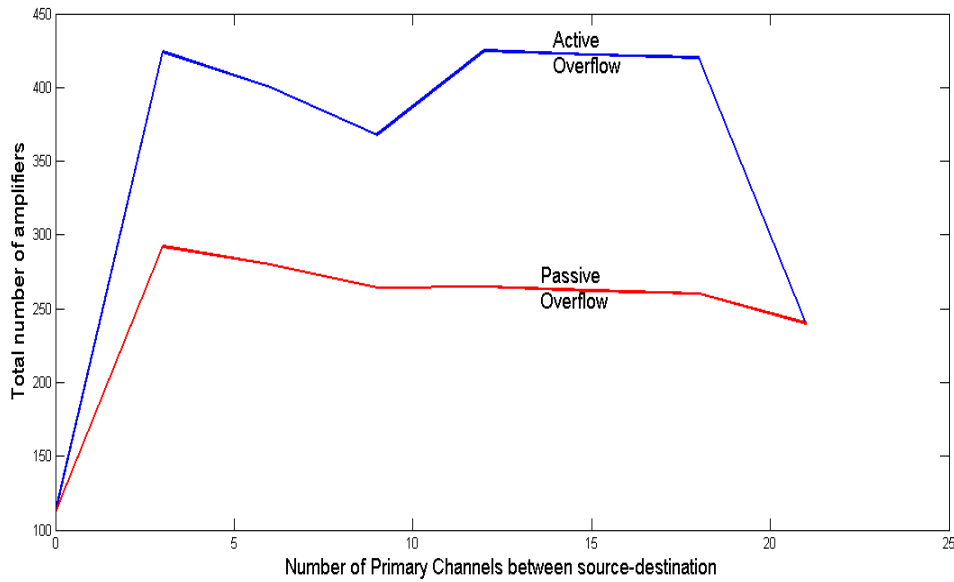


Figure 4.17 Amplifiers to overcome switching loss. Offered load is 6 Erlangs.

Hybrid operation may not lower the number of amplifiers required in the switch, when compared to a non-hybrid operation, as seen in [Figures 4.15, 4.16](#) and [4.17](#). For all three values of loads considered, hybrid operation increases the need for amplifiers. It is assumed that a single amplifier can overcome about 30 dB of loss. It is also assumed that the splicing loss of 10 dB occurs at the wavelength selective switch, which forms the center stage of B-S architecture for both active and passive overflow schemes. Yet another splicing loss of 10 dB may occur at the overflow gates for active overflows. On the other hand, splitter loss of 3 dB may occur at the overflow splitters for passive overflow. Both active and passive overflows are subjected to loss occurring at the splitter prior to the WSC stage but after the overflow stage. Loss at this splitter depends on the dimension of the standalone switch, which in turn depends on the number of output channels. For a non-hybrid operation, however, there is no overflow stage, which may minimize need for amplification, as evident from the dip in the plots at the two ends of the x-axis.

The number of amplifiers in a B-S switch depends on the number of wavelength selective switches (WSCs), in its center stage. Number of WSCs may decrease due to hybrid operation and this may help reduce the number of amplifiers required to overcome the splicing loss of 10 dB occurs at the WSC interface. For an offered load of 3 Erlangs, in [Figure 4.16](#), there is

pronounced dip in the number of amplifiers within the range of the hybrid operation, for the case when active overflow switches are used. In this curve, it appears as if, lowering of losses in the WSC, is almost equal to the loss due to the overflow switches. If this were the case, similar dip should also occur for the design using passive splitters. However, due to the fact that an amplifier is required for all losses less than 30 dB, makes it necessary to use one, even if losses were reduced by a certain value. Had the amplifiers been limited to overcome a smaller loss, the dip in number of number of amplifiers due to the hybrid operation would have been more apparent. For an offered load of 6 Erlangs (in [Figure 4.17](#)) also, there is a small dip in the number of amplifiers during hybrid operation for an OB-switch using active overflow switches. This dip is also reflected in the OB-switch that uses passive splitters, instead of active switches. For an offered load of 0.75 Erlangs in [Figure 4.12](#), the lowering of WSCs is small and this does not help to lower the number of amplifiers.

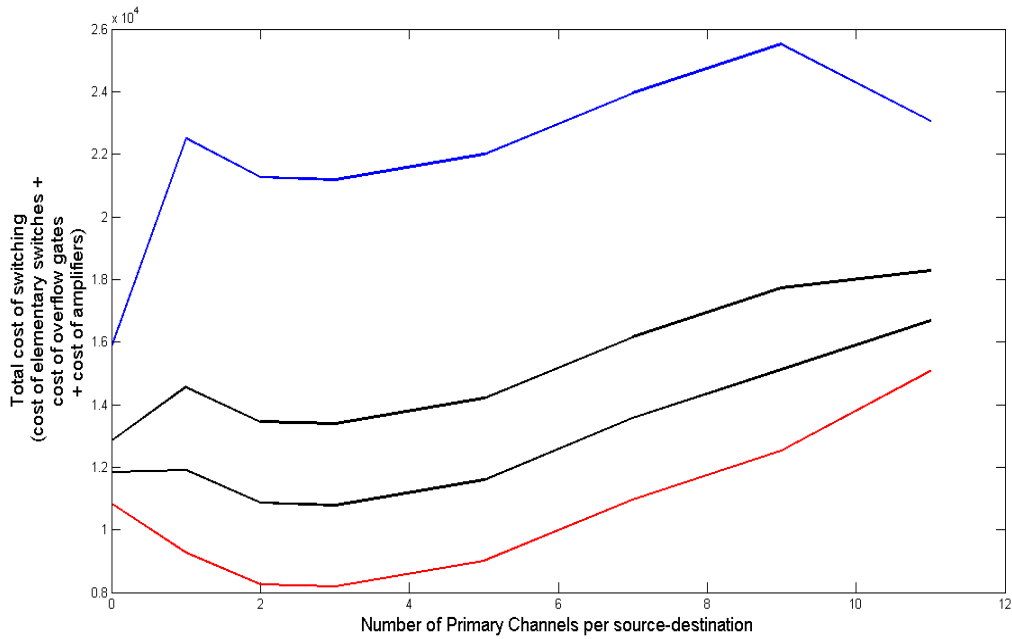


Figure 4.18 Total cost of switching for various values of CR amp. Offered load is 0.75 Erlangs

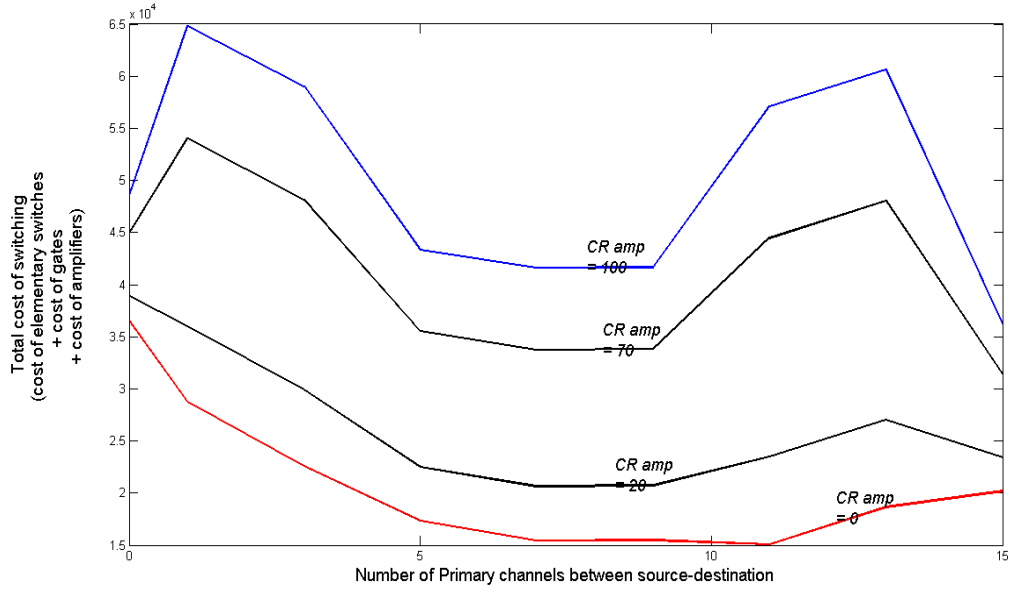


Figure 4.19 Total cost of switching for various values of CR_{amp} . Offered load is 3 Erlangs

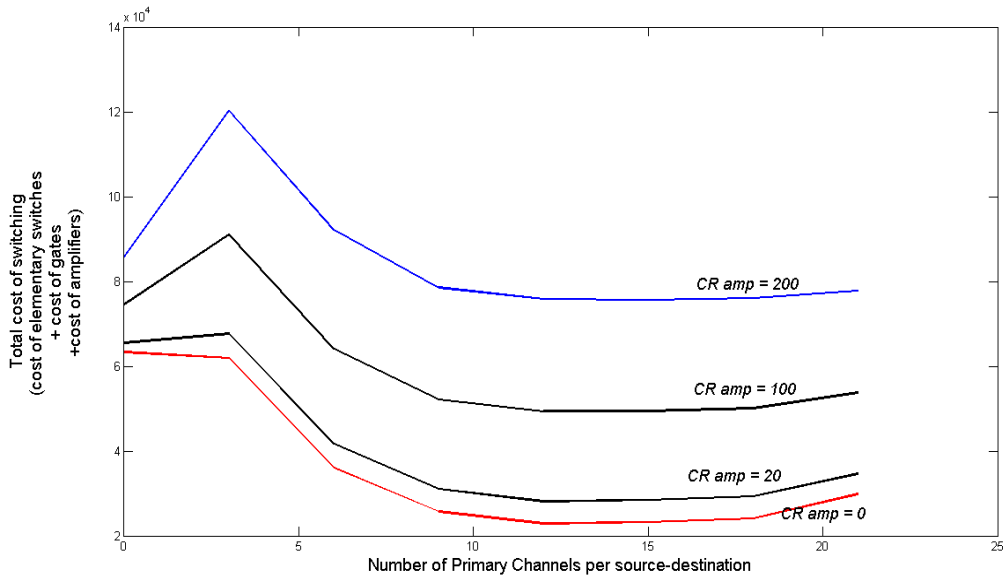


Figure 4.20 Total cost of switching for various values of CR_{amp} . Offered load is 6 Erlangs.

For non-zero values of CR_{amp} , the hybrid cost advantage is lost as CR_{amp} gets larger, as seen in [Figures 4.18](#), [4.19](#) and [4.20](#). It is also seen that the benefit of reducing 1x1 contacts becomes apparent only when the cost of 1x1 contacts dominates the switching cost largely. If the cost of a 1x1 contact is small compared to the cost of amplifiers, hybrid operation may become less cost effective when compared to non-hybrid operation.

4.6.2 B-S ARCHITECTURE WITH MULTI-WAVELENGTH CHIPS

The B-S architecture can also be implemented using arrays of multi-wavelength 1x1 switches on a single chip, as discussed in section 4.2.2.2. In this case, an elementary switch is a multi-wavelength 1x1 switch on a chip. Integrating several switch contacts may result in modifying the total number of elementary switches required. We analyze the following test cases, which will consider arrays of 10-wavelength 1x1 switches on a chip. It is assumed that a splicing loss of 10 dB occurs at the chip-fiber intersection. Similarly, the overflow gates are integrated in a chip with an array of 10 wavelengths. The overflow gates are also integrated on a chip and the gates, too, produce a splicing loss of 10 dB.

[Figures 4.21](#), [4.22](#) and [4.23](#) shows the number of 10-wavelength , 1x1 switching elements required to construct the OB-switch, for an offered load per source of 0.75, 3 and 6 Erlangs, respectively. The OB-switches contain either passive splitters, or active overflow switches. In all these three figures, cost of an amplifier, which is given by the value of CR_{amp} , is assumed to be zero.

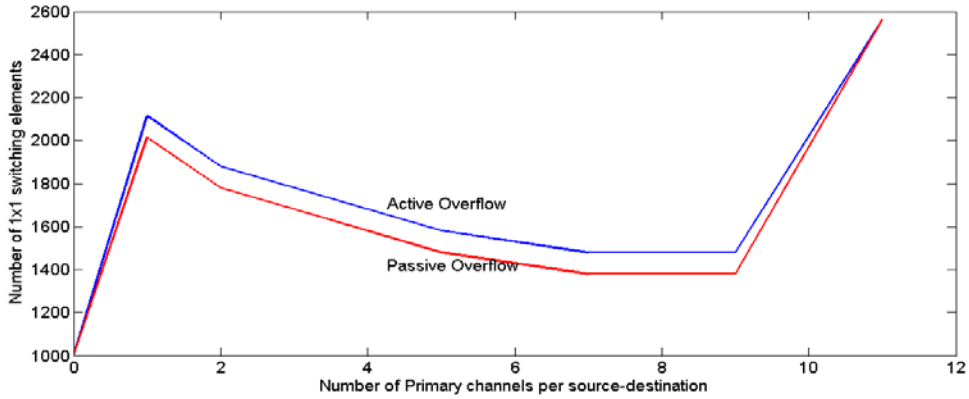


Figure 4.21 Total number of multi-wavelength 1x1 switches. Offered load = 0.75 Erlangs ; $CR_{amp}=0$

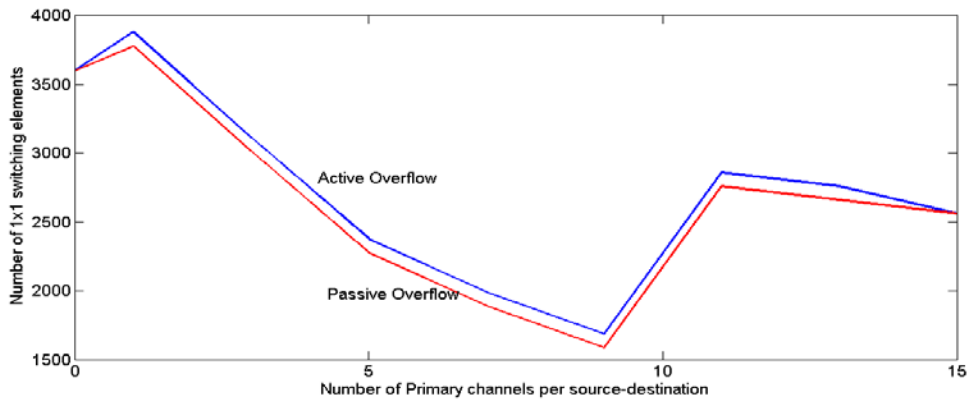


Figure 4.22 Total number of multi-wavelength 1x1 switches. Offered load = 3 Erlangs ; $CR_{amp}=0$

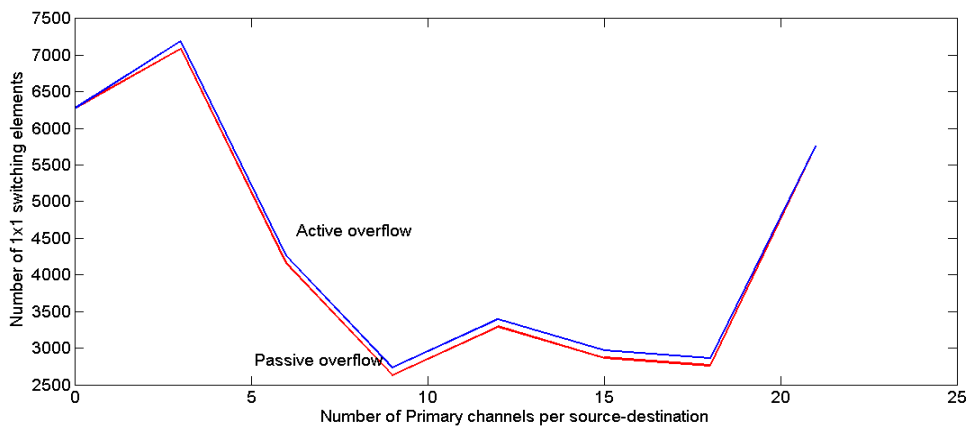


Figure 4.23 Total number of multi-wavelength 1x1 switches. Offered load = 6 Erlangs ; $CR_{amp}=0$

For multi-wavelength integrated 1x1 switches, there are 10 gates per chip, each tuned to a different wavelength. All the gates on a chip may not be used, because the number of input/output channels per standalone MxM switch may not always be an integer multiple of the number of wavelengths per fiber. This is particularly the case for nodes under low loads, where the total number of unused gates adds to the total switching costs. Thus, the benefit of hybrid operation in reducing the switch sizes of primary and overflow layers may be compensated by unused gates. It can be observed from [Figure 4.21](#) that for an offered load of 0.75 Erlangs, hybrid operation may not lower the switching costs. On the other hand, there is lowering of switching costs due to hybrid operation, as it can be observed from [Figures 4.22](#) and [4.23](#), for 3 and 6 Erlangs respectively.

Hybrid cost advantage is not obtained in [Figure 4.21](#), for an offered load of 0.75 Erlangs, because total switching cost is minimum for the non-hybrid operation with zero primary channels. Only a ‘partial hybrid cost advantage’ is obtained for an offered load of 3 and 6 Erlangs. It can be observed from [Figures 4.22](#) and [4.23](#) that hybrid cost advantage is lost for smaller values of p , and it is obtained for larger values of p . At $p = 1$, there is a sudden rise in the number of switching elements. This is explained due to the unused switching elements in the array of 10-wavelength 1x1 switch and also due to extra overflow switches, not present at $p = 0$.

A ‘global maximum value of hybrid cost advantage’ is obtained in [Figure 4.22](#) for an offered load of 3 Erlangs. In this figure, the global minimum for total switching cost occurs at $p = 9$. For an offered load of 6 Erlangs, in [Figure 4.23](#), a ‘strong local maximum value of hybrid cost advantage’ is obtained at $p = 7$ and at $p = 17$. This is because of the interaction between the value of p , the number of overflow channels, ov and the fact that the switching elements come wavelength division multiplexed (WDMed) for 10 wavelengths. Such an effect is not observed in [Figure 4.14](#), where the 1x1 switch is not WDMed and it operates only on a single wavelength.

[Figures 4.24](#), [4.25](#) and [4.26](#) show the total cost of an OB-switch for 0.75, 3 and 6 Erlangs of offered load per source. These figures include the cost of the switching elements and the cost of the amplifiers, used to overcome losses in the switch.

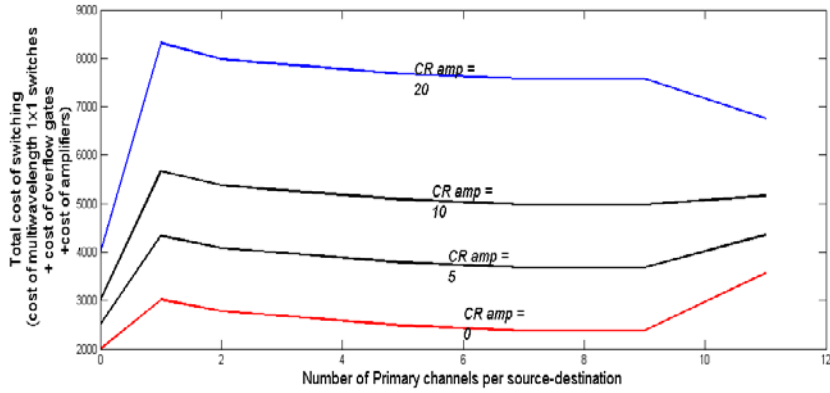


Figure 4.24 Total cost of switching for various values of CR_{amp} . Offered load = 0.75 Erlangs

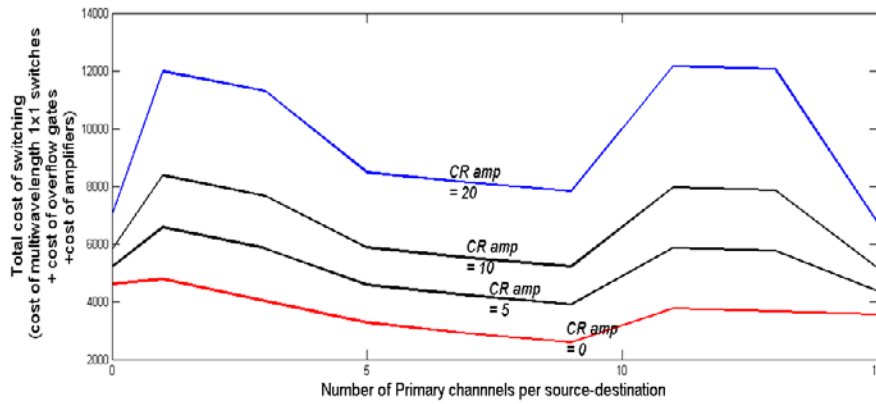


Figure 4.25 Total cost of switching for various values of CR_{amp} . Offered load = 3 Erlangs

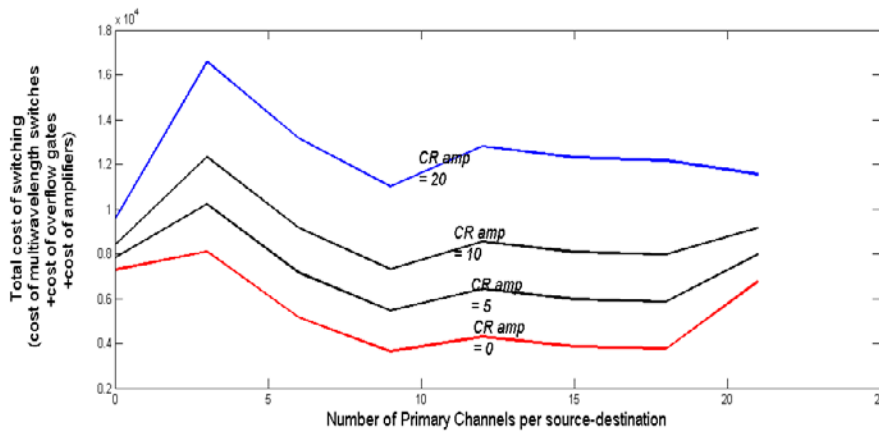


Figure 4.26 Total cost of switching for various values of CR_{amp} . Offered load = 6 Erlangs

The number of amplifiers required in an OB-switch does not depend on the number of wavelengths in a multi-wavelength switching element. Since fiber amplifiers amplify an entire fiber, including its entire constituent wavelengths, number of required amplifiers for an OB-switch made of 10-wavelength 1x1 switches, is the same as in [Figures 4.15, 4.16 and 4.17](#). Since hybrid operation introduces an additional switching stage, switching loss increases, thereby requiring more amplifiers in the switch. The hybrid cost advantage due to lowering the number of elementary switches may be compensated by the high cost of amplifiers. At high values of CR_{amp} , the hybrid cost advantage is lost. Also, compared to total cost of a non-integrated hybrid switch, the cost of an integrated switch is highly sensitive to CR_{amp} . It is seen that hybrid cost advantage is lost for a smaller value of CR_{amp} , when compared to values of CR_{amp} for un-integrated B-S architecture.

Thus, for an OB-switch constructed using the B-S architecture, we can conclude that hybrid operation may help reduce switching costs by reducing the number of elementary switches in the node. At lower offered loads, integration of gates may lead to wasting of gates on the chip, thus adding to the total cost of hybrid switches. For both cases, fiber amplifiers may have to be used to combat switching losses at the overflow and the space switching stages. A very high cost ratio of fiber amplifiers may hinder the cost effectiveness of hybrid operation.

6.05 BENES ARCHITECTURE USING 2X2 SWITCHES

Figures 4.27, 4.28 and 4.29 shows the total number of single wavelength 2x2 switching required to construct a hybrid OB-switch based on Benes architecture, for an offered load of 0.75, 3 and 6 Erlangs. In these figures, both active and passive overflows are considered for the OB-switch.

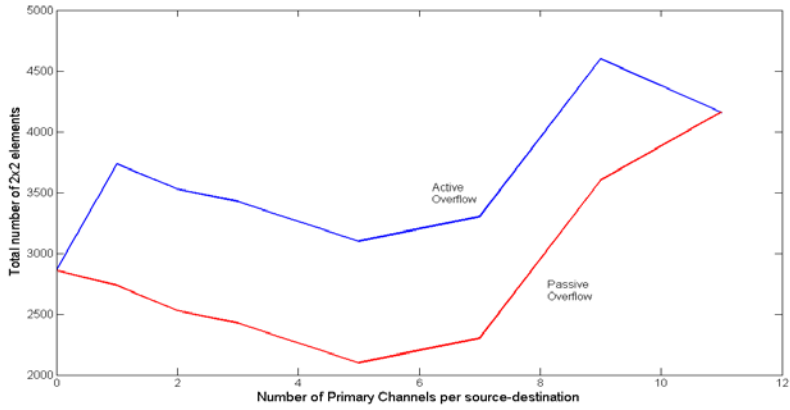


Figure 4.27 Total number of 2x2 switches. Offered load = .75 Erlangs.

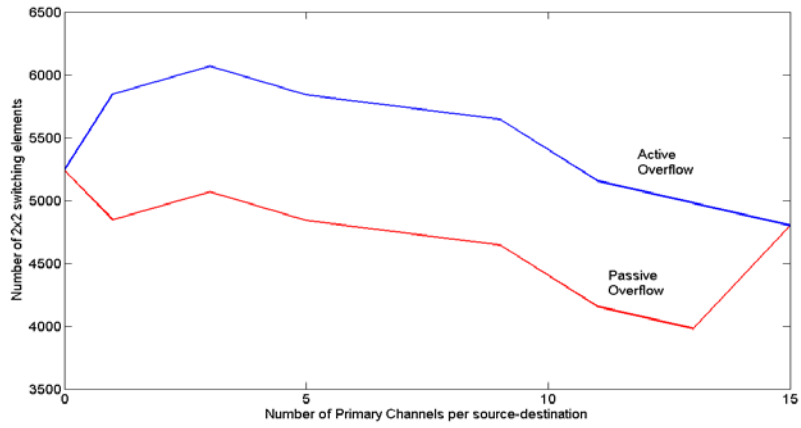


Figure 4.28 Total number of 2x2 switches. Offered load = 3 Erlangs.

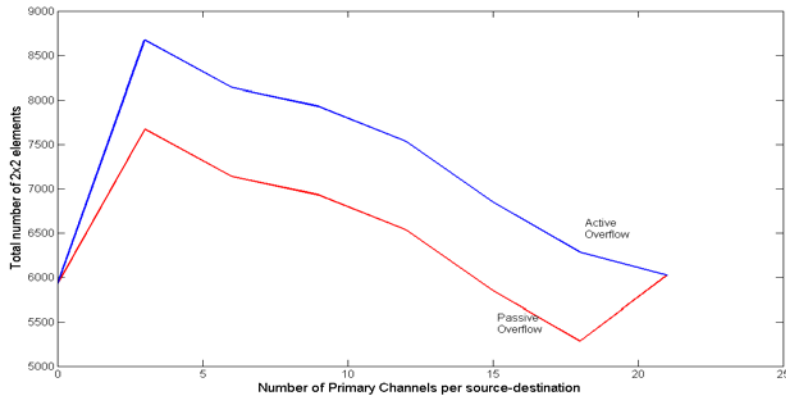


Figure 4.29 Total number of 2x2 switches. Offered load = 6 Erlangs.

It can be observed from Figures 4.27, 4.28 and 4.29 that Hybrid Nodes with the Benes architecture and active overflow do not provide minimum number of 2x2 elements. Hence, hybrid cost advantage is not possible if the hybrid OB-switch is constructed using Benes architecture and if it contains active overflows. On the other hand, Hybrid Nodes with passive overflow are able to achieve minimum number of 2x2 elements. For all the three offered load values, a partial hybrid cost advantage is obtained. The minimization of 2x2 elements is more pronounced at lower loads such as .75 and 3 Erlangs, compared to an offered load of 6 Erlangs.

Figures 4.30, 4.31 and 4.32 represents the total number of amplifiers required for a 2x2 Benes based OB-switch, for an offered load of 0.75, 3 and 6 Erlangs, respectively.

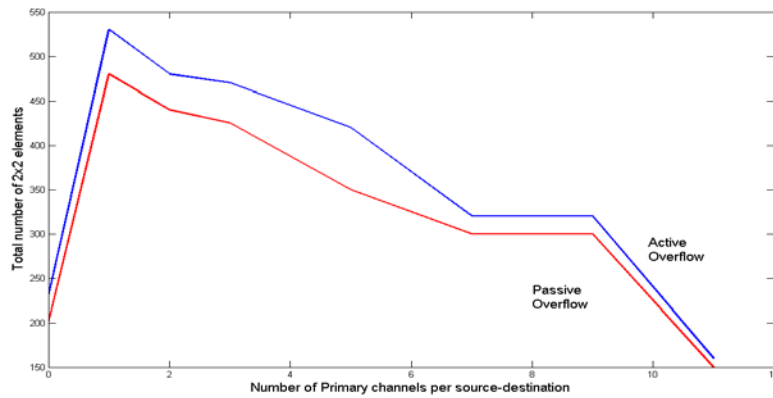


Figure 4.30 Amplifiers to overcome switching loss. Offered load is 0.75 Erlangs.

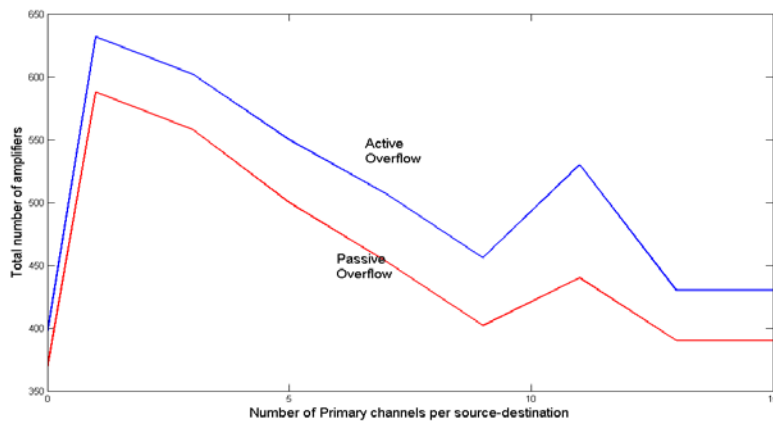


Figure 4.31 Amplifiers to overcome switching loss. Offered load is 3 Erlangs.

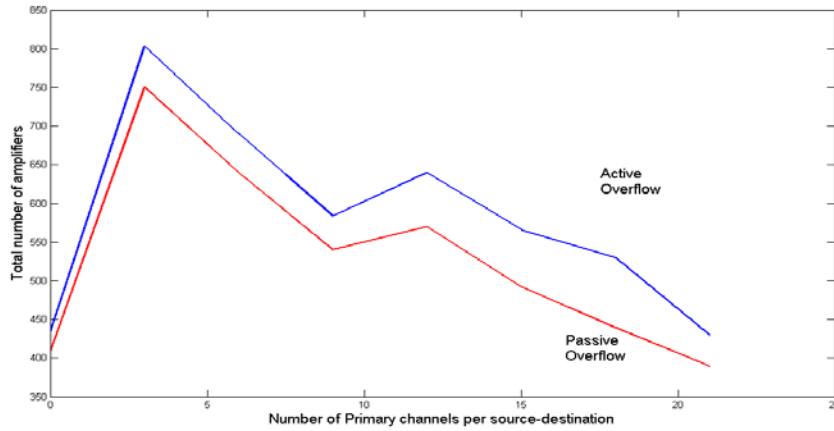


Figure 4.32 Amplifiers to overcome switching loss. Offered load is 6 Erlangs.

It can be observed from [Figures 4.30](#), [4.31](#) and [4.32](#) that hybrid operation is not a favorable mode of operation, when it comes to minimizing total number of amplifiers in the node. This is because hybrid operation adds an additional stage of loss, either at the active overflow gates, or at the passive overflow splitters.

[Figures 4.33](#), [4.34](#) and [4.35](#) represent the total switching cost of a Hybrid Node constructed using 2x2 Benes fabric and passive overflows. The total switching cost of a Hybrid Node is equal to the cost of 2x2 elements and the cost of amplifiers used to overcome losses in the switch.

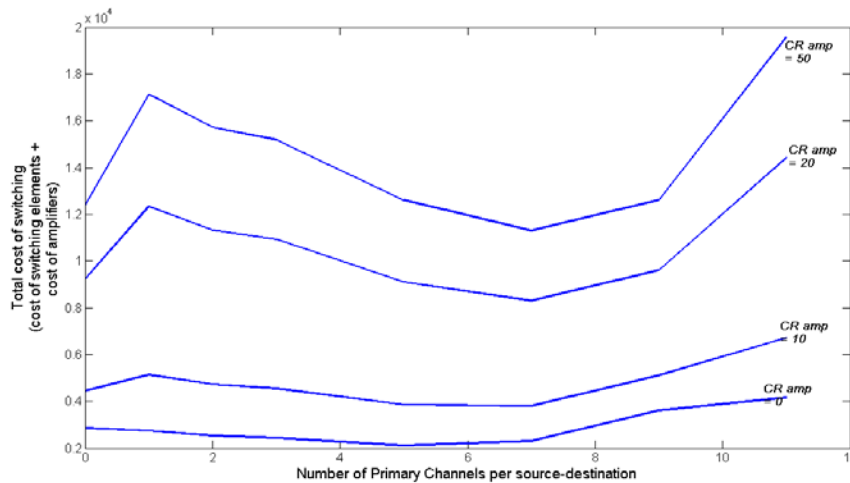


Figure 4.33 Total cost of switching for various values of CR_{amp} . Offered load = 3 Erlangs

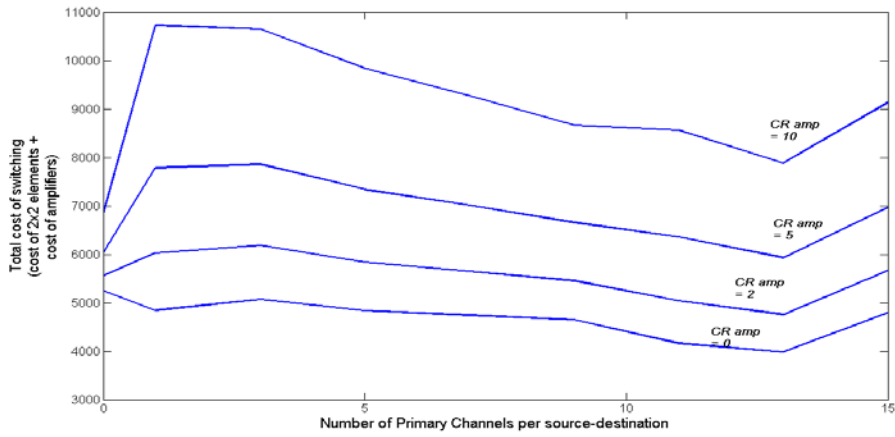


Figure 4.34 Total cost of switching for various values of CR_{amp} . Offered load = 3 Erlangs

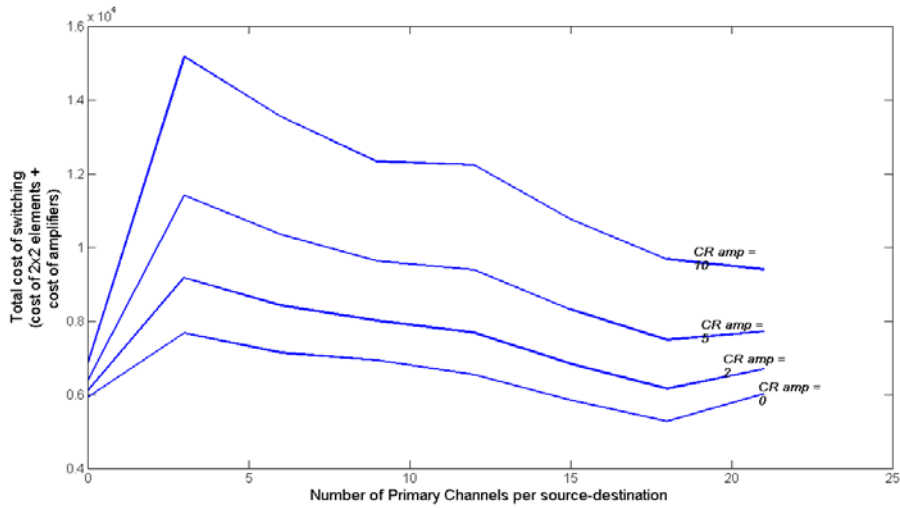


Figure 4.35 Total cost of switching for various values of CR_{amp} . Offered load = 6 Erlangs

It can be observed from [Figures 4.33](#), [4.34](#) and [4.35](#) that for Hybrid Nodes minimization of total node cost is very sensitive to values of CR_{amp} , particularly at low loads. The advantage of hybrid operation in minimizing total node cost is lost with a large value of CR_{amp} .

4.6.4 BENES ARCHITECTURE USING MULTIWAVELENGTH INTEGRATED 2X2 SWITCHES

A hybrid switch may be based on the Benes architecture that uses arrays of multi-wavelength 2x2 switches integrated on a single chip. In this case, the switching costs are calculated with respect to the chip cost. Figures 4.36, 4.37 and 4.38 shows the total number of multi-wavelength 2x2 switching elements needed to construct a Hybrid Node, for an offered load of 0.75, 3 and 6 Erlangs, respectively.

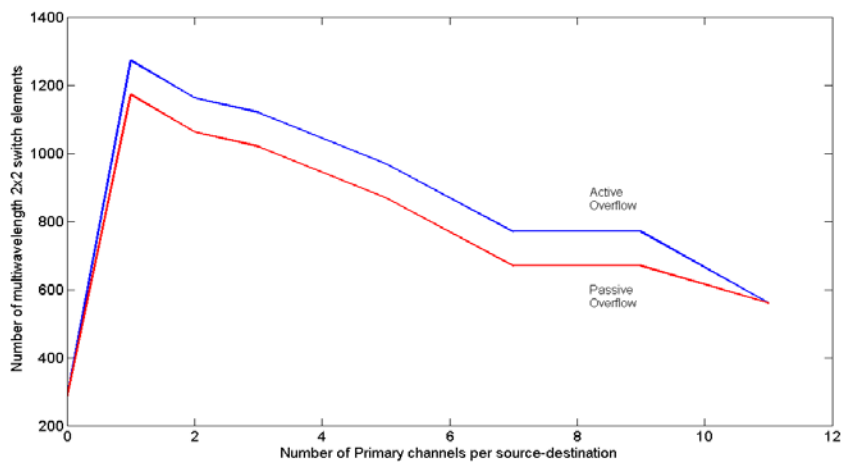


Figure 4.36 Total number of 2x2 chips. Offered load = 0.75 Erlangs.

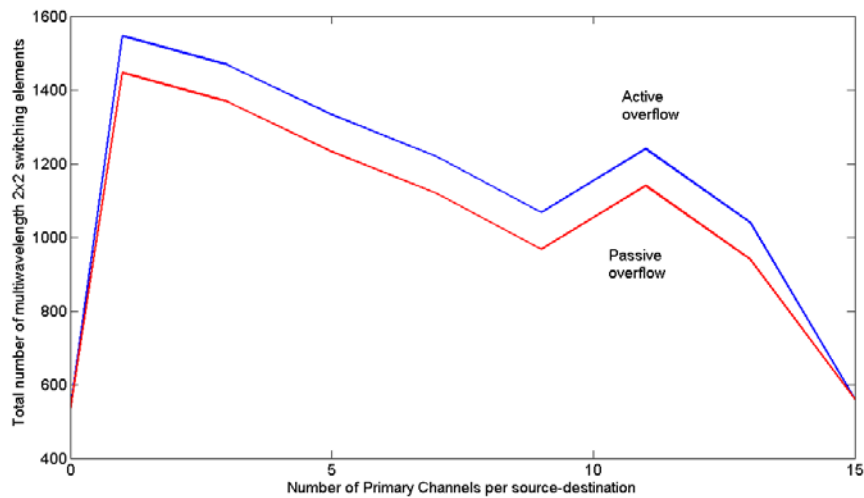


Figure 4.37 Total number of 2x2 chips. Offered load = 3 Erlangs.

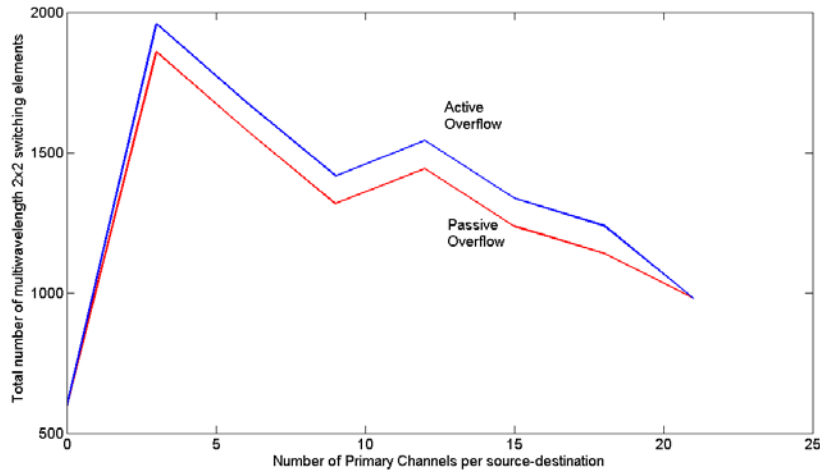


Figure 4.38 Total number of 2x2 elements. Offered load = 6 Erlangs.

For a Hybrid Node based on the Benes architecture using multi-wavelength 2x2 integrated switches, hybrid operation does not minimize the number of elementary switches. In all the three cases of offered load, hybrid operation requires more 2x2 elements compared to a non-hybrid operation.

607 CLOS ARCHITECTURE USING 4X4 SWITCHES

For a Hybrid Node implemented using the Clos architecture, we consider a multi-wavelength 4x4 switch as the basic switching element. The 4x4 switch may be constructed using the Benes architecture and splicing loss for each chip is assumed to be 10 dB. The Clos fabric is assumed to be rearrangeably non-blocking. The overflow gates used for passive overflow are also constructed using multi-wavelength 4x4 switches.

Figures 4.39, 4.40 and 4.41 show the total cost of constructing a Hybrid Node using Clos architecture. In these figures, the curve labeled $CR_{amp} = 0$, gives the total number of multi-wavelength 4x4 elementary switch.

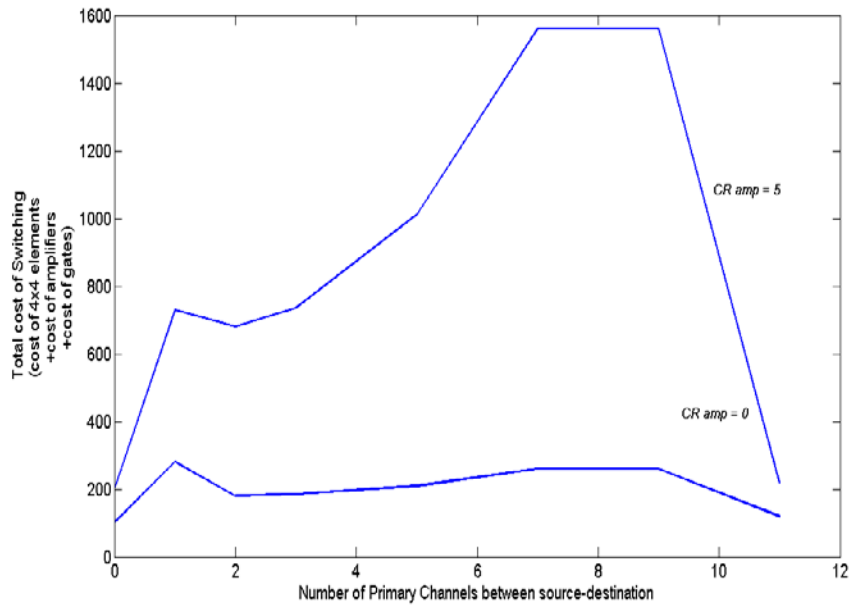


Figure 4.39 Total cost of switching for various values of CR_{amp} for a load of 0.75 Erlangs

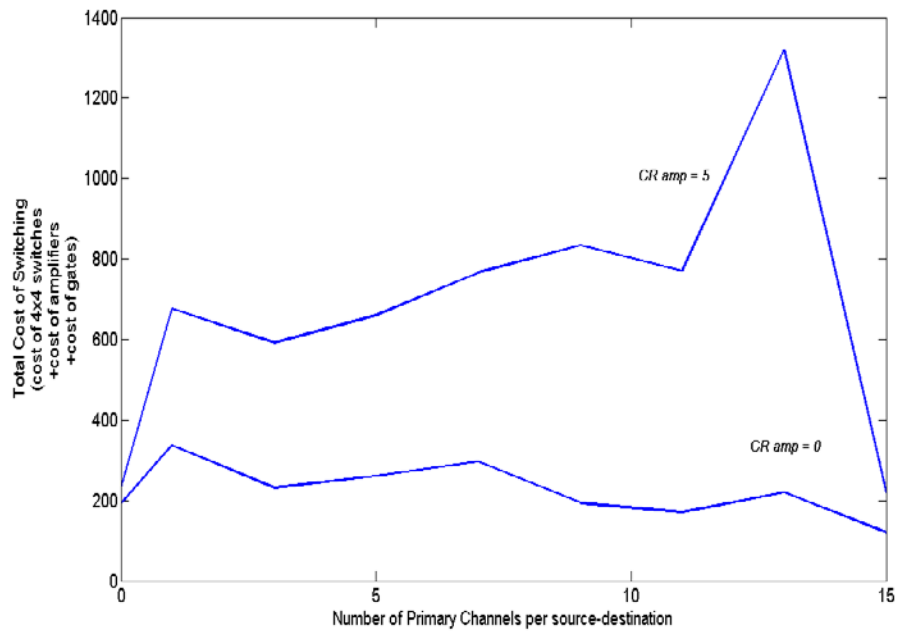


Figure 4.40 Total cost of switching for various values of CR_{amp} for a load of 3 Erlangs

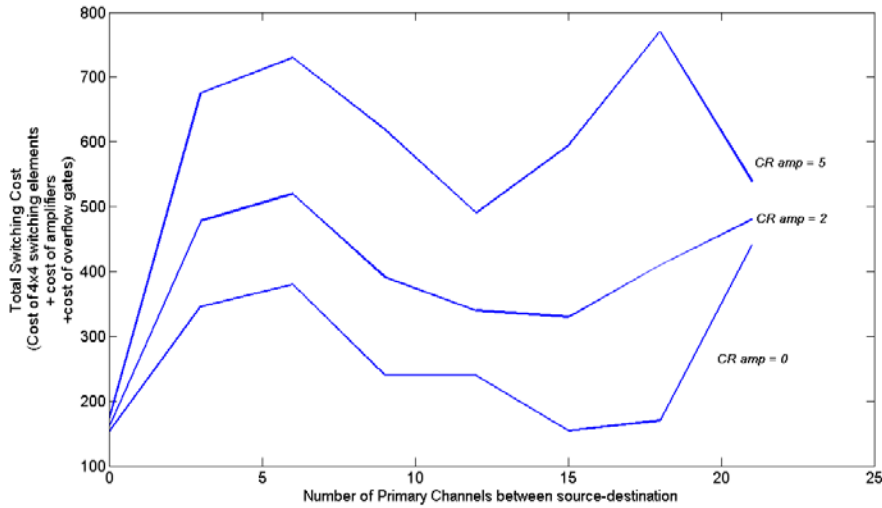


Figure 4.41 Total cost of switching for various values of CR_{amp} for a load of 6 Erlangs

It can be observed from Figures 4.39, 4.40 and 4.41 that cost minimization due to hybrid operation occurs for an offered load 3 Erlangs and 6 Erlangs, but not for 0.75 Erlangs. A partial hybrid cost advantage occurs at $CR_{amp} = 0$ for 3 and 6 Erlangs. The effect of higher values of CR_{amp} is to negate the hybrid advantage that occurs due to minimization of 4x4 switches.

4.6.6 TRANSPORT COSTS

Transport cost includes all channel-related costs that may increase linearly with the channel count. There are two main components to the channel cost: the number of channels and the cost per channel. The number of channels depends on the number of primary and overflow channels and we quantify the cost of a channel using a cost ratio CR_{output} , which relates the channel cost to the cost of a switching element. The intention of considering the transport costs in this manner is to study how the two main cost components may affect the total cost of a Hybrid Node.

4.6.6.1 TOTAL NUMBER OF CHANNELS Transport cost depends on the total number of output channels, which includes the primary channels (which is part of the primary light-paths) and the overflow channels. The cost of a single channel is quantified relative to the cost of an elementary switch, which is used to construct the Hybrid Node. As mentioned in [equation 4.32](#),

the cost ratio CR_{output} relates the transport cost to the switching cost. The advantage of a lower number of cross-points in a hybrid switch, compared to non-hybrid operation, may be lost due to higher transport costs. This is because every additional primary channel will lower channel utilization and improve the overall loss performance obtained by the traffic source. Thus, transport costs rise with an increase in the number of primary channels. Figure 4.42 shows the total number of output channels (wavelengths) required in a hybrid OB-switch that is offered 0.75, 3 and 6 Erlangs. In addition to the offered load, the output channels also depend on the number of primary and overflow path destinations. It is assumed that the traffic sources are identical with respect to their offered load and that all routes (between the Hybrid Node and the destinations) are equally loaded.

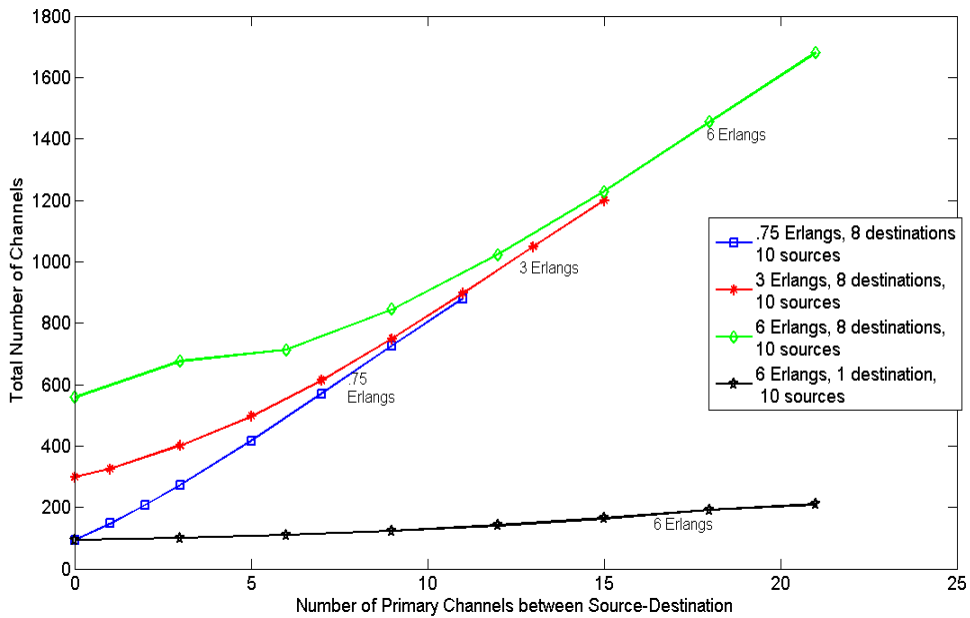


Figure 4.42 Total number of output channels

Figure 4.42 shows that the total number of output channels increases almost linearly with an increase in the number of primary channels for an offered load in the range 0.75 Erlangs to 6 Erlangs. The total number of output channels also depends on amount of sources/destination traffic multiplexed onto the output channels. It is assumed that each source-destination traffic load offers equal load on the hybrid channels. For instance in Figure 4.42, when traffic to 8 destinations are multiplexed together on the overflow channels, the increase in the total number

of channel is nearly linear. Whereas, when traffic to only one destination uses the overflow channels, the total channel remains more flat. Flattening of the total channel curve also occurs for high average traffic loads. For instance, in Figure 4.42, when traffic to 8 destinations share the overflow channels, there is greater flattening of total channel curve for a load of 6 Erlangs, compared to the total channel curve of 0.75 Erlang traffic.

Flattening of the total number of channels occurs when an increase in the primary channels (per source-destination), is ‘somewhat’ cancelled by a decrease in the number of overflow channels, so that the net increase in the total number of channels becomes very small. On the other hand, the total number of channels increases linearly when an increase in the number of primary channels (per source-destination) is substantial compared to the decrease in the number overflows channels. Therefore, as the number of routes (destinations) increases, a small increase in the number of primary channels (per source-destination) results in a substantial increase in the total number of primary channels. In order to counter this increase in the number of primary channels, there is a higher statistical multiplexing gain at the overflow layer. However, when the number of primary channels is already very high the overflow gain, which is described in section 3.3 drops. A small overflow gain corresponds to a small decrease in the number of overflow channels, in response to an increase in the number of primary channels.

4.6.6.2 COST RATIO CR_{OUTPUT} Total channel cost not only depends on the total number of channels, but also on the value of CR_{output} , which relates the cost per channel to the cost per switching element. As the relative cost of a channel becomes very small, which causes to tend toward zero; the Hybrid Node will be able to obtain the cost advantage due to lowering of the number of cross-points. However, if CR_{output} becomes very large, it may be more prudent to conserve channels rather than conserve switch cross-points. In such a case, it may become prohibitively expensive to provide primary channels in addition to overflow channels. Without primary channels, the loss performance of each source becomes equal to the loss provided by the overflow layer.

For a low value of CR_{output} , it is possible to realize a minimum-cost node by minimizing the number of switch contacts. Even if channel costs become infinitely cheap compared to the cost of a switch contact, it may not be cost optimal to operate with primary

channels alone. Some amount of overflow channels will be required to provide a minimum cost node, as it is apparent from the curve labeled $CR_{amp} = 0$, in [Figure 4.43](#).

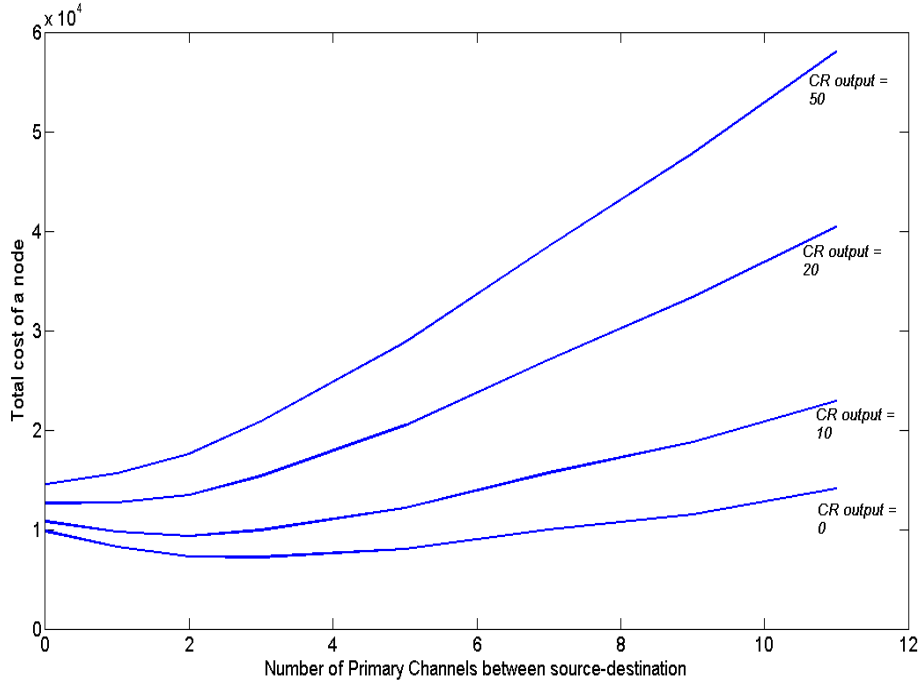


Figure 4.43 Total cost of a node.

[Figures 4.43](#), [4.44](#) and [4.45](#) shows the total cost of a Hybrid node constructed using un-integrated B-S architecture and for an offered load of 0.75, 3 and 6 Erlangs, respectively.

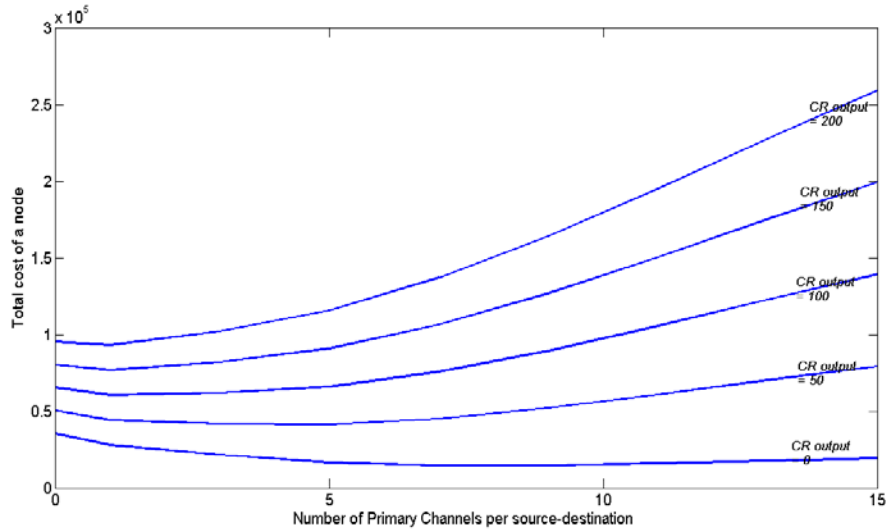


Figure 4.44 Total cost of a node. Offered load = 3 Erlangs

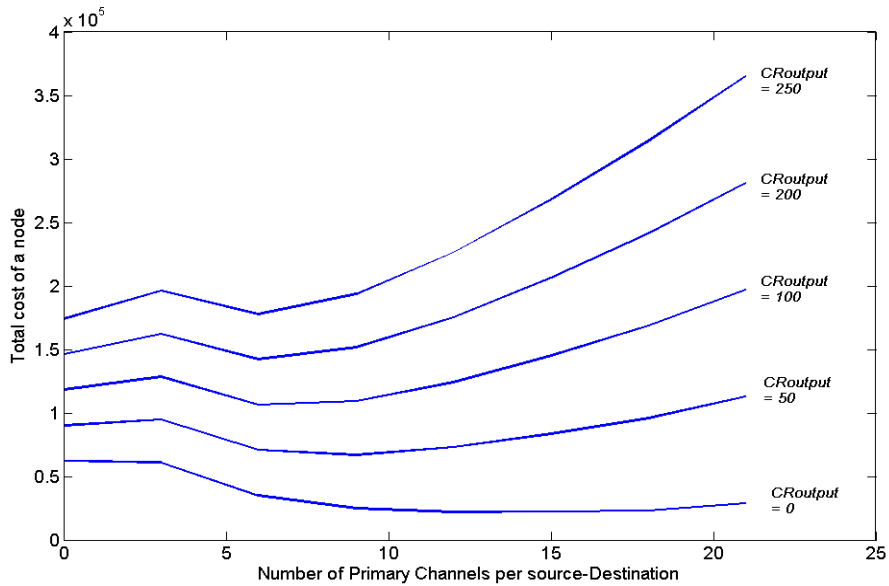


Figure 4.45 Total cost of a node. Offered load is 6 Erlangs.

From [Figures 4.43, 4.44](#) and [4.45](#), it can be seen that channel cost affects the hybrid advantage for the B-S architecture. The effect of transport cost on undoing the advantage of hybrid operation on switching cost is felt more, at lower offered loads. For instance, in [Figure 4.43](#), the hybrid cost advantage is lost, when minimum total cost occurs when the number of

primary channels per source-destination is either 0, or 11. In this figure, it requires a CR_{output} of 20 to overcome the hybrid cost advantage. On the other hand, in [Figure 4.45](#), for a 6 Erlangs offered load, CR_{output} should be as high as 100 to overcome the hybrid advantage. At a CR_{output} of 100, the total cost of the node is minimum when $p = 21$, which indicated a non-hybrid operation with only primary channels. In this figure, for a CR_{output} that is less than 100, hybrid cost advantage is always obtained for values of p between (but not including) 0 and 21.

For a core-node constructed using the Benes architecture, hybrid operation provides a minimization of cross-points over a wide range of primary channels. This advantage is lost when total cost includes a large transport cost. It is also seen that, for a smaller value of offered load, such as 0.75 Erlangs, the total cost curve is highly sensitive to transport costs, compared to a core node with an offered load of 6 Erlangs. Figures 4.46, 4.47 and 4.48 shows the total cost of a node constructed using Benes architecture, whose basic element is a single-wavelength 2x2 switch.

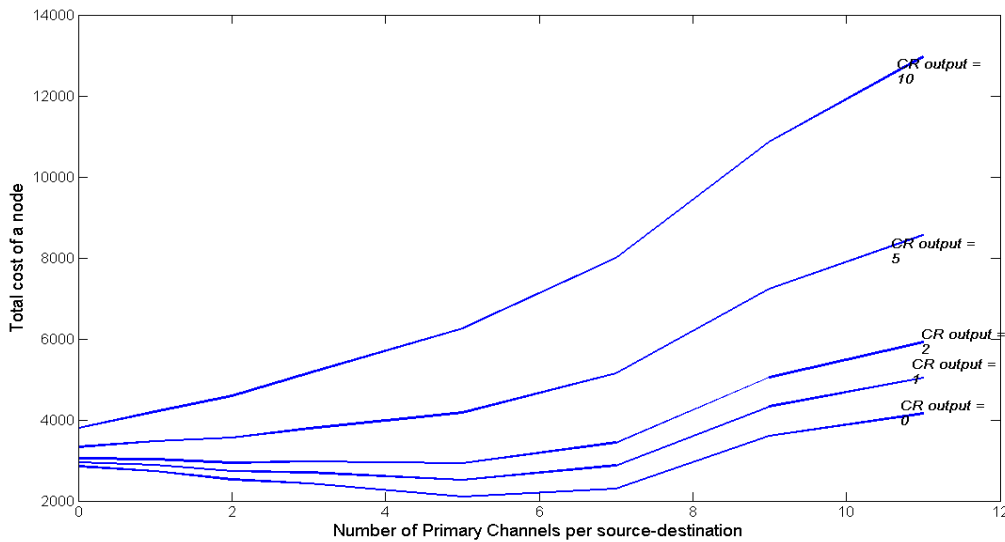


Figure 4.46 Total cost for a core node with an offered load of 0.75 Erlangs per source-destination.

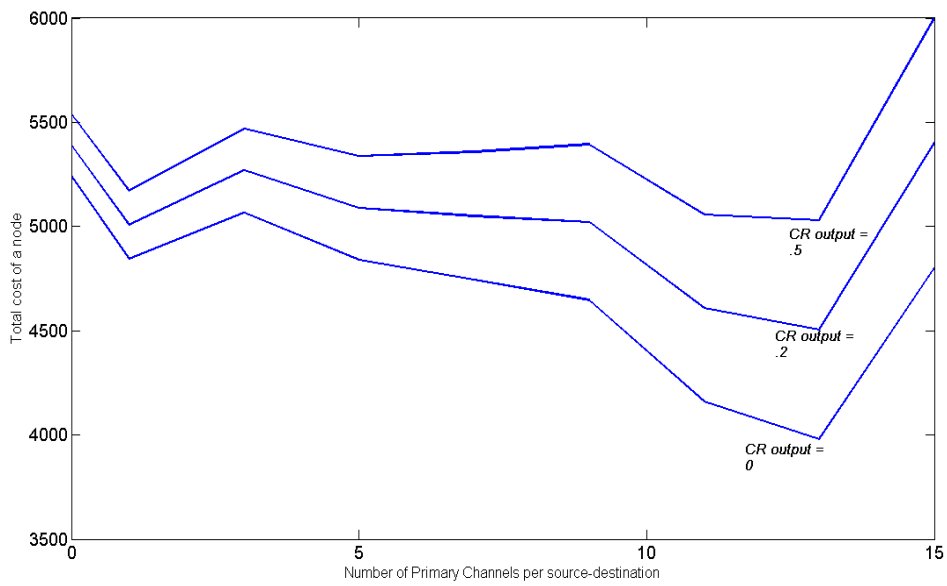


Figure 4.47 Total cost for a core node with an offered load of 3 Erlangs per source-destination.

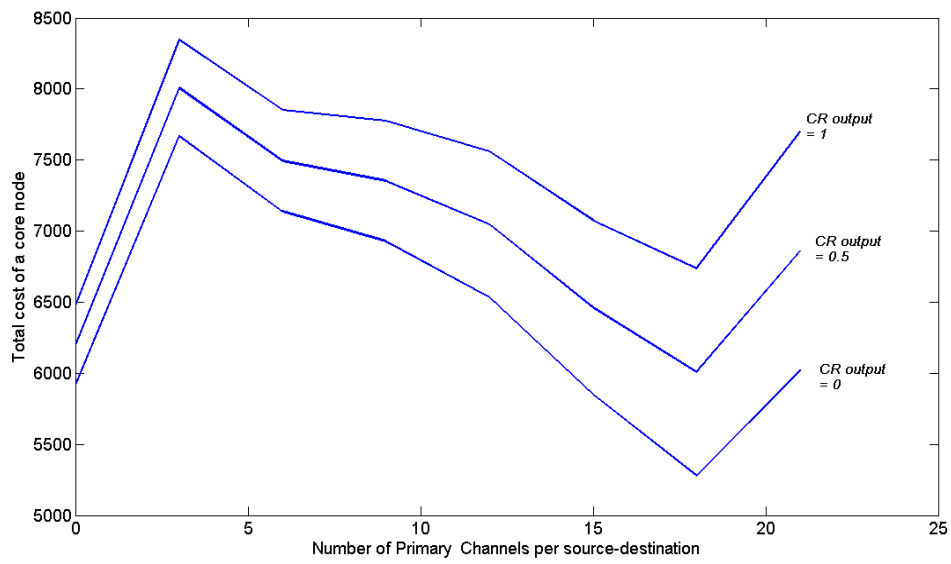


Figure 4.48 Total cost for a core node with an offered load of 6 Erlangs per source-destination.

4.7 HYBRID COST ADVANTAGE

4.7.1 HYBRID COST ADVANTAGE FOR $CR_{AMP} = 0$ AND $CR_{OUTPUT} = 0$

The hybrid cost advantage due to lowering of the number of cross-points can be obtained by setting values of CR_{amp} and CR_{output} at zero in the $Total\ cost(p)$ in [equation 4.30](#). A maximum hybrid cost advantage is obtained when $Total\ cost(p)$ is a minimum at p , which is the number of primary channels (per source-destination) at the output of the Hybrid Node. Plots depicted below show the percentage value of hybrid cost advantage for various switching fabric architecture and various values of offered load. Percentage hybrid cost advantage is given by the value of $percent_HCA(p)$, in [equation 4.34](#) and calculated using the minimum value of $Total\ cost(p)$. Minimum value of $Total\ cost(p)$ occurs at a value of p that lies between 0 and P , where P is the number of primary channels allotted to a route when there are no overflow channels in the path. The hybrid cost advantage components at p , $HCA_{prim}(p)$ and $HCA_{overflow}(p)$, are calculated separately for active and passive overflow schemes using [equation 4.33](#). [Figures 4.49, 4.50, 4.51](#) and [4.52](#), shows the percentage value of HCA for a Hybrid node constructed using the B-S, the Benes and the Clos architecture.

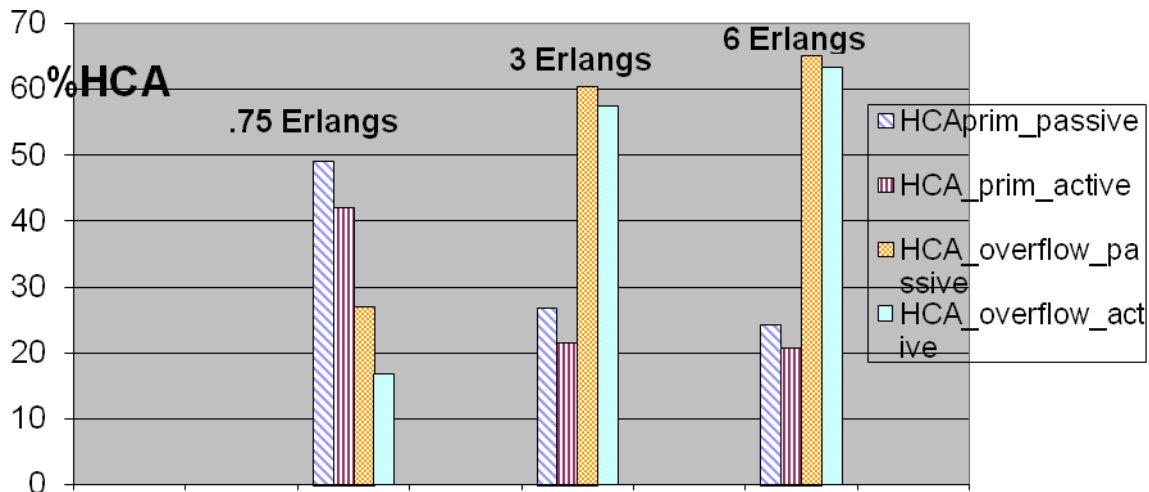


Figure 4.49 Percentage values of HCA for a core node made using B-S architecture.

Comparing the values of HCA in [Figures 4.49](#) and [4.50](#) for the same load values, it is seen that HCA is more pronounced for B-S architecture, specially at higher loads. It is also seen that gates in active overflow case cause HCA to reduce to almost zero for Benes- based core nodes.

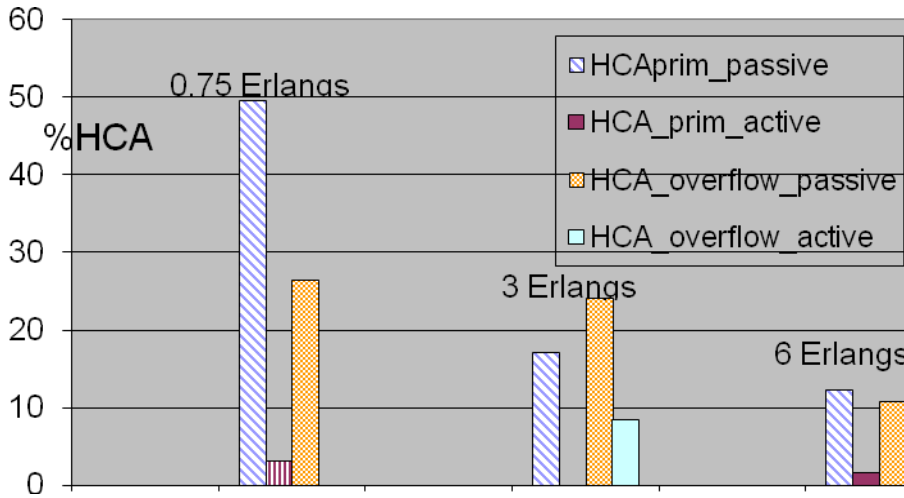


Figure 4.50 Percentage values of HCA for a core node made using Benes architecture

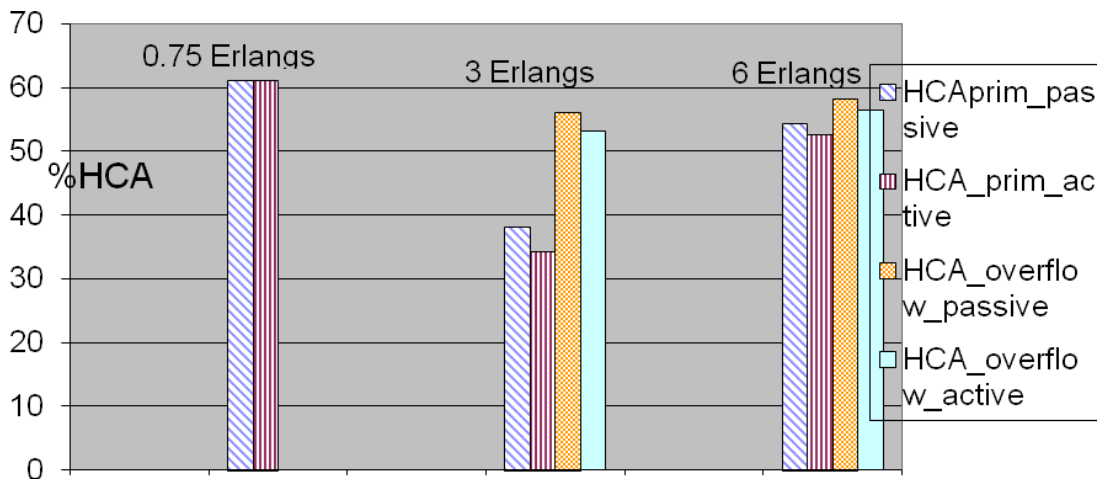


Figure 4.51 Percentage values of HCA for a core node made using Integrated B-S architecture.

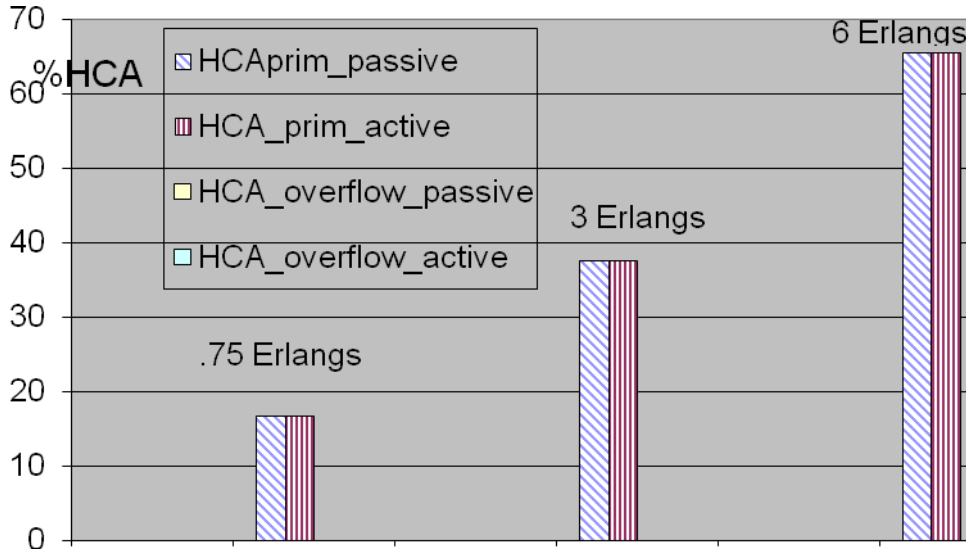


Figure 4.52 Percentage values of HCA for a core node made using Clos architecture

In [Figure 4.51](#), a multi wavelength 1x1 switch is the basic element. In [Figure 4.52](#), the basic element is a multi wavelength 4x4 switch. In [Figure 4.51](#), HCA is realized for higher loads, but in [Figure 4.52](#) HCA is not realized for any of the loads considered, because $HCA_{overflow}$ is zero, since total cost is a minimum when there are no primary channels, as seen in [Figures 4.39](#), [4.40](#) and [4.41](#).

6004 EFFECT OF SWITCH FABRIC ARCHITECTURE

Switch fabric architecture such as Broadcast-Select, Benes and Re-arrangeable Clos, are considered to test the possibility of hybrid advantage. In all the three cases, the hybrid cost advantage occurs with varying sensitivities toward offered load and cost ratios. The Broadcast-and-select architecture shows the minimization of 1x1 switch elements at all three values of offered load (.75 Erlangs, 3 Erlangs and 6 Erlangs) between a source and a destination node. The Benes architecture also shows a minimization of 2x2 switches, but the hybrid advantage seems to be more pronounced at lower values of offered load, compared to higher values of offered load. Also, the hybrid advantage in nodes using Benes architecture is found to be more sensitive to channel and amplifier cost ratios. The Broadcast-and-Select architecture, on the other hand, requires a larger cost ratio to undo the hybrid advantage. The degree of integration also

affects the hybrid advantage of realizing minimum cross-points, in a core node with Benes architecture, compared to B-S architecture.

The hybrid cost advantage is more pronounced in B-S based core node due to the underlying sensitivity of growth in cross points to the growth in the output channels. For an NxN switch, the 1x1 elements in a B-S based switch grows at a rate of N*N, whereas 2x2 elements in a Benes switch of the same dimension, grows at the lower bound of $2 \cdot \log_2 N - 1$. This makes the Benes architecture conserve cross-points, compared to the B-S architecture.

Tables 4.2, 4.3, 4.4 and 4.5 shows the slope of the primary and the overflow OB-switches by measuring the increments in the number of cross-points for B-S and Benes architectures, for a load of 0.75 and 6 Erlangs. The slope of the primary and the overflow layers is obtained by first, calculating the number of overflow channels for a given number of primary channels, using equation (4.3) and then calculating the total number of cross-points for the primary and the overflow switches using [equations \(4.13\)](#) and [\(4.16\)](#), respectively. The slope of the curve depicting the number of cross-points is calculated using a curve fitting procedure, as shown in the tables below. Figure

Table 4.2 Slopes of the primary and overflow layer OB-switch based on B-S architecture for an offered load of 0.75 Erlangs per source-destination.

Primary channels	0	1	2	3	4	5	6	7	8	9	10
Slope of Primary Layer	427.7	400.8	390.6	391.84	399.4	408.15	413	408	390.5	352.4	290.2
Slope of Overflow Layer	-773.6	-472	-570.48	-647	-549.33	-305.33	-44.02	-91.25	-27.06	-156.1	-139.47
<p>Curve fit parameters of the Primary layer curve: $f(x) = p1 \cdot x^4 + p2 \cdot x^3 + p3 \cdot x^2 + p4 \cdot x + p5$ Coefficients with 95% confidence: $p1 = -.214$; $p2 = 3.617$; $p3 = -18.42$; $p4 = 427.7$; $p5 = -4.545$ Goodness of fit : SSE = 539.4 ; R-square = 1</p> <p>Curve Fit parameters for Overflow layer curve: $f(x) = p1 \cdot x^6 + p2 \cdot x^5 + p3 \cdot x^4 + p4 \cdot x^3 + p5 \cdot x^2 + p6 \cdot x + p7$ Coefficients with 95% confidence: $p1 = .1172$; $p2 = -3.63$; $p3 = 40.45$; $p4 = -189.6$; $p5 = 363.3$; $p6 = -773.8$; $p7 = 2865$ Goodness of fit: SSE = 8915; R-square = 0.9991 .</p>											

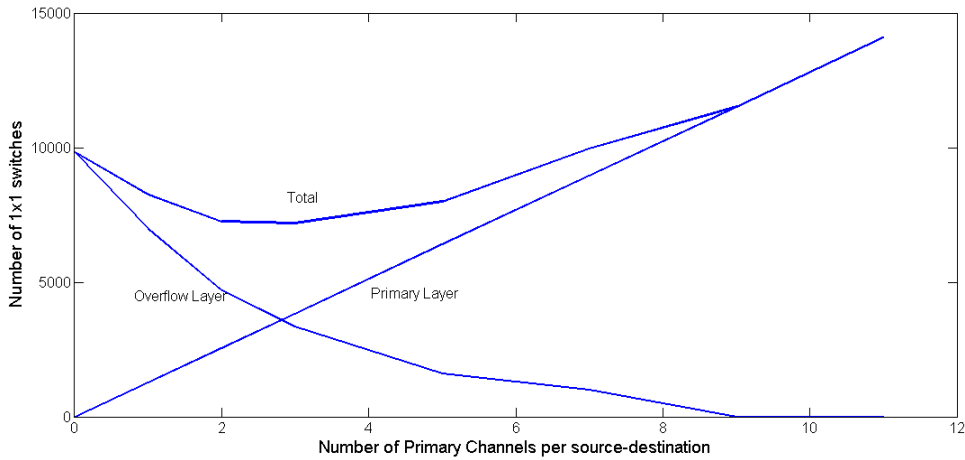


Figure 4.53 Number of 1x1 switches for a core node using B-S architecture and an offered load of .75 Erlangs, 10 sources and 1 destination.

Table 4.3 Slopes of the primary and overflow layer OB-switch based on B-S architecture for an offered load of 6 Erlangs per source-destination.

Primary channels	0	2	4	6	8	10	12	14	16	18	20
Slope of Primary Layer	473.46	377.2	402.73	417.56	374.5	283.17	186.06	131.5	148.31	219.0	215.2
Slope of Overflow Layer	1263	-160	-585	-567	-439.33	-363.58	-369.045	-405.2	-384.5	-229.1	77.9

Curve fit parameters of the Primary layer curve:

$$f(x) = p1*x^6 + p2*x^5 + p3*x^4 + p4*x^3 + p5*x^2 + p6*x + p7$$

Coefficients with 95% confidence:

$$p1 = -.00112 ; p2 = .07066 ; p3 = -1.573 ; p4 = 14.66 ; p5 = -56.7 ; p6 = 473.5 ; p7 = .7752$$

Goodness of fit : SSE = 2062 ; R-square = .9999

Curve Fit parameters for Overflow layer curve:

$$f(x) = p1*x^6 + p2*x^5 + p3*x^4 + p4*x^3 + p5*x^2 + p6*x + p7$$

Coefficients with 95% confidence:

$$p1 = -.002012 ; p2 = 0.1636 ; p3 = -5.048 ; p4 = 74.88 ; p5 = -543.5 ; p6 = 1264 ; p7 = 5918$$

Goodness of fit: SSE = 221.3; R-square = 1

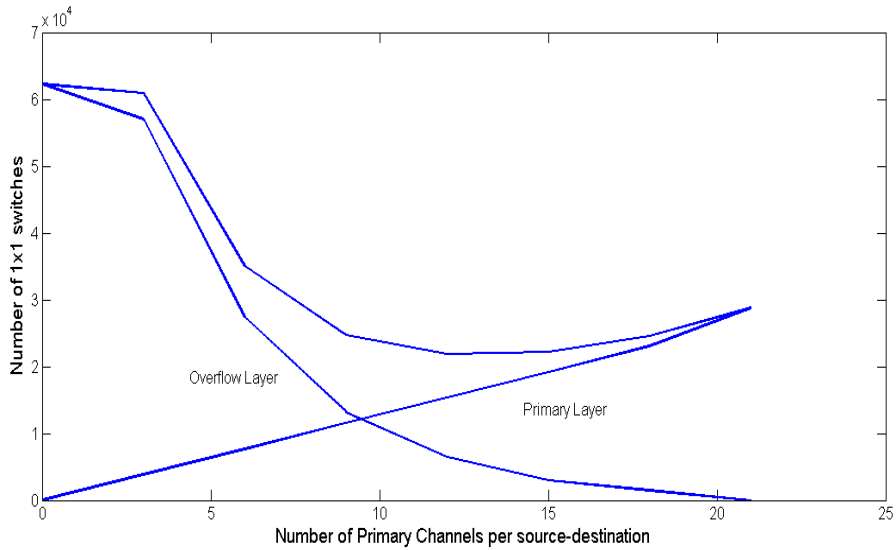


Figure 4.54 Number of 1x1 switches for a core node using B-S architecture and an offered load of .75 Erlangs, 10 sources and 1 destination.

Table 4.4 Slopes of the primary and overflow layer OB-switch based on Benes architecture for an offered load of 0.75 Erlangs per source-destination.

Primary sources	0	1	2	3	4	5	6	7	8	9	10
Slope of Primary	1280	1280	1280	1280	1280	1280	1280	1280	1280	1280	1280
Slope of Overflow	-3116.23	-2547	-1866	-1229	-738.9	-444.8	-346.4	-393.3	-480.6	-454.1	-107.1

Curve Fit parameters for Overflow layer curve: $f(x) = p1*x^5 + p2*x^4 + p3*x^3 + p4*x^2 + p5*x^1 + p6$
Coefficients with 95% confidence:
 $p1 = 0.4282$; $p2 = -9.613$; $p3=51.8$; $p4=225.4$; $p5 = -3116$; $p6 = 9827$
Goodness of fit: SSE = 2.839e+004 ; R-square = 0.9997 .

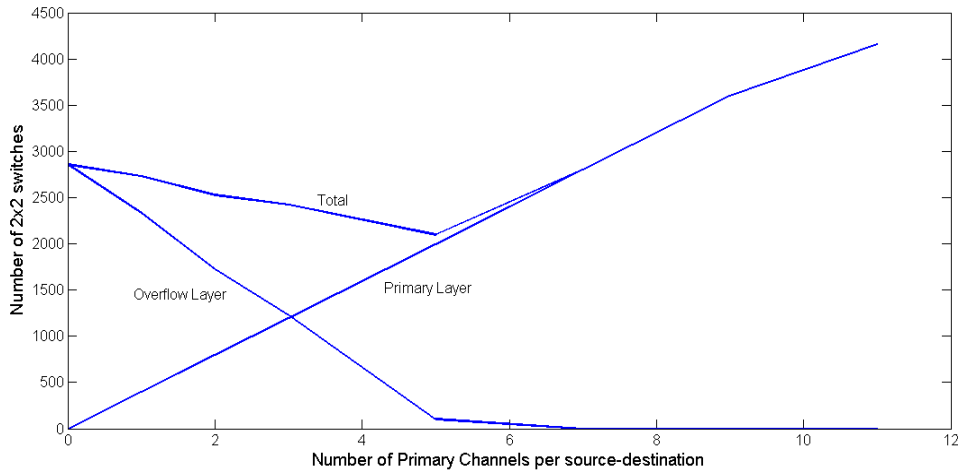


Figure 4.55 Number of 2x2 switches for a core node using Benes architecture and an offered load of .75 Erlangs, 10 sources and 1 destination.

Table 4.5 Slopes of the primary and overflow layer OB-switch based on Benes architecture for an offered load of 6 Erlangs per source-destination.

Primary channels	0	2	4	6	8	10	12	14	16	18	20
Slope of Primary Layer	1458	1350	1272	1225	1207	1220	1263	1337	1440	1574	1737
Slope of Overflow Layer	13769	-6685	-10507	-7751	-4105	-1954	-1445	-1549	-1125	-150.5	-48.23

Curve fit parameters for Primary layer curve: $f(x) = p1 * x^3 + p2 * x^2 + p3 * x + p4$

Coefficients with 95% confidence:

$p1 = 1.257$; $p2 = -30.71$; $p3 = 1458$; $p4 = -116.8$

Goodness of fit: $SSE = 3.91e+.005$; $R\text{-square} = 0.9994$

Curve Fit parameters for Overflow layer curve:

$f(x) = p1 * x^6 + p2 * x^5 + p3 * x^4 + p4 * x^3 + p5 * x^2 + p6 * x + p7$

Coefficients with 95% confidence:

$p1 = -0.04616$; $p2 = 3.382$; $p3 = -96.17$; $p4 = 1316$; $p5 = -8357$; $p6 = 9827$

Goodness of fit: $SSE = 1.053e+006$; $R\text{-square} = 0.9998$.

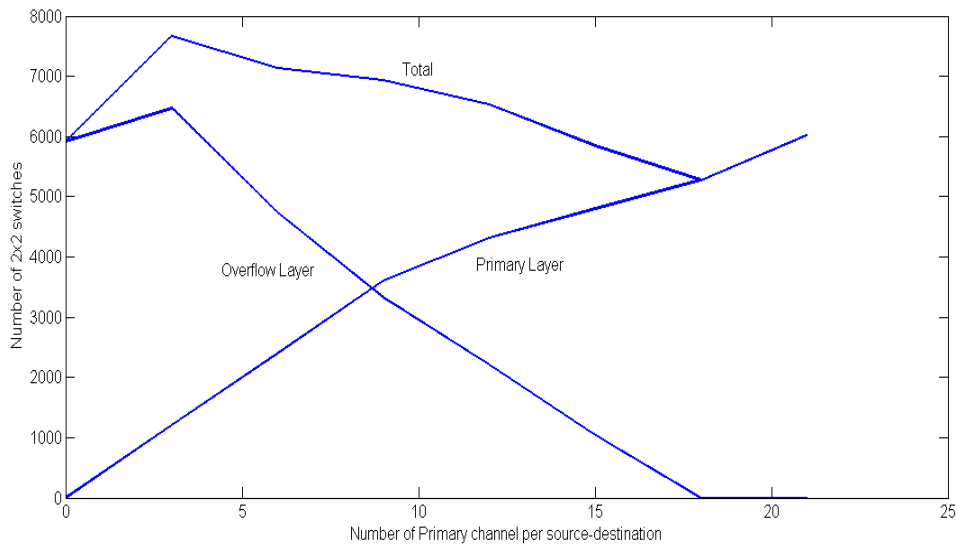


Figure 4.56 Number of 2x2 switches for a core node using Benes architecture and an offered load of 6 Erlangs, 10 sources and 1 destination.

It can be seen from the tables associated with the [Figures 4.53](#) and [4.54](#) that, for the B-S architecture, the slope of the overflow layer decreases continuously. For the Benes architecture in [Tables 4.4](#) and [4.5](#) and in [Figures 4.55](#) and [4.56](#), however, the slope of the overflow layer remains more or less constant over a wide range.

It is also seen that in a Hybrid Node, the growth rate of cross points of the underlying switch architecture also makes hybrid advantage sensitive to the value of cost ratios, such as CR_{amp} and CR_{output} . For instance, by observing [Figures 4.54](#) and [4.56](#), we may compare Hybrid Nodes with B-S and Benes architectures and an offered load of 6 Erlangs. It is seen in [section 4.6](#) that the values of CR_{amp} and $CR_{outputs}$ tend to undo the hybrid cost advantage. It is also seen in [section 4.6](#) that compared to a B-S based node, the Benes based Hybrid Node requires only very small values to CR_{amp} and $CR_{outputs}$ to overcome hybrid advantage completely. This may be explained by the slope of total number of switching elements, labeled as ‘Total’ in the figures above. For a Benes-based Hybrid Node, a relatively ‘stable’ slope of the ‘Total’ curve over different values of number of primary channels makes it more susceptible to absorb cost curves of amplifiers and output transport costs. However, the slope of the ‘Total’ curve for a B-S-based Hybrid Node has a ‘steeper’ slope, which is not easily susceptible to the cost curves of amplifiers and output channel cost. To put it another manner, the incremental cost of the number of

switching elements in a B-S based Hybrid Node has a higher resistance to being influenced by the relative cost structure of amplifiers and channel costs. On the contrary, the incremental cost of the switching elements in a Benes-based Hybrid Node has a low resistance to the relative cost structure of amplifiers and channels costs.

4.8 CHAPTER CONCLUSION

Optical Burst Switching operation plays a central role in implementing a Hybrid Node. In this chapter a general design for the OB-Switch of a Hybrid Node is proposed. The OB-Switch can be constructed using space-switches that may be constructed using any kind of switch fabric architecture. However, the potential of the Hybrid Node to realize the hybrid cost advantage (HCA) strongly depends on the underlying space switch fabric architecture.

A Hybrid Node is cost optimal if the incremental cost of the primary layer is equal to the decremented cost of overflow layer. It is assumed that the predominant cost components of each layer is the switching cost, which depends on the switch architecture and on the transport costs. The switching costs are further classified into the facility switching costs and the OB-switching costs. The OB-switching cost grows at a nearly linear rate for primary layer and at a polynomial rate for the overflow layer of the OB-switch. If we assume the channel related costs and the facility switching to be negligible, the optimality of the OB-switch will decide the optimality of the Hybrid Node.

It is seen that a wide sense non-blocking switch fabric, such as the one constructed using the Broadcast-Select architecture, realizes hybrid cost advantage over a wider range of offered load and it is less sensitive to the changes in non-switching parameters such as CR_{amp} and CR_{output} . The rearrangeably non-blocking space-switch fabrics that minimize the number of switching elements, such as the Benes and Clos, causes the hybrid cost advantage to be highly sensitive to offered load and the non-switching parameters.

Space-switch fabric architectures that help conserve the constructional costs of a Hybrid Node, either via minimizing the number of switching elements or by monolithic integration, may not result in a large hybrid cost advantage. In re-arrangeably non- blocking switch fabrics such, as

the Benes and Clos architectures, the switch size grows slowly with an increase in the number of output channels. On the other hand, space switch fabrics that are not constructionally optimal to begin with, may benefit greatly from the hybrid architecture in cutting the total cost of the node.

Hybrid operation of a core node requires an additional stage of overflow, which is not present in non-hybrid operation. The overflow process can be implemented in a passive manner using splitters or actively using gates. The addition of overflow gates has little effect on the total cost of a B-S switch based node and HCA is seen for both active and passive overflows. For a Benes switch based node, however, active overflows increase the total cost substantially, as to not provide any HCA.

Thus, we conclude that hybrid operation has the potential to reduce total switching cost, which is strongly dependent on the underlying space architecture. Other main costs, such as the cost of amplification and channel costs (including the cost of wavelength conversion on each channel), only increase due to hybrid operation. Hybrid operation has the greatest potential to provide cost advantage if the switching-element cost dominates over other costs and if there is much scope to minimize the number of switch elements in the switch fabric and still maintain the wide-sense non-blocking property.

5.0 ANALYSIS OF A NETWORK OF HYBRID NODES

5.1 INTRODUCTION

A Hybrid Network consists of a set of interconnected Hybrid Nodes, linked together by primary and overflow channels. The primary and overflow channels divide the physical network into two layers, the primary and overflow layers, respectively. To an optical burst entering the core network, the primary path provides a direct ‘virtual’ path to the destination node, although physically, the burst passes through several node hops. Hence, we call the primary layer a ‘virtual layer’.

The average load or channel occupancy of a primary channel in the primary layer is an important metric that can be used to design a hybrid optical network. The channel occupancy of primary channels corresponds to the average load carried by the channel, and it is measured in Erlangs unit. A channel occupancy/load of nearly 1 Erlang corresponds to a channel utilization of nearly one hundred percent. The average load or channel occupancy that is required to be carried by a primary channel, along with the net load offered to the Hybrid Nodes, determines the number of primary/overflow channels in the system. It was seen in Chapter 3 that, for a given offered load at a Hybrid Node, the primary layer modulates the traffic load offered to the overflow layer.

Provisioning a rich primary layer in the proposed overflow network tends to increase the cost due to over-provisioning. However, a rich primary layer also brings down the cost of the overflow layer, because there is a smaller load on the overflow channels. A cost-optimal Hybrid Network will seek to balance these two costs by appropriately selecting the level of primary channel utilization/channel occupancy. An optimal value of primary channel utilization/channel

occupancy can help balance the primary and overflow channel costs in a Hybrid Network, and leads to minimizing the total cost of the core network.

The total cost of a network can be calculated in terms of the total cost of switching and transport infrastructure used to construct the network. Chapter 4 addressed the construction cost of a single Hybrid Node. In a Hybrid Network, however, the Hybrid Nodes are not isolated; instead they are interconnected by the network links, made up of primary/overflow channels. The first goal of this chapter is to determine the number of primary/overflow channels in the links, such that the total switching and transport cost of the entire network is a minimum.

Yet another approach to determine an optimal Hybrid Network is to determine the total cost of all routes in the network. A route exists for every pair of core nodes in the network. A route may contain both primary and overflow paths. The relative cost of an overflow path, with respect to the cost of a primary path along the same route, is given by the path cost ratio, CR_{path} . It was seen in Chapter 3 that, for a fixed value of path cost ratio and for a given offered load, it is possible to obtain the optimal number of primary/overflow channels in the route. However, the path cost ratio itself is dependent on the number of primary channels because cost ratio depends on the possibility of light-path entry in the nodes along the route, as shown by Equation (3.6a) in Chapter 3. If there are more primary channels, the possibility of light-path entry increases and the path cost ratio may possibly decrease. If there are more primary channels available to carry a given offered load, channel load/utilization will decrease. The second goal in this chapter is to consider a network scenario and to determine CR_{path} of all the routes in the network. The value of CR_{path} depends on the probabilities of light-path entry at the network nodes; and the probability of light-path entry in turn, depends on the required primary channel utilization. Thus, a cost-optimal solution of a Hybrid Network may depend on the primary channel utilization with which we choose to operate our primary channels.

Both, total switching cost and total route cost of a network depends on the number of primary and overflow channels in the network links. The number of primary and overflow channels in the links depends on the probability of light-path entry within the network. In this chapter, light-path entry is provided for the optical bursts at a Hybrid Node as long as a primary channel may not carry a load that exceeds a certain given value. In this manner we also specify the amount of over-provisioning provided at the primary layer and we place this constraint on

primary channel performance in addition to the required blocking performance at the overflow layer.

The average carried channel-load in Erlangs, which also corresponds to the average channel utilization, is represented by letter U . For a given value of the offered access load, the total infrastructure cost and the total route costs may depend on the value of U required for the primary channels. Total infrastructure cost and total route costs, which depend on the value of U , are determined for a network topology example. The chapter provides only an ad-hoc solution for the optimality of a Hybrid Network. A general solution is beyond the scope of this chapter.

In this chapter, a method will be provided to determine the number of primary and overflow channels in each link of the network, for a given load, given value of U and given blocking rate B , at the nodes. The method can be used to determine number of primary/overflow channels in each link of the network for different values of U , ranging from 0 to 1. By knowing the number of primary and overflow channels in the links, the total infrastructure cost and the total route cost will be determined. The value of U , for which the cost of the network is at a minimum, is then determined. This value of U , which gives the optimal number of primary and overflow channels, is examined for its dependency of the relative costs of switching and transport components.

5.2 HYBRID NETWORK MODELING

A Hybrid Network, consisting of N nodes and L links, is modeled as a graph containing N vertices and L edges. The primary layer is modeled using two interrelated graphs, one of which is the graph representing the virtual connections made by the primary channel and the other one contains the actual physical mapping of the virtual connections on the network graph. The following graphs are used to model a Hybrid Network,

1. A physical network graph, G_N
2. A virtual primary-layer graph, G_V
3. A physical primary-layer graph, G_P
4. An overflow-layer graph, G_O

5.2.1 GRAPH DEFINITIONS AND EXAMPLES

Consider a core network, whose nodes N , and physical links L , are shown in [Figure 5.1](#).

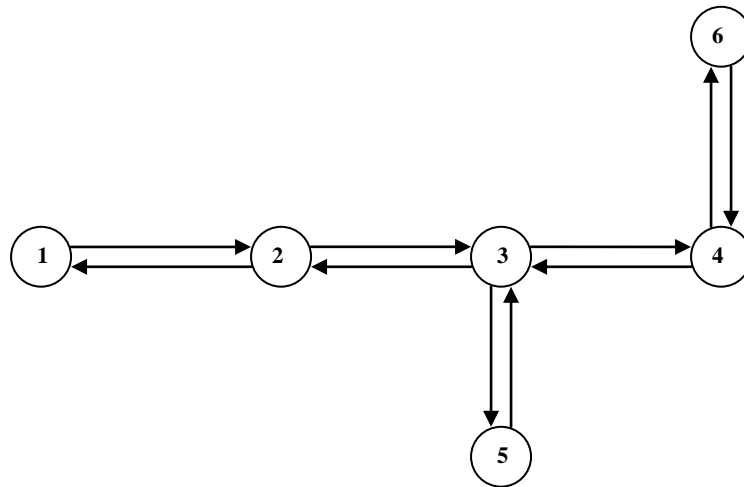


Figure 5.1 A example core-network topology

In the example shown above, $N = 6$ and $L = 10$. The core-network topology in the figure above can be mapped into its Network Graph, G_N , as defined below.

- Definition 5.1: Network Graph, G_N

For a given physical network consisting of N Hybrid Nodes and L links, a unidirectional physical network graph, G_N , consists of vertices v_i and edges e_{ij} ,

where $i = 1, 2, \dots, N$; $j = 1, 2, \dots, N$ and i is not equal to j .

The incidence matrix of G_N is given by I_N ,

where $I_N(i,j) = 1$ when there exists a physical link between nodes i and j

and $I_N(i,j) = 0$, when there is no physical link between nodes i and j .

The Adjacency matrix of G_N is given by A_N ,

where $A_N(i,j) = A_P(i,j) + A_O(i,j)$. $A_P(i,j)$ and $A_O(i,j)$ are the adjacency matrices of the primary and overflow layer graphs, G_P and G_O , respectively.

The properties of G_P and G_O are defined in definitions 5.3 and 5.4. The incidence matrix I_N is a symmetric matrix but the adjacency matrix A_N may not be so.

For the example shown in [Figure 5.1](#), the network graph, G_N and its incidence matrix I_N is as shown in [Figure 5.2](#).

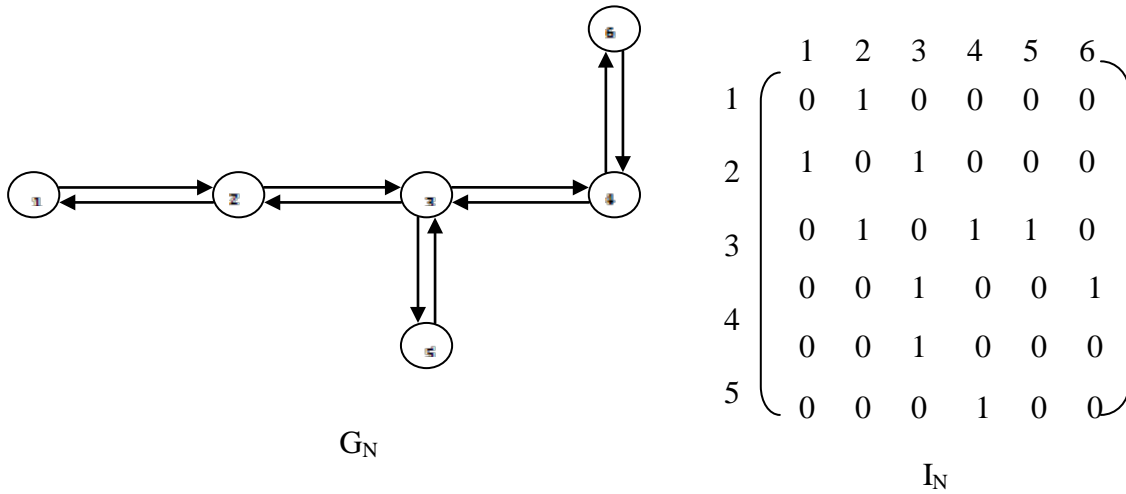


Figure 5.2 An example Network Graph and its Incidence matrix.

- Definition 5.2: Virtual primary layer graph, G_v

For a given network consisting of N Hybrid Nodes and L links, a unidirectional virtual primary layer graph, G_V , consists of vertices v_i and edges e_{ij} ,

$$\text{where } i = 1, 2, \dots, N \ ; \ j = 1, 2, \dots, N \ \text{and } i \text{ is not equal to } j.$$

The incidence matrix of G_V is given by I_V ,

where $I_V(i,j) = 1$ when there exists a primary link/light path between nodes i and j

and $I_V(i,j) = 0$, when there is no primary link/light path between nodes i and j .

The adjacency matrix of G_V is given by A_V ,

where $A_V(i,j)$ is equal to the number of primary light paths between nodes i and j .

Graph G_V is said to be a fully-connected graph if there exists at least one primary light path between every pair of nodes. For a fully connected graph, $I_V(i,j) = 1$ for all values of i and j , except when $i = j$.

The example topology in [Figure 5.1](#) is re-drawn to depict partially connected virtual primary graph, G_V , in which there is no light-path between some nodes.

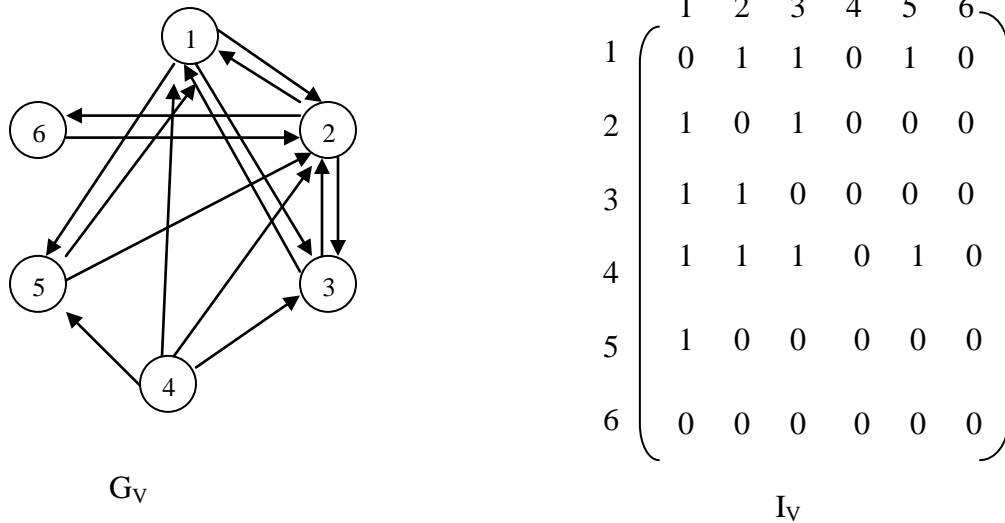


Figure 5.3 Example of a Virtual Primary layer graph.

In a network consisting of hybrid routes the light-paths in the primary layer is made of primary channels in each hop of the path. Therefore, a virtual primary layer graph can be mapped into its associated primary layer graph, as shown in [Figure 5.4](#) below, for the example in [Figure 5.3](#). In the above figure, node 6 is not connected to the other nodes using primary light-paths and node 4 does not have any incoming primary light-paths/channels. Therefore, column 6 and the entry (3,4) in the I_N matrix is a zero.

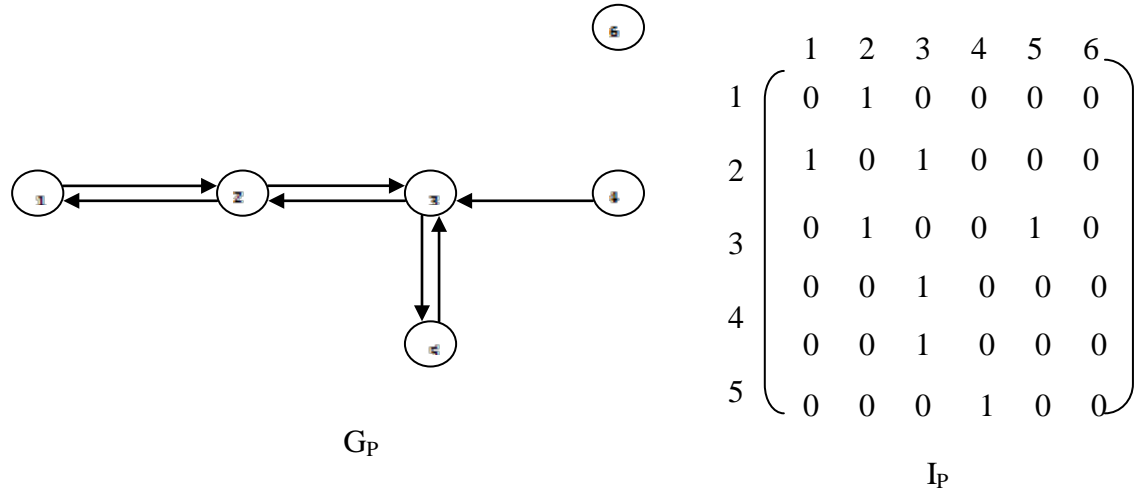


Figure 5.4 An example physical primary layer graph.

- Definition 5.3: Physical primary layer graph, G_P

For a given network consisting of N Hybrid Nodes and L links, a unidirectional physical primary layer graph, G_P , consists of vertices v_i and edges e_{ij} ,

where $i = 1, 2, \dots, N$; $j = 1, 2, \dots, N$ and i is not equal to j .

The incidence matrix of G_P is given by I_P ,

where $I_P(i,j) = 1$ when there exists a primary channel between nodes i and j and $I_P(i,j) = 0$, when there is no primary channel between nodes i and j .

The adjacency matrix of G_P is given by A_P ,

where $A_P(i,j)$ is equal to the number of primary light paths between nodes i and j .

A physical primary layer graph, G_P , can be constructed from a physical network graph, G_N , and a virtual primary graph, G_V , using appropriate path-routing principle. The routing function $R(i,k, G_N)$ produces an ordered set of edges, $E = (e(i,j_1), e(j_1,j_2), e(j_2,j_3), \dots, e(j_{n-1},j_n), e(j_n,k))$, where j_k is a vertex from V , which belongs to set $(1, 2, \dots, N)$. For each non-zero value of $I_V(i,j)$, which stands for the primary light-path connection between nodes i and j , the values of

$(I_P(i,j_1), I_P(j_1,j_2), I_P(j_2,j_3), \dots, I_P(j_{n-1},j_n), I_P(j_n,k))$, in I_P are reset to 1. Also, the matrix A_P is updated by updating the values of elements, $A_P(i,j_1), A_P(j_1,j_2), A_P(j_2,j_3), \dots, A_P(j_{n-1},j_n), A_P(j_n,j)$, by the amounts $e(i,j_1), e(j_1,j_2), e(j_2,j_3), \dots, e(j_{n-1},j_n), e(j_n,k)$, respectively. The values of edges $e(j_k, j_{k+1})$ are the number of primary channels in each link needed to complete the primary path connection between nodes i and k .

While the physical primary layer graph maps only the primary layers in a link, the overflow graph, G_o gives the overflow channels in each link of the network. The overflow graph, G_o , will contain an edge between two vertices, if there is an overflow channels between the corresponding nodes. Unlike G_v , the overflow graph G_o can have edges between two vertices only if the two vertices are neighbors in the actual physical topology. An overflow graph can be defined as :

- Definition 5.4 : Overflow graph, G_o

For a given network consisting of N Hybrid Nodes and L links, a unidirectional physical primary layer graph, G_o , consists of vertices v_i and edges e_{ij} ,

$$\text{where } i = 1, 2, \dots, N \ ; \ j = 1, 2, \dots, N \ \text{and } i \text{ is not equal to } j.$$

The incidence matrix of G_o is given by I_o ,

where $I_o(i,j) = 1$ when there exists an overflow channel between nodes i and j and $I_o(i,j) = 0$, when there is no overflow channel between nodes i and j .

The adjacency matrix of G_o is given by A_o ,

where $A_o(i,j)$ is equal to the number of overflow channels between nodes i and j .

[Figure 5.5](#) shows an overflow graph for the example network in [Figure 5.2](#).

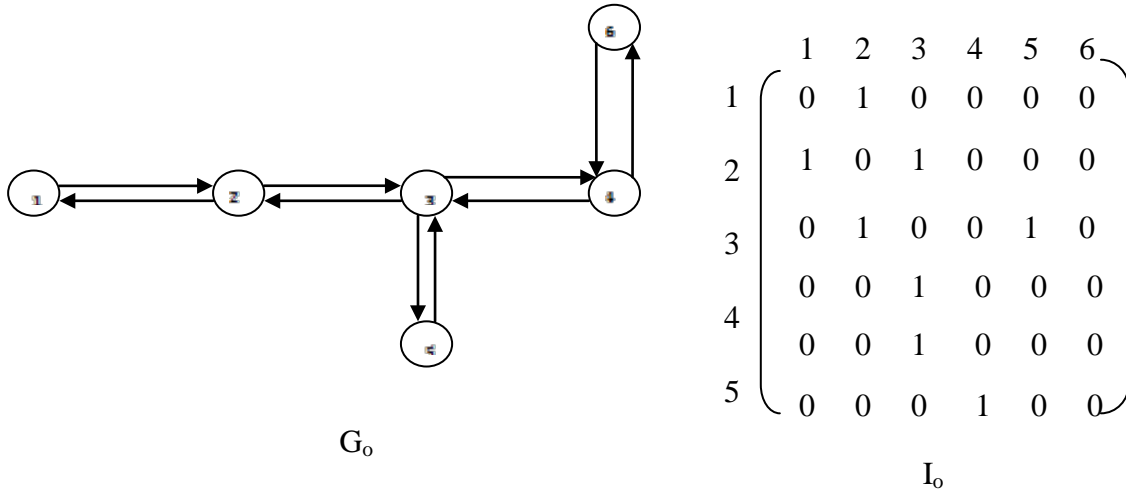


Figure 5.5 Example of an overflow layer graph

5.2.2 ROUTE AND TRAFFIC LOAD MATRICES

For a given graph, G_N , prior to determining the graphs, G_P , G_V and G_O , the route matrix and the traffic matrix is determined. In order to calculate the matrices G_P , G_V and G_O , the physical topology graph, G_N , and the load offered to each edge node is assumed to be provided. In addition, it is assumed that each edge node sends equal burst traffic load to all other nodes.

5.2.2.1 ROUTE MATRIX The optical bursts entering a primary path or a secondary overflow path at a Hybrid Node are assumed to follow the same shortest path to the destination. Using the physical topology graph G_N , a shortest path table is created for every pair of source-destination nodes. Floyd’s algorithm is used to create the shortest path table [52][53]. The algorithm provides a predecessor matrix, $P(G_N)$ and the adjacency matrix $A(G_N)$. Each element of $A(G_N)$, is identified/indexed by a unique integer valued identifier and placed in link matrix $L(G_N)$, which labels the physical links between two Hybrid Nodes. The Predecessor matrix, $P(G_N)$, gives the next hop-node to the destination, along a shortest path from a given source node. In addition, we identify each route between a pair of source and destination nodes, as elements of a route matrix, $R(G_N)$. If there are N nodes in a network, the $R(G_N)$ matrix is an $N \times N$ matrix, in which each

element is assigned a distinct integer value to signify a Route-Id. Element $R(i,j)$ gives the Route Id for a route from node i to node j .

The example network topology in [Figure 5.1](#), is re-drawn below in [Figure 5.6](#), along with the link Id for each link.

- **Step 1:** Obtain, $I(G_N)$ the incidence matrix of G_N .

The rows and columns of the incidence matrix identify the source and destination nodes, respectively.

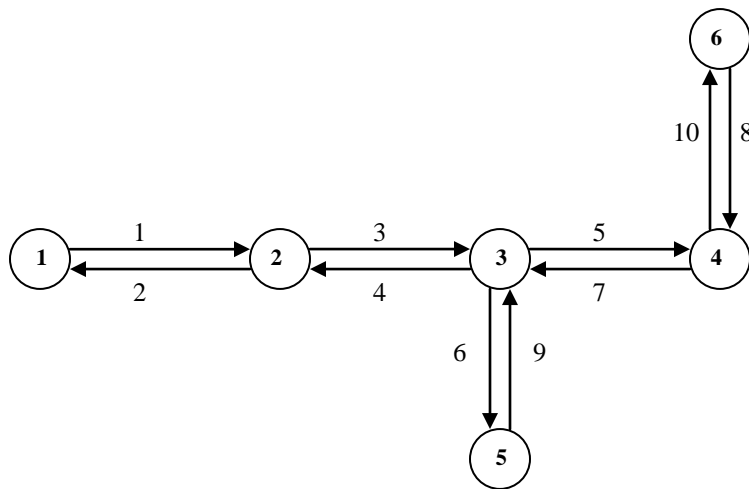


Figure 5.6 Physical Network in the example with link IDs .

Incidence matrix, $I(G_N) =$

$$\begin{bmatrix} 0 & 1 & 0 & 0 & 0 & 0 \\ 1 & 0 & 1 & 0 & 0 & 0 \\ 0 & 1 & 0 & 1 & 1 & 0 \\ 0 & 0 & 1 & 0 & 0 & 1 \\ 0 & 0 & 1 & 0 & 0 & 0 \\ 0 & 0 & 0 & 1 & 0 & 0 \end{bmatrix},$$

Where, rows give the source node and columns, the next hop destination.

- **Step 2:** Map $I(G_N)$ into the appropriate Link matrix, $L(G_N)$, by giving each unidirectional link a link-Id. Also, map $I(G_N)$ into the appropriate route matrix, $R(G_N)$, by identifying the route between a pair of nodes with a route-Id. The rows identify the source and the columns identify the destination in both matrices.

$$L(G_N) = \begin{bmatrix} 0 & 1 & 0 & 0 & 0 & 0 \\ 2 & 0 & 3 & 0 & 0 & 0 \\ 0 & 4 & 0 & 5 & 6 & 0 \\ 0 & 0 & 7 & 0 & 0 & 8 \\ 0 & 0 & 9 & 0 & 0 & 0 \\ 0 & 0 & 0 & 10 & 0 & 0 \end{bmatrix} \quad R(G_N) = \begin{bmatrix} 1 & 2 & 3 & 4 & 5 & 6 \\ 7 & 8 & 9 & 10 & 11 & 12 \\ 13 & 14 & 15 & 16 & 17 & 18 \\ 19 & 20 & 21 & 22 & 23 & 24 \\ 25 & 26 & 27 & 28 & 29 & 30 \\ 31 & 32 & 33 & 34 & 35 & 36 \end{bmatrix}$$

$L(G_N)$ matrix names each link in the physical network and $R(G_N)$ identifies each end-to-end path in the physical network.

- **Step 3:** Determine the predecessor matrix, $P(G_N)$, using Floyd's algorithm.

$$P(G_N) = \begin{bmatrix} 2 & 2 & 2 & 2 & 2 & 2 \\ 1 & 1 & 3 & 3 & 3 & 3 \\ 2 & 2 & 2 & 4 & 5 & 4 \\ 3 & 3 & 3 & 3 & 3 & 6 \\ 3 & 3 & 3 & 3 & 3 & 3 \\ 4 & 4 & 4 & 4 & 4 & 4 \end{bmatrix}$$

The rows of the predecessor matrix identify the source nodes and columns identify destination nodes. Each element of the matrix gives the next hop node to the end destination.

5.2.2.2 TRAFFIC LOAD MATRIX A Traffic Load Matrix, $T(G_N)$, is created to obtain the overflow traffic of a particular route, which passes through a physical unidirectional link of G_N . $T(G_N)$ has $N \times N$ rows and $2 * E$ columns, where $2 * E$ is the number of unidirectional edges of G_N .

An entry, $T(r,s)$, of the $T(G_N)$ matrix gives the amount of overflow traffic of route ‘ r ’ that is present in link ‘ s ’. Route r , which begins in node i and ends in node j , has its Route-Id r , obtained from $R(i,j)$ element in matrix $R(G_N)$. Link s , which links node p to node q , is the value of entry $L(p,q)$ of link matrix $L(G_N)$.

The $T(G_N)$ matrix provides a decomposition of the overflow load on a route, on a link-by-link basis. Traffic decomposition is important to consider because the OBS control plane will decompose headers and queue them on the outgoing links of a node based on their route information. The route information will provide the source and destination of the header, as mentioned in section 3.3.1.

Each entry in the $T(G_N)$ matrix is determined by considering the load entering the overflow channels of a link, after considering the loss probability and the probability of primary path entry, for a given offered load to the Hybrid Node, as shown in [Figure 5.7](#). Losses occur, when a burst-traffic load offered to a Hybrid Node cannot be accommodated on the overflow link considered. In addition, due to primary light path entry of some of the bursts, only a fraction of the total offered load is carried along the overflow links.

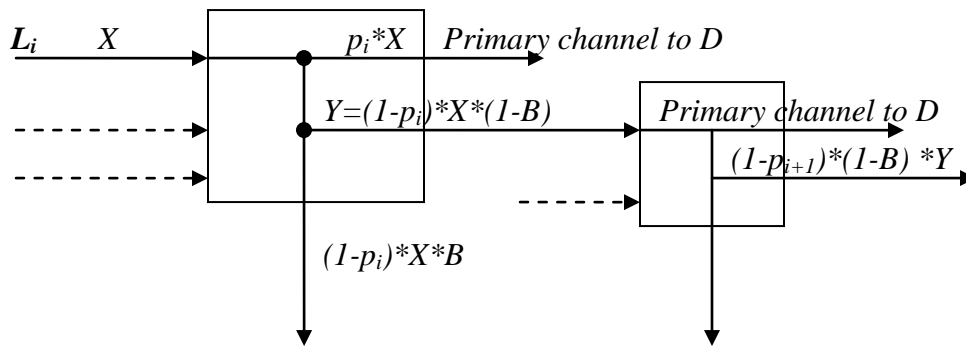


Figure 5.7 Calculating overflow traffic on each hop of the path

Let X Erlangs of traffic load going to a destination ‘ D ’, enter a Hybrid Node from a neighboring node via the overflow links L_i . At the Hybrid Node, a fraction p , of X Erlangs enters an appropriate primary light path reserved between the neighboring node from which the burst arrives, N_s , and the destination node, D . Out of the remaining $(1-p) * X$ Erlangs, only a fraction $(1-B)$ is carried by the outgoing overflow link L_o . The overflow link may consist of multiple

wavelengths that constitute the link. A similar operation takes place at the next hop on the route to the destination. At the next hop, however, the value of fraction p may vary from that of the current hop. At all hops, the value of B is assumed to be a constant.

The method by which the traffic matrix $T(G_N)$ will be calculated for a given graph G_N , is explained by Step 4, for the given example network topology. In order to determine the traffic matrix, we assume that 3 Erlang traffic load is offered between every pair of source-destination nodes (routes) in the network.

- **Step 4:** The graph, shown in Figure 5.6, has $N = 6$ nodes and $E = 5$ edges. Create an empty traffic matrix, $T(G_N)$ matrix with $N*N=36$ rows and $2*E=10$ columns. This matrix will be updated with overflow load values in the subsequent steps.

$$T(G_N) = \text{all_zero_matrix } [36,10]$$

- **Step 5:** For each row of $T(G_N)$, determine the source and destination nodes i and j . Starting from node i determine the next links in the route until destination j is reached. Loop on the $P(G_N)$ matrix for the next hop link, until the next hop is the destination j . The pseudo-code for this algorithm is shown below.

For route between source node i and destination j

Begin loop

Loop until Next_hop = j

Let Current_hop = t

Link_number = n, gives the nth link traversed along the route.

Determine Next_hop = $P_N(\text{current_hop}, j)$

Link_id of next_hop = $L(G_N)(\text{current_hop}, \text{next_hop})$

Set Current_hop = Next_hop

For each *Next_hop* link, assume the probability of light-path entry, $p = 0$ and the blocking probability at the overflow layer, $B = 0.001$. Update the carried route traffic of the link, in the following steps of the algorithm.

Begin with, offered edge node load, $X=3$, $p = 0$ and $B = 0.001$

For route between source i and destination j , determine $Route_id$, $R_N(i,j)$

Update load in $T(G_N)$ ($Route_id$, $Link_id$)

$$T(G_N)(Route_id, Link_id) = X*(1-B)^n*(1-p)$$

Set $current_hop = next_hop$

Set $n = n+1$

Continue the loop

Step 5 gives the overflow traffic matrix $T(G_N)$, such that there are no lightpaths for any route. While calculating the overflow load on each link, it is assumed that average burst load from each route is independent.

- **Step 6:** For each column of the traffic load matrix $T(G_N)$, add all the elements in the column to obtain the total traffic in the corresponding link and place it in a overflow link matrix T_o . T_o has six rows, where each row corresponds to a destination node. The number of columns in T_o , is equal to the number of links in the physical network. In the example, there are 10 links and 6 nodes, hence T_o has 10 columns and 6 rows. While T_o gives the average load in each link, Z_o gives the net Peakedness of this load.

In the example, it is assumed that each access source offers an average load of 3 Erlangs, which has a Peakedness of 2, to every other Hybrid Node in the network.

$$T_o = \begin{bmatrix} 0 & 14.9610 & 0 & 11.976 & 0 & 0 & 5.991 & 0 & 2.99 & 2.99 \\ 2.99 & 0 & 0 & 11.976 & 0 & 0 & 5.991 & 0 & 2.99 & 2.99 \\ 2.99 & 0 & 5.991 & 0 & 0 & 0 & 5.991 & 0 & 2.99 & 2.99 \\ 2.99 & 0 & 5.991 & 0 & \textcircled{11.976} & 0 & 0 & 0 & 2.99 & 2.99 \\ 2.99 & 0 & 5.991 & 0 & 0 & 14.9670 & 5.991 & 0 & 0 & 2.99 \\ 2.99 & 0 & 5.991 & 0 & 11.976 & 0 & 0 & 14.961 & 2.99 & 0 \end{bmatrix}$$

$$Z_o = [2 \quad 2 \quad 2]$$

Each element of T_o gives the link traffic that is destined to a particular destination. For instance the circled element in the T_o matrix shows the load on link 5 (which connects node 3 and 4) that is destined to go to node 4 is 11.976 Erlangs. This load contains bursts originating at nodes 1,2 ,3 and 5, destined to go to node 4. In the example, for an offered access load of 3 Erlangs with no primary channels available, the load offered to the overflow layer is $X = 3$ Erlangs and the load carried is 2.996 Erlangs (after considering blocking at the node). This load suffers an additional blocking at subsequent nodes. In the example of T_o , it is assumed that $p = 0$, since there is no light path entry at any nodes. Therefore, the elements of T_o consider-only link blocking probability B .

The Peakedness of the overflow load is assumed to be 2, which also the peakedness of the access load offered to the proposed network. The Peakedness is maintained at a value of 2, by assuming independent addition of variances and means of individual traffic streams. Peakedness of load is assumed to be constant along the entire route. We may neglect the smoothing effect of traffic carried along overflow channels, which is found to be very small for a blocking probability of $B = 0.001$, for carried traffic on the links. Matrix Z_o gives the Peakedness of each link load.

- **Step 7.** By adding all elements of a column of matrix T_o , total link traffic for the link represented by the respective column is obtained. For each link, number of overflow channels that yield a blocking probability of 0.001 is obtained.

Divide T_o with $(1-.001)$, to consider the offered link traffic to each link prior to the loss. By adding up all the elements of the column, we may obtain,

Offered traffic to each link= [15 15 24 24 24 15 24 15 15 15]

Number of overflow channels required to yield a blocking probability of 0.001 in each link is determined using the method described in section 3.3.1.

Number of overflow channels = [35 35 48 48 48 35 48 35 35 35]

- **Step 8.** Determine matrices

$$G_N = G_O \quad G_P = G_V = \text{all zero matrices}$$

$$\text{Adjacency matrices, } A_N = A_O = \begin{bmatrix} 0 & 35 & 0 & 0 & 0 & 0 \\ 35 & 0 & 48 & 0 & 0 & 0 \\ 0 & 48 & 0 & 48 & 35 & 0 \\ 0 & 0 & 48 & 0 & 0 & 35 \\ 0 & 0 & 35 & 0 & 0 & 0 \\ 0 & 0 & 0 & 35 & 0 & 0 \end{bmatrix}$$

The adjacency matrices give the number of overflow channels in each link of the network, by assuming that there no primary channels in the network. In the remaining steps of the example, possibility of light-path entry is introduced in the analysis.

5.3 LIGHTPATH ENTRY OF OVERFLOW TRAFFIC

The matrix $T(G_N)$ decomposes the route traffic in all links of G_N by assuming there is absolutely no primary layer in the network. This means, the adjacency matrices of G_V and G_P are assumed to be zero. This is the case when all the offered edge traffic is carried by the overflow layer and remains in the overflow channel though out the core network, without any possibility of light-path entry. In this section, we begin to introduce primary channels in varying amounts at the edge nodes. Light-path entry is provided for optical bursts at intermediate nodes of its route, but

only if the light-path is occupied by a certain amount U . U is the average Erlang-load carried by a primary channel. The Average primary light-path utilization/occupancy of a certain number of primary channels originating at the Hybrid Node, PL , is shown in [Table 5.1](#). It is assumed in [Table 5.1](#) that the offered access load is 3 Erlangs and Peakedness is 2.

Table 5.1 Primary channels for each route at edge node.

Primary Channels, PL, For given access load	Avg. channel Utilization, U	Overflow percent, p_o at the Hybrid Node
1	60%	40%
3	53%	47%
5	45.8%	55%
7	38.1%	62%
9	31.9%	68%
11	26.9%	73.1%
13	22.1%	77.9%
15	20%	80%

In [Table 5.1](#), PL is the amount of primary channels that accepts a part of the offered load, which is 3 Erlangs and a Peakedness of 2. The percentage of the offered load which is not accepted by PL channels overflows. Therefore, the percentage of offered load carried by PL number of primary channels is found out by knowing the probability of overflow at the primary channels. The value of U , which is the amount of load carried by each primary channel out of a group of PL channels, is found by dividing the total carried load by PL . This value of carried load per primary channel is also the channel utilization, which is given by the value of U in [Table 5.1](#). In calculating the value of U , it is assumed that all PL channels are equally loaded. The amount of offered load per primary channel that overflows is given by the value of p_o in [Table 5.1](#).

Each Hybrid Node, is assumed to be connected to just one access node that sends an aggregate load of 3 Erlangs, with a Peakedness of 2, to another Hybrid Node in the network. Each Hybrid Node, is also assumed to be connected to its ‘physical’ neighboring nodes. For each Hybrid Node, as depicted in Figure 3.4, one of its sources is the access traffic source and all other sources are neighboring core nodes that offer their overflow traffic. In this section a

method of light-path entry is discussed, in which primary light-paths, PL , are provided to each access source, as shown in [Table 5.1](#). Each value of PL is associated with a value of average primary channel utilization, U , as shown in [Table 5.1](#). If the value of offered access load is changed, the value of U changes.

The access traffic-load that overflows from PL primary channels at the edge node, appears at a subsequent core node along the traffic path. At any core node, the incoming links contain aggregated overflow traffic that may enter a light-path only if the light-path can be utilized by an amount of U . For instance if there are Y Erlangs of overflow load, destined to node 'D', along an incoming link 'K' of core node 'S'. There will be as many light-paths from node 'S' to node 'D', carrying a portion of the offered Y Erlangs load, such that the light-paths are utilized by a given amount U . This value of U , corresponds to PL , which is the number of light paths given to each access source at the core node. Thus, number of primary light-paths assigned at any core node.

5.3.1 ITERATING OVERFLOW TRAFFIC LOAD MATRIX

Prior to allotting the primary light-paths to a route, an overflow traffic matrix, T_o is formed, as shown in Step 6 of example in Section 5.1.2 and plotted in [Figure 5.8](#). The matrix has $2 \cdot E$ columns and N rows. The columns identify the link and the row corresponds to the destination node. Each entry $T_o(i,j)$ corresponds to the sum of all traffic elements, whose final destination is node i and passes through link j .

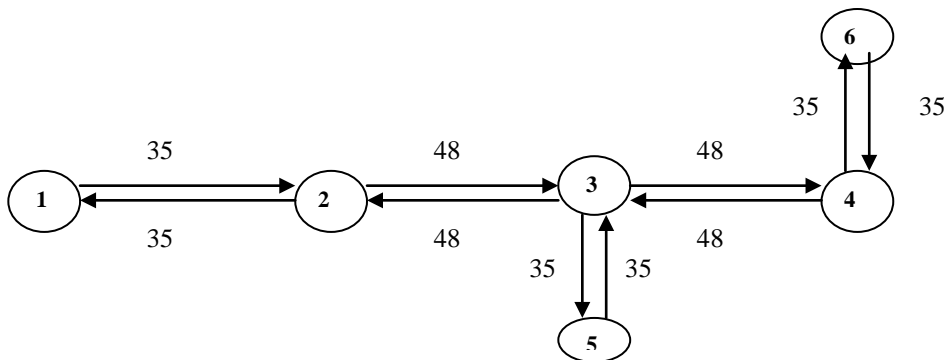


Figure 5.8 Number of overflow channels in the example network, with out any primary channels.

The T_o matrix is updated whenever a primary light-path is provided at any of the Hybrid Nodes. Primary light paths are added in a step-by-step manner for all possible routes and, each time a primary light-path is added, the load in the overflow layer is recalculated and the T_o matrix is updated. A primary light-path is provided for a route only if the average primary path-utilization has a value U .

5.3.2 ADDING PRIMARY LIGHTPATHS IN EXAMPLE 1

Let a given value of utilization, U , be obtained to carry the access traffic using PL light-paths originating at the Hybrid Nodes. Starting from each of the N nodes in the Hybrid Network, PL light-paths are added along the shortest routing-path to the other $N-1$ nodes. The addition of primary light-paths, which only carries load from a single access source, results in a ‘new’ value of overflow load at each link of the network shown in [Figure 5.8](#).

The overflow load, on each link of the network, which is given by each element of T_o matrix, was calculated, along with the Peakedness values, using steps 1 to 8 of Example 1. The overflow traffic matrix, T_o , was updated by considering the value of the overflow percentage, p_o , for the respective value of PL and U . Steps 5 and 6 of the example were performed after updating value of p_o , in order to obtain the new overflow matrix. Step 9 in this example performs this iteration on the T_o matrices for an offered access load of 3, Peakedness of 2, $U = 0.53$, $PL = 3$ and $p_o = 0.47$.

- **Step 9 : Add light paths for each access source:** Redo Step 5 with offered load $X = 3*p$. Then perform step 6 to obtain the updated T_o matrix.

In this step, the overflow layer is provided with an overflow traffic of $3*p_o$ Erlangs, whose Peakedness can be calculated using Rapp’s approximation, as described in Section 3.3.1. By ignoring the smoothing effect of the link traffic due to loss at each node, we may assume the Peakedness of the link traffic to be a constant. For an offered load of 3 Erlangs and $p_o = 0.47$, we may obtain Peakedness of the overflow to be 2.3286, which is slightly greater than the offered Peakedness of 2.

$$T_o = \begin{bmatrix} 0 & 7.032 & 0 & 5.629 & 0 & 0 & 2.816 & 0 & 1.408 & 1.408 \\ 1.408 & 0 & 0 & 5.629 & 0 & 0 & 2.816 & 0 & 1.408 & 1.408 \\ 1.408 & 0 & 2.816 & 0 & 0 & 0 & 2.816 & 0 & 1.408 & 1.408 \\ 1.408 & 0 & 2.816 & 0 & 5.629 & 0 & 0 & 0 & 1.408 & 1.408 \\ 1.408 & 0 & 2.816 & 0 & 0 & 7.032 & 2.816 & 0 & 0 & 1.408 \\ 1.408 & 0 & 2.816 & 0 & 5.629 & 0 & 0 & 7.032 & 1.408 & 0 \end{bmatrix}$$

$$Z_o = [2.328 \quad 2.328 \quad 2.328]$$

- **Step 10.** Matrices G_v and G_p are updated to account for primary light paths.

In the example, for the given load and a utilization of 53%, $PL = 3$. Matrix A_v , which is the adjacency matrix of G_v , is updated by adding PL to all the entries. Similarly G_p is updated by updating the adjacency matrix A_p with the traffic in all the links. For instance, in the link between nodes 1 and 2 of [Figure 5.9](#), there are 5 primary paths going to each of the five nodes in the network. Each primary path on link 1 (between nodes 1 and 2) consists of $PL=3$ light-paths/primary channels, resulting in 15 primary channels. The adjacency matrix element $A_p(1,2)$, which represents link 1, is updated to 15.

$$A_v = \begin{bmatrix} 0 & 3 & 3 & 3 & 3 & 3 \\ 3 & 0 & 3 & 3 & 3 & 3 \\ 3 & 3 & 0 & 3 & 3 & 3 \\ 3 & 3 & 3 & 0 & 3 & 3 \\ 3 & 3 & 3 & 3 & 0 & 3 \\ 3 & 3 & 3 & 3 & 3 & 0 \end{bmatrix}$$

$$A_p = \begin{bmatrix} 0 & 15 & 0 & 0 & 0 & 0 \\ 15 & 0 & 24 & 0 & 0 & 0 \\ 0 & 24 & 0 & 24 & 15 & 0 \\ 0 & 0 & 24 & 0 & 0 & 15 \\ 0 & 0 & 15 & 0 & 0 & 0 \\ 0 & 0 & 0 & 15 & 0 & 0 \end{bmatrix}$$

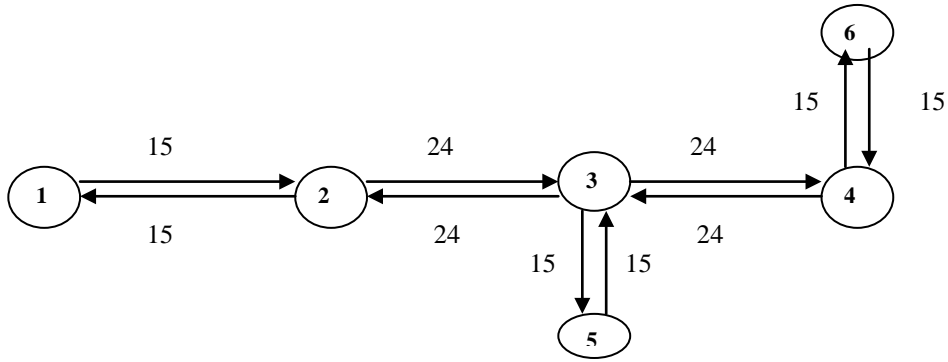


Figure 5.9 G_p for the given example network, after performing Step 10.

- **Step 11 Adding primary light-paths to carry load from neighboring nodes**

In Step 10, the primary light-paths carrying access load from only one (access) source were added to the Hybrid Network at the Hybrid Node. In this step, the possibility of adding more light-paths is examined. As mentioned earlier, light-paths are added such that each light-path will have a mean occupancy of U . From the traffic matrix T_o obtained in Step 9, select all routes on any link that can be assigned N primary light-paths with utilization U . In the T_o matrix below, the highlighted entries correspond to the decomposed load values in link 3, that can be each provided a primary light-path. Update the A_v and A_p matrices by N on the respective links of the path.

Table 5.2 Value of T_o after Iteration 1

Link	1	2	3	4	5	6	7	8	9	10
	0	7.0576	0	5.6495	0	0	2.8262	0	1.4138	1.4138
	1.4138	0	0	5.6495	0	0	2.8262	0	1.4138	1.4138
	1.4138	0	2.8262	0	0	0	2.8262	0	1.4138	1.4138
	1.4138	0	2.8262	0	5.6495	0	0	0	1.4138	1.4138
	1.4138	0	2.8262	0	0	7.0604	2.8262	0	0	1.4138
	1.4138	0	2.8262	0	5.6495	0	0	7.0576	1.4138	0
Prim. Ch. added					2	1		1		

$Z_o = 2.3286$	2.3286	2.3286	2.3286	2.3286	2.3286	2.3286	2.3286	2.3286	2.3286
nodes	1	2	3	4	5	6			
p_o	0	0	0.806	0	0	0			
Orig.Lightpath			3						

Figure 5.10 shows the newly added primary channels on Links 5, 6 and 8, as 2, 1 and 1 channels, respectively. For instance, we may select Link 3, which contains bursts going to nodes 3,4, 5 and 6. Each traffic component on Link 3 can be put into a light-path to yield a utilization close to $U = 53\%$, which we require in this example. There are four traffic components on Link 3, destined to nodes 3, 4, 5 and 6. Two out of the four traffic components on Link 3, also pass through Link 5. Thus, Link 5 gets 2 light-paths/primary channels originating at Node 3. Also, one component passes through Link 6, through which, there is a light-path that originates at Node 3. At this stage of the iteration, the primary light-paths originate from node 2, where the probability of light-path entry, p_o is 19.4% and the probability of overflow $p_o = 80.6\%$

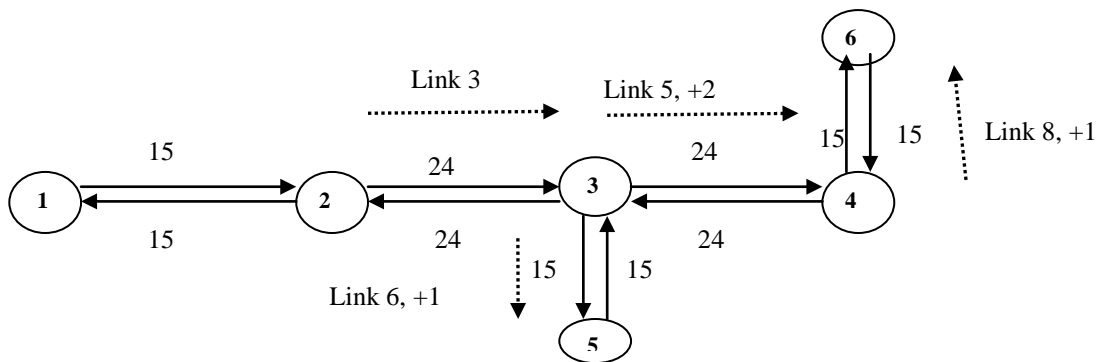


Figure 5.10 Gp for the example network, after Iteration 1.

- **Step 12.** Updating T_o and Z_o , as result of light-paths added in Step 11

With the new value p_o , obtained Step 11, Step 5 is re-run in order to obtain the new matrix T_o . Also the values of Z_o on each link are updated.

Z_o is updated on all links to which new primary channels are added. In the example, the Peakedness of Links 3, 5, 6 and 8 are to be updated. The Peakedness of Link 3 traffic is equal to the Peakedness of overflow traffic, which is found to be 2.454 by Rapp's approximation. All components of Link 3 load is equal. Any one component of link 3, after light-path entry, produces an overflow of $2.826 \cdot .806 = 2.2779$, Erlangs, which is offered to, say, Link 5. Overflow load along Link 5 is updated, due to change in overflow from Link 3 and all this process is carried out in Step 5, with probability of light-path entry $p = .194$ (or $p_o = .806$).

The change in Peakedness of the load offered by Link 3 due to light-path entry at Node 3, will result in change in Peakedness of overflow load in Link 5. Link 5 carries, not only the traffic carried from Links 3 and 9, but also some traffic native to Node 3. Link 3 now offers a load of 2.2779 Erlangs with a Peakedness of 2.454. In addition, on Link 5, there is 2.82 Erlangs native to node 3, and this load has a Peakedness of 2.3286. The Peakedness of overflow load in link 5 given by [37]

$$Z_0(5) = (2.2779 \cdot 2.454 + 2.82 \cdot 2.3286) / (2.2779 + 2.82) = 2.3849$$

Similarly, Peakedness of links 6 and 8, which gets effected by light-path entry of Link 3 load at Node 3, is updated as shown in Table 5.3.

Table 5.3, shows the updated value of link-loads and Peakedness. In Iteration 2, load offered by Link 4 is selected for light-path entry. As a result, 7 light-paths are added on Link 2, as shown in Table 5.3 and Figure 5.11

Table 5.3 Value of T_o after Iteration 2

Links	1	2	3	4	5	6	7	8	9	10
	0	7.0576	0	5.6495	0	0	2.8262	0	1.4138	1.4138
	1.4138	0	0	5.6495	0	0	2.8262	0	1.4138	1.4138
	1.4138	0	2.8262	0	0	0	2.8262	0	1.4138	1.4138
	1.4138	0	2.8262	0	5.1018	0	0	0	1.4138	1.4138
	1.4138	0	2.8262	0	0	6.5127	2.8262	0	0	1.4138
	1.4138	0	2.8262	0	5.1018	0	0	6.5104	1.4138	0
Prim.								7		

Ch. added									
$Z_o =$ 2.3286	2.3286	2.3286	2.3286	2.3849	2.3179	2.3286	2.3719	2.3286	2.3286

nodes	1	2	3	4	5	6
p_o			0.806	0.2712		
Orig. Lightpath			3	7		

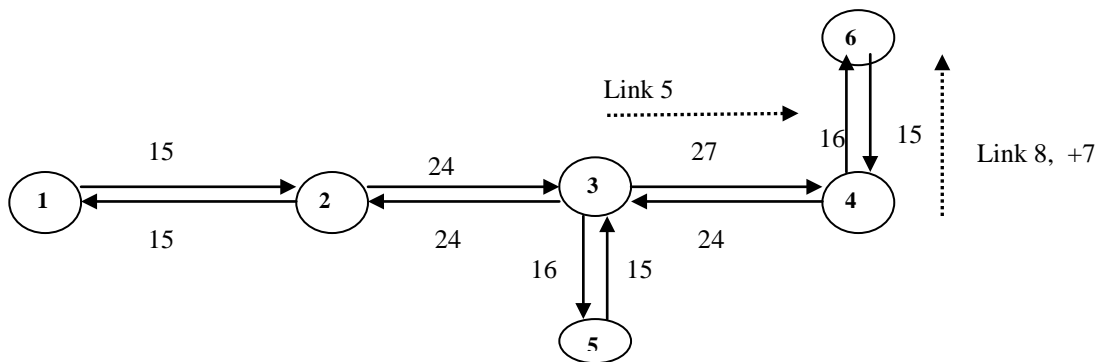


Figure 5.11 G_p after addition of 7 primary channels after Iteration 2.

- **Step 13** Further updating T_o and Z_o

Primary light-paths are added to the outgoing links of yet another node and the T_o matrix is updated. The iteration process continues until there is no link traffic element in the T_o matrix that can be provided a primary light-path with utilization U .

In this example, the next node we consider is Node 4. A primary light-path is provided to all traffic elements in Link 5. For a traffic load of 5.1018 on Link 5, 7 primary light-paths can be provided, resulting in channel utilization of 52.8%. Since Link 5 carries traffic from two route paths, there are 14 primary channels in the Link. The addition of primary light-paths in Link 5 has an effect on traffic elements in Link 8, which is also provided 7 primary channels. Node 3's

overflow percentage, p_o , is 0.2712 and the T_o matrix is updated by running step 5. The Peakedness of the traffic elements in Links 5 and 8 is updated, using the method in Step 12. [Figure 5.11](#) shows addition of new primary channels on G_p obtained from Iteration 1.

The process of updating T_o , Z_o and G_p continues for several rounds until there is no traffic element in T_o that can be assigned a light-path.

[Table 5.4](#), shows the updated value of link-loads and Peakedness. In Iteration 3, load offered by Link 7 is selected for light-path entry. As a result, 2 light-paths are added on Link 3 and one channel each on Links 2 and 5, as shown in [Table 5.4](#) and [Figure 5.12](#).

Table 5.4 Iteration 3

Links	1	2	3	4	5	6	7	8	9	10
0	7.0576	0	5.6495	0	0	2.8262	0	1.4138	1.4138	
1.4138	0	0	5.6495	0	0	2.8262	0	1.4138	1.4138	
1.4138	0	2.8262	0	0	0	2.8262	0	1.4138	1.4138	
1.4138	0	2.8262	0	5.1018	0	0	0	1.4138	1.4138	
1.4138	0	2.8262	0	0	6.5127	2.8262	0	0	1.4138	
1.4138	0	2.8262	0	5.1018	0	0	2.796	1.4138	0	
Prim. Channels	1	2			1					
$Z_o = 2.3286$	2.3286	2.3286	2.3286	2.3849	2.3719	2.3286	2.7116	2.3286	2.3286	
nodes	1	2	3	4	5	6				
p_o			0.806	0.2712						
Orig. Lightpath			6	7						

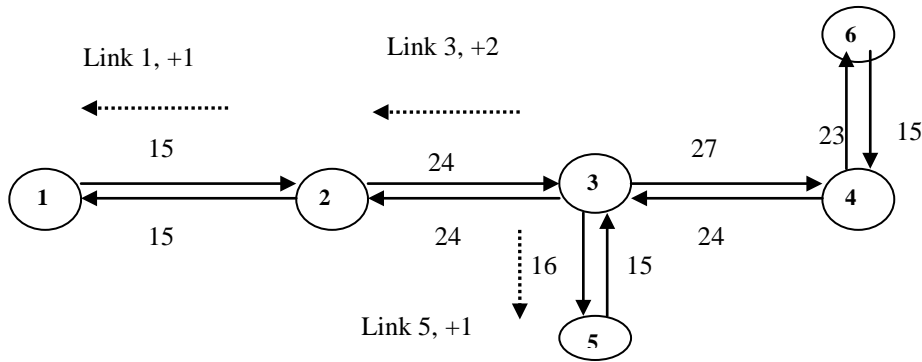


Figure 5.12 Addition of light-paths in Iteration 3

Table 5.5, shows the updated value of link-loads and Peakedness. In Iteration 4, load offered by Link 4 is selected for light-path entry. As a result, 7 light-paths are added on Link 2, as shown in Table 5.5 and Figure 5.13.

Table 5.5 Iteration 4

Links	1	2	3	4	5	6	7	8	9	10
	0	6.5104	0	5.1018	0	0	2.8262	0	1.4138	1.4138
	1.4138	0	0	5.1018	0	0	2.8262	0	1.4138	1.4138
	1.4138	0	2.8262	0	0	0	2.8262	0	1.4138	1.4138
	1.4138	0	2.8262	0	5.1018	0	0	0	1.4138	1.4138
	1.4138	0	2.8262	0	0	5.965	2.8262	0	0	1.4138
	1.4138	0	2.8262	0	5.1018	0	0	2.796	1.4138	0
$Z_o =$	2.3286	2.3719	2.3286	2.3286	2.3849	2.3692	2.3286	2.7116	2.3286	2.3286
Prim Ch. added		7								
nodes	1	2	3	4	5	6				
p_o	0	0.2664	0.806	0.2712	0	0				
Orig. Lightpath	0	7	6	7	0	0				

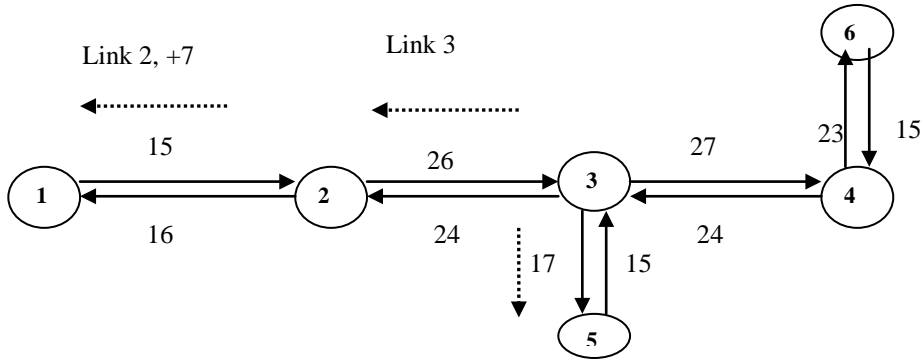


Figure 5.13 Gp after addition of primary channels on link 2.

The final T_o matrix gives the link-load elements of the overflow layer that do not enter any primary light-paths. At the last round of the iterative process, the final values of p (or p_o) are obtained, which gives probability of light-path (overflow path) entry at each node.

Table 5.6, shows the updated value of link-loads and Peakedness. In the final iteration, there are no link-loads for light-path entry. This final step is shown in Table 5.6 and Figure 5.13.

Table 5.6 Final Iteration

Links	1	2	3	4	5	6	7	8	9	10
0	2.7715	0	5.1018	0	0	2.8262	0	1.4138	1.4138	
1.4138	0	0	5.1018	0	0	2.8262	0	1.4138	1.4138	
1.4138	0	2.8262	0	0	0	2.8262	0	1.4138	1.4138	
1.4138	0	2.8262	0	5.1018	0	0	0	1.4138	1.4138	
1.4138	0	2.8262	0	0	5.965	2.8262	0	0	1.4138	
1.4138	0	2.8262	0	5.1018	0	0	2.796	1.4138	0	
$Z_o =$										
2.3286	2.6819	2.3286	2.3286	2.3849	2.3692	2.3286	2.7116	2.3286	2.3286	
nodes	1	2	3	4	5	6				
p_o	0	0.2664	0.806	0.2712	0	0				

- **Step 14.** Updating G_o and G_p matrices

The Adjacency matrix A_o , which gives the number of overflow channels in each link, is obtained from the matrix T_o . In order to obtain the number of overflow channels in a link, the

total traffic passing through the link is obtained by adding all the elements of the corresponding column in T_o . Queuing analysis is performed on the link to obtain the number of overflow channels for which a loss of B is obtained.

In the example, channel blocking is assumed to be 0.001. For this example, the final adjacency matrix of the overflow graph is determined as,

$$A_o = \begin{bmatrix} 0 & 25 & 0 & 0 & 0 & 0 \\ 19 & 0 & 32 & 0 & 0 & 0 \\ 0 & 30 & 0 & 30 & 23 & 0 \\ 0 & 0 & 29 & 0 & 0 & 19 \\ 0 & 0 & 25 & 0 & 0 & 0 \\ 0 & 0 & 0 & 25 & 0 & 0 \end{bmatrix}.$$

[Figure 5.14](#) compares the overflow graph obtained after light-path entry, with that in which there is no light-path entry.

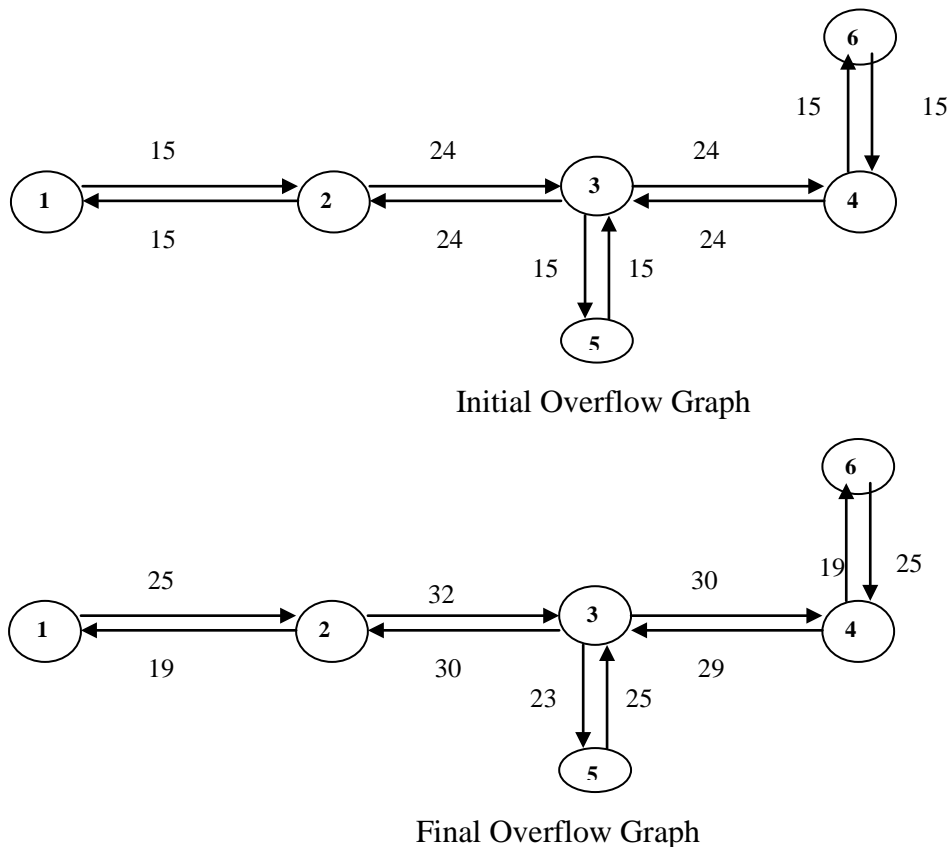
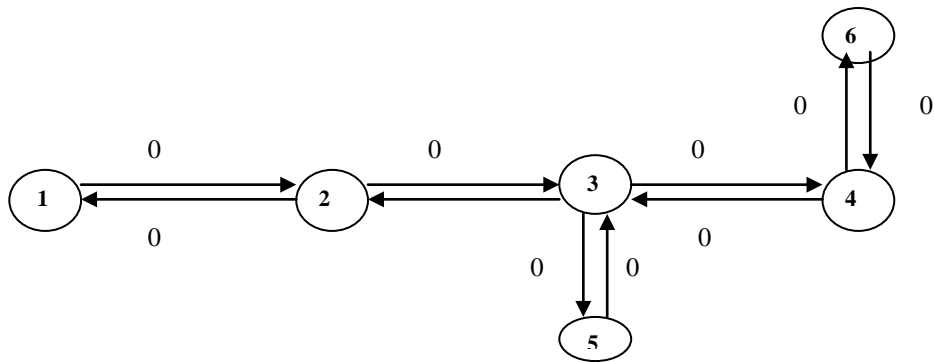


Figure 5.14 Initial and Final Overflow Graphs.

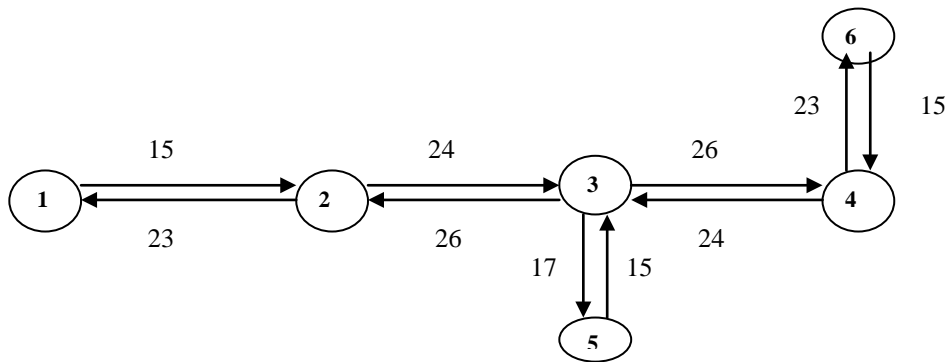
Adjacency matrix, A_p , of graph G_p , whose links are utilized with an average utilization of U is found to be,

$$A_p = \begin{bmatrix} 0 & 15 & 0 & 0 & 0 & 0 \\ 23 & 0 & 24 & 0 & 0 & 0 \\ 0 & 26 & 0 & 26 & 17 & 0 \\ 0 & 0 & 24 & 0 & 0 & 23 \\ 0 & 0 & 15 & 0 & 0 & 0 \\ 0 & 0 & 0 & 15 & 0 & 0 \end{bmatrix}.$$

[Figure 5.15](#) compares the initial and final Primary layer graph.



Initial Primary Layer Graph



Final Primary Layer Graph

Figure 5.15 Initial and final Primary Layer Graph.

5.3.3 RESULTS: PRIMARY AND OVERFLOW CHANNELS IN THE LINKS

In the previous section, the average channel utilization of the primary layer was assumed to be 53%. We may also consider several other possible values of primary channel utilization, as given in [Table 5.1](#). The A_p and A_o matrices are determined for all the cases of primary channel utilization.

1) Utilization of 60%

$$A_o = \begin{bmatrix} 0 & 31 & 0 & 0 & 0 & 0 \\ 23 & 0 & 42 & 0 & 0 & 0 \\ 0 & 20 & 0 & 36 & 25 & 0 \\ 0 & 0 & 42 & 0 & 0 & 23 \\ 0 & 0 & 31 & 0 & 0 & 0 \\ 0 & 0 & 0 & 31 & 0 & 0 \end{bmatrix}$$

$$A_p = \begin{bmatrix} 0 & 5 & 0 & 0 & 0 & 0 \\ 17 & 0 & 8 & 0 & 0 & 0 \\ 0 & 16 & 0 & 16 & 13 & 0 \\ 0 & 0 & 8 & 0 & 0 & 17 \\ 0 & 0 & 5 & 0 & 0 & 0 \\ 0 & 0 & 0 & 5 & 0 & 0 \end{bmatrix}$$

2) Utilization of 53%

$$A_o = \begin{bmatrix} 0 & 25 & 0 & 0 & 0 & 0 \\ 19 & 0 & 32 & 0 & 0 & 0 \\ 0 & 30 & 0 & 30 & 23 & 0 \\ 0 & 0 & 29 & 0 & 0 & 19 \\ 0 & 0 & 25 & 0 & 0 & 0 \\ 0 & 0 & 0 & 25 & 0 & 0 \end{bmatrix}$$

$$A_p = \begin{bmatrix} 0 & 15 & 0 & 0 & 0 & 0 \\ 23 & 0 & 24 & 0 & 0 & 0 \\ 0 & 26 & 0 & 26 & 17 & 0 \\ 0 & 0 & 24 & 0 & 0 & 23 \\ 0 & 0 & 15 & 0 & 0 & 0 \\ 0 & 0 & 0 & 15 & 0 & 0 \end{bmatrix}$$

3) Utilization of 46%

$$A_o = \begin{bmatrix} 0 & 19 & 0 & 0 & 0 & 0 \\ 17 & 0 & 20 & 0 & 0 & 0 \\ 0 & 25 & 0 & 25 & 19 & 0 \\ 0 & 0 & 20 & 0 & 0 & 17 \\ 0 & 0 & 19 & 0 & 0 & 0 \\ 0 & 0 & 0 & 19 & 0 & 0 \end{bmatrix}$$

$$A_p = \begin{bmatrix} 0 & 25 & 0 & 0 & 0 & 0 \\ 28 & 0 & 40 & 0 & 0 & 0 \\ 0 & 46 & 0 & 46 & 25 & 0 \\ 0 & 0 & 40 & 0 & 0 & 28 \\ 0 & 0 & 25 & 0 & 0 & 0 \\ 0 & 0 & 0 & 25 & 0 & 0 \end{bmatrix}$$

4) Utilization of 38.15%

$$A_o = \begin{bmatrix} 0 & 15 & 0 & 0 & 0 & 0 \\ 15 & 0 & 17 & 0 & 0 & 0 \\ 0 & 17 & 0 & 17 & 15 & 0 \\ 0 & 0 & 15 & 0 & 0 & 15 \\ 0 & 0 & 15 & 0 & 0 & 0 \\ 0 & 0 & 0 & 15 & 0 & 0 \end{bmatrix}$$

$$A_p = \begin{bmatrix} 0 & 35 & 0 & 0 & 0 & 0 \\ 35 & 0 & 56 & 0 & 0 & 0 \\ 0 & 56 & 0 & 56 & 35 & 0 \\ 0 & 0 & 56 & 0 & 0 & 35 \\ 0 & 0 & 35 & 0 & 0 & 0 \\ 0 & 0 & 0 & 35 & 0 & 0 \end{bmatrix}$$

5) Utilization of 31.9%

$$A_o = \begin{bmatrix} 0 & 12 & 0 & 0 & 0 & 0 \\ 12 & 0 & 13 & 0 & 0 & 0 \\ 0 & 13 & 0 & 13 & 12 & 0 \\ 0 & 0 & 13 & 0 & 0 & 12 \\ 0 & 0 & 12 & 0 & 0 & 0 \\ 0 & 0 & 0 & 12 & 0 & 0 \end{bmatrix}$$

$$A_p = \begin{bmatrix} 0 & 45 & 0 & 0 & 0 & 0 \\ 45 & 0 & 72 & 0 & 0 & 0 \\ 0 & 72 & 0 & 72 & 45 & 0 \\ 0 & 0 & 72 & 0 & 0 & 45 \\ 0 & 0 & 45 & 0 & 0 & 0 \\ 0 & 0 & 0 & 45 & 0 & 0 \end{bmatrix}$$

6) Utilization of 26.9%

$$A_o = \begin{bmatrix} 0 & 10 & 0 & 0 & 0 & 0 \\ 10 & 0 & 10 & 0 & 0 & 0 \\ 0 & 10 & 0 & 10 & 10 & 0 \\ 0 & 0 & 10 & 0 & 0 & 10 \\ 0 & 0 & 10 & 0 & 0 & 0 \\ 0 & 0 & 0 & 10 & 0 & 0 \end{bmatrix}$$

$$A_p = \begin{bmatrix} 0 & 65 & 0 & 0 & 0 & 0 \\ 65 & 0 & 104 & 0 & 0 & 0 \\ 0 & 104 & 0 & 104 & 65 & 0 \\ 0 & 0 & 104 & 0 & 0 & 65 \\ 0 & 0 & 65 & 0 & 0 & 0 \\ 0 & 0 & 0 & 65 & 0 & 0 \end{bmatrix}$$

7) Utilization of 22%

$$A_o = \begin{bmatrix} 0 & 9 & 0 & 0 & 0 & 0 \\ 9 & 0 & 9 & 0 & 0 & 0 \\ 0 & 9 & 0 & 9 & 9 & 0 \\ 0 & 0 & 9 & 0 & 0 & 9 \\ 0 & 0 & 9 & 0 & 0 & 0 \\ 0 & 0 & 0 & 9 & 0 & 0 \end{bmatrix}$$

$$A_p = \begin{bmatrix} 0 & 65 & 0 & 0 & 0 & 0 \\ 65 & 0 & 104 & 0 & 0 & 0 \\ 0 & 104 & 0 & 104 & 65 & 0 \\ 0 & 0 & 104 & 0 & 0 & 65 \\ 0 & 0 & 65 & 0 & 0 & 0 \\ 0 & 0 & 0 & 65 & 0 & 0 \end{bmatrix}$$

8) Utilization < 21%

$$A_o = \begin{bmatrix} 0 & 0 & 0 & 0 & 0 & 0 \\ 0 & 0 & 0 & 0 & 0 & 0 \\ 0 & 0 & 0 & 0 & 0 & 0 \\ 0 & 0 & 0 & 0 & 0 & 0 \\ 0 & 0 & 0 & 0 & 0 & 0 \\ 0 & 0 & 0 & 0 & 0 & 0 \end{bmatrix}$$

$$A_p = \begin{bmatrix} 0 & 75 & 0 & 0 & 0 & 0 \\ 75 & 0 & 120 & 0 & 0 & 0 \\ 0 & 120 & 0 & 120 & 75 & 0 \\ 0 & 0 & 120 & 0 & 0 & 75 \\ 0 & 0 & 75 & 0 & 0 & 0 \\ 0 & 0 & 0 & 75 & 0 & 0 \end{bmatrix}$$

9) Utilization >60%

$$A_o = \begin{bmatrix} 0 & 35 & 0 & 0 & 0 & 0 \\ 35 & 0 & 48 & 0 & 0 & 0 \\ 0 & 48 & 0 & 48 & 35 & 0 \\ 0 & 0 & 48 & 0 & 0 & 35 \\ 0 & 0 & 35 & 0 & 0 & 0 \\ 0 & 0 & 0 & 35 & 0 & 0 \end{bmatrix} \quad A_p = \begin{bmatrix} 0 & 0 & 0 & 0 & 0 & 0 \\ 0 & 0 & 0 & 0 & 0 & 0 \\ 0 & 0 & 0 & 0 & 0 & 0 \\ 0 & 0 & 0 & 0 & 0 & 0 \\ 0 & 0 & 0 & 0 & 0 & 0 \\ 0 & 0 & 0 & 0 & 0 & 0 \end{bmatrix}$$

Entries in the A_o and A_p matrices depend on the utilization of primary channels. It is seen from the entries in the matrices that for a utilization of 60%, 53% and 48%, the number of primary and overflow channels are not the same for the bidirectional links between a pair of nodes. For instance, for a utilization of 60%, there are 15 primary channels from Node 1 to Node 2 (Link 1) and 23 primary channels from Node 2 to Node 1 (Link 2). The difference between the number of channels in the bidirectional link reduces, as primary channel utilization decreases. For instance, for a utilization of 48%, there are 25 channels in Link 1 and 28 channels in Link 2. This difference in number of channels disappears as utilization becomes 38.1%. Similar behavior is observed for the graph A_o .

5.3.4 SWITCHING COST OF NODES

We saw in Chapter 4 that the switching cost of a node depends on the number of switching elements in the primary and overflow layers within the Hybrid Node. We also saw that the number of switching elements in a Hybrid Node depends on number of primary and overflow channels on the outgoing links. We may use the A_p and A_o matrices, for each case of U , to determine the number of switching elements in each node of the Hybrid Network.

Each node of the primary network performs the following switching functions

- 1) To provide light-path entry for access traffic via a 'primary_access_switch'.
- 2) To provide light-path entry for core overflow traffic via a 'primary_core_switch'.
- 3) To provide overflow channel entry for both sources via a single 'overflow_switch'.
- 4) To direct incoming traffic from each source to either the primary or overflow switches.

In order to determine the number of switching elements in a ‘primary_access_switch,’ we require the number of fibers coming from the access source to the Hybrid Nodes, the number of incoming overflow fibers, and the number of outgoing primary fibers. The number of incoming access fibers is assumed to be 10 fibers each carrying 10 wavelengths. The number of outgoing fibers is determined from the A_p and A_o matrices.

The A_p and A_o matrices give the number of primary and overflow wavelengths, respectively. Assuming there are 10 wavelengths per fiber, we use the following method to determine the number of primary and overflow fibers in each link. Consider an $N \times N$ Link_Fiber_matrix, whose elements represent the number of fibers in each link. Also consider an $N \times N$ primary fiber matrix and an $N \times N$ overflow_fiber_matrix that gives the number of fibers carrying primary and overflow channels, respectively. It is assumed that primary and overflow channels are packed onto fibers in the most efficient manner; so it is possible for primary and overflow channels of a link to be on the same fiber.

For each link, between nodes i and j , where $i, j = 1, 2, \dots, N$ and W is the number of wavelengths per fiber,

$$\begin{aligned}
 \text{Link_Fiber_matrix}(i, j) &= \left\lceil \frac{(A_p(i, j) + A_o(i, j))}{W} \right\rceil \\
 \text{Primary_fiber_matrix}(i, j) &= \left\lceil \frac{A_p(i, j)}{W} \right\rceil \quad \dots\dots\dots (5.1) \\
 \text{Overflow_fiber_matrix}(i, j) &= \left\lceil \frac{A_o(i, j)}{W} \right\rceil
 \end{aligned}$$

The primary fiber matrix gives the total number of primary fibers in a link, which contain the primary channels originating in the core nodes and the primary channels bypassing the core node. In order to determine the dimension of a primary switch, we need the number of primary channels originating at the core node. The iterative process described in Section 5.2.2 creates new light-paths originating at a node during each iterative step. [Table 5.2](#) gives number of light-paths originating from each node for a given value of primary channel utilization and an offered load of 3 Erlangs with a Peakedness of 2.

[Figure 5.17](#) shows the number of primary fibers in each Link of the network. [Figure 5.16](#) shows overflow channels in each link.

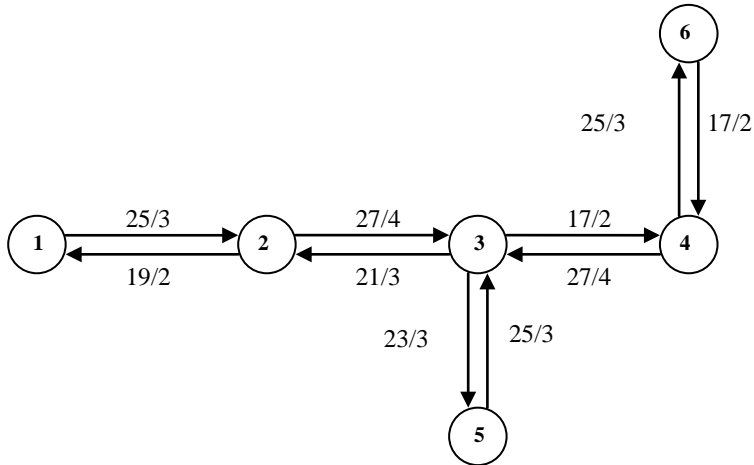


Figure 5.16 Links showing overflows channels/overflow fibers of each link

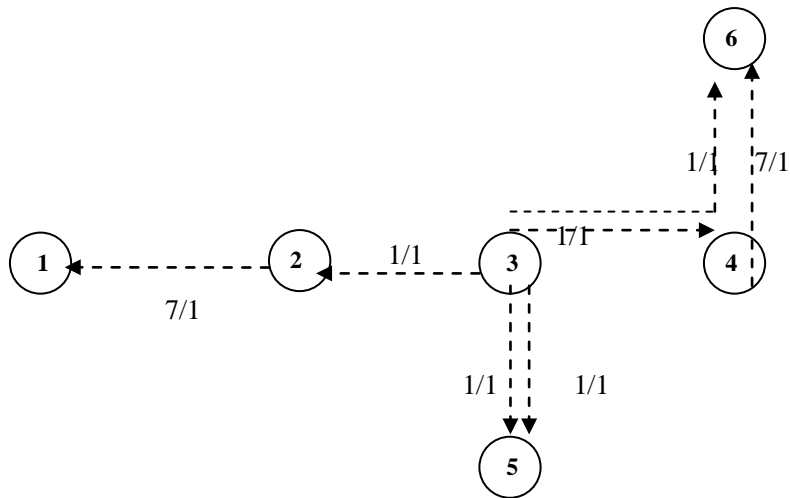


Figure 5.17 Primary lightpaths/fiber emanating from nodes 2, 3 and 4.

Table 5.7 Number of input and out put fibers at each node.

U=53.8%, load of 3 Erlangs, Z = 2 ; W =10 wavelength/fiber, 10 access input channels; B= .001						
Nodes \ Switch	1	2	3	4	5	6
Access input	10	10	10	10	10	10
Prim_access	5	5	5	5	5	5
Core_input	0	3	(4,3)	3	0	0
Prim_core	0	1	(3,3)	1	0	0
Overflow_in	10	16	20	16	10	10
Overflow_out	3	6	9	5	3	3

In [Table 5.7](#), Access input is the number of input access fibers, assumed to be 10 fibers. Prim_access is the number of primary channels provided for each access source and this number depends on the primary channel utilization and offered load. For a primary channel utilization of 53.8% and an offered load of 3 Erlangs/Peakedness of 2, *PL* is always 3 channels per destination node and these many channel can be accommodated in one single fiber. Since there are 5 destination nodes, there should be 5 prim_access fibers emanating from a ‘prim_access_switch,’ one fiber going to each destination. Therefore, the ‘prim_access_switch’ should be of dimension 10 * 5, where 10 is the number of access_input fibers and 5 is the number of Prim_access output fibers.

Core_input gives number of overflow fibers entering a core node that may be connected to primary channels at the core node. Core_input contains overflow fibers from all the input links that may be connected to the node. Overflow fibers in a link is calculated using [Equation \(5.1\)](#). It is seen in [Table 5.7](#) that for Node 3, there are two different values for Core_input because there are 4 input fibers from Nodes 2 and 4 and 3 input fibers from Node 5.

By determining the number of input and output fibers in a node, number of switching elements in the primary and overflow OB-switches can be determined using the method developed in Chapter 4.

For a core node *i*, we may calculate total number of switching elements as,

9						
Switching elements, $u=26.9\%, PL=11$	650	790	1000	790	650	650
Switching elements, $u=22.9\%, PL=13$	740	866	1055	866	740	740
Switching elements, $u=20\%, PL=15$	750	750	750	750	750	750
Switching elements, $u>60\%, PL=0$	300	2085	3700	2085	300	300

5.4 COST OF A HYBRID NETWORK

The cost of a Hybrid Network may be considered to be equal to the sum of its switching and transmission costs. The total transmission cost of a network is assumed linearly dependent on the total number of wavelength channels that constitute all the links of a network. The total number of elementary switches used to construct all the nodes of the network may determine the total switching cost of a network. Both switching and transmission costs depend on the number of primary and overflow channels in the network links.

5.4.1 SWITCHING COSTS

The number of switching elements in each node of the Hybrid Network, which is given in [Table 5.8](#), is shown in [Figure 5.18](#), for different values of primary light-paths PL provided to each access source. The hybrid switches are constructed using the architecture described in Chapter 4.

The switch fabric is assumed to use the Broadcast-and-Select architecture, which is made of 1*1 switching elements.

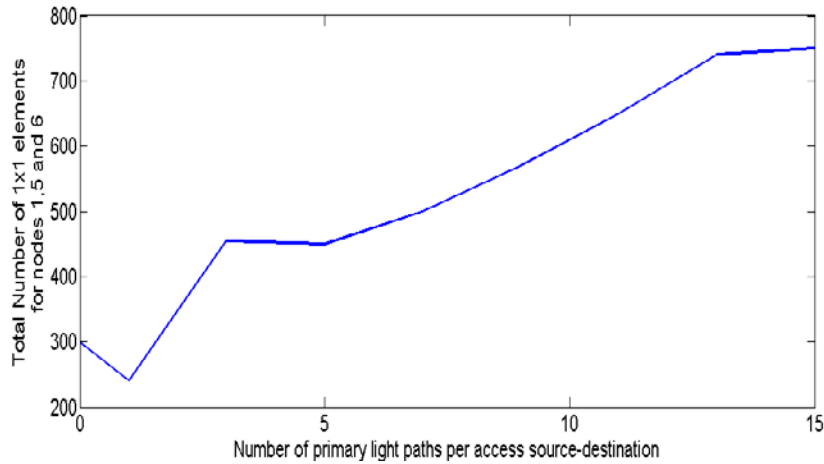


Figure 5.18 Number of 1x1 elements for nodes 1, 6 and 5.

[Figure 5.18](#) shows the total number of 1*1 elements, for different values of PL , for Node1 in the given example network. Nodes 5 and 6 also contain the same number of 1*1 elements. All three nodes are connected to their respective access source and to one other node in the network. [Figure 5.18](#) shows that with an increase in PL , the number of 1x1 switching elements also increases. This is because Nodes 1, 5 and 6 groom incoming access-traffic to outgoing primary and overflow channels. With an increase in PL , the number of primary channels used to carry this access load increases and as a result, the size of ‘access_prim_switch’ increases. It is also observed in the given example that the size of ‘access_prim_switch’ increases at a rate that is faster than the corresponding decrease in the size of the overflow switch.

[Figure 5.19](#) shows total number of 1*1 elements for node 3 that not only connects to the access source but also to three other core switches. Node 3 provides light-path entry for traffic offered by Nodes 2 and 4. It is observed from [Table 5.1](#) that as the value of PL increases the corresponding value of U decreases. In order to provide light-path entry at Node 3 for any incoming optical bursts, via overflow channels from Nodes 2 or 5, the average primary channel utilization should be of the required value, U . With an increase in the value of PL , large amount of access traffic is placed on primary light-paths with only a small amount left for the overflow layer. Hence, only a small amount of overflow traffic from Node1 and 2 reaches Node 3 for light-path entry. Thus, for a large value of PL , the number of light-paths originating in Node 3

decreases. In the same manner, a small value of PL results in a heavy overflow from Nodes 1 and 2, so there is more overflow traffic along Link 3. Therefore, in order to provide an average channel utilization of U (corresponding to the value of PL) for the light-paths originating at Node 3, more primary channels are required. Thus, a small value of PL corresponds to more light-paths originating at Node 3.

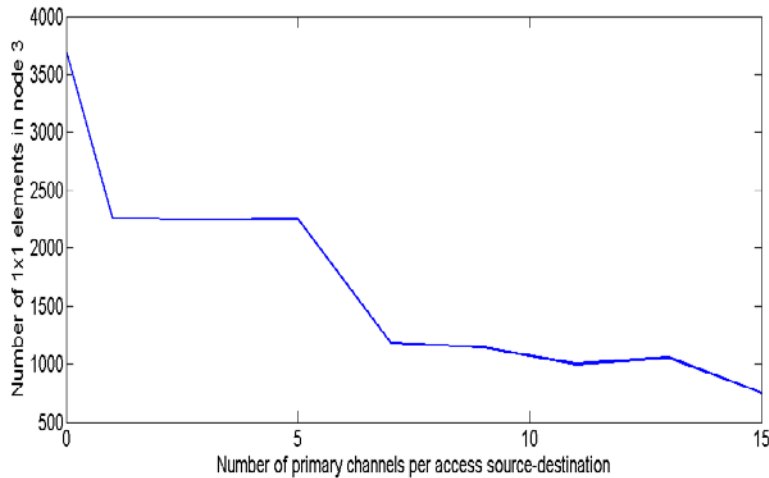


Figure 5.19 Number of 1*1 elements for node 3

For the given example, it is seen that the number of 1*1 elements in Node 3 decreases due to an increase in the value of PL . As PL increases, the number of primary light-paths used to carry the access load increases. At the same time, the number of primary channels used to provide light-path entry decreases, along with a decrease in the number of overflow channels emanating from Node 3. The net effect is that the dimension of the Node-3 switch becomes smaller, there-by requiring fewer 1*1 elements.

[Figure 5.20](#) shows that Core-Nodes 2 and 4 are connected to one access source and two other core nodes. Core-Node 2 does not receive as much overflow load as Node 3 does, but it receives more overflow traffic than Node 1 does. It is seen that the number of 1*1 elements for Core-Nodes 2 and 4, decreases slightly with an increase in value of PL . The net percentage decrease in the number of 1*1 elements between $PL = 0$ and $PL = 15$ is about 70% for Node 3, 46% for Node 4 and 37% for Node 2.

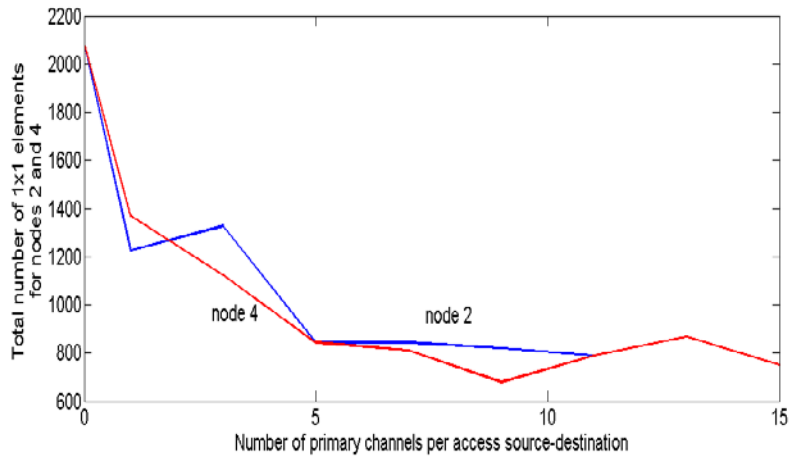


Figure 5.20 Number of 1x1 elements in nodes 2 and 4

[Figure 5.21](#) shows the variation of the total number of 1*1 elements in the entire network. It can be seen that there is a balance between the increase in the number 1*1 elements in Nodes 1, 5 and 6 and the decrease in the number of 1*1 elements in Nodes 2 , 3 and 4. The minimum number of 1x1 elements occurs at $PL = 7$.

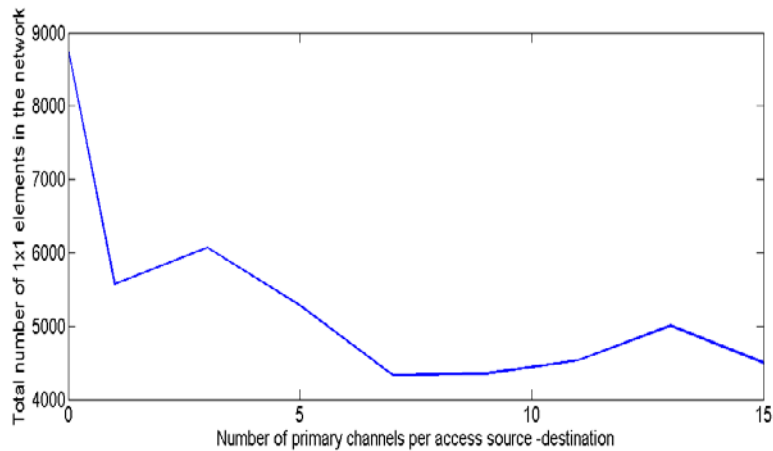


Figure 5.21 Number of 1x1 elements in the entire network

5.4.2 TRANSMISSION COSTS

The total number of wavelength channels in a network is one of the main factors that dictate total transport cost of the network. We assume that the cost of a link is linearly dependent on the total number of channels in the link and that all channels have the same transmission rate. [Figure 5.22](#) shows the total number of transmission channels, including both primary and overflow channels, in the network. The total number of channels is obtained by summing up the elements of the A_p and A_o matrices for each value of utilization U (which corresponds to a value of PL).

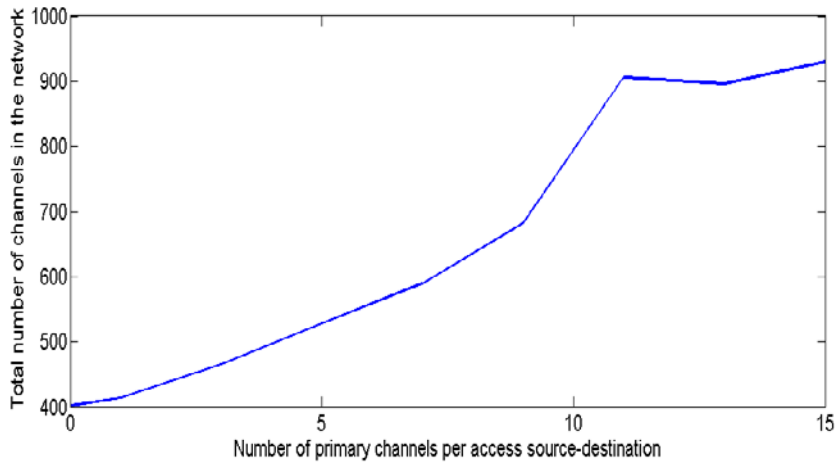


Figure 5.22 Total number of channels in the network

The total cost of a Hybrid Network depends on the relative cost of transporting a channel to the cost of switching a channel. In order to calculate total cost, we introduce the metric CR_{trans} , which is the relative cost of a wavelength channel, to the cost of a switching element. [Figure 5.23](#) shows the total cost of a Hybrid Network for different values of CR_{trans} . The total cost of a network is calculated using [Equation 5.3](#).

$$\begin{aligned}
 Total_cost_network = \\
 Total_channels * CR_trans + Total_switching_elements.....(5.3)
 \end{aligned}$$

For a small value of CR_{trans} , total cost curve resembles the curve in [Figure 5.21](#). For higher values of CR_{trans} , total cost is dominated by the transport costs and resembles the curve in [Figure 5.22](#).

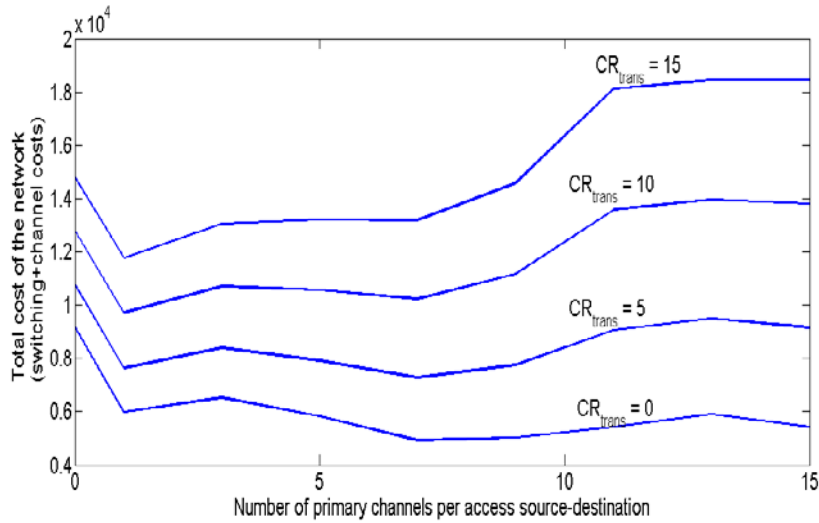


Figure 5.23 Total cost of the network for different values of CR_{trans}

The total cost of a Hybrid Network depends on the value of CR_{trans} . The total transport cost of the network increases as channel over-provisioning increases. In order to get an optimal Hybrid Network, the increase in total transport cost must be balanced by the decrease in switching costs. For the given network and its access loads, switching costs depend on the degree of over-provisioning, represented by the value of U/PL , for the primary light-paths used to carry the access load. The total switching cost of a node may increase, with an increase in the value of PL , if the node is directly linked to fewer core nodes. At the same time, an increase in the value of PL results in lowering the switching costs of a highly-linked node.

5.5 COST OF ROUTES

A Hybrid Network consisting of ‘N’ nodes will contain ‘N*(N-1)’ routes between core nodes. Each route in the Hybrid Network is associated with a path, which is made of the nodes traversed by a burst to get from the source node of the route, to its destination node. Each route path may be characterized by its path cost ratio, as discussed in Chapter 3. In order to determine the path cost ratio CR_{path} , we use Equation (3.6e) in Chapter 3. The probability of light-path entry at the i th node of the route path, p_i , is determined using the iterative technique described in Section 5.2. We may calculate cost ratios for all routes in the network, using [Equation \(3.6\)](#) from Chapter 3.

In order to calculate the cost of all route paths, we need to determine the value of CR_{path} for all routes in the given network. A Matrix CR_{path_PL} , contains all values of CR_{path} , for a given value of PL. In calculating the cost ratio of each route, it is assumed that all nodes and links have identical costs. The cost of switching may be approximated to be the same in all nodes, as internal paths through a B-S fabric constitute just one 1*1 element. All transport links are assumed to be of equal cost.

5.5.1 COST OF ROUTES IN EXAMPLE 1

Prior to calculating the costs of network routes, the value of CR_{path} associated with each route has to be determined. CR_{path} of each route, as provided in [Equation \(3.6e\)](#) of Chapter 3 is modified, by assuming that the cost of switching is one unit and the cost of transport is K units per-hop. The cost ratio, $CR_{path_PL}(i)$ of route i , is obtained by modifying [Equation \(3.6d\)](#) in Section 3.4.2.1.

$$CR_{path_PL}(i) = \frac{\left[\sum_{N=1}^{hops(i)} \left[\prod_{k=1}^N (1 - p_k) \right] * p_{N+1} * (1 - B)^N * (N + 1) \right] + hops(i) * K}{1 + hops(i) * K}$$

or,

$$CR_{path_PL}(i) = \frac{avg_overflow_hops_PL(i) + hops(i) * K}{1 + hops(i) * K} \dots\dots\dots(5.4)$$

For the network in the example with N nodes, the N*N hops matrix, whose elements are the actual physical hops in a route is given by,

$$hops = \begin{bmatrix} 0 & 1 & 2 & 3 & 3 & 4 \\ 1 & 0 & 1 & 2 & 2 & 3 \\ 2 & 1 & 0 & 1 & 1 & 2 \\ 3 & 2 & 1 & 0 & 2 & 1 \\ 3 & 2 & 1 & 2 & 0 & 3 \\ 4 & 3 & 2 & 1 & 2 & 0 \end{bmatrix}$$

$$avghops = 2.0333$$

$$avghops = \frac{\sum_i^{(N-N)} \sum_j^{(N-N)} hops(i,j)}{N * N} \dots\dots\dots(5.5)$$

In the hops matrix, the rows are the source nodes of a route and columns are the destinations. An entry $hops(i,j)$ in the hops matrix gives the number of hops taken by an overflow path between the source and the destination nodes. The average number of hops for all routes of the network is given by $avghops$.

The value of p_i , which is the probability of light-path entry at the i th node, is obtained from the iterative process described in Section 5.2. Using the formula given in Equation (5.3), $avg_overflow_hops$ is obtained for each route, for a given value of PL/U . It is observed that for varying values of PL , the entries in $avg_overflow_hops_PL$ are always less than or equal to the corresponding values in the (physical) hops matrix. Due to light-path entry in the overflow path, the average switching hops traversed by a burst will be less than the actual number of physical hops in the path.

For $PL=1$; average overflow hops is given as :

$$avg_overflow_hops_1 = \begin{bmatrix} 0 & .99 & 1.97 & 2.46 & 2.46 & 2.58 \\ .99 & 0 & .99 & 1.48 & 1.48 & 2.08 \\ 1.3 & .99 & 0 & .99 & .99 & 1.3 \\ 2.08 & 1.12 & .99 & 0 & 1.12 & .99 \\ 2.42 & 2.49 & .99 & 2.49 & 0 & 2.41 \\ 2.41 & 1.44 & 1.99 & .99 & 1.48 & 0 \end{bmatrix}$$

For PL=3; average overflow hops is given as :

$$avg_overflow_hops_3 = \begin{bmatrix} 0 & .99 & 1.97 & 2.79 & 2.79 & 2.96 \\ .99 & 0 & .99 & 1.80 & 1.80 & 1.99 \\ 1.26 & .99 & 0 & .99 & .99 & .81 \\ 2.61 & .62 & .99 & 0 & 1.80 & .99 \\ 2.75 & 2.162 & .99 & 1.80 & 0 & 2.76 \\ 2.43 & 2.79 & 1.97 & .99 & 2.79 & 0 \end{bmatrix}$$

For PL=5, 7, 9, 11,13 $CR_{path_5} = CR_{path_7} = CR_{path_9} = CR_{path_{11}}$ average overflow hops is given as:

$$avg_overflow_hops_5 = \begin{bmatrix} 0 & .99 & 1.98 & 2.99 & 2.99 & 3.98 \\ .99 & 0 & .99 & 1.96 & 1.96 & 2.91 \\ 1.98 & .99 & 0 & .99 & .99 & 1.98 \\ 2.99 & 1.96 & .99 & 0 & 1.96 & 1.96 \\ 2.99 & 1.98 & .99 & 1.98 & 0 & 2.99 \\ 3.98 & 2.99 & 1.98 & .99 & 2.99 & 0 \end{bmatrix}$$

The average value of $avg_overflow_hops_PL$ is obtained for each value of PL as,

<i>PL</i>	0	1	3	5	7	9	11	13
$avg(avg_overflow_hops_PL)$.98	1.65	1.76	2.08	2.08	2.08	2.08	0

In terms of cost of a primary path, the total cost of a hybrid path,

$$Total_cost_ (PL) = (avg_CR_{path}(PL)) * \sum_{l=1}^{10} Ro_PL(l) + * \sum_{l=1}^{10} Rp_PL(l)$$

where,

$$avg_CR_{path}(PL) = \frac{avg(avg_overflow_hops_PL) + K * avg_hops}{1 + K * avg_hops} \dots\dots\dots(5.6)$$

In [Equation \(5.6\)](#), $Ro_PL(l)$ is the number of overflow channels in link l of the network and $Rp_PL(l)$ is the number of primary light-paths in link l . $Rp_PL(l)$ primary light-paths on link l span an average number of hops equal to $avg_hops(PL)$. On the other hand due to light-path entry at intermediate hops, $Ro_PL(l)$ overflow channels $avg(avg_overflow_hops(PL))$ hops across the network.

Table 5.9 Number of primary and overflow channels in each link.

Link,l	0	1	3	5	7	9	11	7	13	
PL = 0										
Ro_0	35	35	48	48	48	35	48	35	35	35
Rp_0	0	0	0	0	0	0	0	0	0	0
PL = 1										
Ro_1	31	23	42	20	36	25	42	23	31	31
Rp_1	5	14	4	10	10	9	3	9	5	5
PL = 3										
Ro_3	19	17	20	25	25	19	20	17	19	19
Rp_3	15	10	12	8	8	5	9	10	15	15
PL = 5										
Ro_5	15	15	17	17	17	15	15	15	15	15
Rp_5	25	5	20	10	10	5	15	5	25	25
PL = 7										
Ro_5	12	12	13	13	13	12	13	12	12	12
Rp_5	35	7	28	14	14	7	21	7	35	35
PL = 9										
Ro_5	10	10	10	10	10	10	10	10	10	10

Rp_5	45	9	36	18	18	9	27	9	45	45
PL = 11										
Ro_5	9	9	9	9	9	9	9	9	9	9
Rp_5	55	11	44	22	22	11	33	11	55	55
PL = 13										
Ro_5	0	0	0	0	0	0	0	0	0	0
Rp_5	65	13	52	26	26	13	26	13	65	65

In order to determine the cost of all network routes, we add up all elements of $Total_cost_PL(l)$ matrix to obtain $Total_cost(PL)$. PL varies from 0 to 13 in [Table 5.9](#).

5.5.2 ANALYSIS OF NETWORK ROUTE COSTS FOR EXAMPLE 1

$Total_cost(PL)$ depends on value of K , as seen in [Equations \(5.6\)](#). [Table 5.10](#) gives the $avg_CR_{path}(PL)$ and the $Total_cost(PL)$ for different values of PL and K .

Table 5.10 Total cost of the Hybrid Network

PL	0	1	3	5	7	9	11	13
K = 1								
$Avg_CR_{path}(PL)$.99	1.2136	1.2481	1.356	1.356	1.356	1.356	2
$Total_cost(PL)$	400	443	356	690	371	397	441	377
K = 10								
$Avg_CR_{path}(PL)$.99	1.03	1.035	1.05	1.05	1.05	1.05	2
$Total_cost(PL)$	401	388	314	567	333	366	413	377
K = 0.5								
$Avg_CR_{path}(PL)$.99	1.2136	1.2481	1.356	1.356	1.356	1.356	2
$Total_cost(PL)$	398	475	381	762	394	414	457	377

The value of K, which is the ratio of cost of transmitting a channel along a link to the cost of switching the channel, determines the total cost of network. If the value of K is large, a hybrid operation may yield better savings in total cost, compared to the cost of non-hybrid operation. In the worked out example above, Hybrid Operation attains a minimum for K =10 and for K =1. For K = 10, minimum total cost is obtained for PL = 3 and for K = 1, minimum point occurs at PL = 3, as well. However, for a smaller value of K, hybrid operation may not be cost optimal. For instance, for K = .5, total cost of network in the example is a minimum if there are absolutely no overflow channels.

In order to understand the table entries, let us consider the case when K =1 and PL =5. The example network, when provided with PL =5, obtains a utilization of 48.5% , as it can be obtained from [Table 5.1](#). With this value of utilization, the adjacency matrices of the primary and overflow layer graphs, A_p and A_v , can be obtained by the Iterative technique described in Sections 5.2 and 5.3. The values of A_p and A_v are:

$$A_o = \begin{bmatrix} 0 & 19 & 0 & 0 & 0 & 0 \\ 17 & 0 & 20 & 0 & 0 & 0 \\ 0 & 25 & 0 & 25 & 19 & 0 \\ 0 & 0 & 20 & 0 & 0 & 17 \\ 0 & 0 & 19 & 0 & 0 & 0 \\ 0 & 0 & 0 & 19 & 0 & 0 \end{bmatrix} \quad A_p = \begin{bmatrix} 0 & 25 & 0 & 0 & 0 & 0 \\ 28 & 0 & 40 & 0 & 0 & 0 \\ 0 & 46 & 0 & 46 & 25 & 0 \\ 0 & 0 & 40 & 0 & 0 & 28 \\ 0 & 0 & 25 & 0 & 0 & 0 \\ 0 & 0 & 0 & 25 & 0 & 0 \end{bmatrix}$$

From the primary and overflow layer adjacency matrices, number of primary and overflow channels , $Rp_{PL}(l)$ and $Ro_{PL}(l)$ is obtained for all the ten links, l in the example.

Link,l	0	1	3	5	7	9	11	7	13	
PL = 5										
Ro_5	15	15	17	17	17	15	15	15	15	15
Rp_5	25	5	20	10	10	5	15	5	25	25

Sum of Ro_{PL} and Rp_{PL} is taken and substituted in [Equation \(5.6\)](#).

$$\sum_{l=1}^{10} R_o PL(l) = 156 \text{ and } \sum_{l=1}^{10} R_p PL(l) = 142$$

In order to determine the total cost of all routes, the average value of path cost ratio has to be determined. In order to determine the average cost ratio over all routes, we first off all determine the *hops* and *avg_hops_PL* matrix, as in [Equation \(5.4\)](#).

$$avg_overflow_hops_5 = \begin{bmatrix} 0 & .99 & 1.98 & 2.99 & 2.99 & 3.98 \\ .99 & 0 & .99 & 1.96 & 1.96 & 2.91 \\ 1.98 & .99 & 0 & .99 & .99 & 1.98 \\ 2.99 & 1.96 & .99 & 0 & 1.96 & 1.96 \\ 2.99 & 1.98 & .99 & 1.98 & 0 & 2.99 \\ 3.98 & 2.99 & 1.98 & .99 & 2.99 & 0 \end{bmatrix}$$

For each route in the network between Nodes i and j, [Equation \(5.4\)](#) is used to obtain the element of the *avg_overflow_hops_5* matrix. Due to light-path entry, each element of the *avg_overflow_hops_PL* matrix will be less than the corresponding values in the hops matrix. Average of all elements of this matrix is taken to obtain $avg(avg_overflow_hops_5)$, which is equal to 2.08. This value along with the value of K, is substituted in [Equation \(5.6\)](#) to obtain $avg_CR_{path_PL}$, which is the average cost ratio over all routes for the example network. From the value of $avg_CR_{path_PL}$, [Equation \(5.4\)](#) is used to obtain the total cost, $Total_cost(PL)$.

5.6 CHAPTER CONCLUSION

An example network has been analyzed for hybrid operation. The example brings together two approaches, developed in Chapters 3 and 4, in order to assess the total cost of a Hybrid Network. The total cost of a Hybrid Network is obtained by calculating the total switching and the total transport cost of the given network. The total cost of the Hybrid Network is also obtained by

considering the total cost of all the routes in the network. For both approaches, the total cost of the network is analyzed for different values of primary channel utilization.

Prior to calculating the total cost of the Hybrid Network using either of the two approaches, an iterative method is developed to obtain the total number of primary and overflow channels in all the links. Once the number of input and output channels in a node is known, total switching cost of the nodes are determined. The Hybrid Nodes are assumed to possess the switching architecture outlined in Chapter 4. Assuming that the core node is constructed using Broadcast-Select architecture, the total switching cost is assumed proportional to number of 1×1 elements in the node.

It is observed that the number of 1×1 elements in each node of the example network depends on the average primary channel utilization/channel load. Since the primary channel utilization of the network corresponds to a fixed number of primary channels for the access source, we see that the number of 1×1 elements depends on number of access primary channels. As the number of access primary channels increases, the number of 1×1 elements also increases for nodes with a degree of one. On the contrary, for the node with degree-3, the number of 1×1 elements decreases with an increase in number of access primary channels. Overall, the total number of 1×1 elements in the network obtains a minimum while operating in the hybrid mode with 9 access primary channels per source- destination.

The total cost of a Hybrid Network is assumed to be the sum of the total switching and the total transport costs. The transport cost of the network is assumed to be directly proportional to the number of channels in the network. Both switching and transport costs are related by a cost ratio, CR_{trans} , which is the ratio of a channel cost to the cost of a 1×1 switching element. If value of CR_{trans} is very small, total cost of the network follows the cost curve of the switching cost and obtains a minimum for hybrid operation. As the value of CR_{trans} increases, the total cost curve tends to resemble the total channel curve, which increases with an increase in the number of access primary channels.

The total cost of a Hybrid Network is also obtained by calculating the total cost of all Hybrid Routes in the networks. A Hybrid Route, as explained in Chapter 3, consists of primary and overflow paths and the cost of the two paths are related via the notion of path cost ratio, CR_{path} . The value of CR_{path} depends on the average number of switching hops taken by a burst that was put on the overflow path by the source node. Due to the possibility of light-path entry at

all intermediate hops between the source and destination nodes of a route path, the average number of hops at which the burst has to be switched reduces. The possibility of light-path entry increases when there are only few access primary channels and when there is a huge overflow at the edge nodes. Under this condition, the possibility of light-path entry at the core nodes increases and therefore, CR_{path} decreases. Thus, it is seen that for smaller number of primary channels per access source, the average path cost ratio of the network decreases and for a large number of access primary channels, the average path cost ratio increases.

The value of CR_{path} is determined for all routes in the network assuming a fixed value of K , which is the ratio of the per-link transmission cost and the per-hop switching cost. The total cost of the network is determined for each value of access primary channels. It is observed that hybrid operation may provide minimum total cost, subject to the value of K . When K is large cost savings due to hybrid operation is found to be large and when K is small, the cost savings decreases.

6.0 CONCLUSION

A hybrid OCS/OBS operation can be realized in core optical networks by providing hybrid OCS/OBS routes between the network nodes. The OCS-based primary path of a hybrid route will provide a guaranteed connection between the source and destinations of the route and the OBS-based overflow path is a best-effort path used to carry primary path overflows. The allotment of primary and overflow paths to the incoming channel requests are performed at the control layer of a hybrid node and the operation is performed for burst headers arriving from, access and core links. Once the control layer sets up a route path for the burst header, the switch hardware is configured to set up an internal path through the hybrid node. In this dissertation, both hybrid routes and hybrid nodes are analyzed for its cost effectiveness that may lead to cost optimality.

The results obtained by analyzing a Hybrid Route, a Hybrid Node and an example Hybrid Network, point to the possibility of realizing a cost optimum core network. However, in order to make the analyses tractable several simplifying assumptions were made. In order to extend the work performed in this dissertation, more studies have to be performed by considering a heterogeneous mix of offered traffic and its effect of cost-optimality of core optical networks. In addition, more focus needs to be paid to cost and complexity of the access-core interface that shapes the incoming access traffic. Several other cost issues that may potentially effect the cost structures of the Hybrid Routes, such as alternate path routing, heterogeneous loading of routes etc have to be considered.

The Hybrid Network analysis performed in this work is limited to solving an example analytically. However, in order to arrive at a general network solution simulations studies have to be performed to a large variety of networks carrying a diverse traffic with diverse requirements.

Thus, the existing work is an initial step towards realizing a cost-optimal core optical network using OBS based overflow channels.

6.1 SUMMARY OF RESULTS

Cost optimality of a hybrid route depends on statistics of the load offered by each source to the route, the number of sources sharing the route, and the relative costs of primary and overflow paths. Optimality of a hybrid route depends on offered-load statistics such as the smoothness of the burst arrivals, through the value of ‘overflow gain’. At the point of cost optimality, overflow gain is directly proportional to the number of sources sharing the overflow path and inversely proportional to the relative costs of primary and overflow paths. This relation between overflow gain, number of sources, and path cost ratio, gives the optimality condition. The optimality condition states that a hybrid route is cost optimal only if the incremental cost of primary path in the route is equal to the corresponding decremented cost of the overflow path.

The hybrid route optimality condition is tested in Chapter 3 for a set of offered loads and its Peakedness values, the number of sources sharing the overflow channels, and for a range of path cost ratios. The overflow gain is obtained under the condition that the blocking probability of an overflow link is fixed. The feasibility of hybrid operation is analyzed by determining, for each case of offered load and number of sources, the window of path-cost ratios for which optimal hybrid operation can be obtained. It is seen that hybrid operation becomes cost-optimal compared to a non-hybrid operation, for a larger window of path-cost ratio when the Peakedness of offered load is high and overflow gain is small. The window of path cost ratio also increases when there are larger number of sources, which corresponds to the case when overflow gain is small.

A hybrid network is made of hybrid nodes that provide switching and transmission hardware to set up hybrid route. The function of a hybrid node is to bypass incoming primary channels and optical-burst switch(OB-switch) incoming overflow and access links onto outgoing primary and overflow channels. Chapter 4 outlines a switching node architecture, which is divided into several ‘source-specific’ primary OB-switches and a large overflow OB-switch. In

addition to the switching hardware, there are other devices such as wavelength converters, amplifiers and transmitters/receiver ports, in the primary and overflow layers of the hybrid node.

A hybrid node is cost-optimal if incremental cost of the primary layer is equal to the decremented cost of the overflow layer. It is assumed that the predominant cost components of each layer are the switching cost, which depends on the switch architecture and channel dependent costs that scale linearly with the number of output channels. The switching cost grows at a nearly linear rate in the primary layer of the hybrid node and at a polynomial rate for overflow layer of the hybrid node. If we assume channel-related costs to be negligible, the optimality of the hybrid switch will decide the optimality of the hybrid node.

The cost advantage of an optimal hybrid switch, called the ‘hybrid advantage’ is higher for the un-integrated Broadcast-And-Select architecture. Both the Benes architecture and the integration of switching elements on a chip reduce this ‘hybrid advantage’. Thus, the hybrid advantage is more pronounced if the underlying switch architecture of primary and overflow layers is not cost-optimal. Both the Benes architecture and the integration of switching elements are traditionally used to minimize switching costs in the electronic domain. Although not considered cost-optimal, un-integrated switches and the Broadcast-Select architecture are easier to realize in the optical domain.

Chapter 5 provides an example to test the optimality conditions for hybrid routes and hybrid nodes at a network level. The hybrid network provides fixed channel utilization at the primary layer and fixed blocking probability at each node of the overflow layer. If we assume a fixed blocking probability at the overflow links, the cost optimality of a hybrid network depends on the value of primary channel utilization. In order to obtain this value, the total cost of the network is calculated using two approaches. First, the total cost of the hybrid nodes and links is obtained, over a range of primary channel-utilization. In the second approach, the total cost of hybrid network is obtained as the total cost of all routes in the network.

From the network analysis, it is seen that the total switching cost of nodes with a smaller degree, depends on the cost of the primary layer, which increases with a decrease in primary channel utilization. On the other hand, the cost of nodes with a higher node-degree, depends on the cost of the overflow layer, which decreases for a lower value of primary channel utilization. Overall, the total cost of switching obtains a minimum cost by operating in the hybrid mode.

This hybrid advantage will help minimize total cost of network, if ratio of cost of a channel, to the cost of a switching element is small.

The total cost of the example network, when viewed as a collection of routes, obtains a minimum value due to hybrid operation. While calculating the route costs it is seen that the average path cost-ratio of all the routes increases by lowering the primary channel utilization. Cost optimality of the hybrid network depends on cost ratio via the value of primary channel utilization and on the value of K , the cost ratio of per-link and per-node costs for an overflow path. In the example, cost optimality is lost when K becomes very small.

6.2 FUTURE WORK

In the future work on hybrid networks, the aim will be to obtain a general solution for optimal hybrid operation in a network. In this dissertation, the light-path entry mechanism of a hybrid route proceeds from the source to the destination nodes of hybrid route. The dual of the optimal-route problem is to consider light-path entry happening near the source node and overflow path entry nearer to the destination node. Both the problems are part of a larger problem to optimally choose the method of light path and overflow path entry for a route.

Efficiency and robustness of a hybrid network depends on its performance when subjected to a dynamic load. Under such a case, some wavelengths will be re-allotted between primary and overflow layers during epochs of load change. Optimal design of such a dynamic capacity switched network will be an interesting topic for future work. Cost efficiency of such a 'capacity switched' network will require design of switch that will contain interconnections between the primary and overflow layers.

The hybrid network proposed in the dissertation may be used to provide spare capacity in the event of link/node failures. Spare capacity may be provided in the form of primary and/or overflow channels. Spare capacity allocation methods in the existing literature can be extended to the use of hybrid networks [\[59\]](#). Cost of optimality of a hybrid network with spare capacity may depend on several cost parameters such as channel costs, switching costs, topology etc.

The hybrid operation proposed in the dissertation may be used to provide performance differentiation under fixed number of channels in the links. By tweaking the number of primary and overflow paths available to each class, performance differentiation can be provided. Preliminary analytical and simulation studies on this topic has provided two different approach to provide performance differentiation [61][62]. An efficient control algorithm that will monitor offered load of each class and adjust primary/overflow channel capacity accordingly is being currently studied.

The primary and overflow channels help modify the topology of existing core networks. While primary light-paths overlay a virtual ‘mesh’ topology on the existing network, overflow channels conserve existing physical topology. As the network parameters such as the traffic load characteristics of the access layer and the cost structure of the network varies, the degree of mesh overlay also varies. From a topology perspective, the problem solved in Chapter 5 provides a mesh overlay on an existing physical network, using the ‘virtual graph, G_v .

While the problems solved in the dissertation assumes homogenous traffic sources and identical switching architecture of the hybrid node, the solution to cost optimal network is constrained to a large extent. In reality however, traffic sources may be heterogeneous and the nodes may vary in their switching architecture and the solution space for optimal network becomes very large. It is also important to consider the evolution of networks with respect to possible cost structures and traffic types, in order to strategically design a core network. However, strategic designs also require a high degree of combinatorial analyses of possible traffic and cost structures. In order to determine optimal topology for a more realistic network consisting of a large solution space, cost optimization may be performed using genetic algorithms that can help provide a global optimum in an efficient manner [60]. It will be interesting to determine if there are optimal topologies that can help balance cost, performance and survivability of core networks.

BIBLIOGRAPHY

- [1] Thompson R. A (2000), "Telephone Switching Systems," Artech House.
- [2] Harrington.E., "Voice/Data Integration Using Circuit Switched Networks," *Communications, IEEE Transactions on [legacy, pre - 1988]*, Volume 28, June 1980. Page(s): 781-793.
- [3] Easton, R.; Hutchison, P.; Kolor, R.; Mondello, R.; Muise, R., "TASI-E Communications System," *Communications, IEEE Transactions on [legacy, pre - 1988]* Volume 30, Issue 4, Apr 1982 Page(s):803 – 807.
- [4] Bohm . C., P. Lindgren, L. Ramfelt and P. Sjödin, "The DTM Gigabit Network", *Journal of High Speed Networks*, Vol. 3, No. 2, pp. 109-126, 1994.
- [5] Joel. A. E., Photonic Switching, United States Patent #4,736,462, April 1988.
- [6] Simmons J. M., "Analysis of wavelength conversion in all-optical express backbone networks," presented at the *Optical Fiber Communication Conf. (OFC)*, Anaheim, CA, Mar. 17–22, 2002, Paper TuG2.
- [7] D. Banerjee and B. Mukherjee., "A practical approach for routing and wavelength assignment in large wavelength-routed optical networks," *IEEE Journal on Selected Areas in Communications*, 4(5):903.908, 1996.
- [8] D. Banerjee and B. Mukherjee., "Wavelength-routed optical networks: linear formulation, resource budgeting tradeoffs, and a reconfiguration study," *IEEE/ACM Transactions on Networking*, 8(5):598.607, 2000.
- [9] Saleh, A.A.M.; Simmons, J.M, "Evolution Toward the Next-Generation Core Optical Network," *Journal of Lightwave Technology*, volume 24, Sept. 2006.
- [10] Hunter.D.K, Adnovich.I, "Approaches to Internet Packet Switching," *IEEE Communications Magazine*, Sept. 2000.
-

- [11] Xu.L., Perros.H.G, Rouskas.G., “ **Techniques for Optical Packet Switching,**” *IEEE Communications Magazine*, January 2001.
- [12] O’Mahony M. J. *et al.*, “**The Application of Optical Packet Switching in Future Communication Networks,**” *IEEE Commun. Mag.*, vol. 39, no. 3, 2001.
- [13] Hunter.D.K, Adnovich.I., Chia.M.C., “**Buffering in Optical Packet Switches,**” *Journal of Lightwave Technology*, December 1998.
- [14] Yao.s. et. al., “**A Unified Study of Contention Resolution Schemes in Optical Packet Switched Networks,**” *Journal of Lightwave Technology*, Vol.21, February 2003.
- [15] Chen. Y., Qiao.C., Yu.X. “**Optical Burst Switching: A New Area in Optical Networking Research,**” *IEEE Network*, May/June 2000.
- [16] Qiao. C. and M. Yoo, “**Optical Burst Switching (OBS) —A New Paradigm for an Optical Internet,**” *J. High Speed Networks*, vol. 8, no. 1, 1999.
- [17] Gauger .C.M et.al, “**Hybrid optical network architectures: bringing packets and circuits together,**” *Communications Magazine, IEEE* , vol.44, no.8pp. 36- 42, Aug. 2006.
- [18] Gauger C. M. and Mukherjee B, “**Optical Burst Transport Network (OBTN) —A Novel Architecture for Efficient Transport of Optical Burst Data Over Lambda Grids,**” *IEEE High Perf. Switching and Routing*, HongKong, May 2005.
- [19] G. M. Lee *et al.*, “**Performance Evaluation of an optical Hybrid Switching System,**” *IEEE GLOBECOM*, San Francisco, CA, Dec. 2003.
- [20] Kovacevic, M.; Gerla, M., “**HONET: an integrated services wavelength division optical network,**” *Communications, 1994. ICC 94, SUPERCOMM/ICC '94, Conference Record, Serving Humanity Through Communications. IEEE International Conference on*, vol.3, 1-5 May 1994 Page(s):1669 - 1674.
- [21] Zheng .X. *et al.*, “**CHEETAH: Circuit-switched High-Speed End-to-End Transport Architecture Testbed,**” *IEEE Commun.Mag., Opt. Commun. Supp.*, vol. 3, no. 3, 2005.
- [22] de Miguel.I *et al.*, “**Polymorphic Architectures for Optical Networks and Their Seamless Evolution Towards Networks and Their Seamless Evolution Towards Next Generation Networks,**” *Photonic Network Commun.*,vol. 8, no. 2, Sept. 2004.
- [23] Van Breusegern, E et. Al, “**Overspill routing in optical networks: a true hybrid optical network design,**” *Selected Areas in Communications, IEEE Journal on*, Volume 24, Issue 4, Part Supplement, Apr 2006 Page(s):13 – 25.
-

- [24] Van Breusegem. E. *et al.*, “**A Broad View on Overspill Routing in Optical Networks: A Real Synthesis of Packet and Circuit Switching?**” *Optical Switching and Net.*, vol.1, no. 1, 2004, pp. 51–64.
- [25] Iversen. V.B., “Teletraffic Engineering Handbook,” ITU-T SG 2/16 & ITC. [26] Iversen, V.B.; Mirtchev, S.T., “**Generalised Erlang Loss Formula,**” *Electronics Letters*, Volume 32, Issue 8, 11 Apr 1996 Page(s):712 – 713.
- [27] Kosten, L., “**On Blocking Probability of Graded Multiples,**” (in German), *Elektr. Nachy.-Techn.*, Volume. 14, pp. 5-12, 1937.
- [28] Girard. A., “**Routing and Dimensioning in Circuit-Switched Networks,**” Addison-Wesley, 1990
- [29] Brockmeyer, E., “**The Simple Overflow Problem in the Theory of Telephone Traffic,**” (in Danish), *Teleteknik*, volume 5, pp. 361-374, 1954.
- [30] Jagerman. D. L., “**Burstiness descriptors of traffic streams: Indices of dispersion and peakedness,**” in *Proceedings of the Conference on Information Sciences and Systems*, (Princeton, NJ), pp. 24--28, 1994.
- [31] Wilkinson. R. I., “**Theories of toll traffic engineering in the usa,**” *The Bell System Technical Journal*, 35(2):421–514, 1956.
- [32] Akimaru. H. and Kawashima. K., *Teletraffic—Theory and Application*, 2nd ed. London, U.K.: Springer, 1999.
- [33] Kuczura, A., “**The interrupted Poisson process as an over flow process,**” *Bell Sys. Tech. J.* 52, No. 3 (1973) 437-448.
- [34] Bayvel.P and Killey. R., “**Nonlinear optical effects in WDM transmission,**” in *Optical Fiber Telecommunications IV B*, I. Kaminow and T. Li, Eds.New York: Elsevier, 2002.
- [35] El-Mirghani. J.M.H., Mouftah.H.T., “**Technologies and Architectures for Scalable Dynamic Dense WDM,**” *IEEE Communications Magazine*, February 2000.
- [36] Hsueh. Y. *et al.*, “**Traffic grooming on WDM rings using optical burst transport,**” *J. Lightw. Technol.*, vol. 24, no. 1, pp. 44–53, Jan. 2006.
- [37] Kuczura, A. and Bajaj, D., “**A Method of Moments for the Analysis of a Switched Communication Network's Performance,**” *Communications, IEEE Transactions on [legacy, pre - 1988]* , vol.25, no.2pp. 185- 193, Feb 1977.
-

- [38] Tucker R., “**Petabit-per-second routers: Optical vs. electronic implementations,**” *presented at the Optical Fiber Communication Conf. Expo.(OFC)/National Fiber Optic Engineers Conf.(NFOEC)*, Anaheim, CA,Mar. 5–10, 2006, Paper OFJ3.
- [39] Zhou.P., Yang.O., “**How Practical is Optical Packet Switching in Core Networks,**” *Globecom 2003*.
- [40] Xin .C.*et al.*, “**A Hybrid Optical Switching Approach,**” *IEEE GLOBECOM*, San Francisco/CA, Dec. 2003.
- [41] Brandt, A., and Brandt, M., “**On the moments of the over flow and freed carried traffic for the GI/M/C/0 system,**” ZIB-Report ZR-01-09, Konrad-Zuse-Zentrum fur Informationstechnik Berlin (2001) 1-18.
- [42]Gunther Bolch. *et.al*, “**Queueing Networks and Markov Chains: Modeling and Performance Evaluation with Computer Science Applications,**” Wiley-Interscience; 2 edition (April 14, 2006).
- [43] Papadimitriou .G. I. *et al.*, “**Optical switching: Switch fabrics, techniques, and architectures,**” *J. Lightw. Technol.*, vol. 21, no. 2, pp. 384–405, Feb. 2003.
- [44] M.V. Rodrigo and J. Gotz, “**An analytical study of optical burst switching aggregation strategies,**” Workshop on OBS'04, 2004.
- [45] Wilfong. G. *et al*, “**WDM Cross connect Architecture with Reduced Complexity,**” *J. Lightwave Technology.*, vol 17, Oct 1999.
- [46] Renaud. M.*et.al*, “**SOA Based Optical Network Components,**” *Electronic Components and Technology Conference-2001*.
- [47] Renaud M., “**Integrated SOA-components for all-optical networking functions**”, invited paper, *ECIO'01*, Paderborn, Germany, April 4-6, 2001.
- [48] Gambini, *et. al*, “**Transparent optical packet switching: network architecture and demonstrators in the KEOPS project,**” *IEEE JSAC*, Sept 1998.
- [49] Williams. K. A., *et. al*, “**Monolithic Integration of Semiconductor Optical Switches for Optical Cross Connects,**” *IRC-TR-04-018*, October 2004.
- [50] Lacey. J., “**Optical Switching and its Impact on Optical Networks,**” *OFC2001*.
-

- [51] Spanke. R, “ **Architectures For Guided Wave Optical Space Switching Systems,**” IEEE Communications Magazine , May 1987.
- [52] Jungnickle. D. , “ **Graphs, Networks and Algorithms,**” Springer 2007, ISBN 3540727795, 9783540727798.
- [53] Sedgewick. R. , “**Algorithms in C++,**” Addison Wesley Longman Publishing. Co. 1992.
- [54] Rugsachart. A, Thompson. R. A: **Optimal timeslot size for synchronous optical burst switching.** Broadnets 2007: 17-22.
- [55] Artprecha Rugsachart, [Richard A. Thompson](#): “**An analysis of time synchronized optical burst switching,**” HPSR 2006.
- [56] Menon. Pratibha, Thompson. R. A, “ **Optimal Combination of circuit and Packet Switching in Optical core networks,**” HPSR 2006.
- [57] Thompson. R. A et. al, “ **Economic Analysis of an Optical Core Network Architecture,**” ITERA 2007.
- [58] Menon. Pratibha, Thompson. R. A,” **Capacity Management in Optical Core Networks Using Overflow Channels,**” ITERA 2007.
- [59] Al-Rumaih, Tipper.D , Liu. Y and Norman.B,” **Spare Capacity Planning for Survivable Mesh Networks,**” *Lecture notes in Computer Science 1815, Proceedings of the IFIP Networking 2000*, Paris, France, May, 2000.
- [60] Konak, A. and Smith, A.E. (1999). "A hybrid genetic algorithm approach for backbone design of communication networks," *Proceedings of the 1999 Congress on Evolutionary Computation-CEC99 (Cat. No. 99TH8406)*, Washington, DC, USA, IEEE, 1817-23 Vol. 3.
- [61] Menon. Pratibha, Cerroni. W and Reimer.N, “**Overflow Traffic Modeling in Hybrid optical circuit/burst switching nodes with service differentiation,**” *proceedings of OFC* March 2009.
- [62] Ramaswami. R, Sivarajan.K.N., “ **Routing and Wavelength Assignment Problem in All Optical Networks,**” IEEE Transactions on Networking Vol 3, Issue 5 Oct 1995.
- [63] Dutta.R, Kamal. A. E. and Rouskas.G.N (Eds) , “ **Traffic Grooming for all Optical Networks,**” Optical Network series, Springer, 2008.
-

[64] Dixit.S (Ed) , “ **IP over WDM: Building the Next Generation Optical Networks,**” John Wiley and Sons,
2003.

[65] Lin. H , Wang.S , Tsai. C and Hung.M , “ **Traffic Intensity Based alternate Path Routing for all Optical
Networks,**” Journal of Lightwave technology, Vol.26, Issue 22, Nov 2008
